DEPARTMENT OF THE NAVY
DAVID TAYLOR MODEL BASIN

HYDROMECHANICS

○

AERODYNAMICS

○

STRUCTURAL MECHANICS

○

APPLIED MATHEMATICS

TMB 2-, 3-, AND 4-BLADED SUPERCAVITATING

PROPELLER SERIES

by

E. B. Caster

HYDROMECHANICS LABORATORY

RESEARCH AND DEVELOPMENT REPORT

January 1963   Report 1637

TMB 2-, 3-, AND 4-BLADED SUPERCAVITATING

PROPELLER SERIES

by

E. B. Caster

TABLE OF CONTENTS

LIST OF TABLES

NOTATION

BTF	Blade thickness fraction	

C_P Power coefficient $\left(\dfrac{550\, P_s}{\dfrac{\rho}{8}\, \pi\, D^2 V_a^3} \right)$

C_T Thrust coefficient $\left(\dfrac{T}{\dfrac{\rho}{8}\, \pi\, D^2 V_a^2} \right)$

C_σ Pitch correction coefficient

D   Propeller diameter

E A R   Expanded area ratio

g   Acceleration due to gravity

H   Atmospheric pressure plus the submergence pressure at 0.7 section minus the cavity pressure

J   Speed coefficient $\left(\dfrac{V_a}{nD} \right)$

l Chord length

$l_{0.7}$ Chord length at 0.7 radius

n   Revolutions per unit time

P_s Shaft horsepower

P/D   Pitch ratio along the radius for finite cavitation numbers

R   Maximum propeller radius

R_e Reynolds number $\left(l_{0.7} \cdot \dfrac{V\sqrt{V_a^2 + 0.7\pi n D^2}}{\upsilon} \right)$

r   Radius of any propeller blade section

S_C Maximum compressive stress

T   Thrust

t   Section thickness

t_{max} Maximum section thickness along the radius χ

V_a Speed of advance

$(V_r)_{0.7}$ Inflow velocity to section at 0.7 radius

χ Nondimensional radius $\left(\dfrac{r}{R} \right)$

χ_h Nondimensional radius at the hub

χ_l Fractional distance along the chord measured from the leading edge

y   Pressure face ordinate

y_{max} Maximum pressure face ordinate along the radius χ

z   Number of blades

$\Delta(P/D)$ Pitch correction coefficient

η Propeller efficiency $\left(\dfrac{C_T}{C_P} \right)$

υ Kinematic viscosity

ρ Density of fluid

$\sigma_{0.7}$ Cavitation number at 0.7 radius $\left[\dfrac{2gH}{(V_r^2)_{0.7}} \simeq \dfrac{2gHJ^2}{V_a^2(J^2 + 4.84)} \right]$

ABSTRACT

This report presents theoretically derived series of
2-bladed supercavitating propellers with expanded area
ratios of 0.3, 0.4, and 0.5; 3-bladed propellers with
expanded area ratios of 0.4, 0.5, and 0.6; and 4-bladed
propellers with expanded area ratios of 0.5, 0.6, and
0.7. These propellers have a specified radial distri-
bution of the section chord and a hub radius of 0.2 of
the propeller radius. The series data are plotted in
the form of nondimensional coefficients so that the
performance of the propellers can be easily predicted
and a complete design obtained if desired.

INTRODUCTION

Supercavitating (SC) propellers, which have fully developed
cavitation on the suction side (back) of their blades, are of interest
to naval architects since conventional propellers experience an un-
predictable performance breakdown, because of cavitation, when operated
at very high speeds.

This report presents series data which can be used to predict
the performance of SC propellers. Since an experimental series is
costly and time-consuming, a theoretical series is of great value, if
only in a qualitative way. The series presented can be compared with
experimental results[1,2,3] of propellers designed using this method. It
is apparent that there is some deviation from the experimental values,
but this difference is not unreasonable compared to propellers design
from experimentally derived subcavitating series.

A 3-bladed supercavitating propeller series with an expanded
area ratio of 0.5 has already been derived at the Taylor Model Basin.[4]
Since the ultimate aim of a designer is to obtain the best propeller for
a given craft, there is need for a method of predicting the performance
of SC propellers due to variations in number of blades and expanded
ratio. The choice of the number of blades and expanded area ratio is

---

[1]References are listed on page 12.

important in designing propellers since the propeller stress is dependent on these parameters. because the propeller stress is directly related to the loading of SC propellers, which have sections that are usually thin and highly stressed, the choice of these parameters is invaluable.

In addition to stress considerations, the choice of number of blades and expanded area ratio is also important since it has been determined that any type of SC section operating at a given angle of attack has an optimum point, i.e., a minimum drag-lift ratio, which occurs at a specific lift coefficient.[5] This means that the blade chord becomes important in deriving the most efficient propeller.

This report presents a series of 2-, 3-, and 4-bladed SC propellers having various expanded area ratios. The results are plotted in a series of diagrams in the form of nondimensional co-efficients which can be used to predict the performance and character-istics of SC propellers.

METHOD OF APPROACH

The series charts presented here were derived by first designing a number of 2-, 3-, and 4-bladed SC propellers for zero cavitation number operating in uniform flow. Each propeller had a hub radius of 0.2 of the propeller radius. The Reynolds numbers used for calculating the section drag varied from 7.2×10^6 to 7.7×10^7 which corresponds to propellers having a diameter of 3 feet and operating at a speed of ad-vance of 60 knots. It should be noted that these propellers were designed for the same diameter, speed of advance, speed coefficients, and non-viscous thrust coefficients as those propellers designed to derive the series presented in Reference 3, i.e., the speed coefficients covered a range from 0.3142 to 1.5708 and the nonviscous thrust coefficients covered a range from 0.15 to 4.0.

Like the series derived in Reference 4, the nonviscous thrust and power coefficients, ideal efficiency, and hydrodynamic pitch distribution for each of the series of 2-, 3-, and 4-bladed SC propellers were computed using Lerbs' moderately loaded propeller theory.[6] This

2

propeller theory has been programmed for the high-speed computers at the Model Basin.[7]

Once the above calculations were obtained, the next step was to determine the viscous corrections that must be applied to these nonviscous calculations, using the method given in Reference 1. In order to make these calculations, it was necessary to know the values of the section drag-lift ratio, which is dependent mainly on the section lift coefficient and angle of attack. Table 1 gives the radial distribution of the section chord for each series. From these values, the viscous thrust and power coefficients and propeller efficiency were calculated for each propeller.

The next step was to calculate the propeller pitch distribution for nonzero as well as zero cavitation numbers, using the method given in Reference 1. Since the amount of cavitation changes the thrust and power of a propeller, this effect must be compensated for by a corresponding change in the propeller pitch. This was obtained by calculating the pitch of each propeller at cavitation numbers ranging from 0 to 0.205 and comparing the results with the pitch calculated for zero cavitation number.

The section ordinates of the "TMB Modified Tulin Section," used on these propellers, were calculated next. The camber line of this type section is the pressure side (face) of the foil, and the thickness is applied between the camber line and the free-stream line. The camber and thickness ordinates were calculated using the method presented in Reference 1. The blade thickness fraction (BTF) was also calculated for each propeller in order to compute the nominal stress at the blade root of these propellers by a simplified method derived from Reference 8.

PRESENTATION OF DIAGRAMS

Most of the diagrams presented here are designated by a number and letter. The number indicates the propeller parameter and the letter indicates the number of blades and the expanded area ratio (EAR) of the propeller. The letters a, b, and c represent 2-bladed propellers having expanded area ratios of 0.3, 0.4, and 0.5, respectively; the letters d, e, and f represent 3-bladed propellers having expanded area ratios of

3

TABLE 1

Radial Distribution of Blade Chord for Supercavitating Propellers

	2-Bladed Series			3-Bladed Series			4-Bladed Series		
	EAR = 0.3	EAR = 0.4	EAR = 0.5	EAR = 0.4	EAR = 0.5	EAR = 0.6	EAR = 0.5	EAR = 0.6	EAR = 0.7
x	l/D	l/D	l/D	l/D	l/D	l/D	l/D	l/D	l/D
0.2	0.3438	0.4584	0.5730	0.3056	0.3820	0.4584	0.2865	0.3438	0.4011
0.3	0.3438	0.4584	0.5730	0.3056	0.3820	0.4584	0.2865	0.3438	0.4011
0.4	0.3438	0.4584	0.5730	0.3056	0.3820	0.4584	0.2865	0.3438	0.4011
0.5	0.3429	0.4572	0.5715	0.3048	0.3810	0.4572	0.2858	0.3429	0.4001
0.6	0.3357	0.4476	0.5595	0.2984	0.3730	0.4476	0.2798	0.3357	0.3917
0.7	0.3159	0.4212	0.5265	0.2808	0.3510	0.4212	0.2633	0.3159	0.3686
0.8	0.2754	0.3672	0.4590	0.2448	0.3060	0.3672	0.2295	0.2754	0.3213
0.9	0.2070	0.2760	0.3450	0.1840	0.2300	0.2760	0.1725	0.2070	0.2415
0.95	0.1503	0.2004	0.2505	0.1336	0.1670	0.2004	0.1253	0.1503	0.1754
1.0	0	0	0	0	0	0	0	0	0

4

0.4, 0.5, and 0.6, respectively; and the letters g, h, and i represent
4-bladed propellers having expanded area ratios of 0.5, 0.6, and 0.7,
respectively. It should be noted that the 3-bladed series diagrams
presented in Reference 4 are also presented here.

The propeller efficiency contours η and the pitch ratio
calculated at 0.7 radius for zero cavitation number P/D_o are presented
in Appendix A, Figures 1a through 1i, as a function of the thrust co-
efficient $\sqrt{C_T}$ and the speed coefficient J and in Appendix B, Figures 2a
through 2i, as a function of the power coefficient $\sqrt{C_P}$ and J. The
solid efficiency contours in these diagrams indicate the region where
the section-lift coefficient is between 0.0548 and 0.2 and the section
angle of attack is 2 degrees. The dashed portion below the solid
efficiency contours represents the region where the section-lift co-
efficient is less than 0.0548, resulting in flat-face sections having
angles of attack less than 2 degrees. This area should be avoided because
face cavitation is likely to occur on SC sections operating at these small
angles. The dashed portion above the solid efficient contours re-
presents the approximate area where the section-lift coefficient is
greater than 0.2 and the angle of attack greater than 2 degrees. In
this region, the cavities become thick and section loading high, and the
theoretical results may be in question. Also included in these diagrams
are maximum efficiency curves for obtaining the optimum rpm or diameter D.

The thrust coefficient C_T, power coefficient C_P, speed co-
efficient J and propeller efficiency η presented in Figures 1a through
2i were calculated using the following equations:

$$\sqrt{C_T} = \frac{T}{\frac{\rho}{8} \pi \ D^2 V_a^2} \tag{1}$$

$$\sqrt{C_P} = \frac{550 P_s}{\frac{\rho}{8} \pi \ D^2 V_a^3} \tag{2}$$

$$J = \frac{V_a}{nD} \tag{3}$$

5

and

$$\eta = \frac{C_T}{C_P} \qquad [4]$$

where T is the propeller thrust,

P_s is the shaft horsepower,

ρ is the density of the fluid,

D is the propeller diameter,

V_a is the speed of advance, and

n is the revolutions per unit time.

The propeller blade thickness fractions (BTF) derived for these propellers are presented next in Appendix C, Figures 3a through 3i, as a function of $\sqrt{C_T}$ and J so the propeller stress can be calculated. An approximate method for calculating the maximum compressive stress at the blade root derived from Reference 8 is

$$S_C \simeq \frac{1.95 \rho C_T V_a^2}{z \, (BTF)^2} \qquad [5]$$

where BTF is the blade thickness fraction given in Appendix C.

As mentioned above, Appendices A and B give the pitch ratio calculated at 0.7 radius for zero cavitation number P/D_o. Since there is a change in thrust and power of a propeller due to cavitation, a corresponding change in this pitch must be made to offset the variation in thrust or power. This change in P/D_o due to zero cavitation numbers $(\Delta(P/D)C_\sigma)$ is presented in Appendix D, Figures 4 through 4i. The parameter C_σ is plotted in Figure 4 as a function of the section cavitation number at the 0.7 radius $(\sigma_{0.7})$ only, where

$$\sigma_{0.7} \simeq \frac{2gH \, J^2}{V_a^2 \, (J^2 + 4.84)} \qquad [6]$$

and where H is the atmospheric pressure plus the submergence pressure at 0.7 section minus the cavity pressure, and g is the acceleration due to gravity. The other parameter $\Delta(P/D)$ derived for these propellers is also presented in Appendix D, Figures 4a through 4i, as a function of $\sqrt{C_T}$ and J.

The final pitch ratio at 0.7 radius for propellers operating at various cavitation numbers $(P/D)_{0.7}$ can be obtained from the equation

$$(P/D)_{0.7} = P/D_0 - \Delta(P/D)C_\sigma \qquad [7]$$

where C_σ is the pitch correction coefficient from Figure 4 of Appendix D and $\Delta P/D$ is the pitch correction coefficient from Figures 4a through 4i of Appendix D. The radial distribution of $(P/D)_{0.7}$ is presented in Table 2.

The section ordinates at various radii for the propellers are presented in Appendices E and F. The maximum face ordinates are presented in Appendix E, Figures 5a through 8i, and the maximum thickness ordinates are presented in Appendix F, Figures 9a through 12i, as a function of $\sqrt{C_T}$ and J.

A replot of the maximum efficiency curves given in Appendix A is presented in Figures 13 through 20 to show the relationship of number of blades and expanded area ratio to optimum rpm and diameter. The inconsistency in these diagrams is undoubtedly due to the method of fairing used as the curves were not cross-faired on the basis of number of blades nor expanded area ratio. They do indicate, however, the trend with varying number of blades and expanded area ratio.

USE OF DIAGRAMS

For a design based on thrust T, the propeller efficiency η and the 0.7 radius pitch for zero cavitation number P/D_0 can be obtained from Appendix A, Figures 1a through 1i, depending on the number of blades and expanded area ratio, once the thrust coefficient $\sqrt{C_T}$ and speed coefficient J are obtained. Similarily, for a design based on shaft horsepower P_s values of η and P/D_0 can be obtained from Appendix B, Figures 2a through 2i, once the power coefficient $\sqrt{C_P}$ and J are obtained. Equations [1], [2], and [3] can be used to calculate $\sqrt{C_T}$, $\sqrt{C_P}$, and J, respectively.

Figures presented in Appendices A and B can also be used to obtain the optimum rpm or diameter D for a given thrust or power. The optimum rpm for a given diameter is obtained by plotting $\sqrt{C_T}$ or $\sqrt{C_P}$ on the maximum efficiency line for a given C_T or C_P in these figures. This point represents the J that gives the optimum rpm for a given diameter,

and using this J value, the optimum rpm can be calculated using Equation [3]. The optimum diameter D for a given rpm is obtained by assuming a diameter and plotting the calculated J and $\sqrt{C_T}$ or $\sqrt{C_P}$ on the figures presented in Appendices A and B. The J obtained at the intersection of a straight line drawn from the origin of the diagram through this point and the line of maximum efficiency for a given C_T/J^2 or C_P/J^2 represents the J that gives the optimum diameter for a given rpm. Using this J, the optimum diameter D can be calculated using Equation [3].

It should be noted at this point that if the design being considered is based on shaft horsepower, the corresponding C_T must be calculated since the remaining design diagrams are presented as a function of $\sqrt{C_T}$ and J. This value of C_T can be calculated using Equation [4] once η and C_P are obtained from Appendix B for the propeller based on power.

The approximate maximum compressive stress of the propeller can be calculated using Equation [5] where the blade thickness fraction (BTF) is obtained from Appendix C, Figures 3a through 3i. The final pitch ratio for the propeller at the 0.7 radius for any cavitation number $(P/D)_{0.7}$ is calculated using Equation [7] where P/D_0 is obtained from Appendix A or B. C_σ is given in Appendix D, Figure 4, as a function of $\sigma_{0.7}$ which is calculated using Equation [6]; and $\Delta(P/D)$ is given in Appendix D, Figures 4a through 4i. The radial pitch distribution for this propeller is then obtained from Table 2.

The section shape for these propellers can be obtained from Appendix E which gives the maximum face ordinates $(y/l)_{max}$ and Appendix F which gives the maximum thickness ordinates $(t/l)_{max}$ at various radii. Once these ordinates are obtained, faired curves are then drawn to obtain values for $(y/l)_{max}$ and $(t/l)_{max}$ at other radii where from theory, $(y/l)_{max}$ is zero at the hub and tip. Table 1 gives the section chord lengths l chosen for these propellers. Thus, once y_{max} and t_{max} are obtained, the chordwise distribution of the ordinates y and t can be obtained using the distribution given in Table 3. The method of completing the design of a SC propeller, using this series, is identical to the method presented in the Appendix of Reference 3.

TABLE 2

Coefficients for Obtaining Radial Distribution of Pitch

X	$\dfrac{P/D}{(P/D)_{0.7}}$
0.2	0.974
0.3	0.979
0.4	0.984
0.5	0.990
0.6	0.995
0.7	1.0
0.8	1.006
0.9	1.011
0.95	1.011
1.0	1.010

TABLE 3

Coefficients for Obtaining Face and Thickness Distribution along Chord

x_1	$\dfrac{y}{y_{max}}$	$\dfrac{t}{t_{max}}$ When $0 < (\dfrac{t}{l})_{max} \leq 0.051$	$\dfrac{t}{t_{max}}$ When $0.051 < (\dfrac{t}{l})_{max} \leq 0.0753$	$\dfrac{t}{t_{max}}$ When $0.0753 < (\dfrac{t}{l})_{max}$
0	0	0	0	0
0.0075	0.0189	0.0476	0.0343	0.0297
0.0125	0.0324	0.0705	0.0501	0.0429
0.05	0.1419	0.2053	0.1326	0.1068
0.10	0.2915	0.3532	0.2124	0.1626
0.20	0.5669	0.5951	0.3421	0.2513
0.30	0.7846	0.7659	0.4453	0.3311
0.40	0.9319	0.8663	0.5285	0.4082
0.50	1.0000	0.9305	0.6075	0.4925
0.60	0.9834	0.9725	0.6879	0.5866
0.70	0.8780	1.0100	0.7787	0.6963
0.80	0.6806	1.0275	0.8645	0.8064
0.90	0.3886	1.0236	0.9401	0.9104
0.95	0.2065	1.0141	0.9719	0.9570
1.00	0	1.0	1.0	1.0

CONCLUSION

Theoretical results have been presented for 2-bladed SC propellers having expanded area ratios of 0.3, 0.4, and 0.5; for 3-bladed SC propellers having expanded area ratios of 0.4, 0.5, and 0.6, and for 4-bladed SC propellers having expanded area ratios of 0.5, 0.6, and 0.7. This theoretical series should be of great value, if only in a qualitative way, in predicting the performance of SC propellers due to variations in number of blades and expanded area ratio.

Caution must be exercised in using these results in any but a qualitative way. This is especially true for designs which deviate too much from the optimum efficiency curves. Experimental results indicate that, as would be expected, there is more of a variation from the theoretical results than for subcavitating propellers. The theory used is the best available for such propellers, but questions arise as to the validity of the lifting surface corrections used as well as the lift and drag characteristics available for SC sections. These questionable areas should not detract from the usefulness of the series presented since the relative characteristics of different propellers would be expected to change little.

ACKNOWLEDGMENT

REFERENCES

1. Tachmindji, A. J. and Morgan, W. B., "The Design and Estimated Performance of a Series of Supercavitating Propellers," Presented at the Second Symposium on Naval Hydrodynamics (Aug 1958).

2. Venning, E. Jr. and Haberman, W. L., "Supercavitating Propeller Performance," Presented at the 1962 Annual Meeting of the Society of Naval Architects and Marine Engineers.

3. Hecker, R., "Experimental Performance of TMB SC Propellers," David Taylor Model Basin Report 1432 (in preparation).

4. Caster, E. B., "TMB 3-Bladed Supercavitating Propeller Series," David Taylor Model Basin Report 1245 (Aug 1959).

5. Morgan, W. B., "Optimum Supercavitating Sections," David Taylor Model Basin Report C-856 (Aug 1957).

6. Lerbs, H. W., "Moderately Loaded Propellers with a Finite Number of Blades and an Arbitrary Distribution of Circulation," Transactions, Society of Naval Architects and Marine Engineers (1952).

7. Hecker, R., "Manual for Preparing and Interpreting Data of Propeller Problems Which Are Programmed for High-Speed Computers at the David Taylor Model Basin," David Taylor Model Basin Report 1244 (Aug 1959).

8. Morgan, W. B., "Centroid and Moment of Inertia of a Supercavitating Section," David Taylor Model Basin Report 1193 (Aug 1957).

APPENDIX A

C_T-J DIAGRAMS FOR TMB SC PROPELLER SERIES
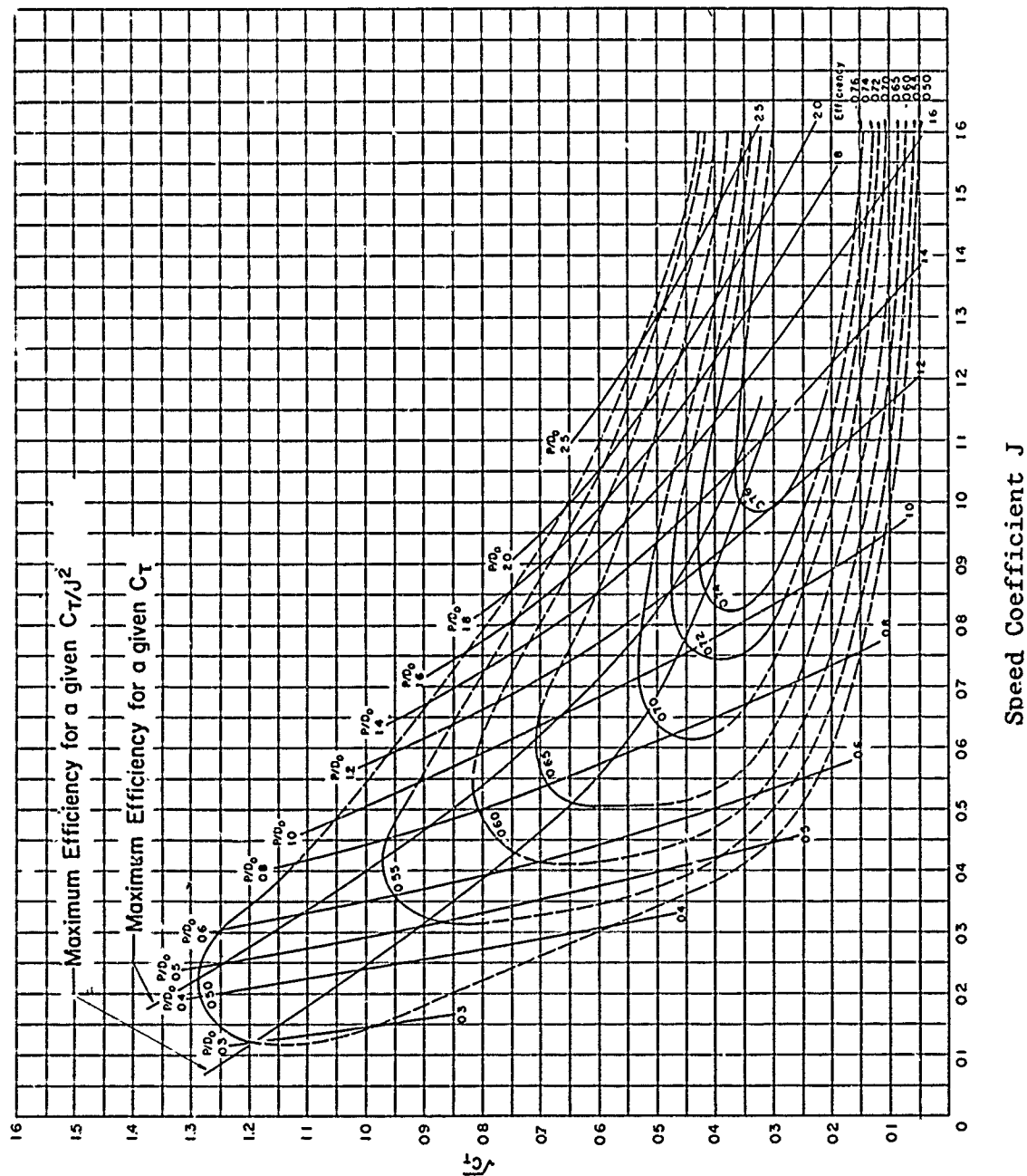
Figure 1a — C_T-J Diagram for TMB 2-Bladed SC Propeller Series, EAR = 0.3

14
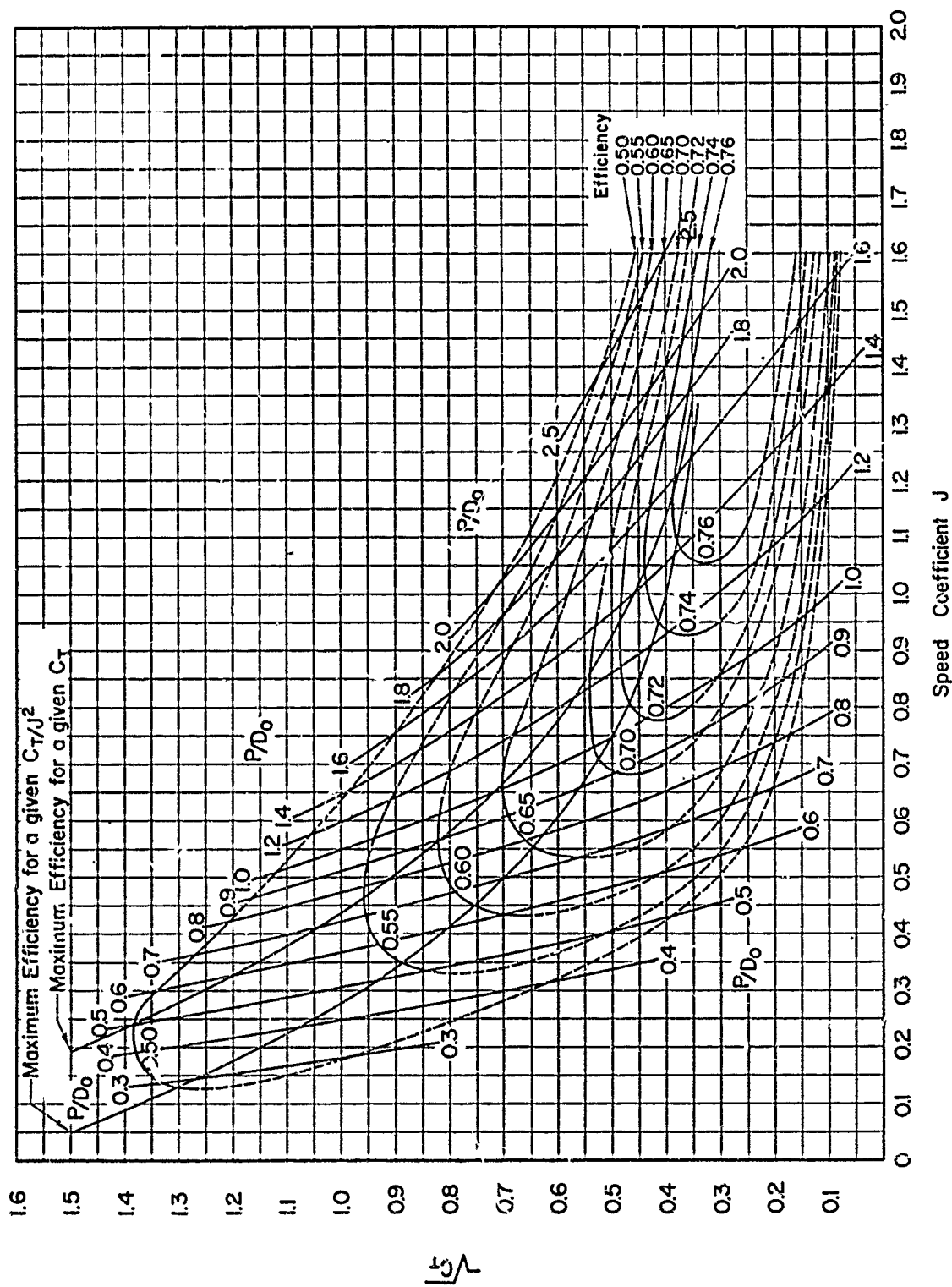
Figure 1b – C_T-J Diagram for TMB 2-Bladed SC Propeller Series, EAR = 0.4

15
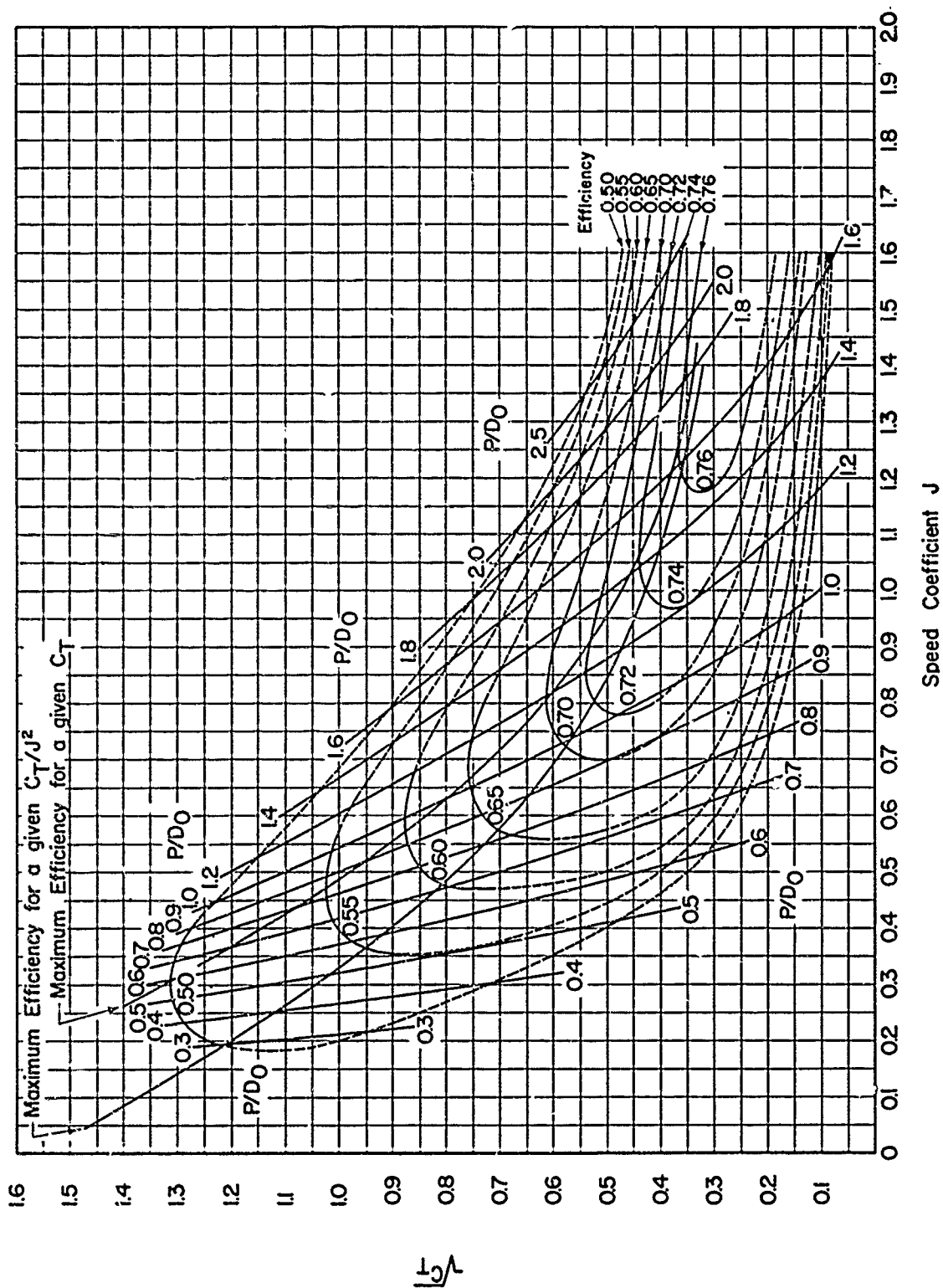
Figure 1c – C_T-J Diagram for TMB 2-Bladed SC Propeller Series, EAR = 0.5

16
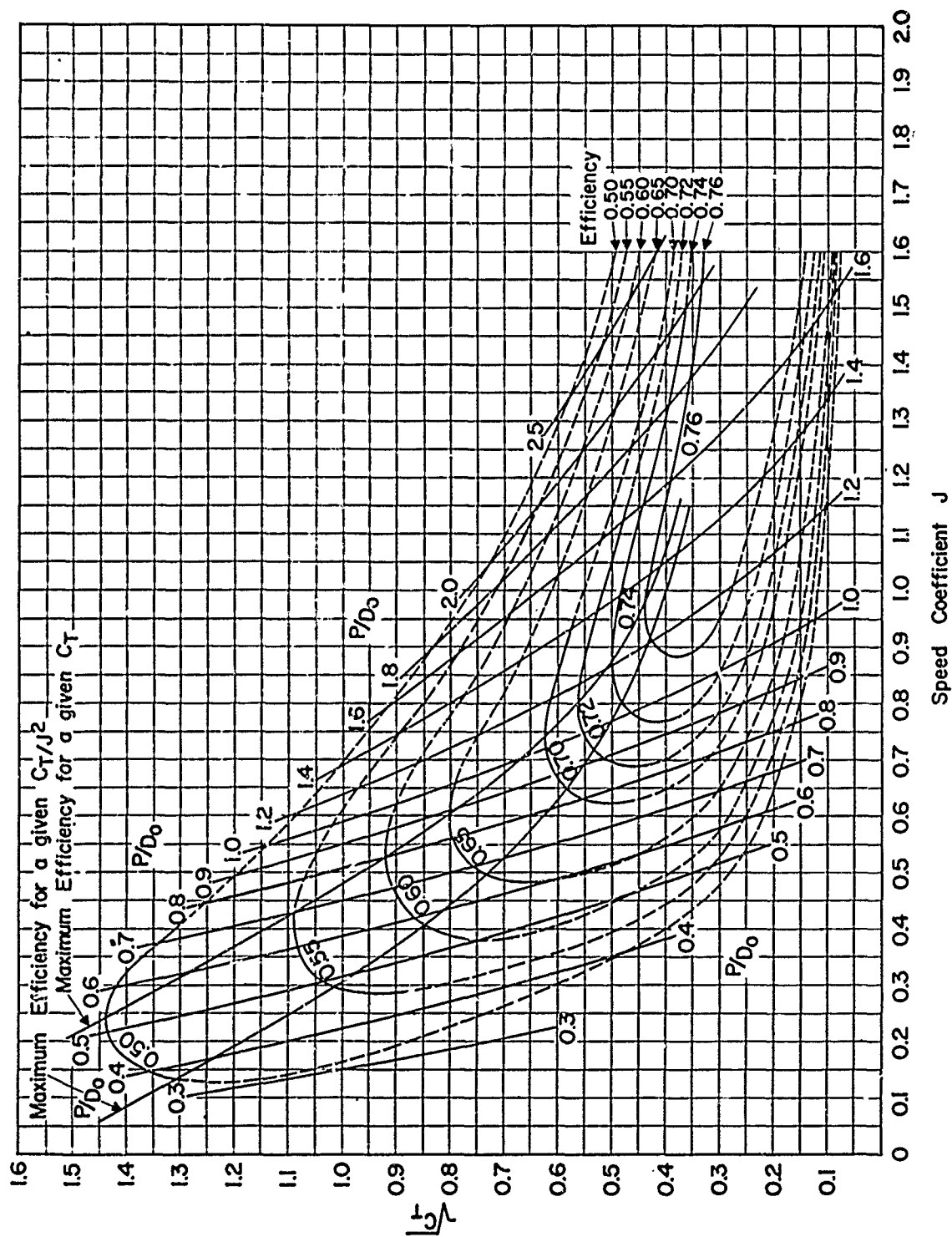
Figure 1d — C_T-J Diagram for TMB 3-Bladed SC Propeller Series, EAR = 0.4

17
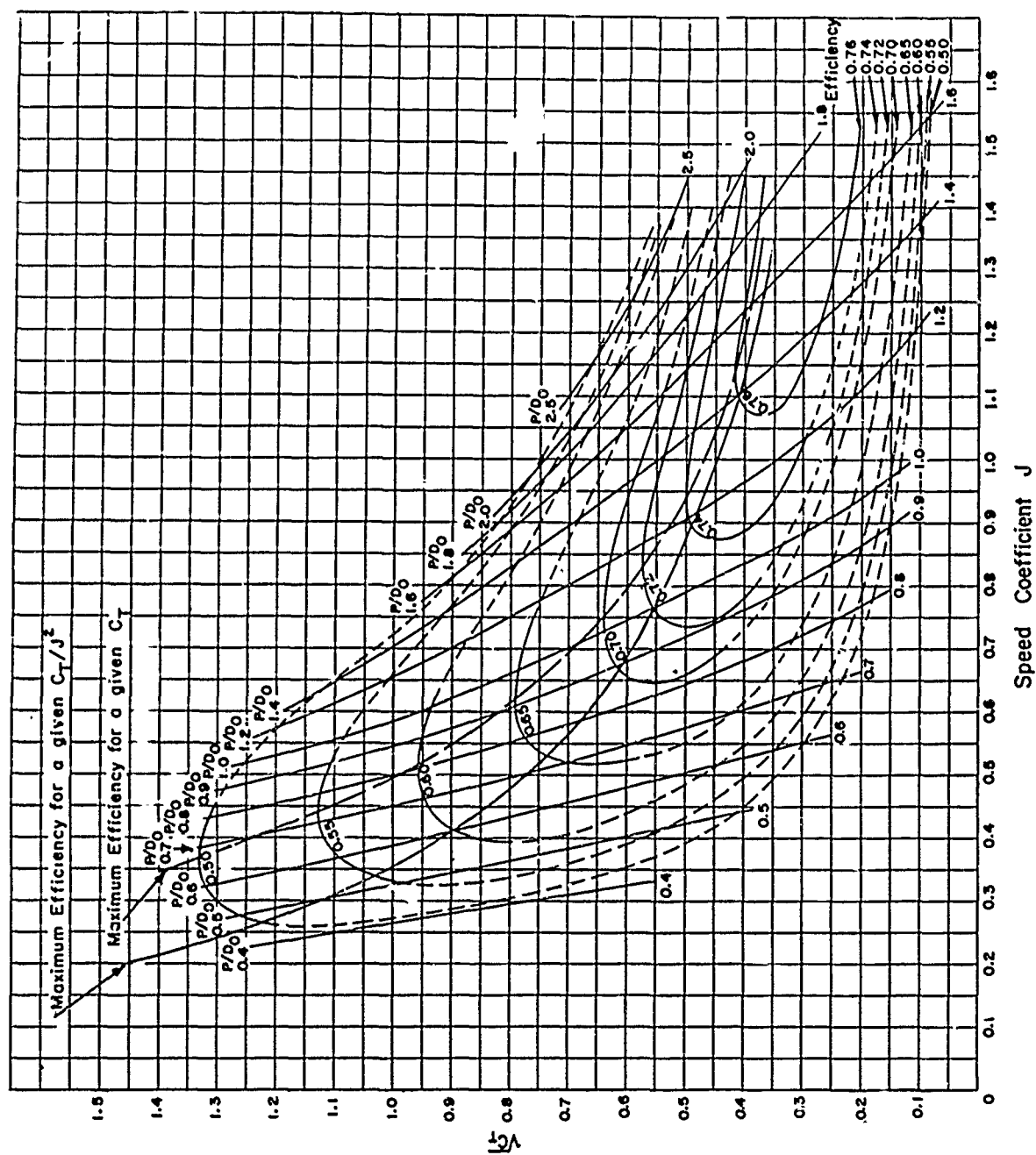
Figure 1e — C_T-J Diagram for TMB 3-Bladed SC Propeller Series, EAR = 0.5

18
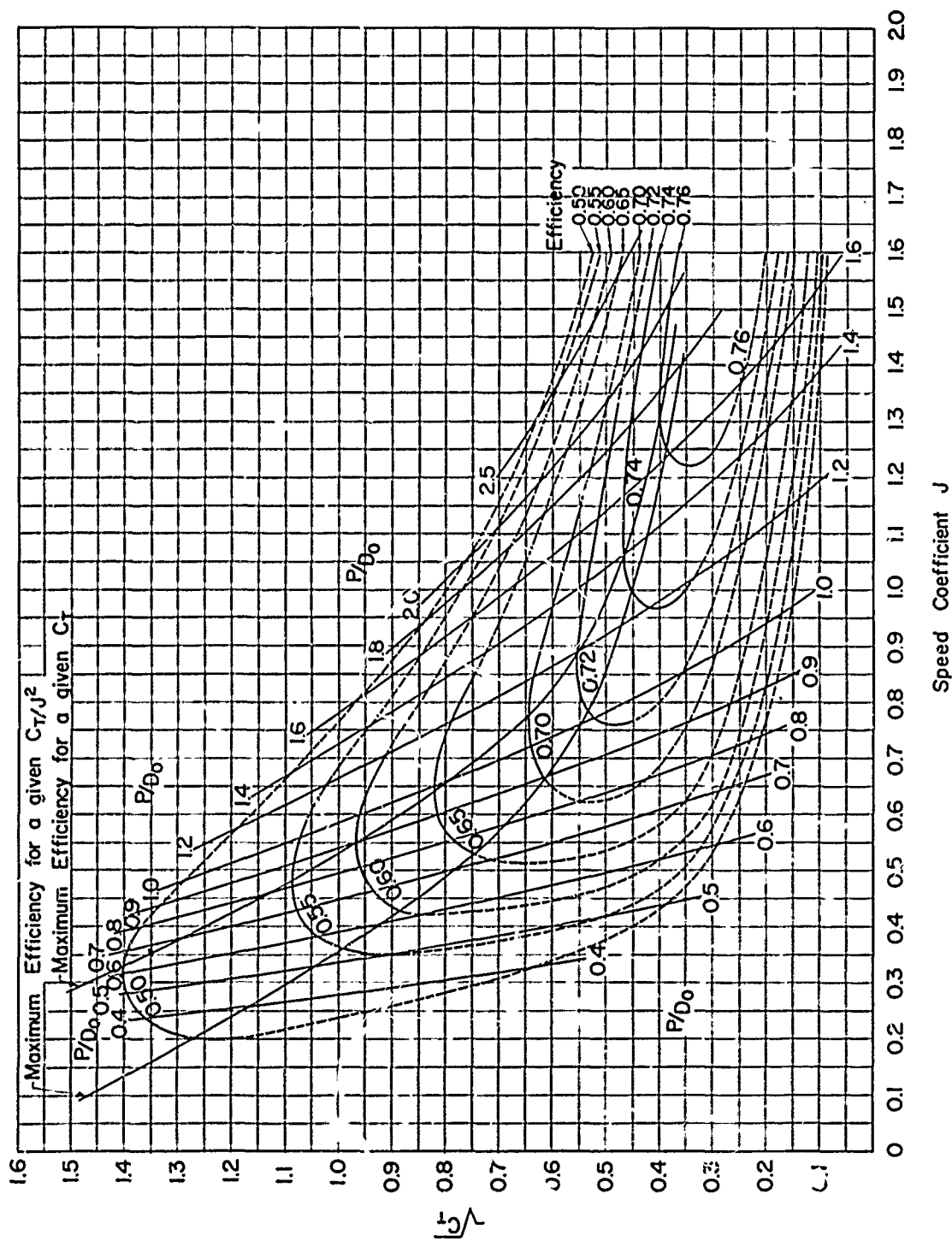
Figure 1f — C_T-J Diagram for TMB 3-Bladed SC Propeller Series, EAR = 0.6

19
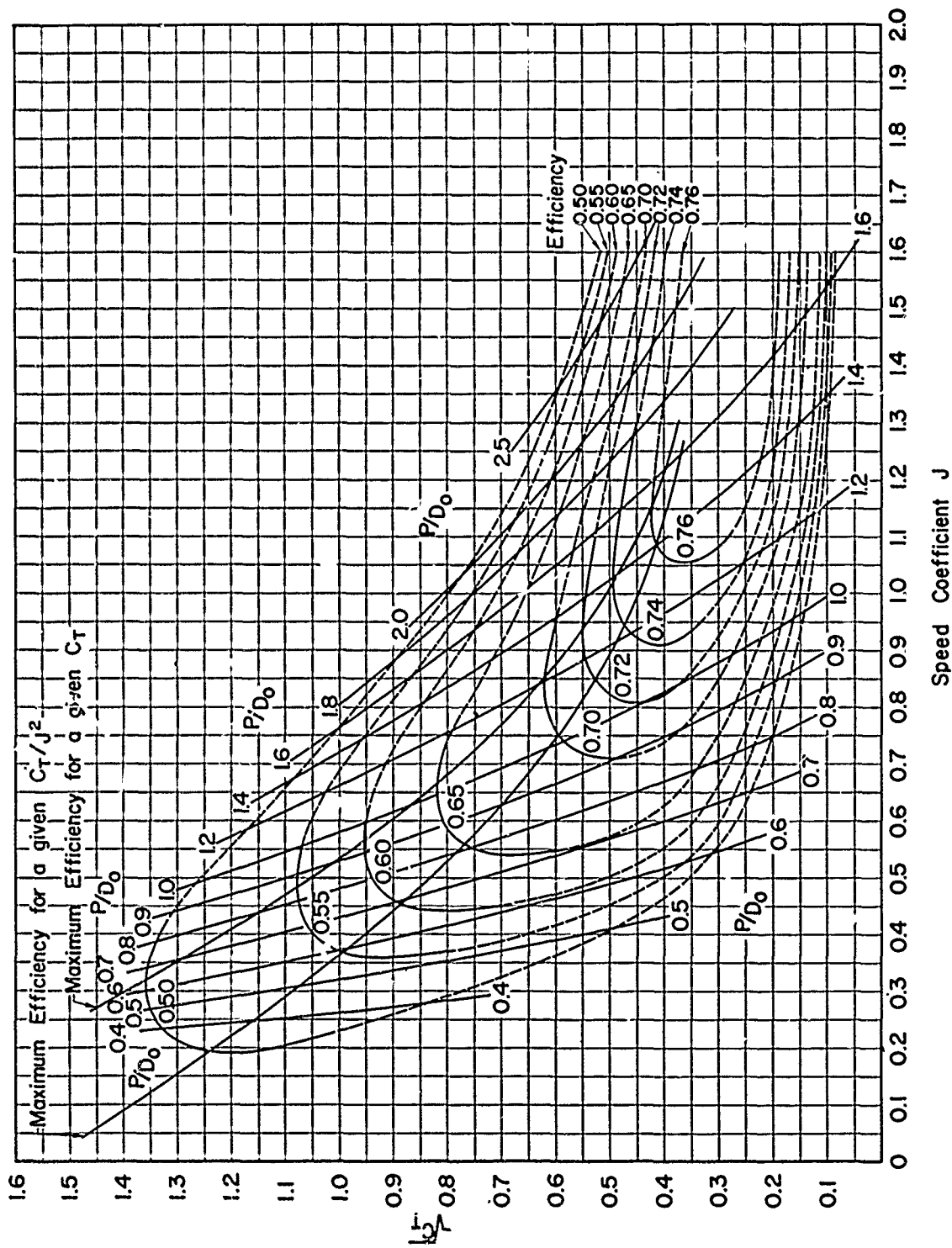
Figure 1g — C_T-J Diagram for TMB 4-Bladed SC Propeller Series, EAR = 0.5

20
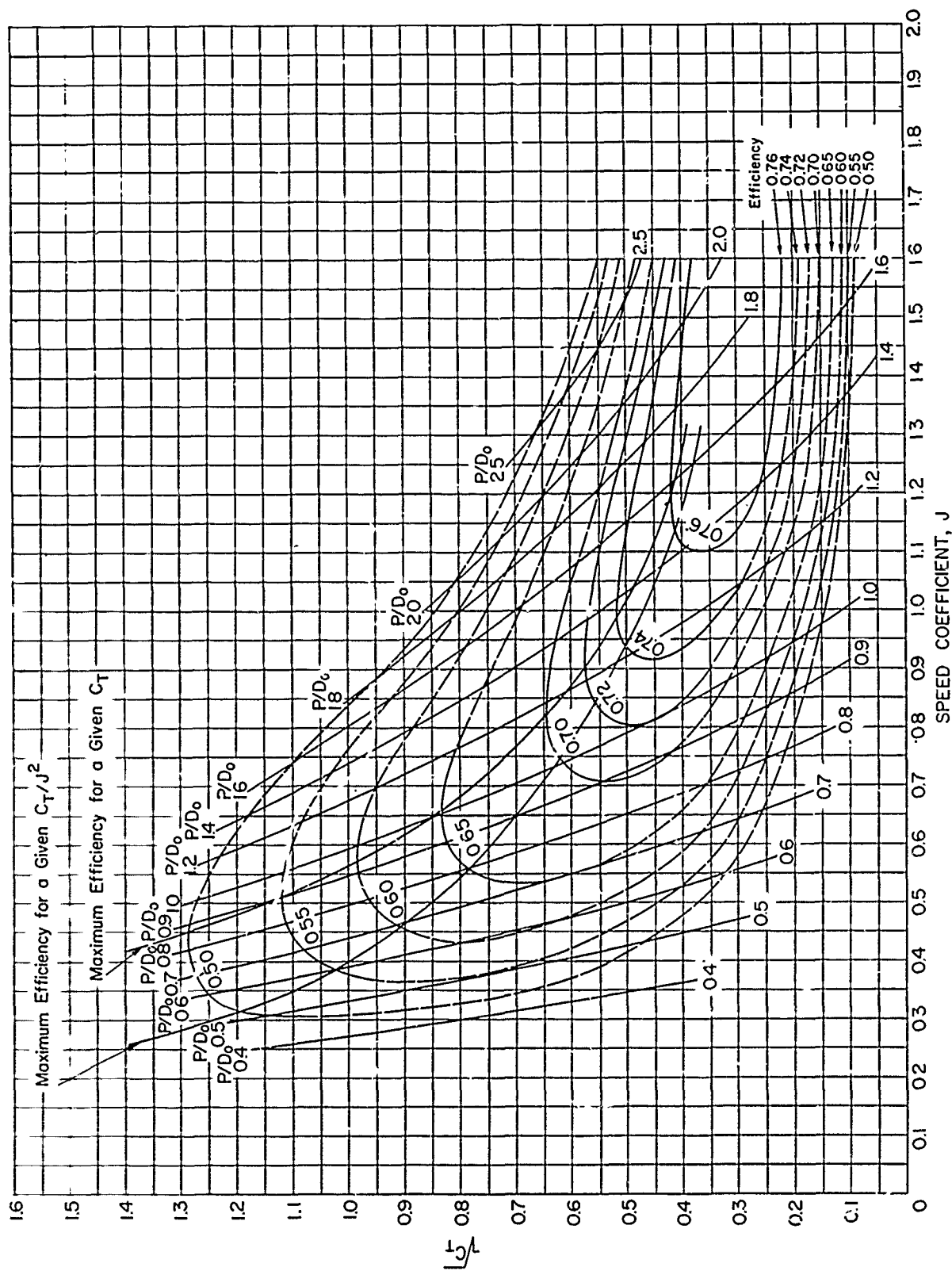
Figure 1h – C_T-J Diagram for TMB 4-Bladed SC Propeller Series, EAR = 0.6

21
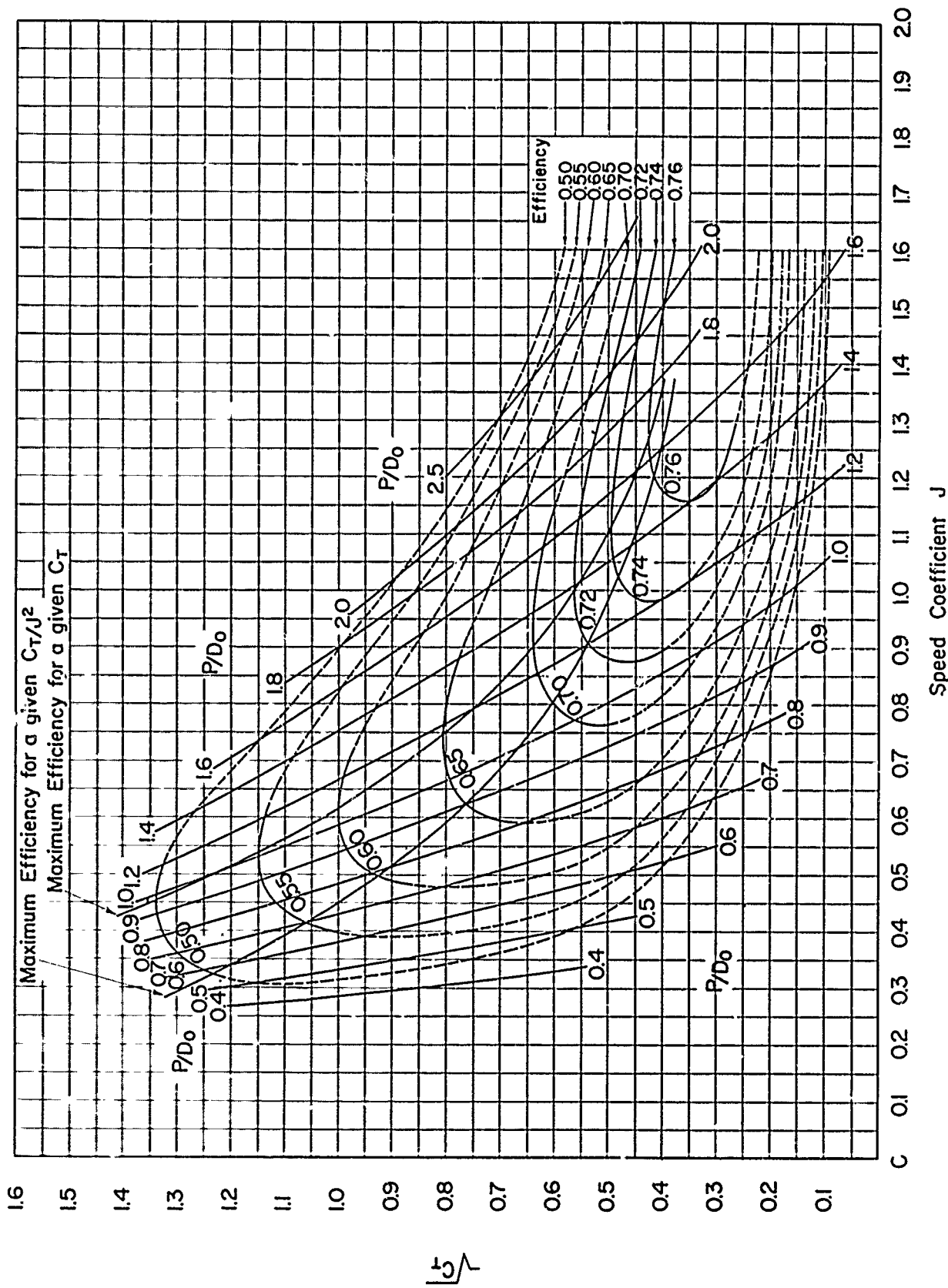
Figure 1i — C_T-J Diagram for TMB 4-Bladed SC Propeller Series, EAR = 0.7

22

APPENDIX B

C_P-J DIAGRAMS FOR TMB SC PROPELLER SERIES
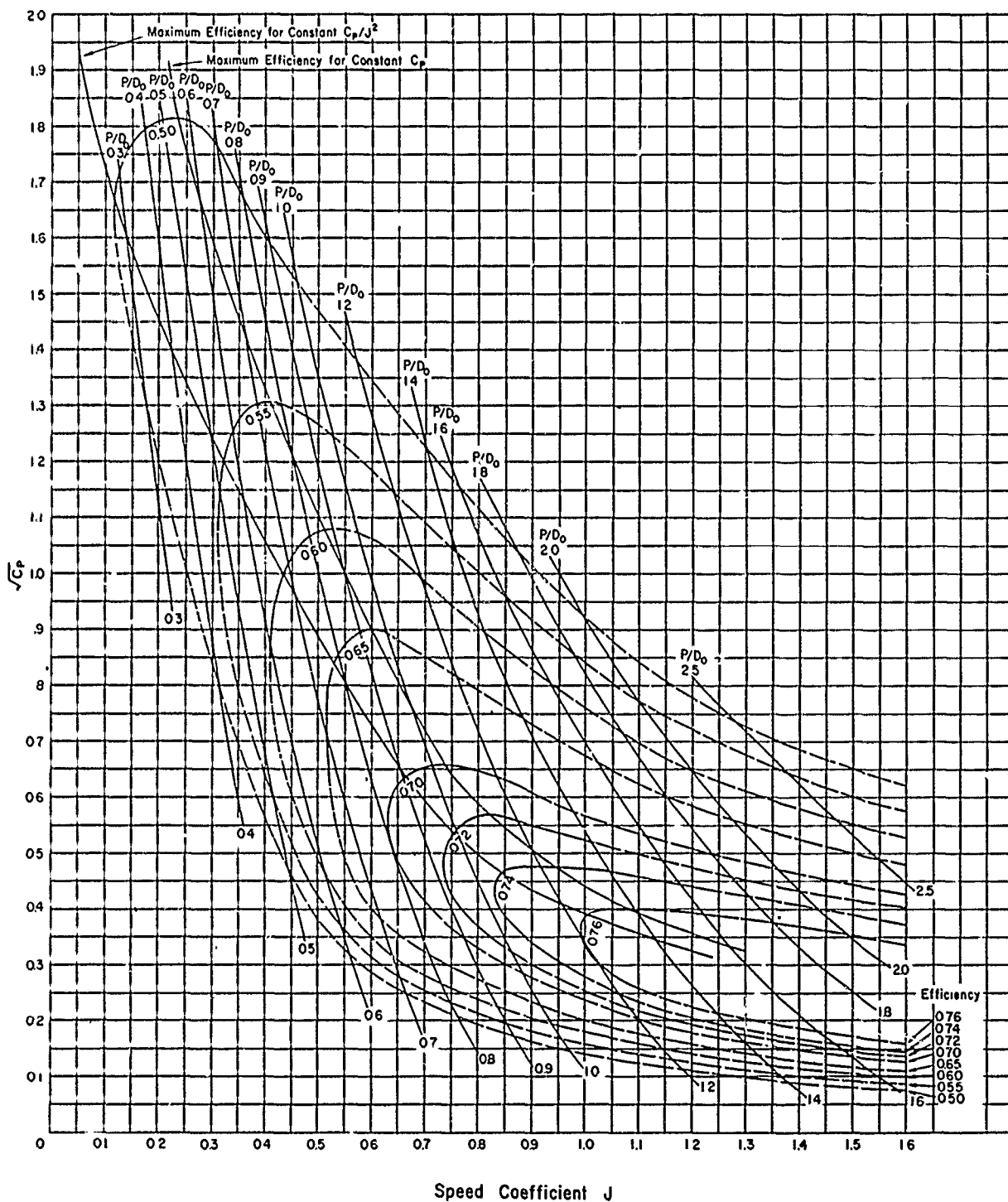
Figure 2a — C_P-J Diagram for TMB 2-Bladed SC Propeller Series, EAR = 0.3

24
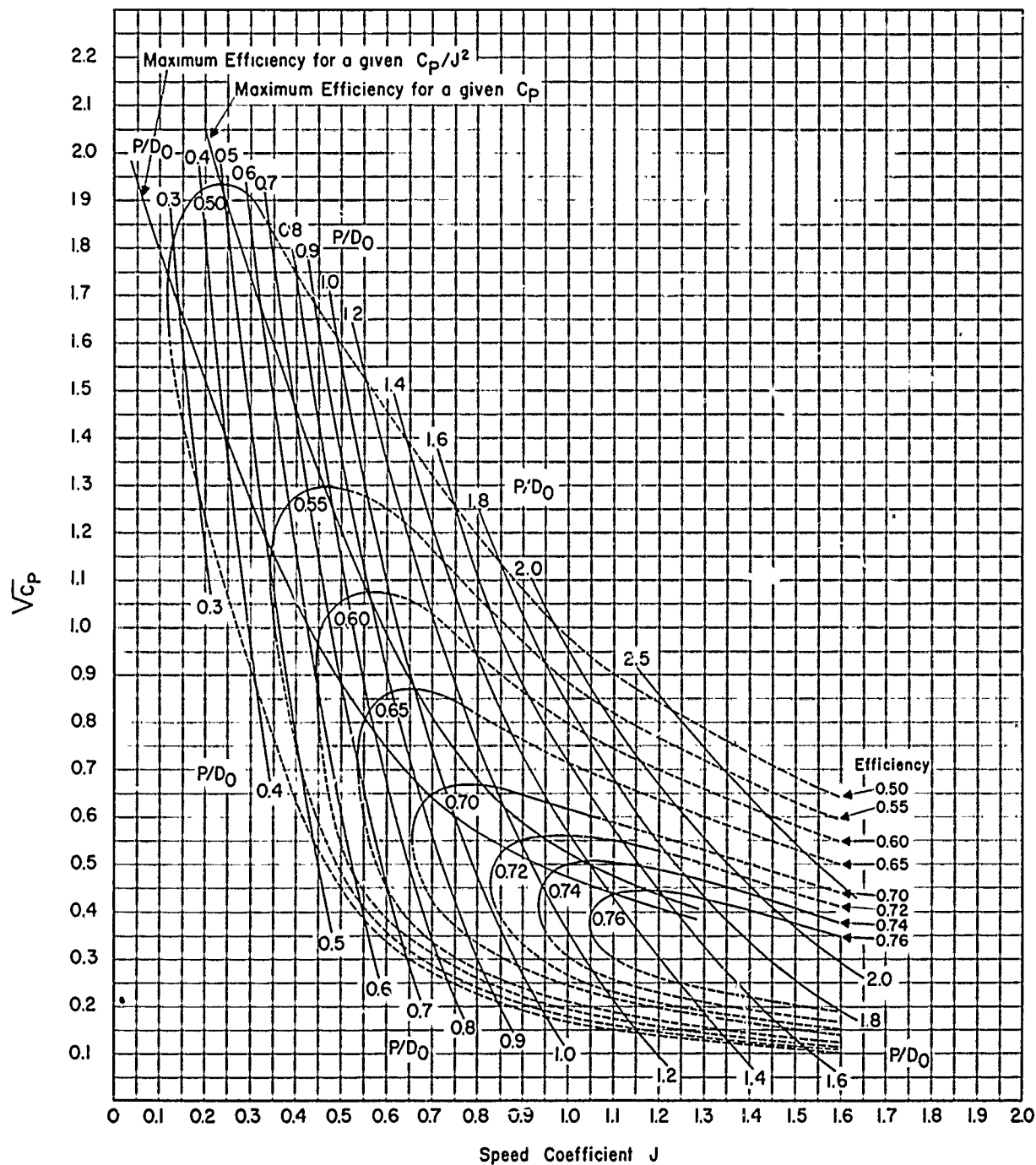
Figure 2b — C_P-J Diagram for TMB 2-Bladed SC Propeller Series, EAR = 0.4

25
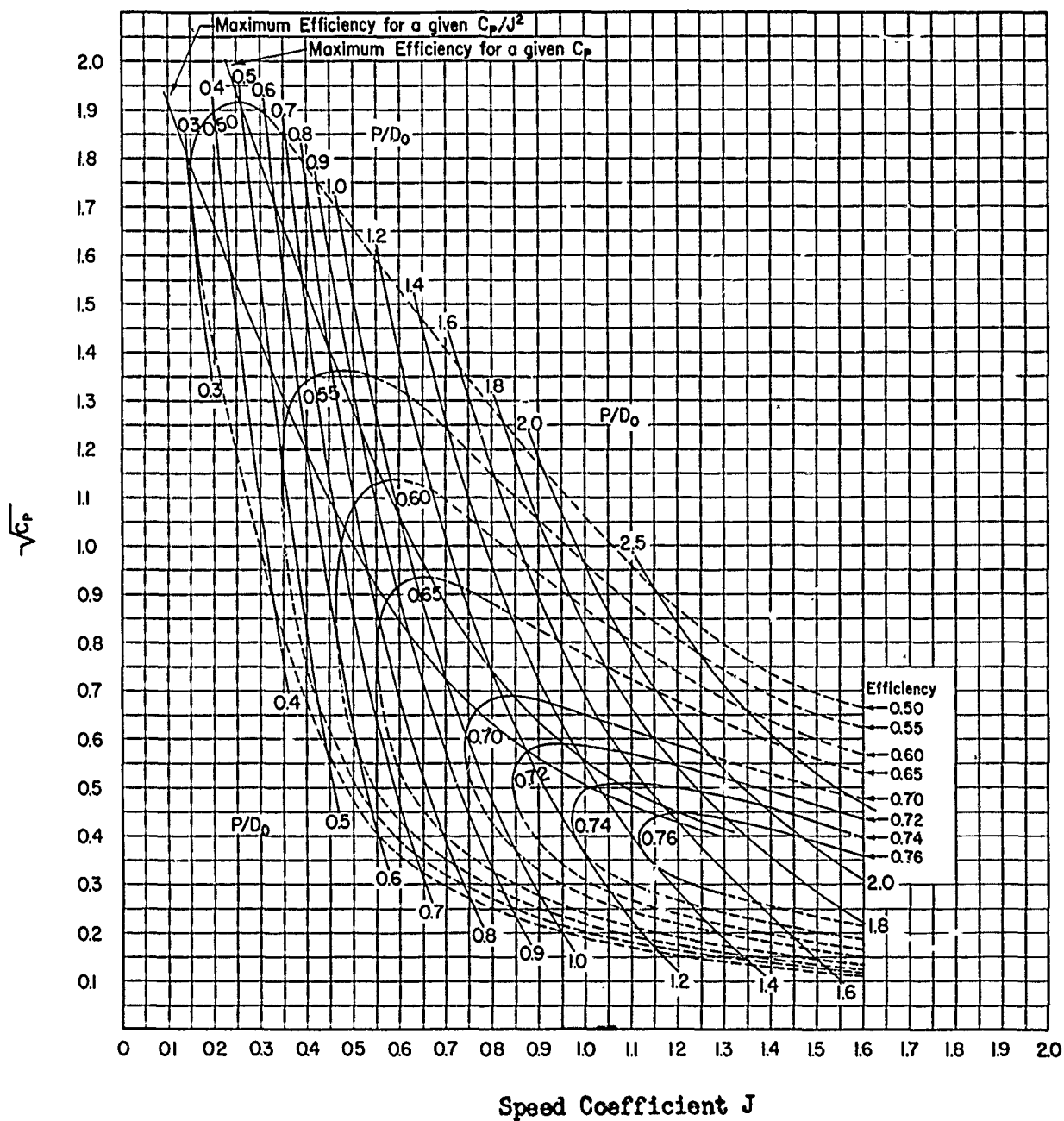
Figure 2c — C_P-J Diagram for TMB 2-Bladed SC Propeller Series, EAR = 0.5

26
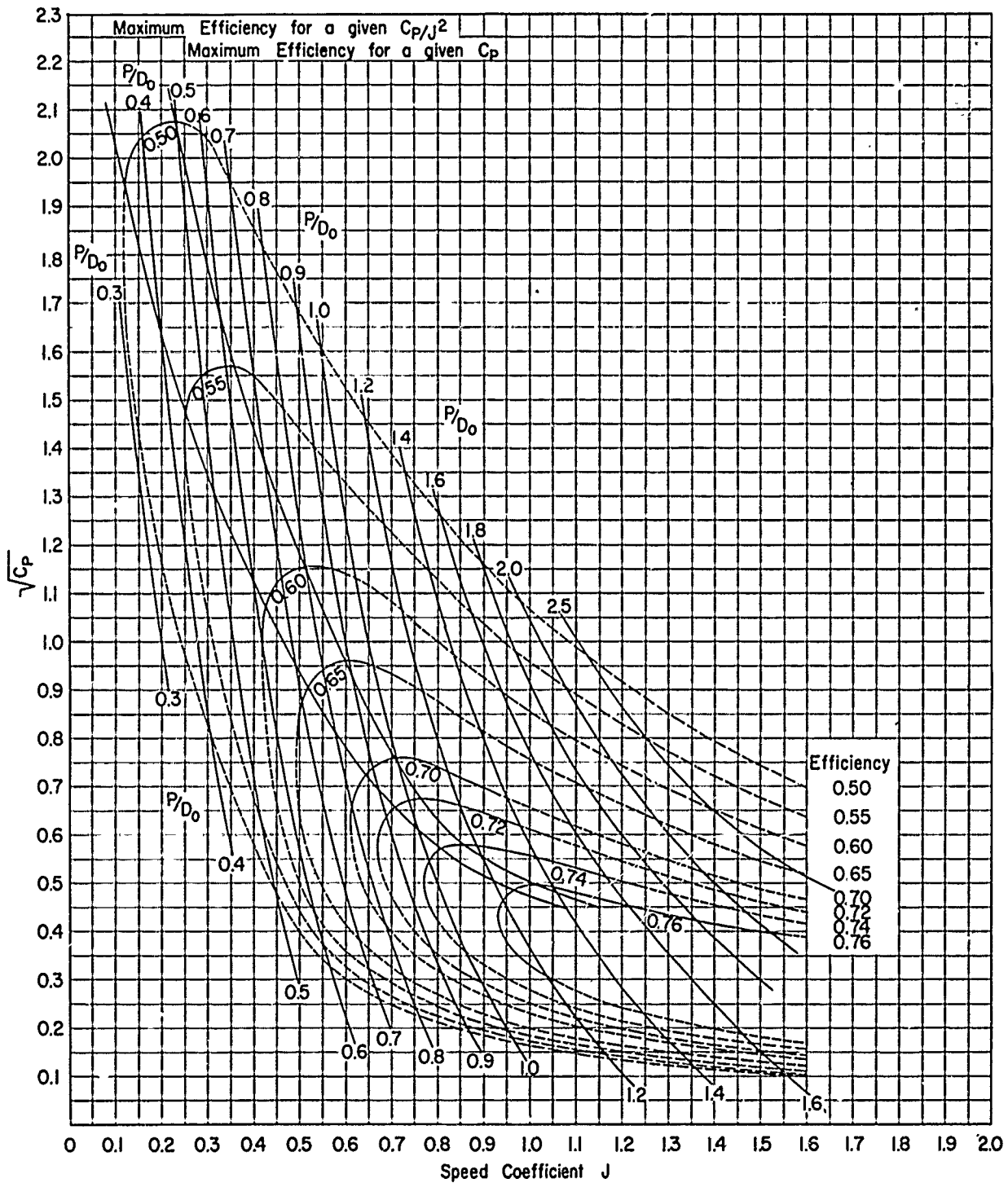
Figure 2d — C_P-J Diagram for TMB 3-Bladed SC Propeller Series, EAR = 0.4

27
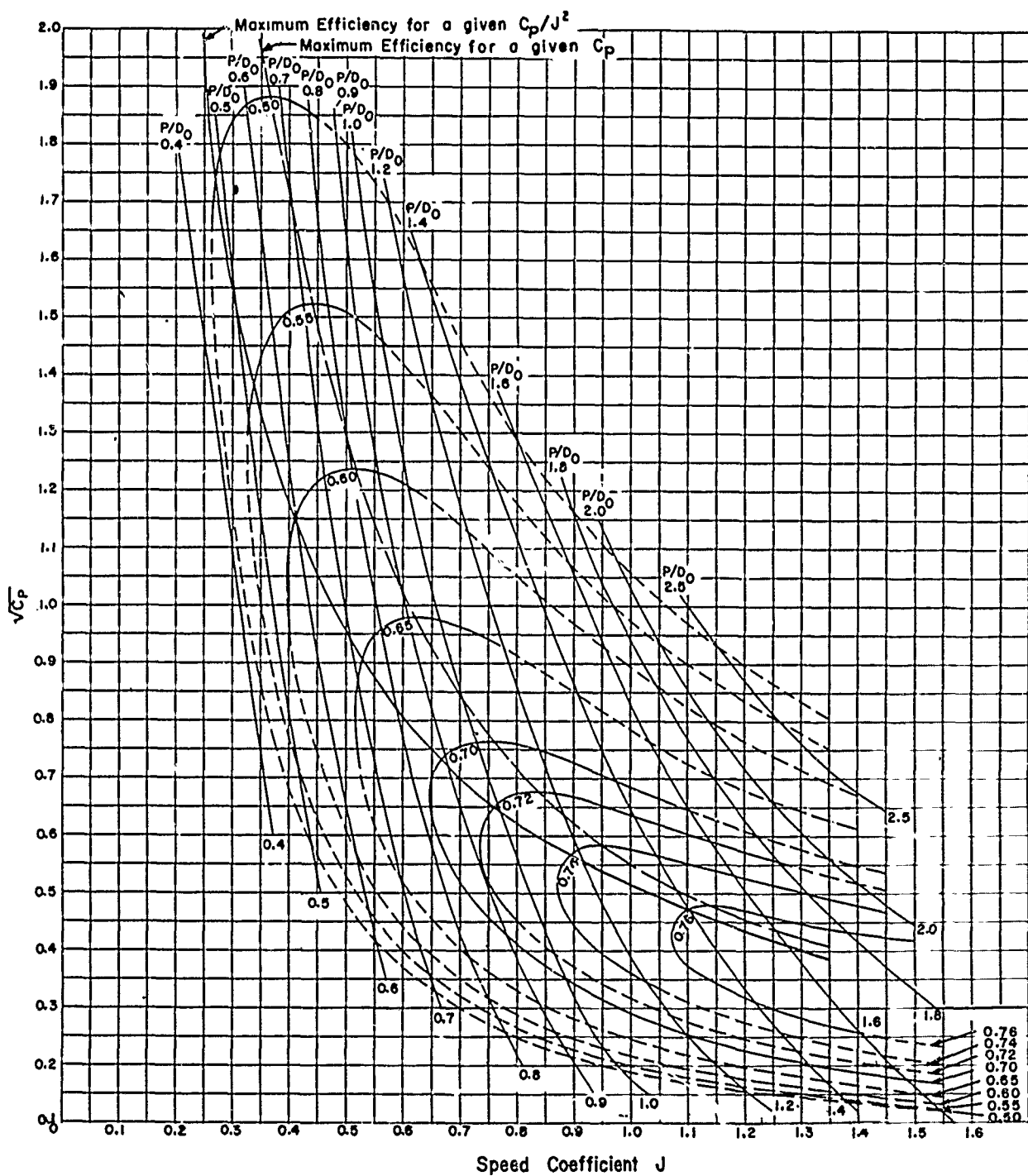
Figure 2e — C_P-J Diagram for TMB 3-Bladed SC Propeller Series, EAR = 0.5

28
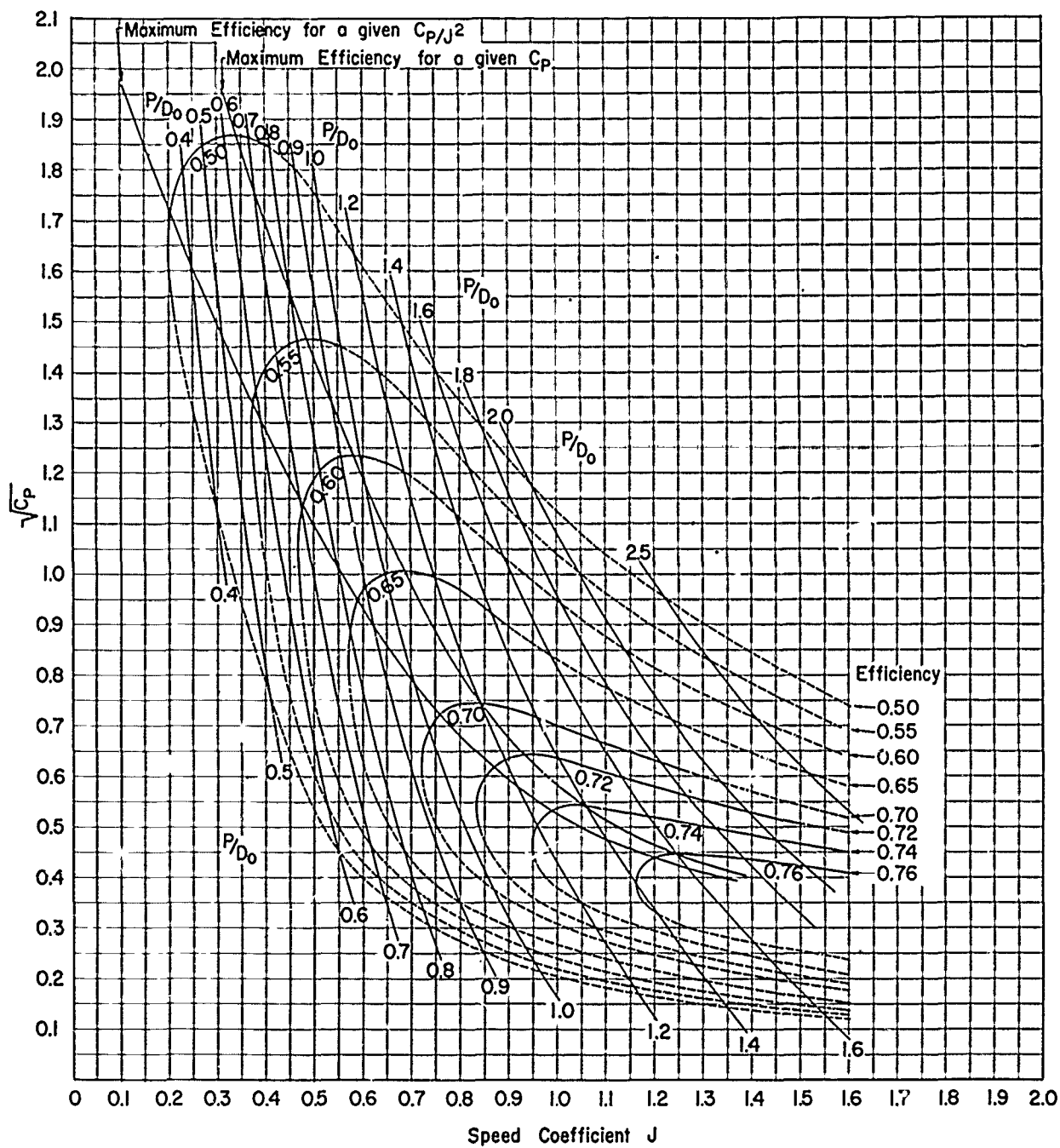
Figure 2f — C_P-J Diagram for TMB 3-Bladed SC Propeller Series, EAR = 0.6

29
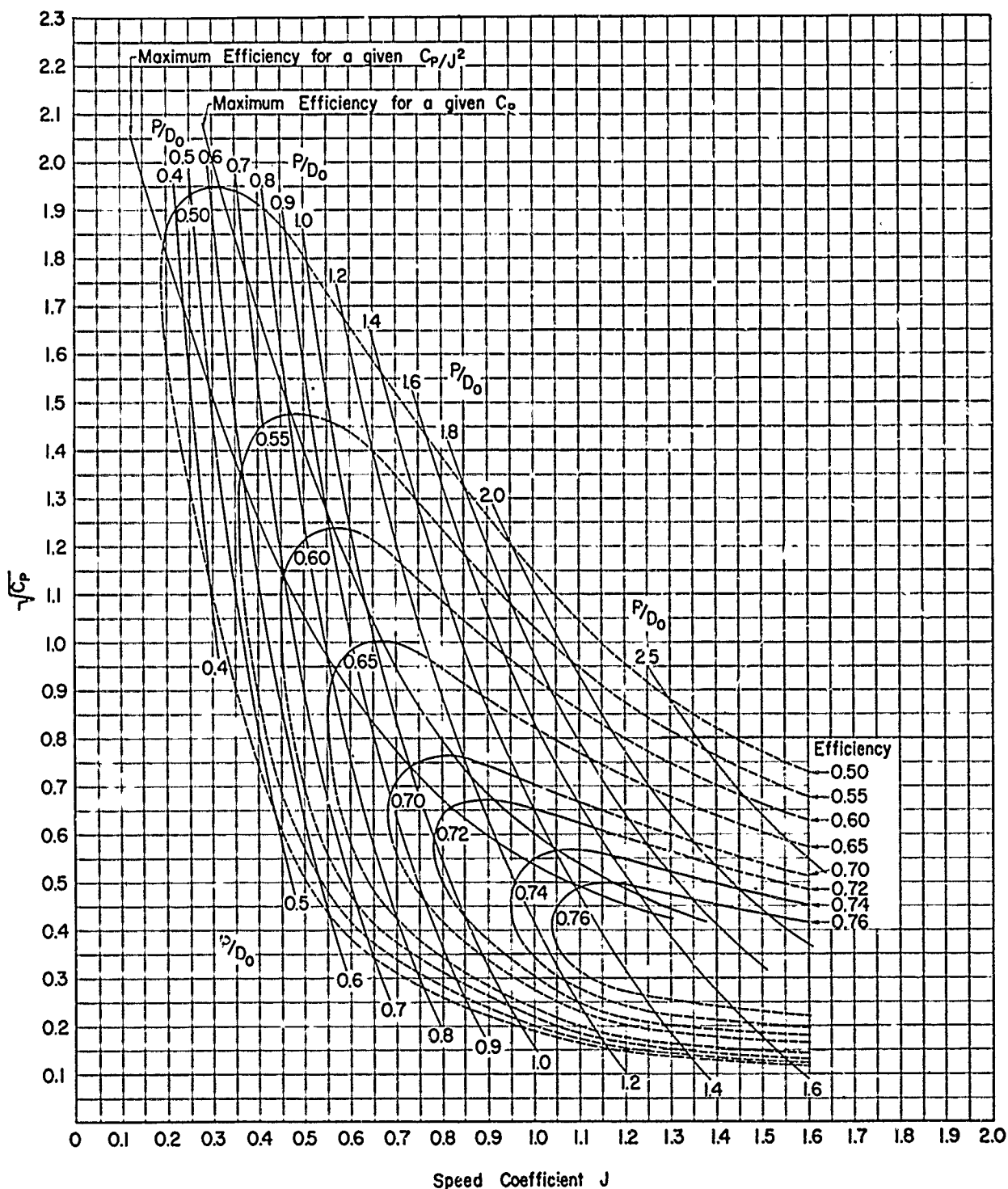
Figure 2g – C_P-J Diagram for TMB 4-Bladed SC Propeller Series, EAR = 0.5

30
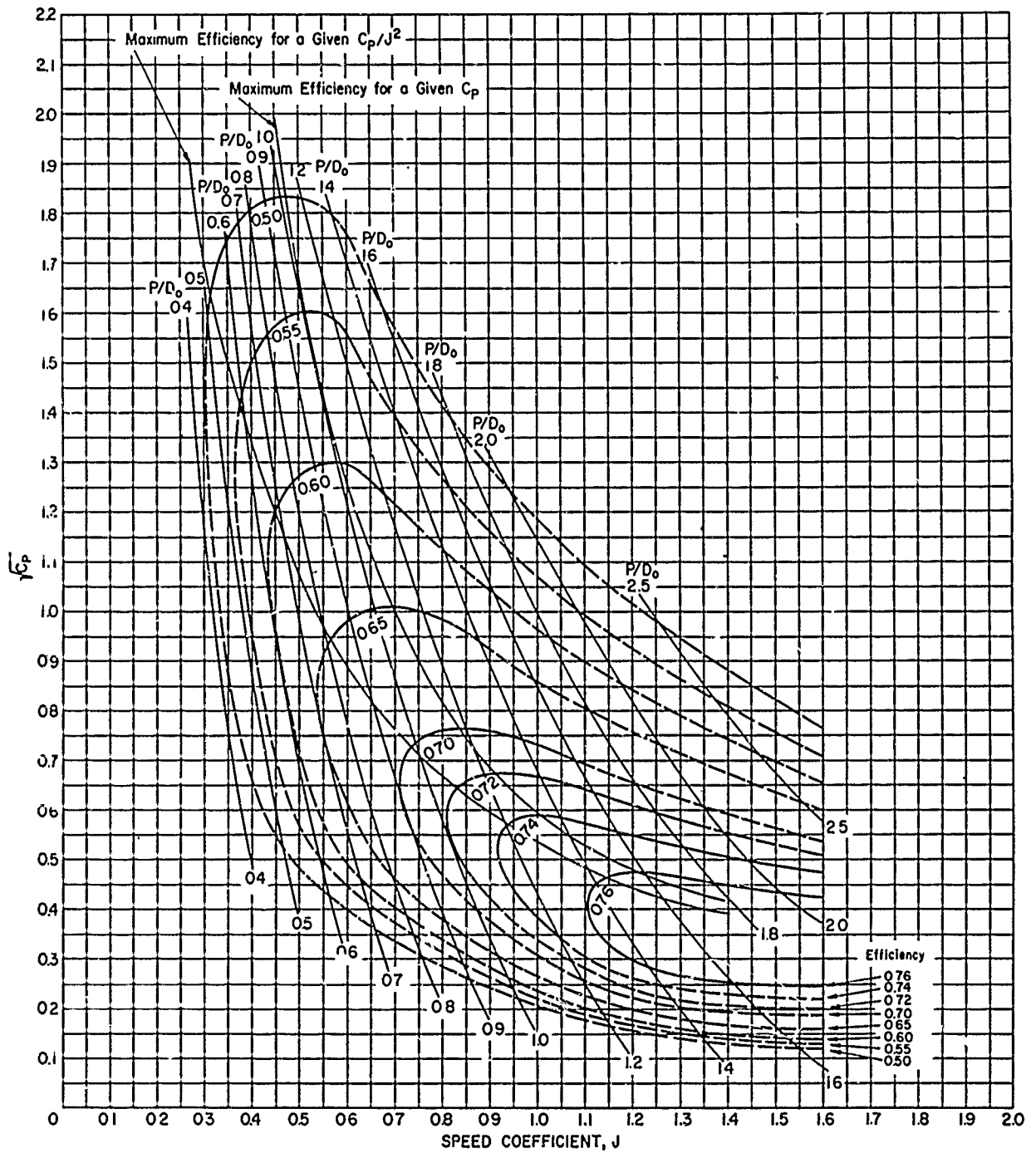
Figure 2h – C_P-J Diagram for TME 4-Bladed SC Propeller Series, EAR = 0.6

31
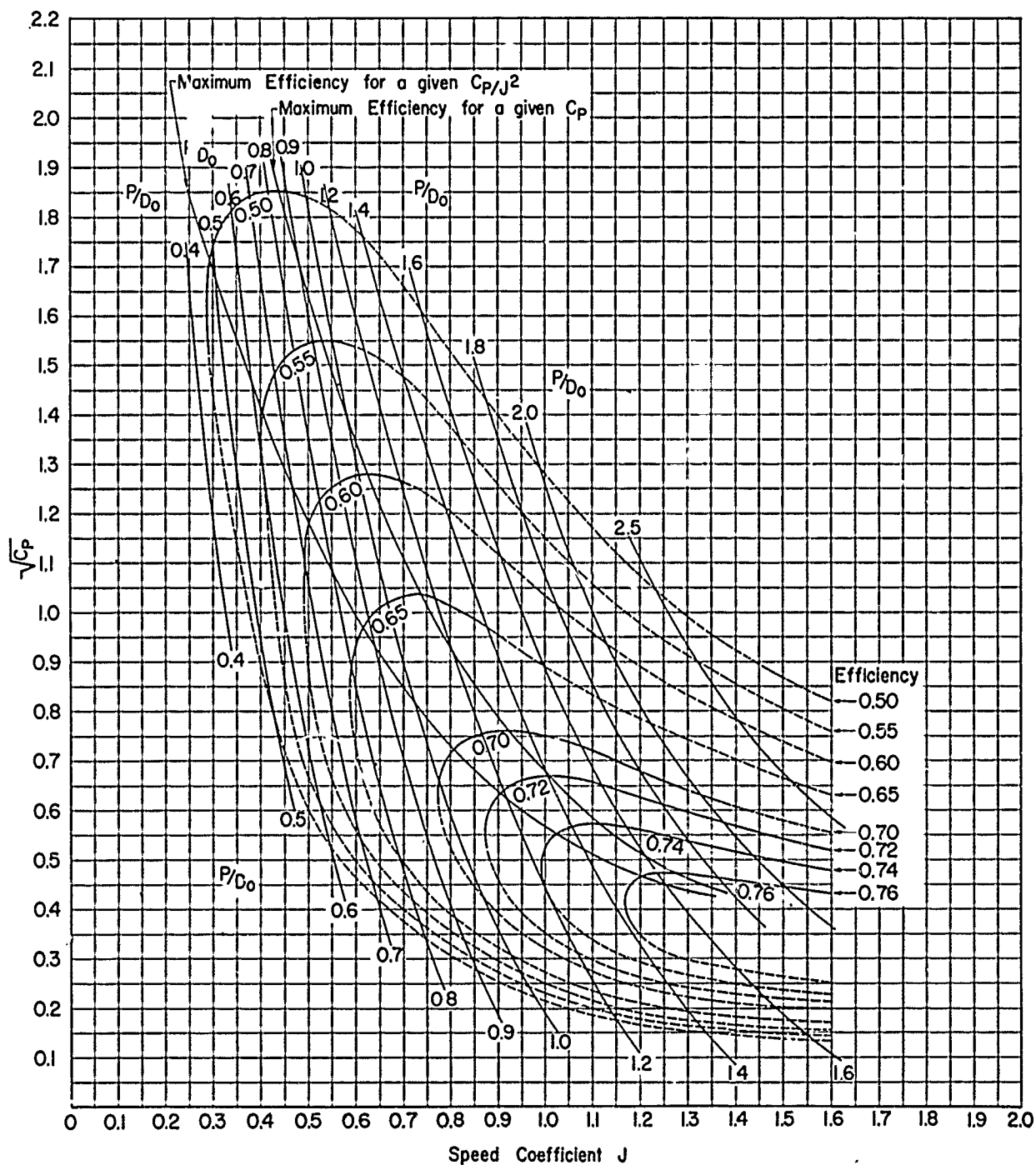
Figure 2i — C_P-J Diagram for TMB 4-Bladed SC Propeller Series, EAR = 0.7

APPENDIX C

BLADE THICKNESS FRACTIONS FOR TMB SC PROPELLER SERIES
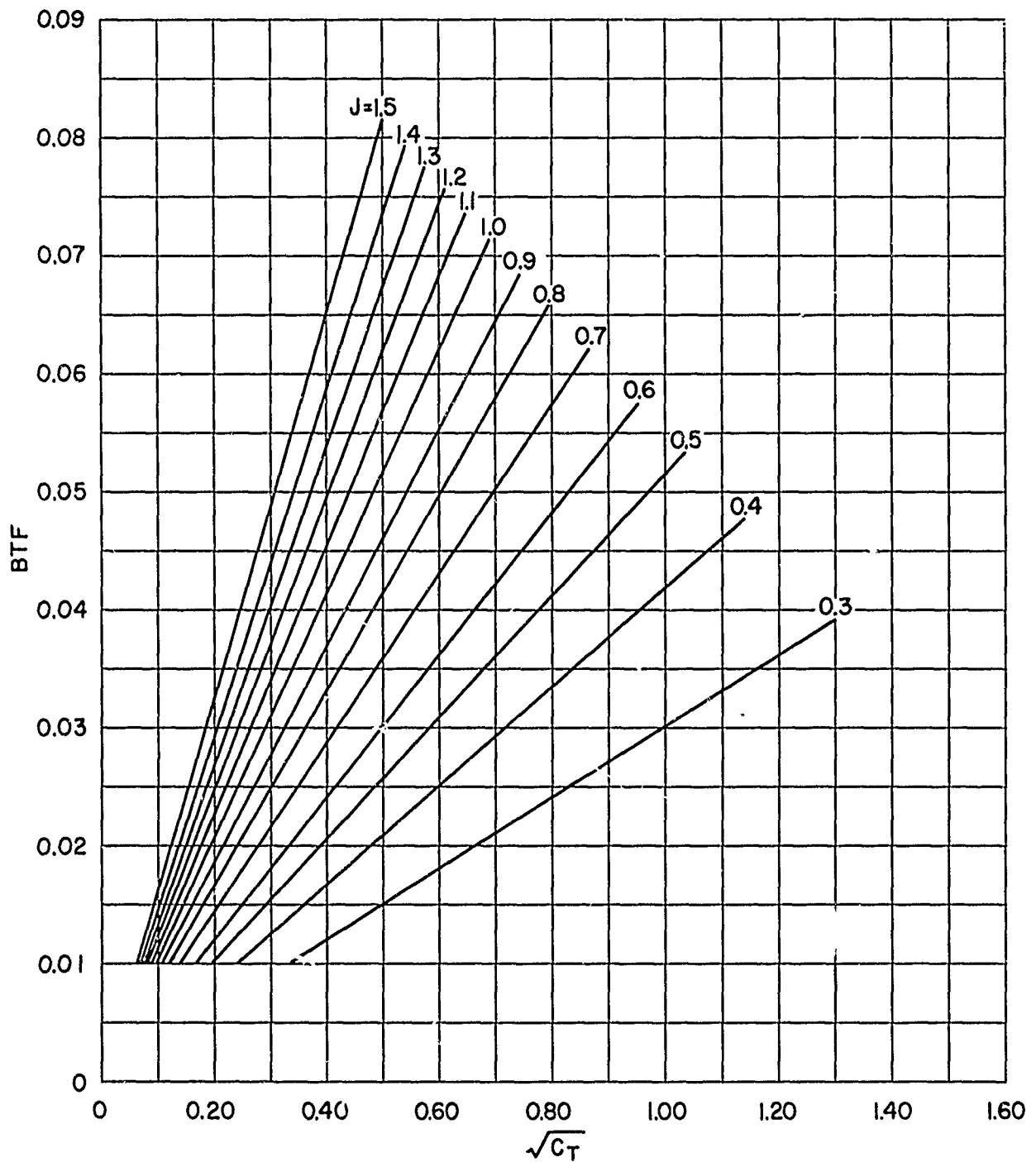
Figure 3a — Blade Thickness Fraction for TMB 2-Bladed SC Propeller Series, EAR = 0.3
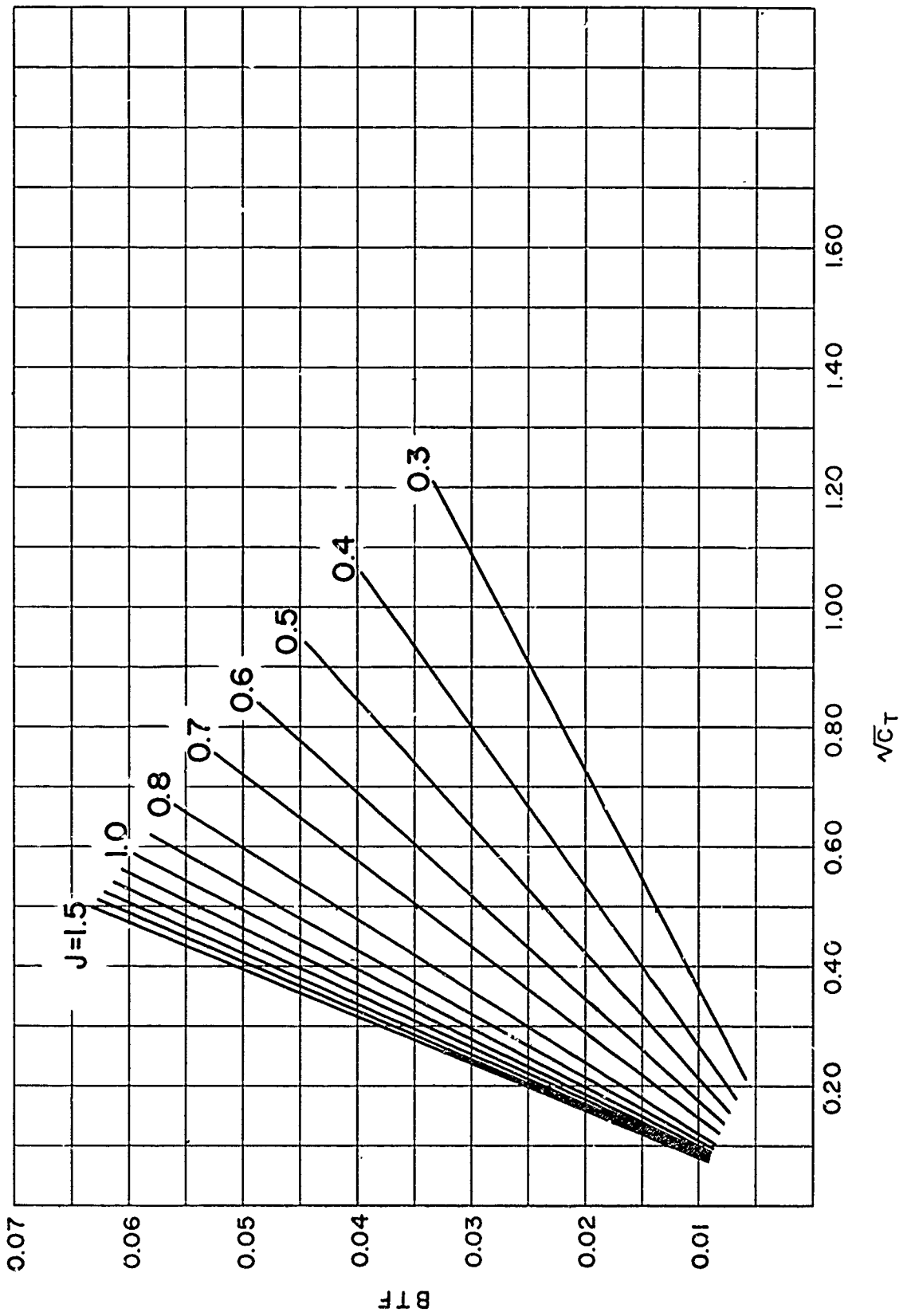
Figure 3b – Blade Thickness Fraction for TMB 2-Bladed SC Propeller Series, EAR = 0.4

35
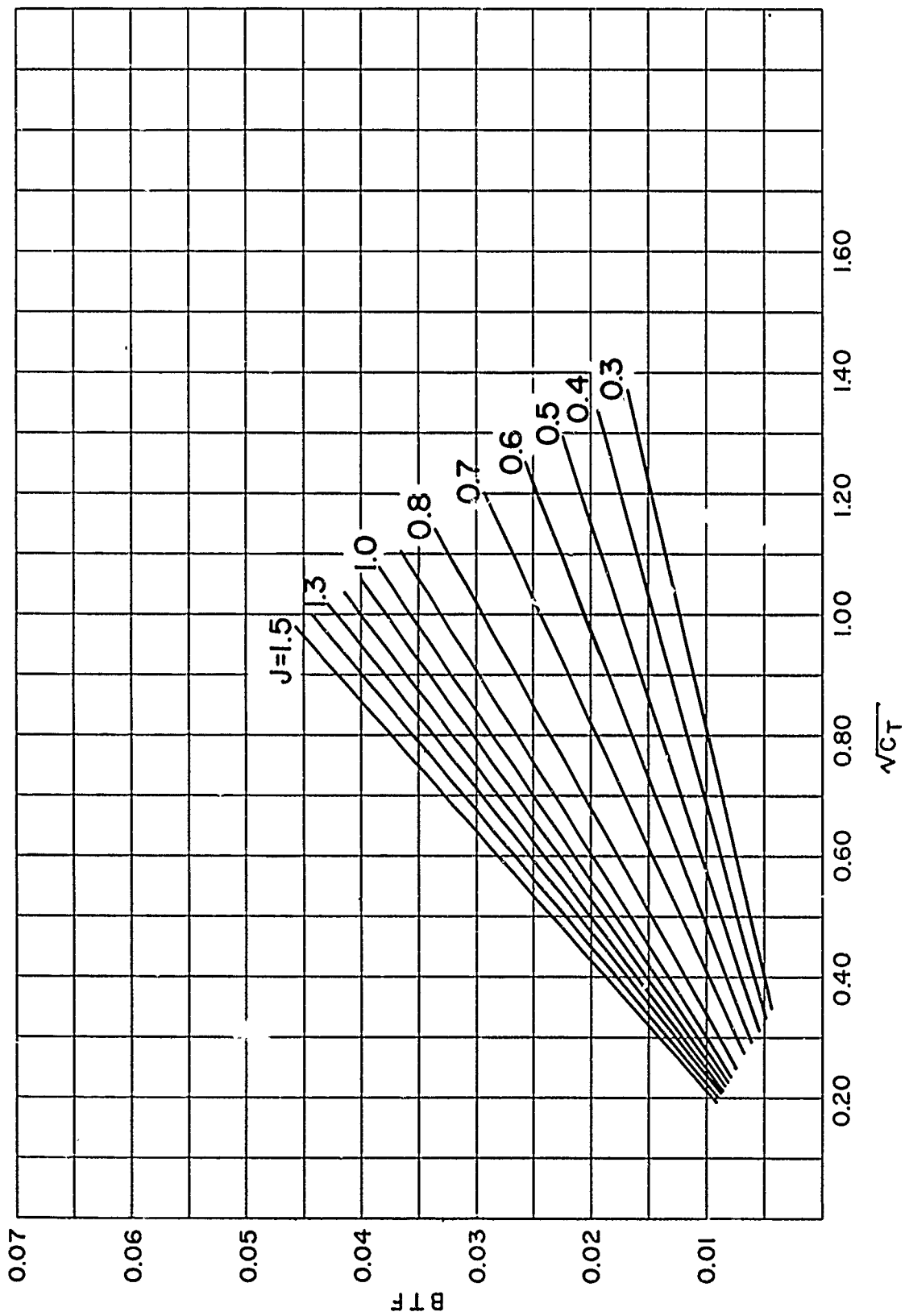
Figure 3c — Blade Thickness Fraction for TMB 2-Bladed SC Propeller Series, EAR = 0.5
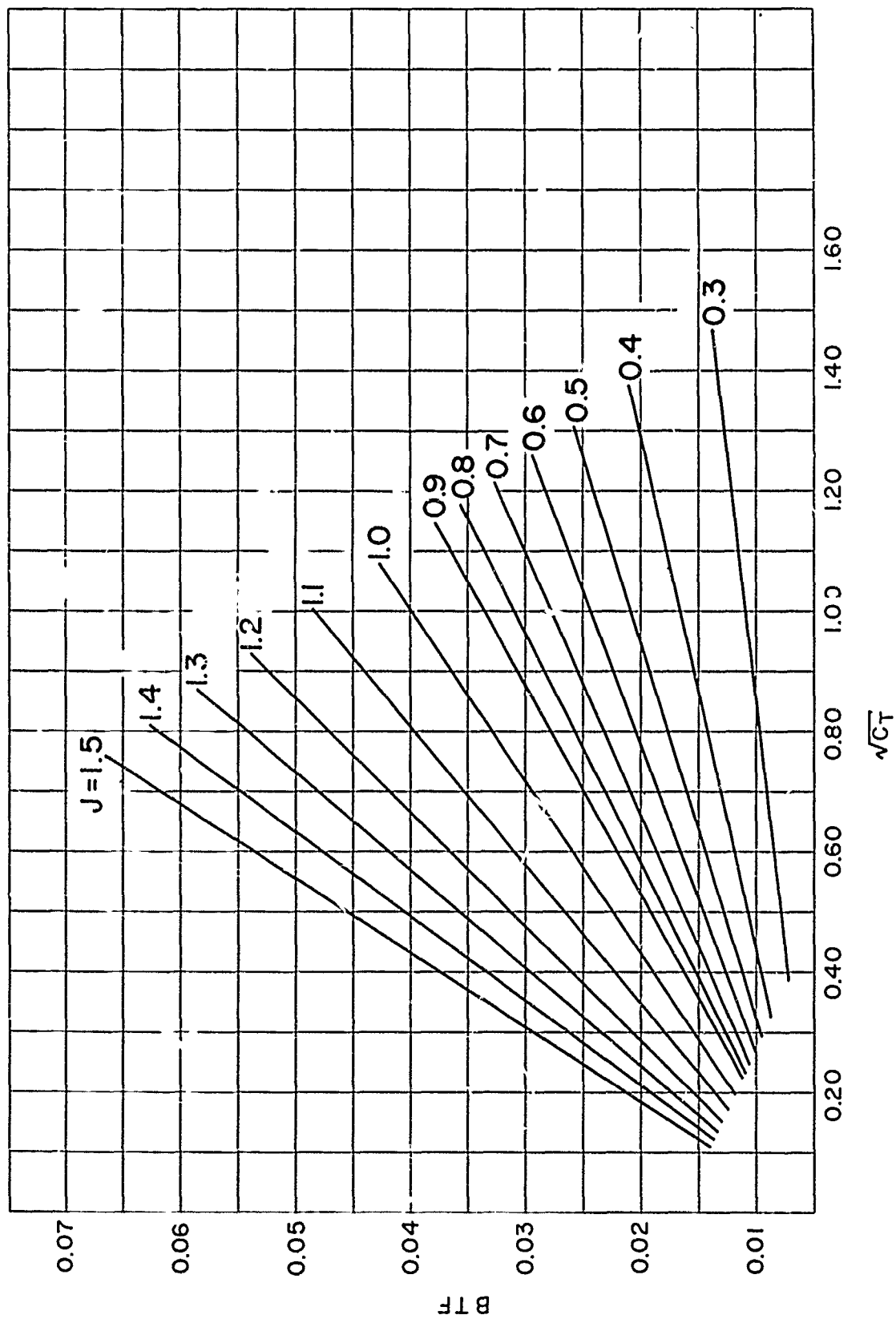
Figure 3d – Blade Thickness Fraction for TMB 3-Bladed SC Propeller Series, EAR = 0.4

37
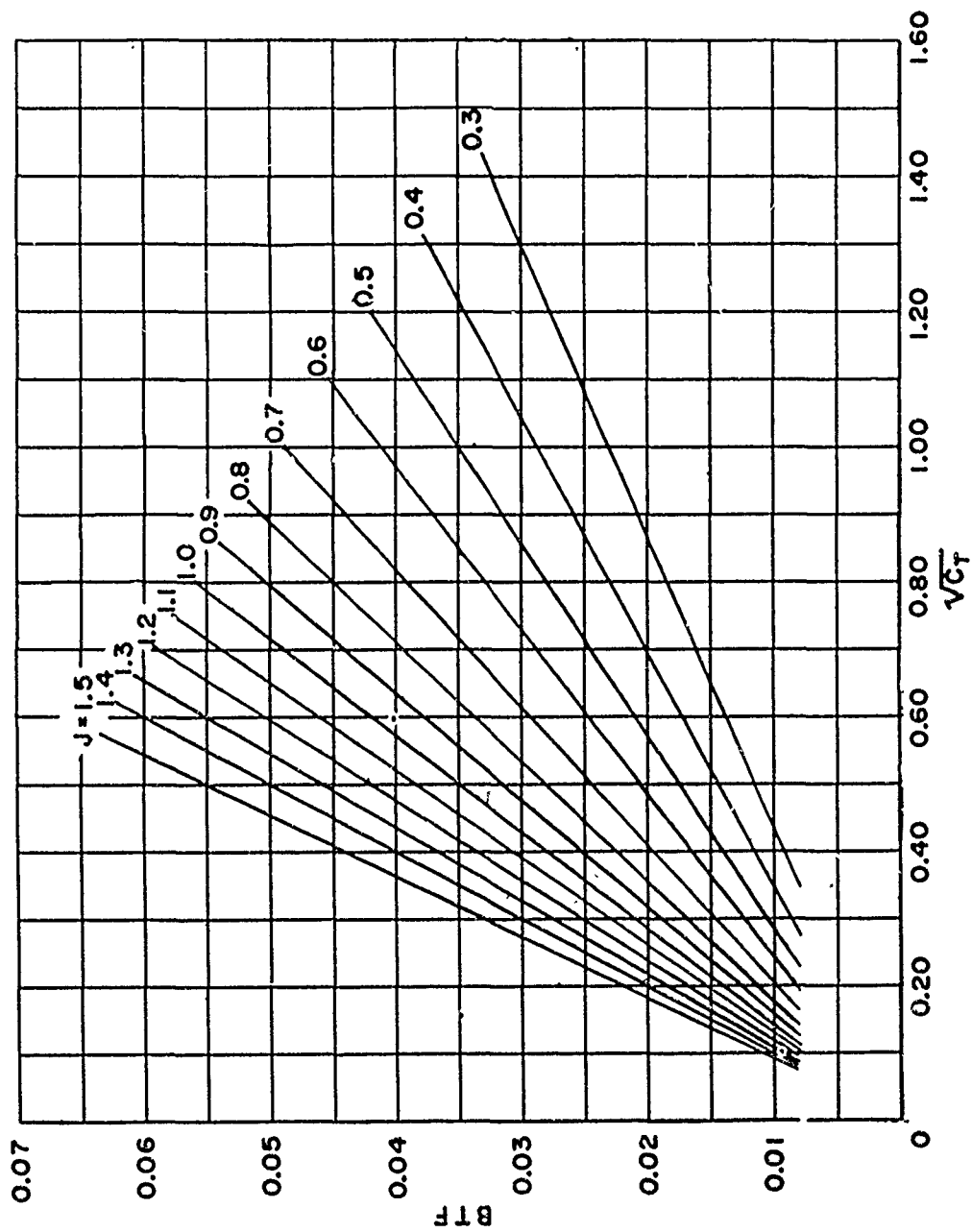
Figure 3e – Blade Thickness Fraction for TMB 3-Bladed SC Propeller Series, EAR = 0.5

38
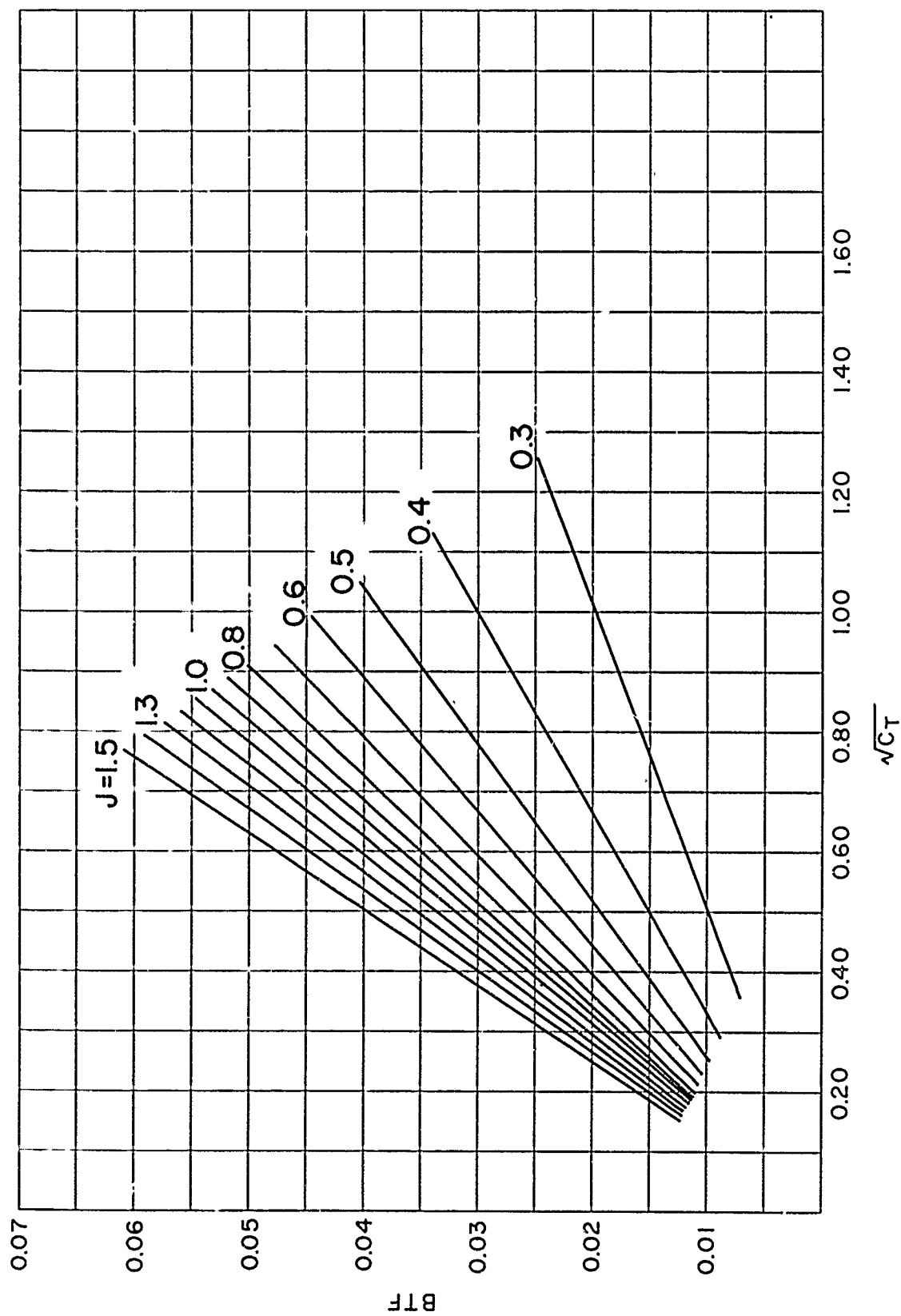
Figure 3f — Blade Thickness Fraction for TMB 3-Bladed SC Propeller Series, EAR = 0.6

39
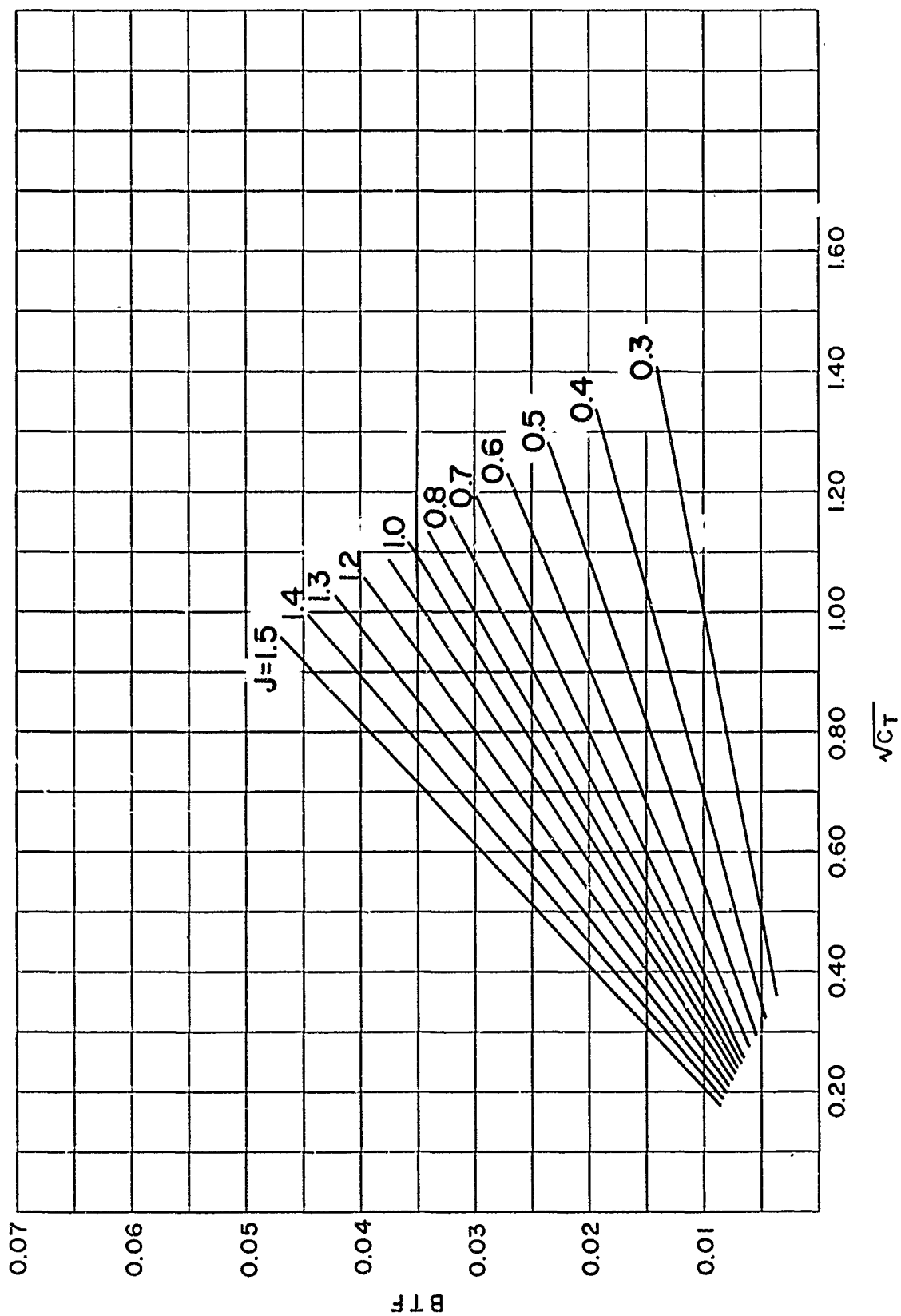
Figure 3g — Blade Thickness Fraction for TMB 4-Bladed SC Propeller Series, EAR = 0.5

40
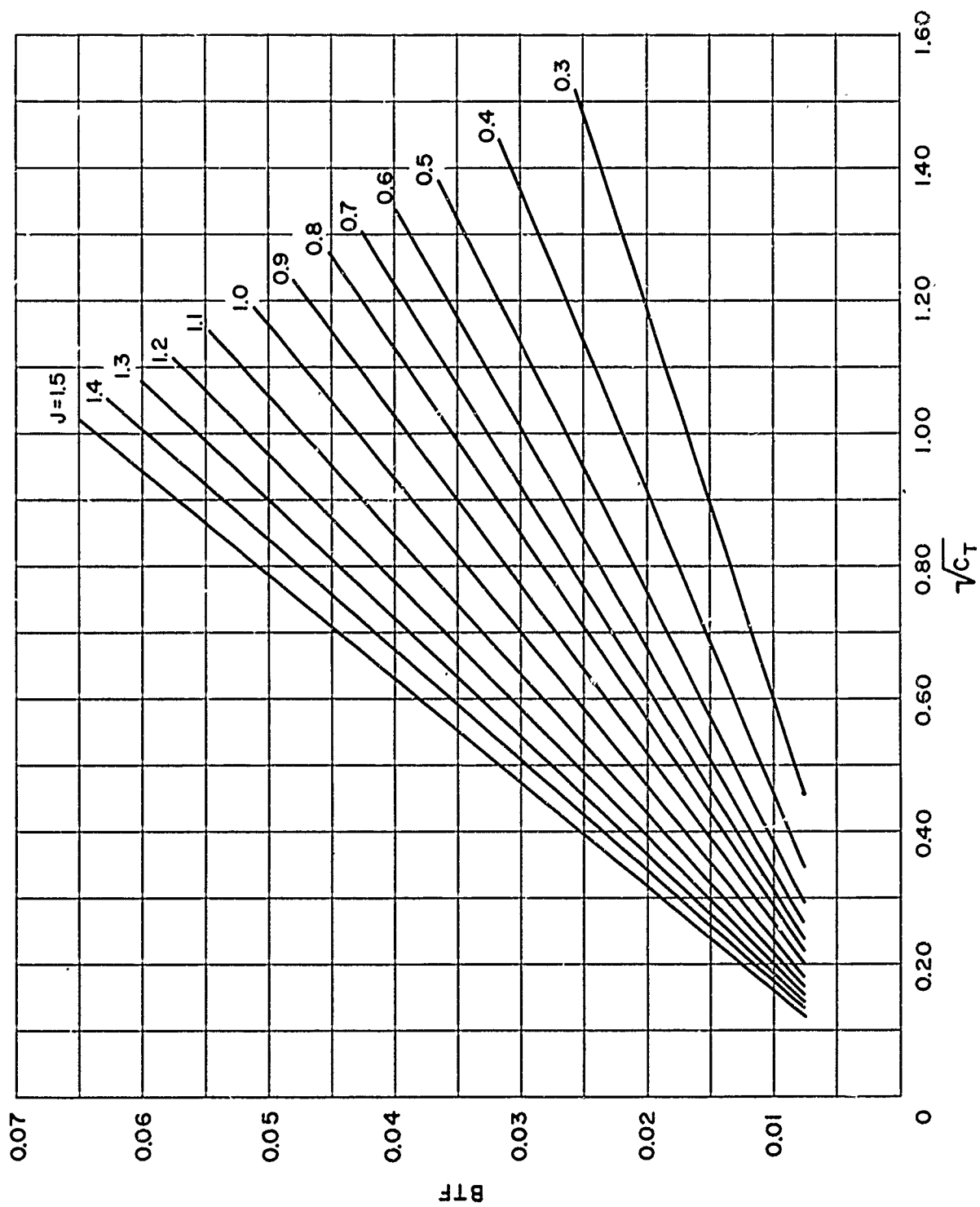
Figure 3h — Blade Thickness Fraction for TMB 4-Bladed SC Propeller Series, EAR = 0.6

41
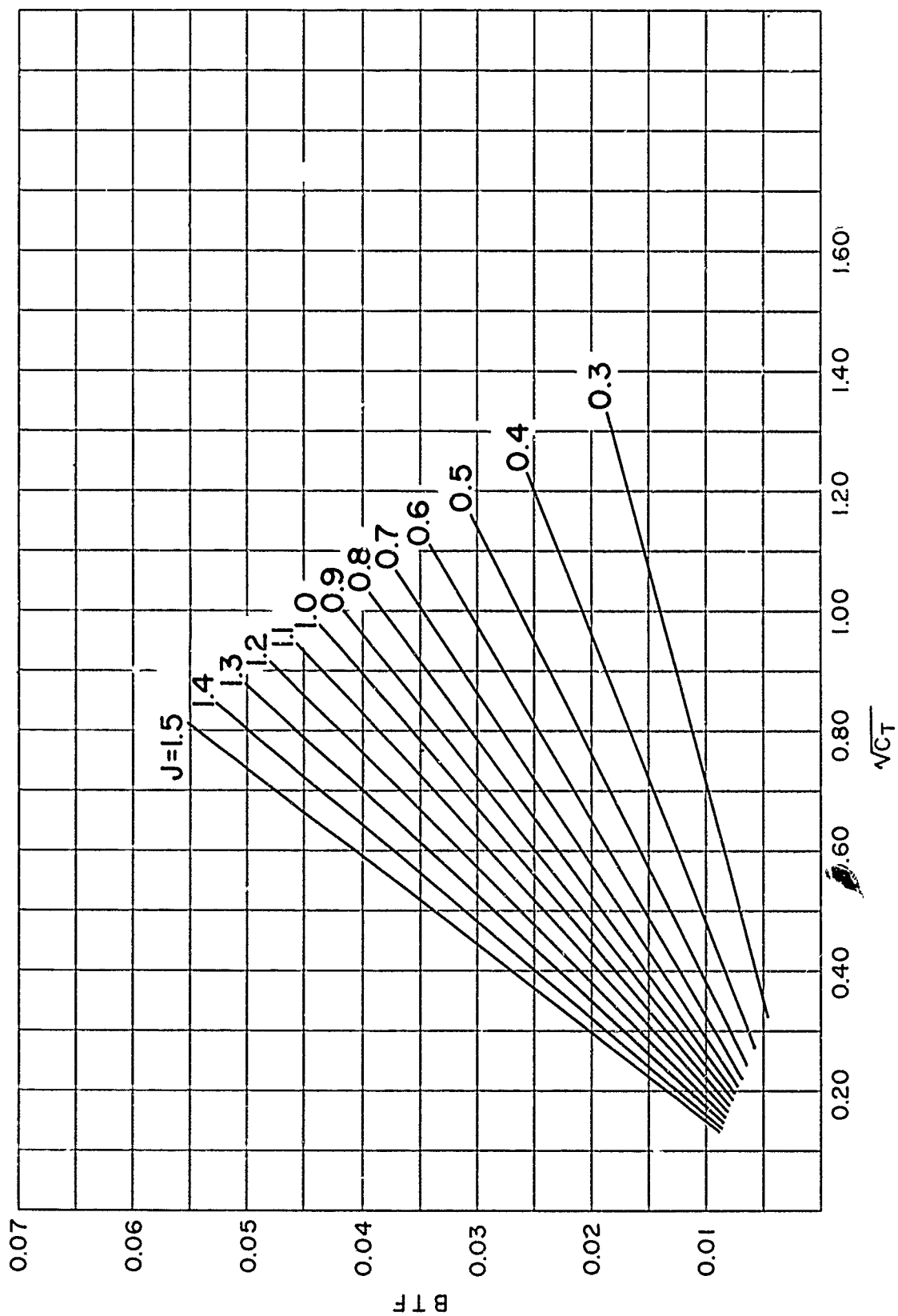
Figure 3i – Blade Thickness Fraction for TMB 4-Bladed SC Propeller Series, EAR = 0.7

42

APPENDIX D

PITCH CORRECTION COEFFICIENTS FOR TMB SC PROPELLER SERIES
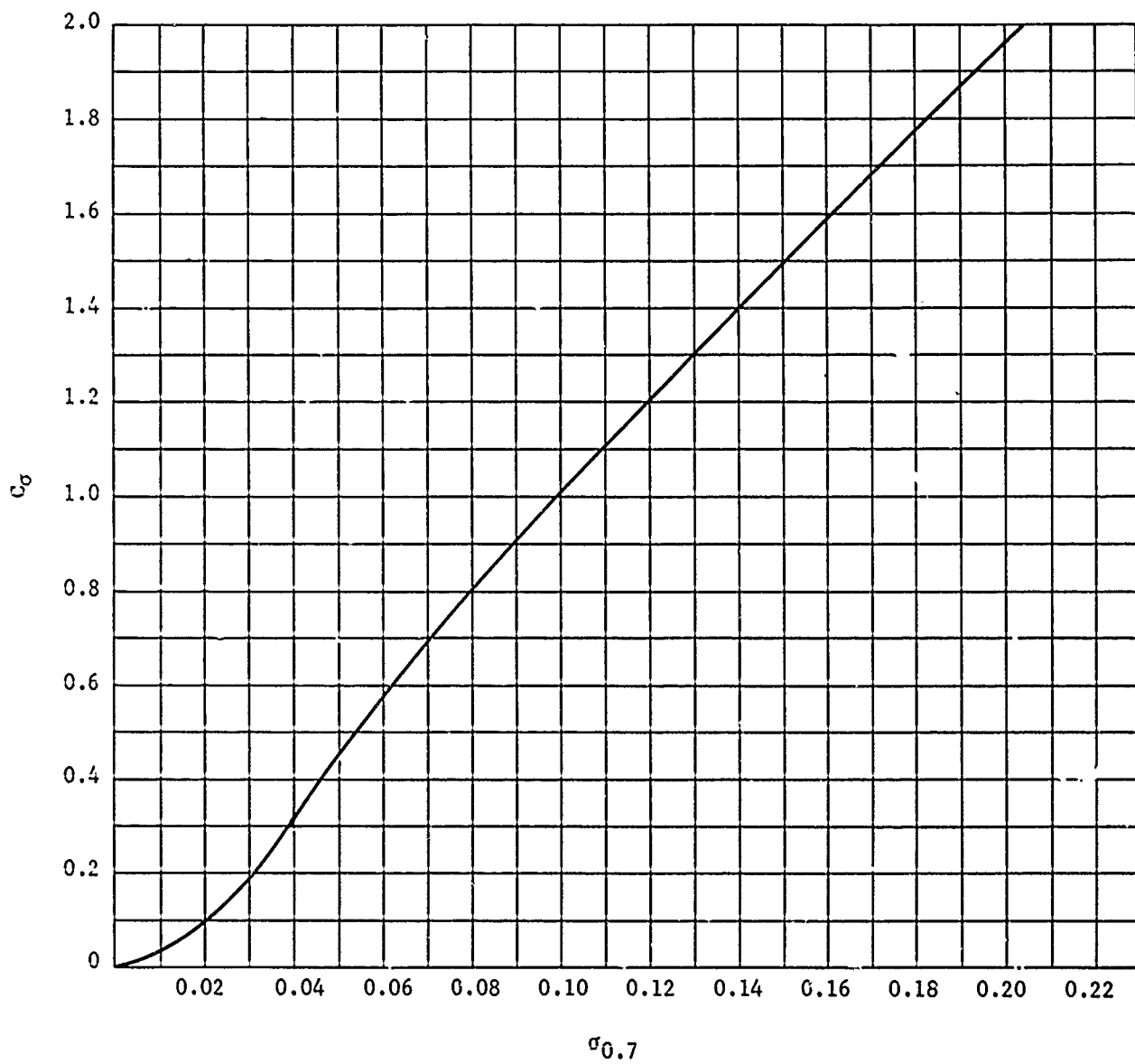
Figure 4 — Pitch Correction Coefficient (C_σ) for Finite Cavitation Numbers for

TMB SC Propeller Series

44
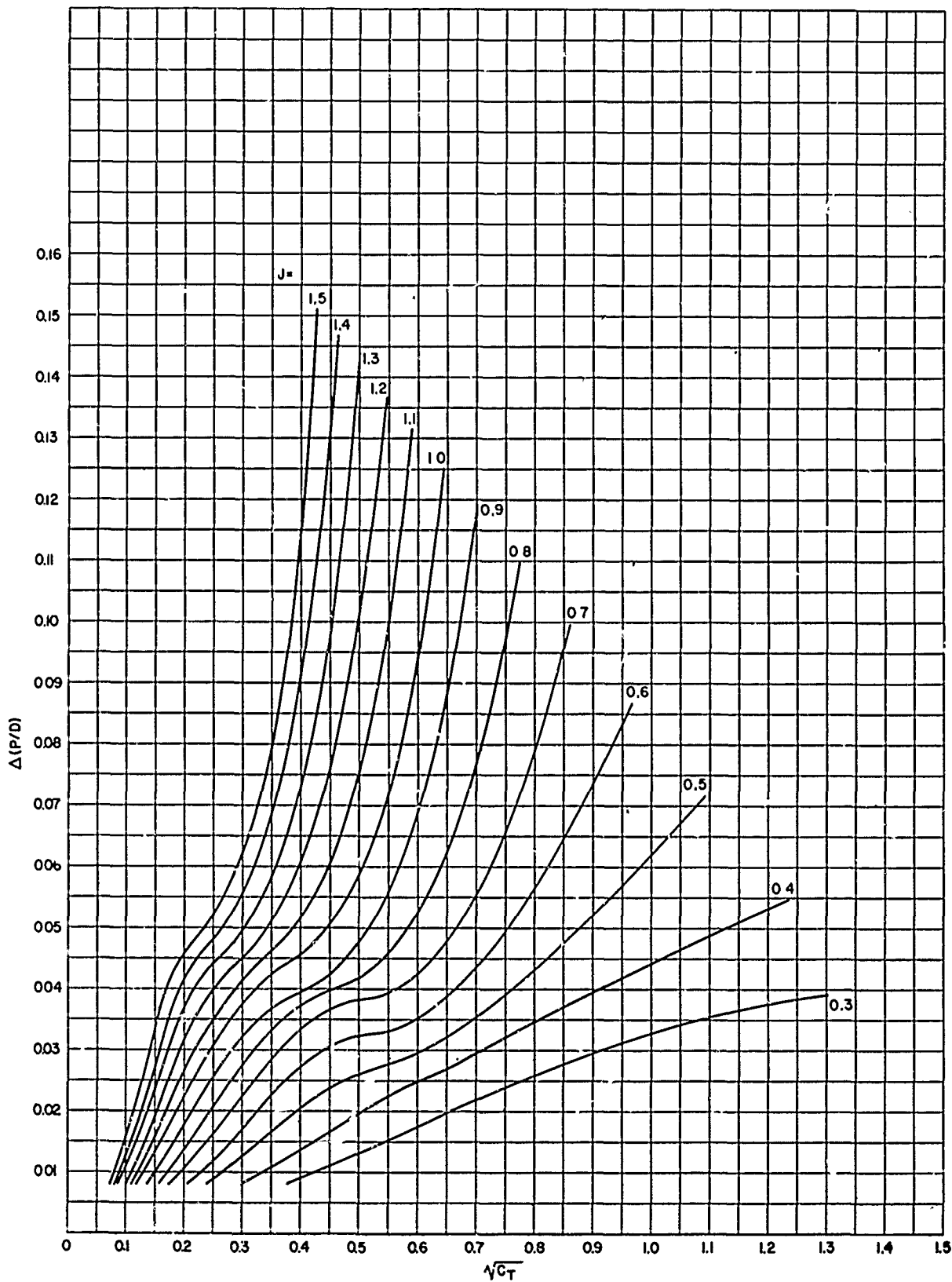
Figure 4a – Pitch Correction Coefficient $\Delta(P/D)$ for Finite Cavitation Numbers for TMB 2-Bladed SC Propeller Series, EAR = 0.3

45
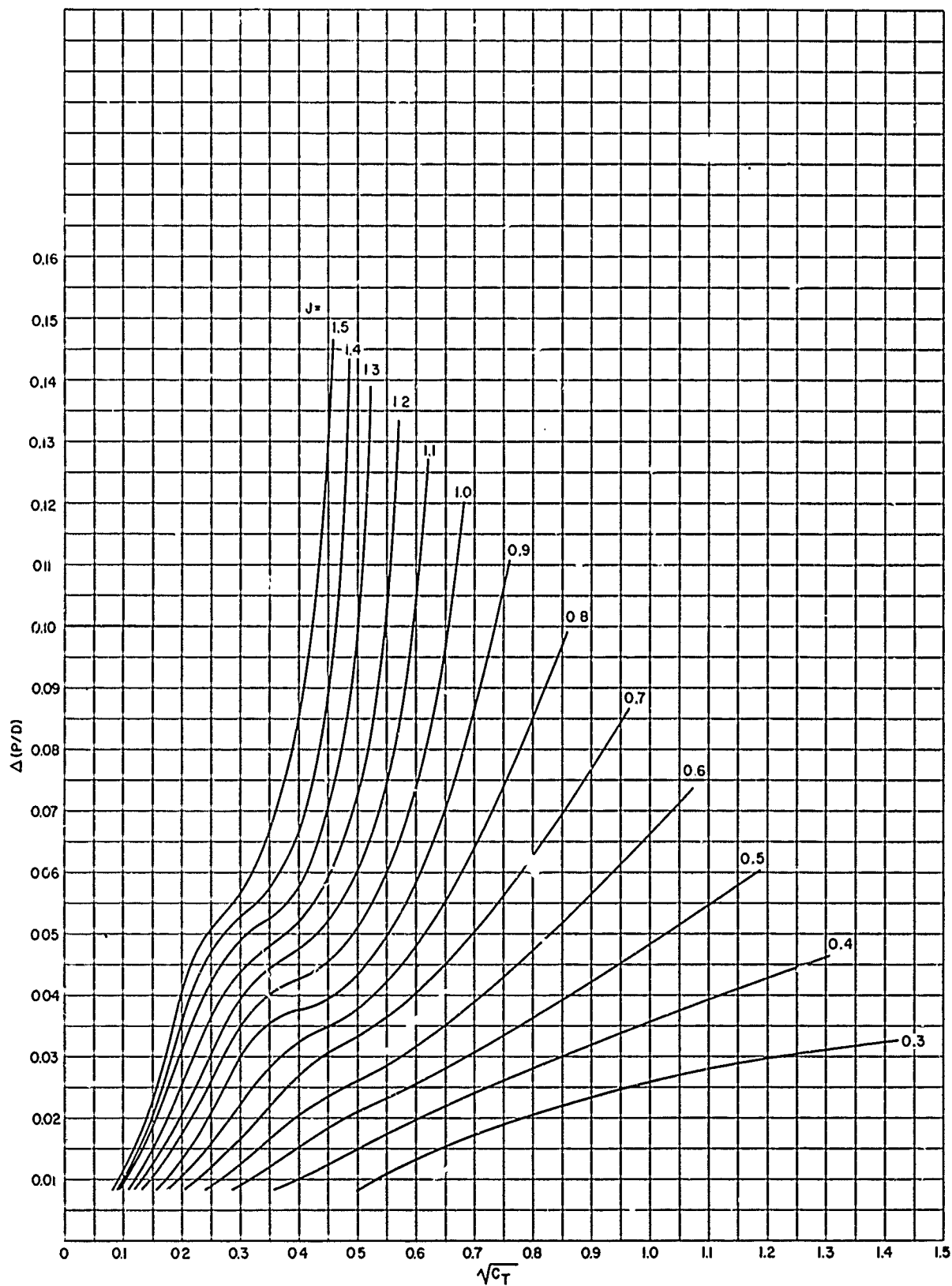
Figure 4b – Pitch Correction Coefficient $\Delta(P/D)$ for Finite Cavitation Numbers for TMB 2-Bladed SC Propeller Series, EAR = 0.4

46
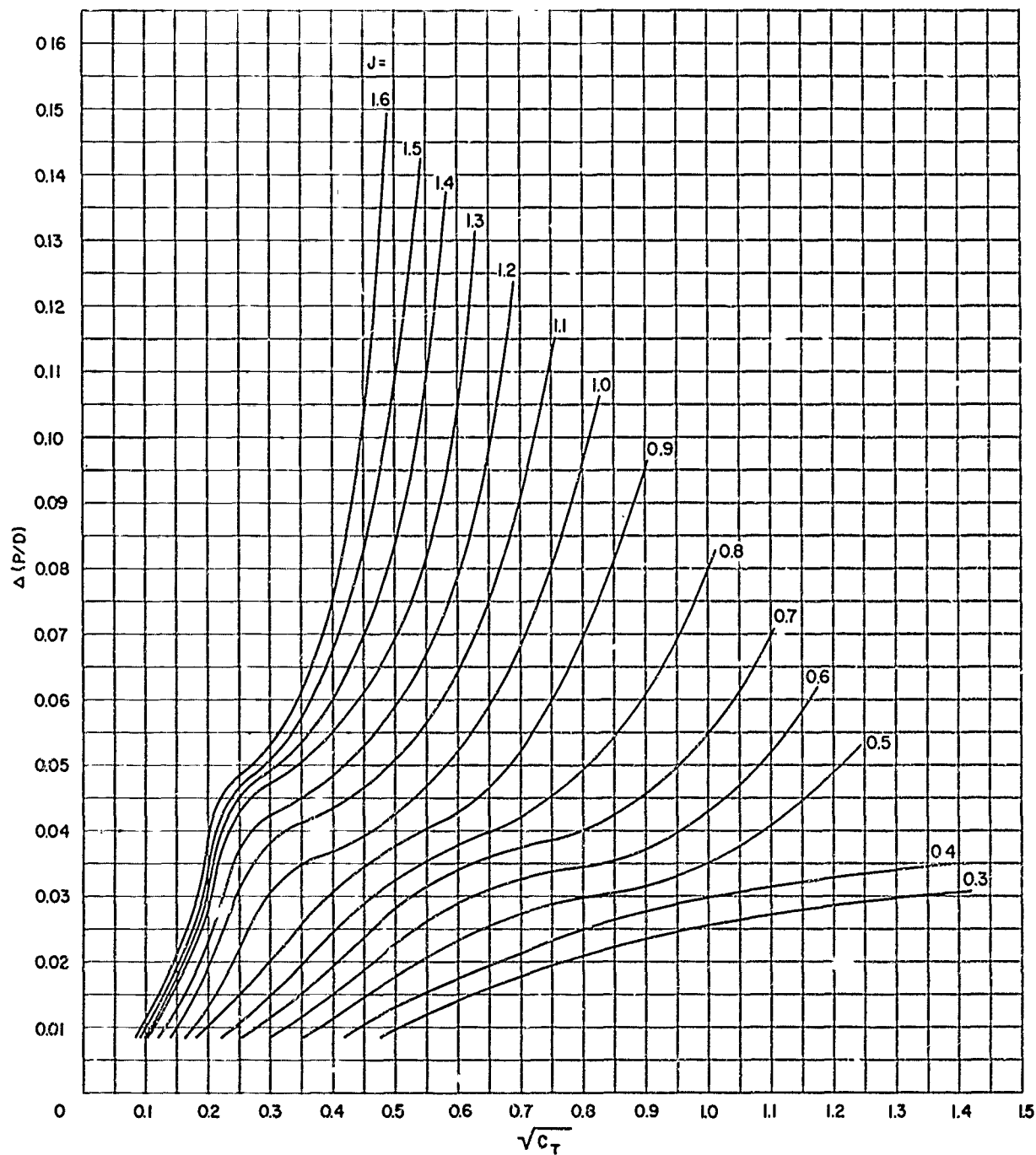
Figure 4c – Pitch Correction Coefficient $\Delta(P/D)$ for Finite Cavitation Numbers for TMB 2-Bladed SC Propeller Series, EAR = 0.5
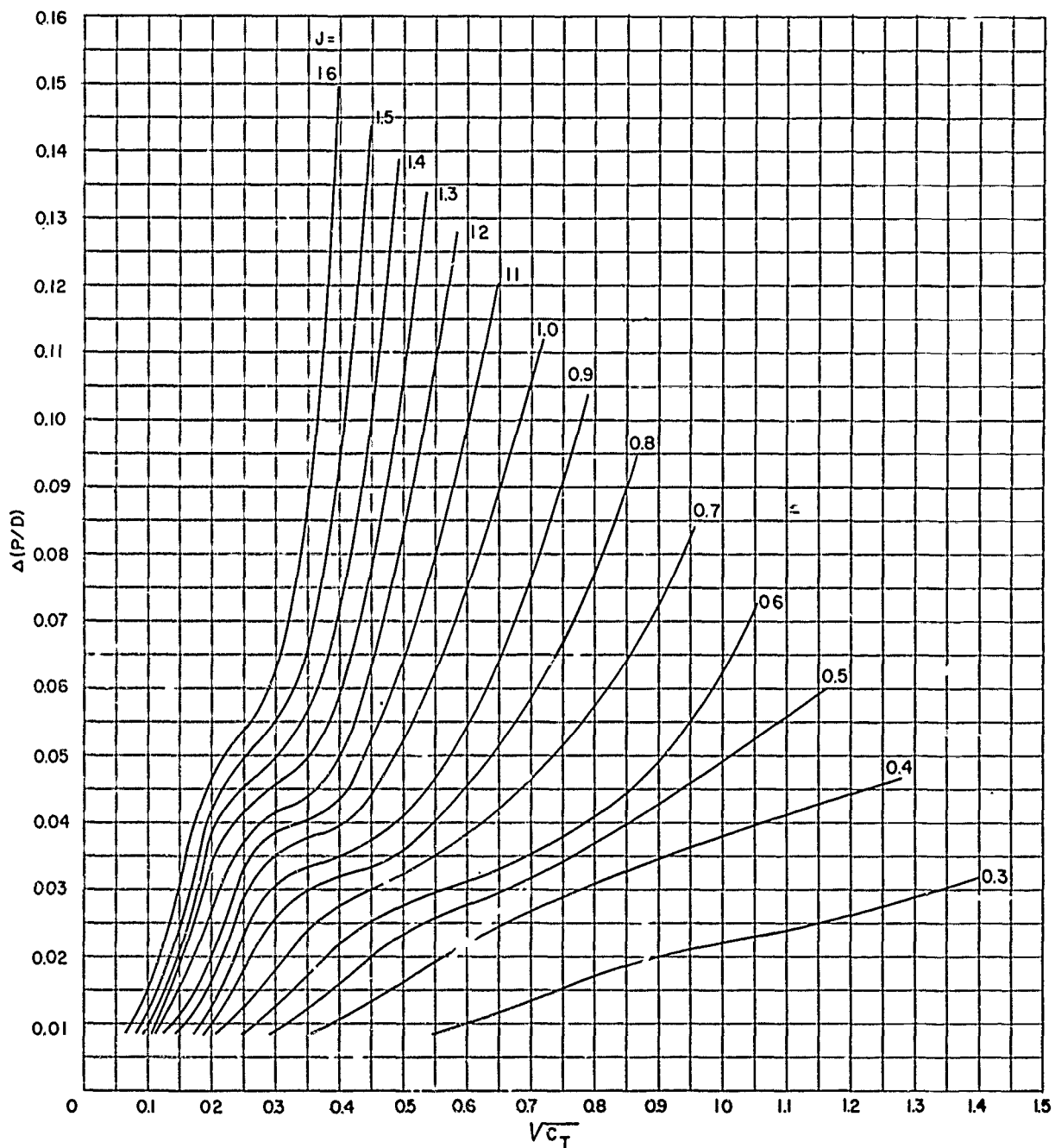
Figure 4d – Pitch Correction Coefficient $\Delta(P/D)$ for Finite Cavitation Numbers for TMB 3-Bladed SC Propeller Series, EAR = 0.4

48
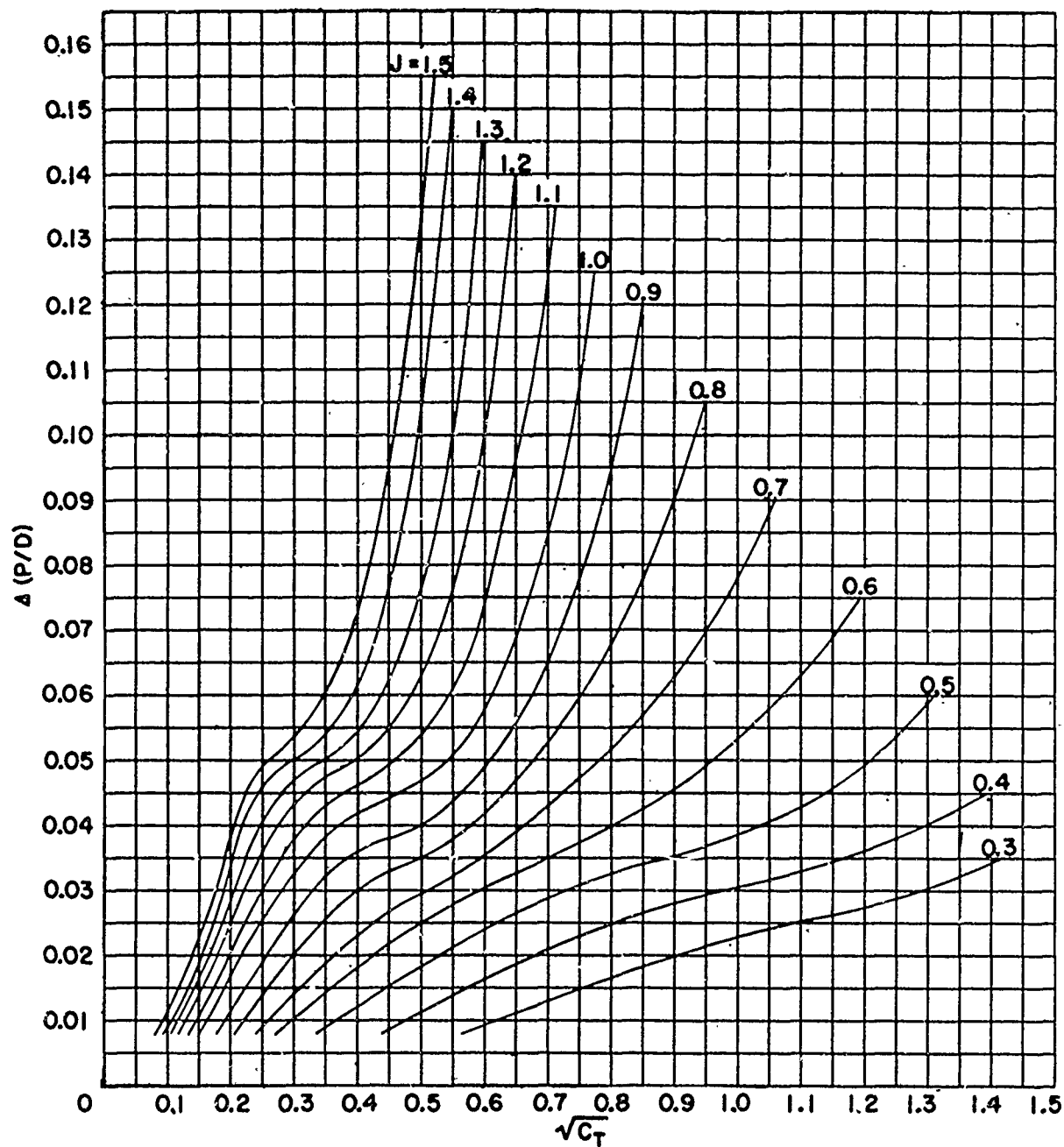
Figure 4e – Pitch Correction Coefficient $\Delta(P/D)$ for Finite Cavitation Numbers for TMB 3-Bladed SC Propeller Series, EAR = 0.5

49
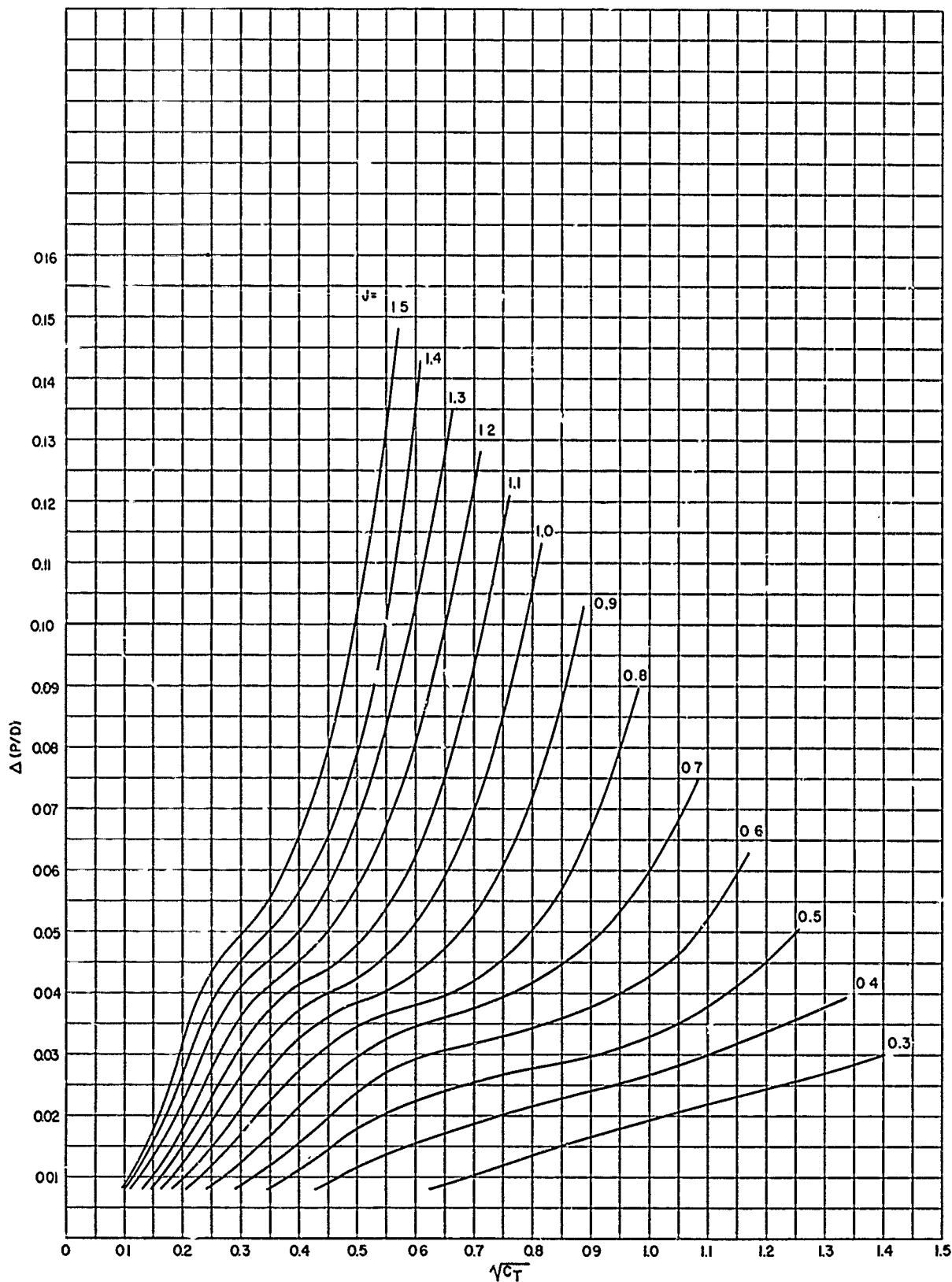
Figure 4f – Pitch Correction Coefficient $\Delta(P/D)$ for Finite Cavitation Numbers for TMB 3-Bladed SC Propeller Series, EAR = 0.6

50
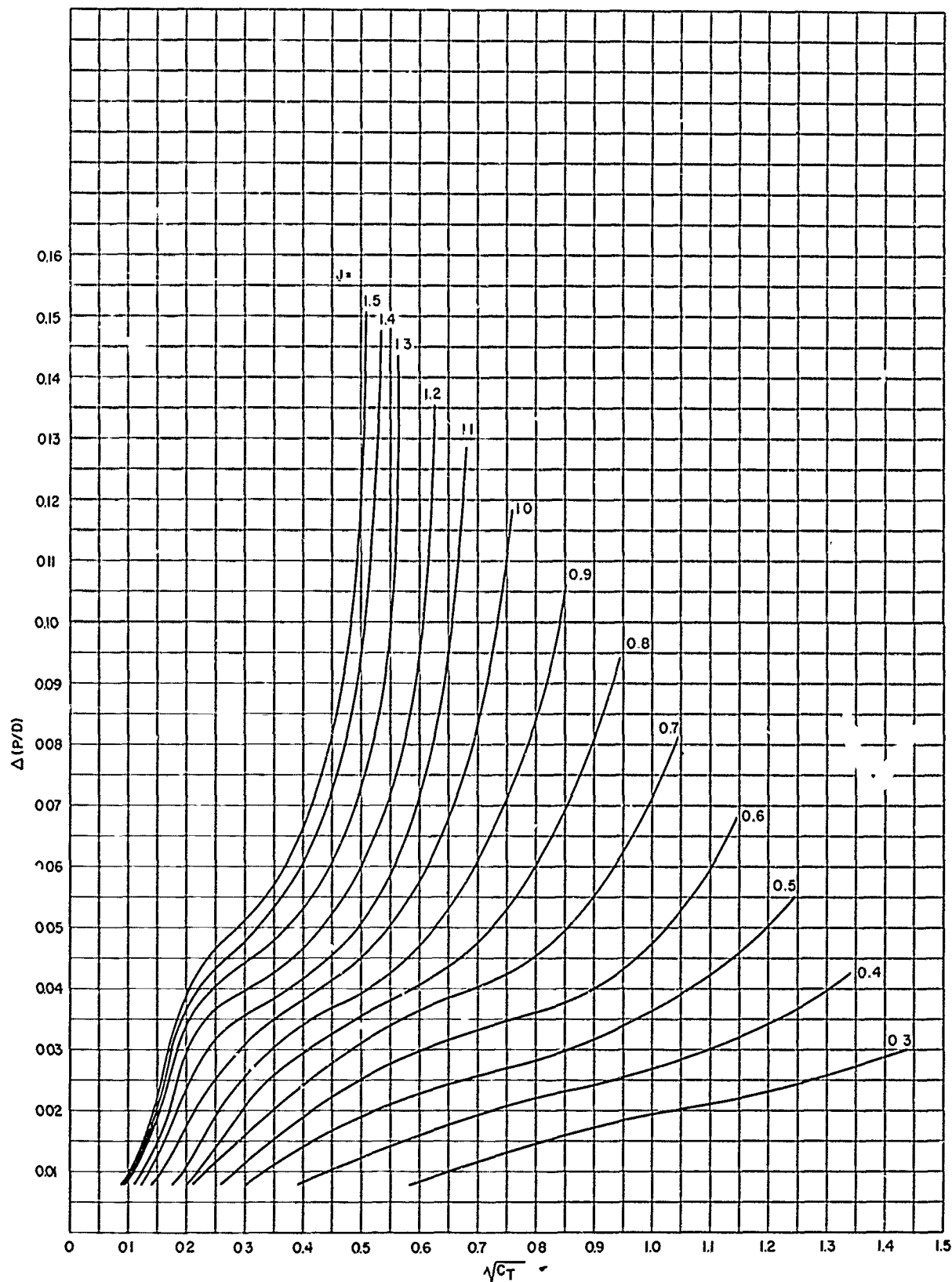
Figure 4g – Pitch Correction Coefficient $\Delta(P/D)$ for Finite Cavitation Numbers for TMB 4-Bladed SC Propeller Series, EAR = 0.5
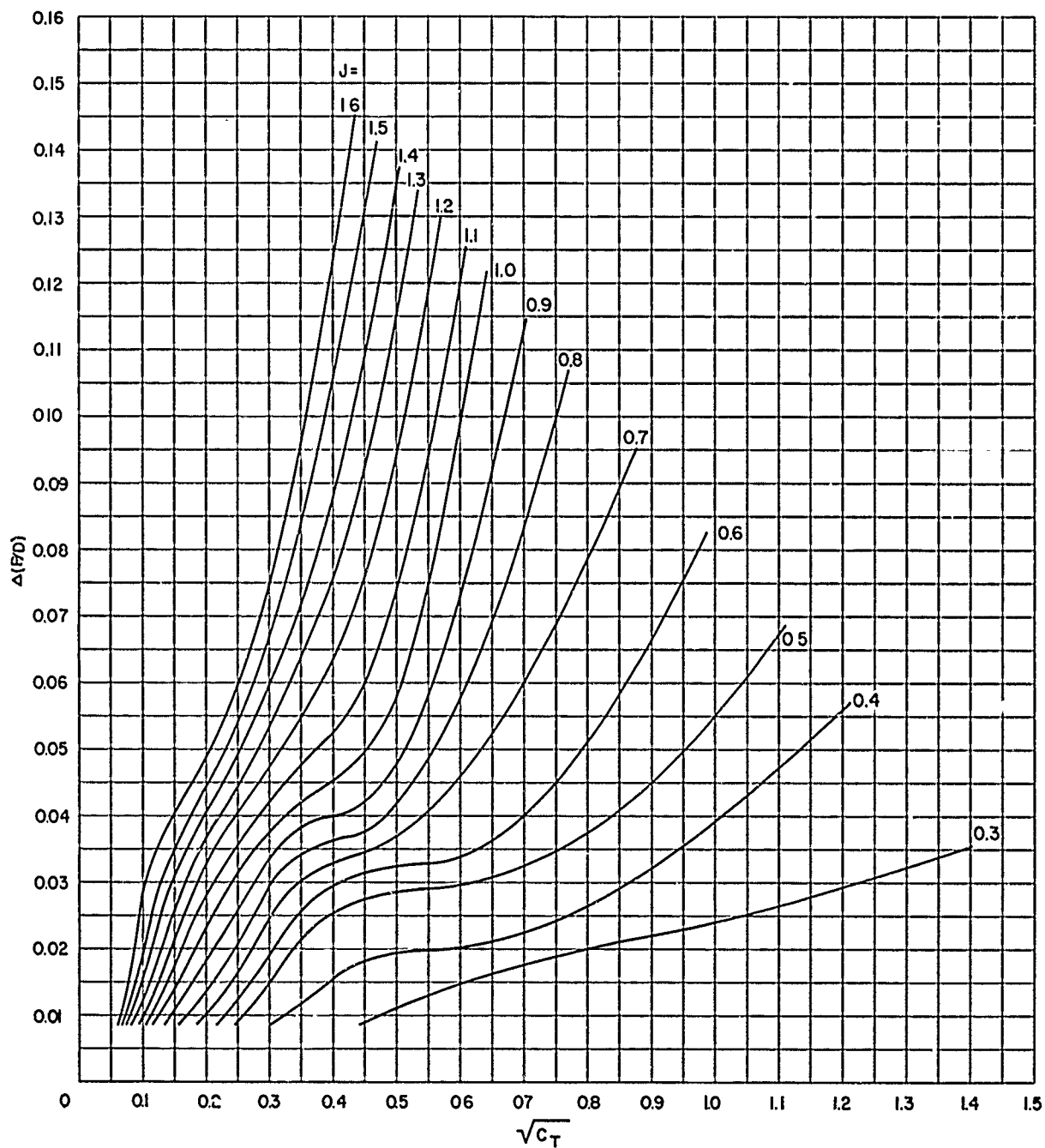
Figure 4h – Pitch Correction Coefficient $\Delta(P/D)$ for Finite Cavitation Numbers for TMB 4-Bladed SC Propeller Series, EAR = 0.6

52
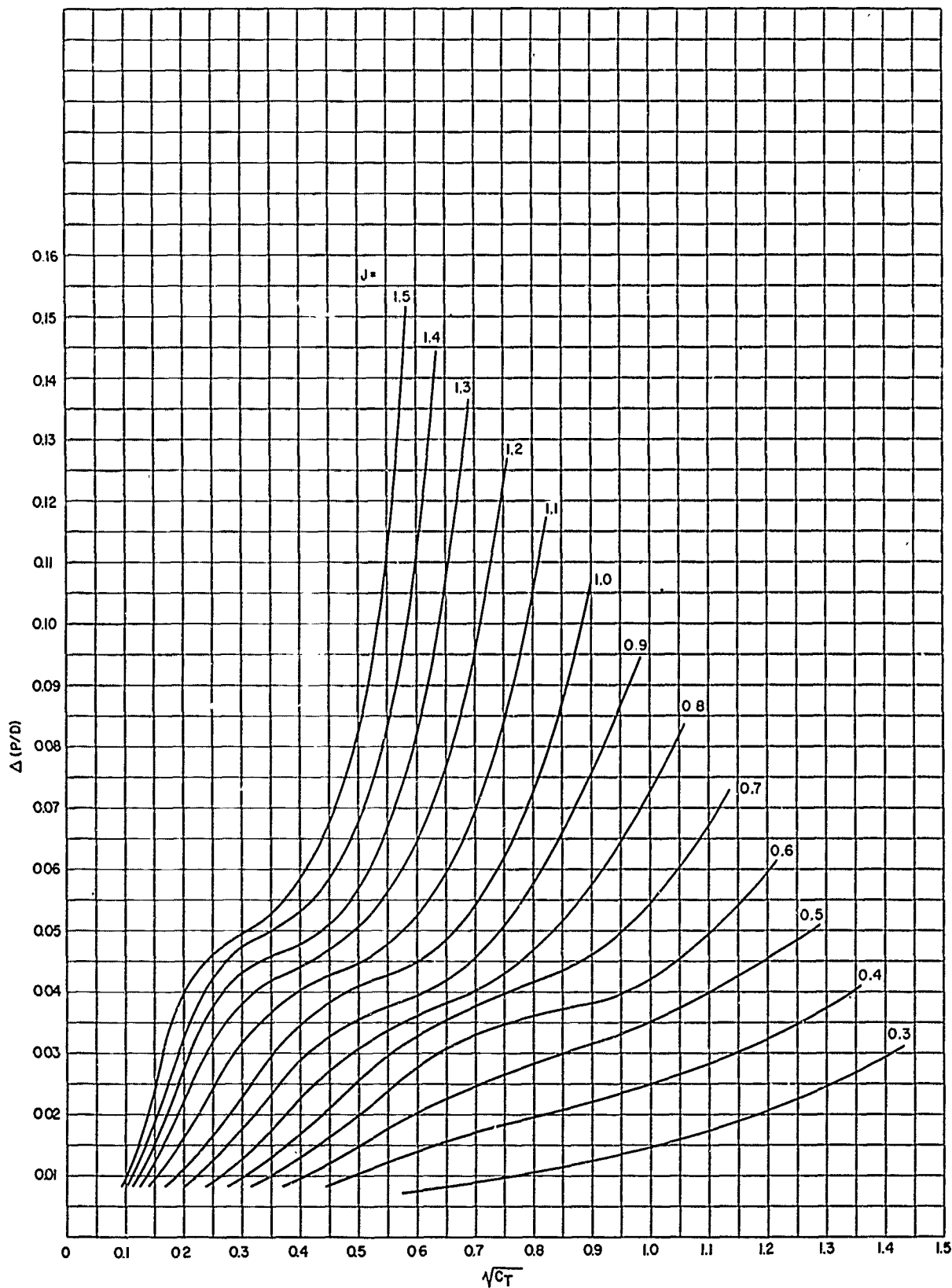
Figure 4i – Pitch Correction Coefficient $\Delta(P/D)$ for Finite Cavitation Numbers for TMB 4-Bladed SC Propeller Series, EAR = 0.7

53

APPENDIX E

MAXIMUM FACE ORDINATES AT 0.3, 0.5, 0.7, AND 0.9 RADIUS FOR TMB SC PROPELLER SERIES
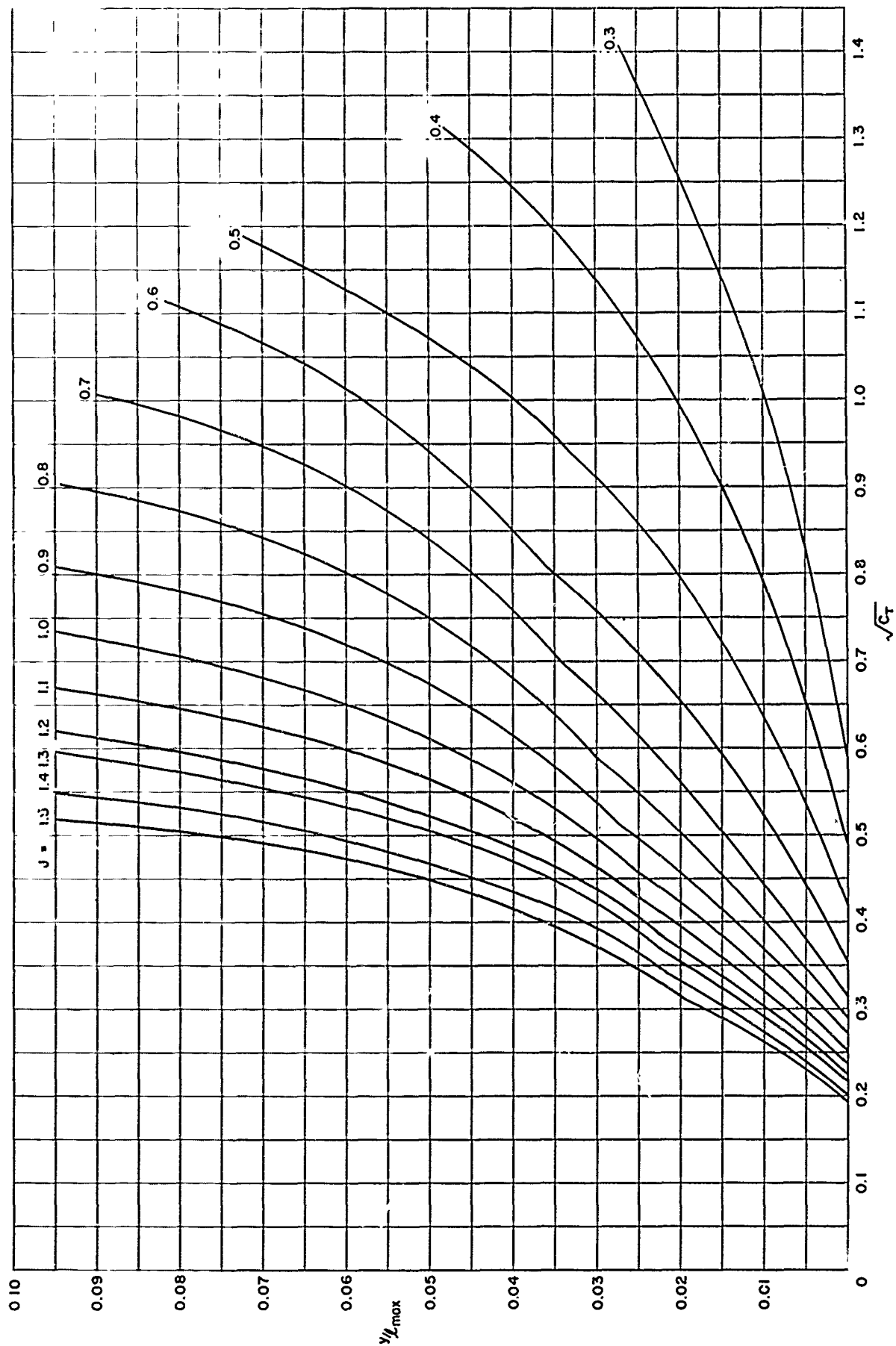
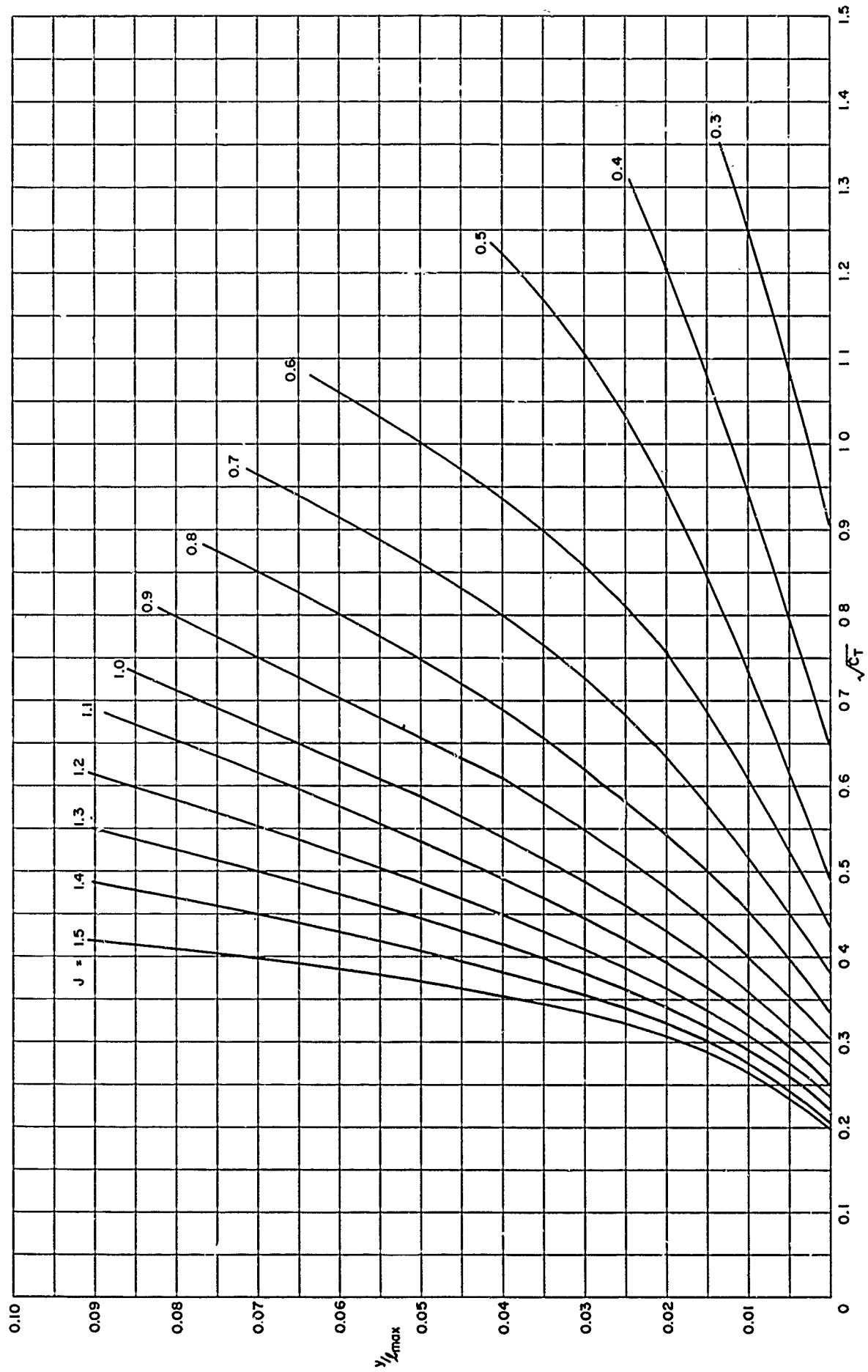Figure 5a — Maximum Face Ordinate at 0.3 Radius for TMB 2-Bladed SC Propeller Series, EAR = 0.3

55
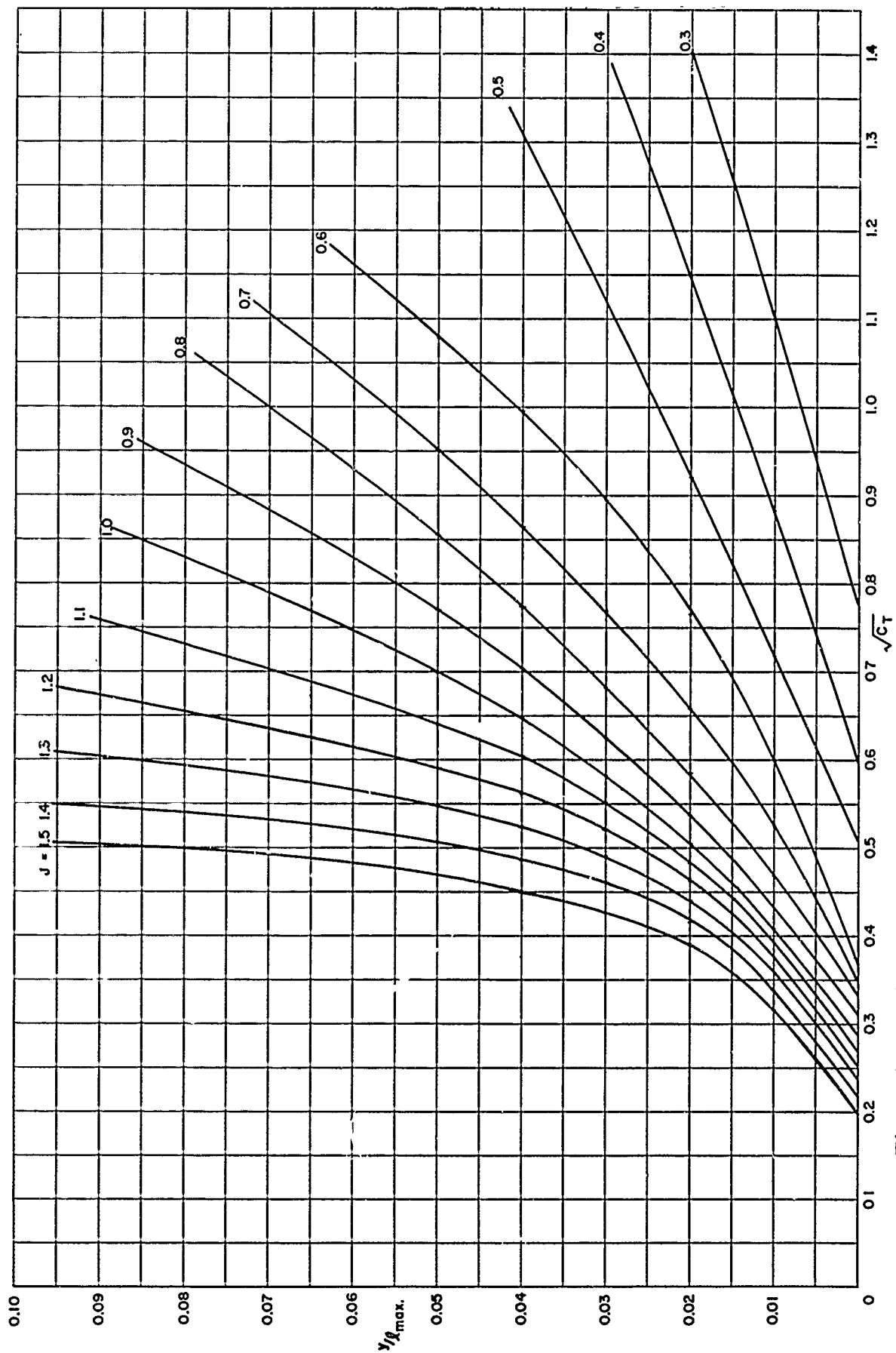
Figure 5b – Maximum Face Ordinate at 0.3 Radius for TMB 2-Bladed SC Propeller Series, EAR = 0.4
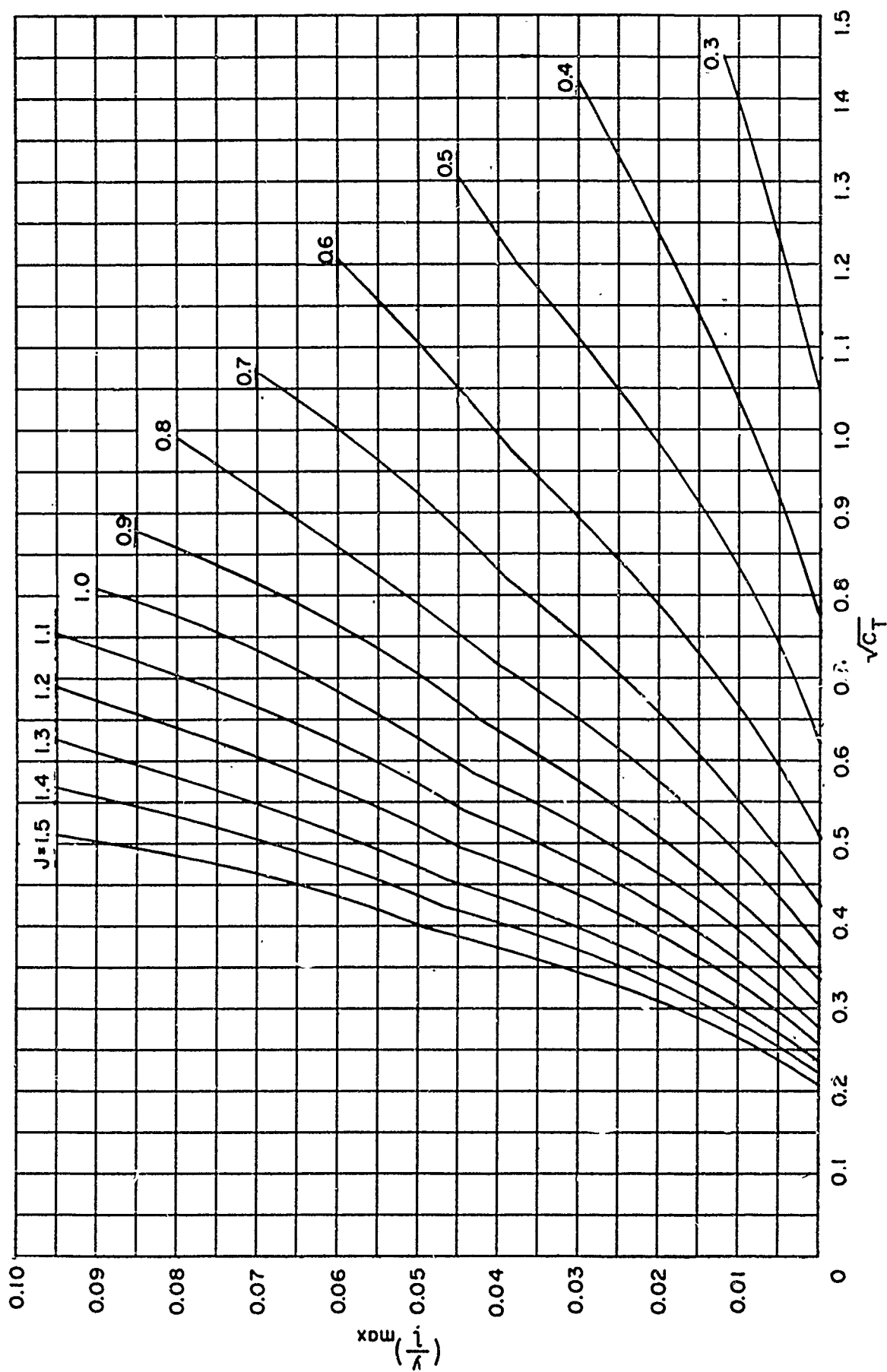
56
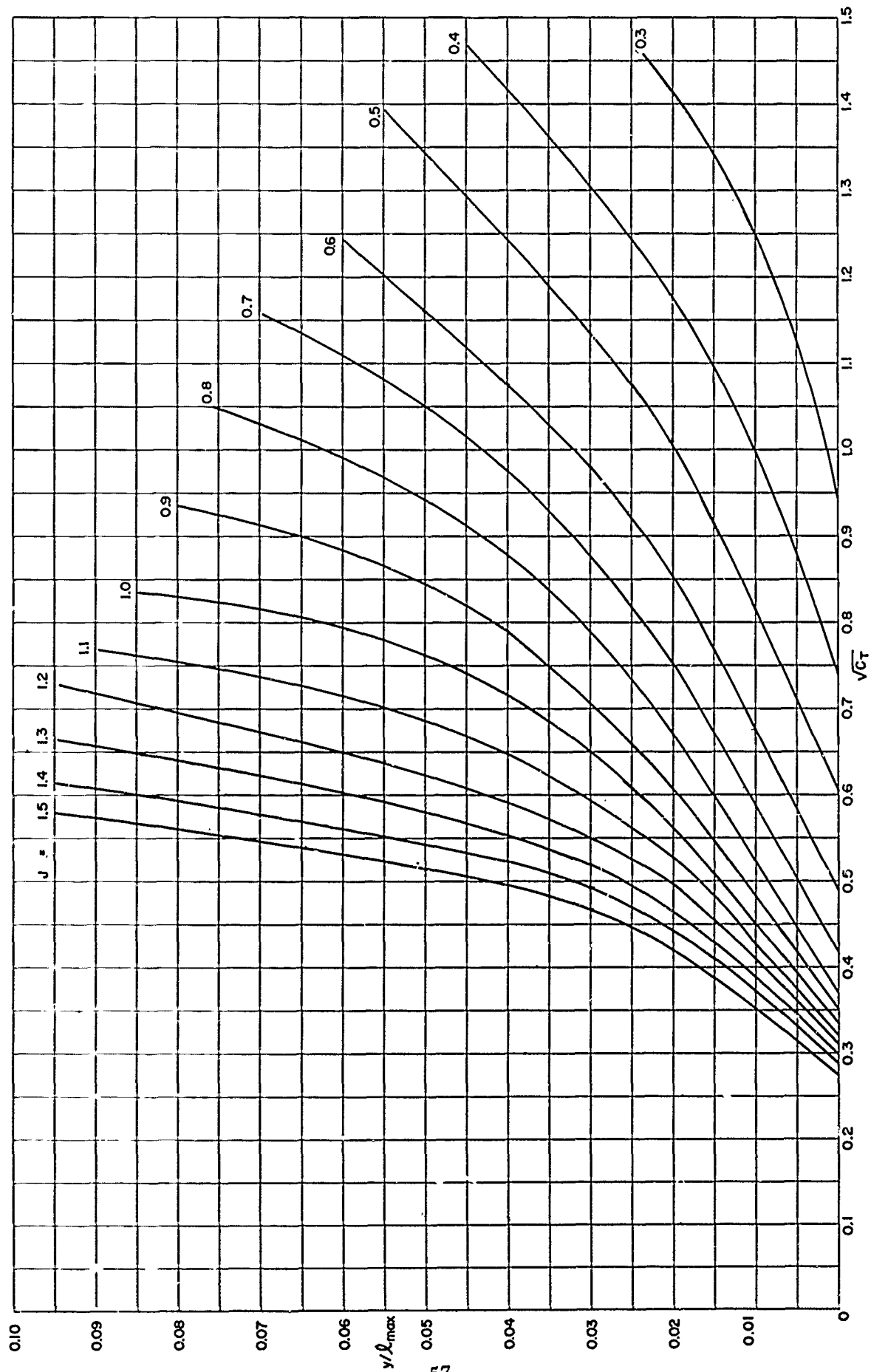
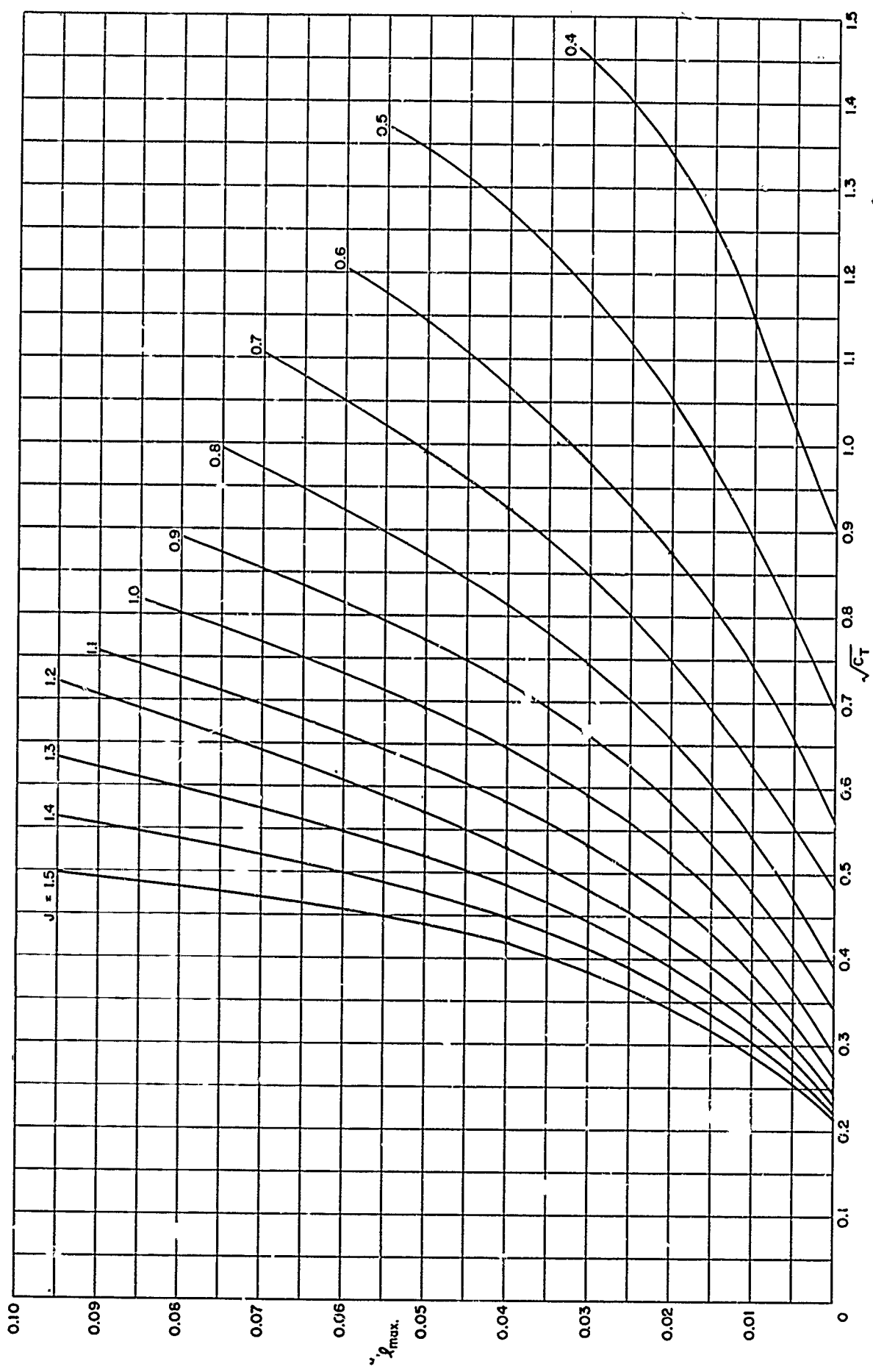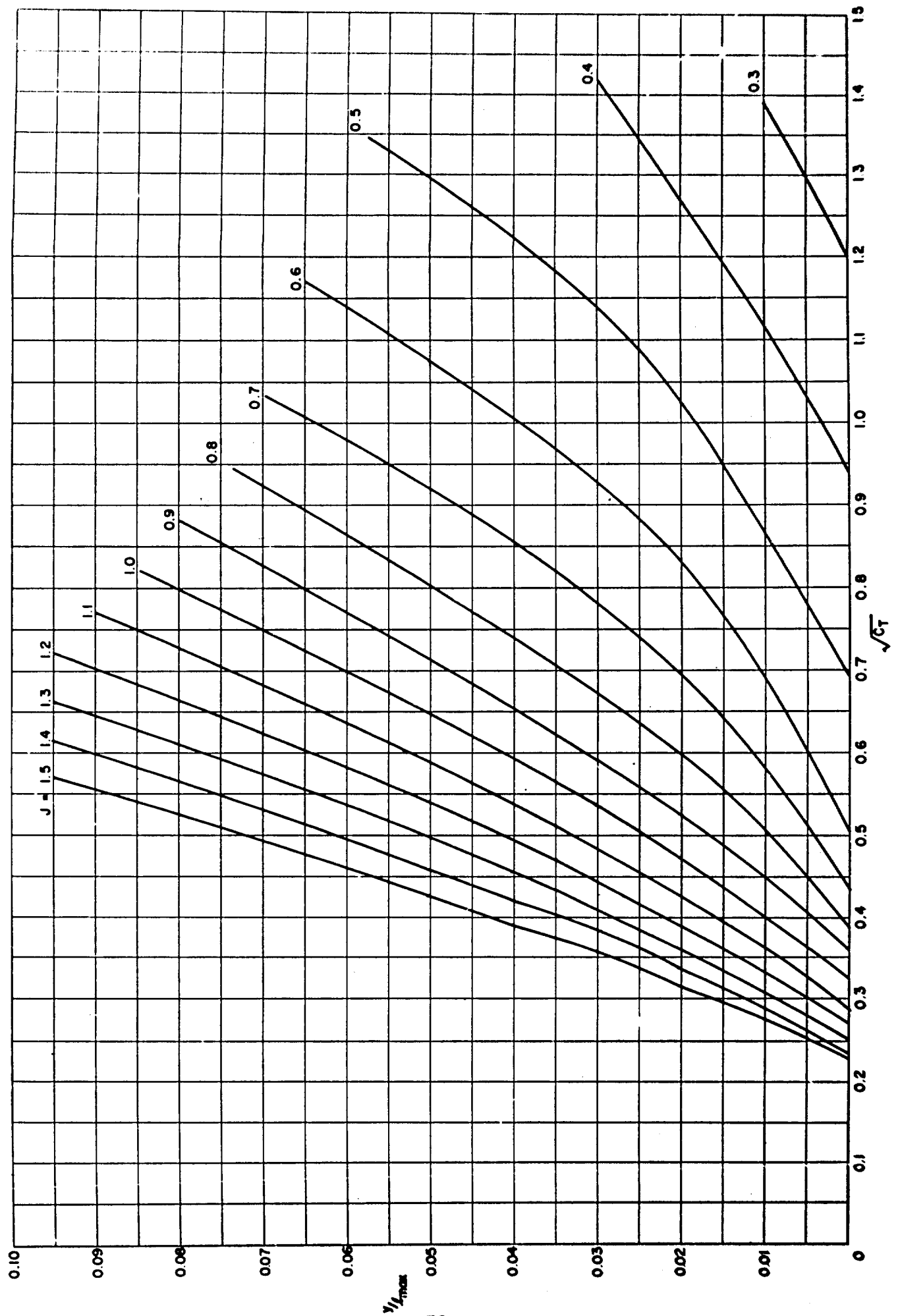Figure 5c — Maximum Face Ordinate at 0.3 Radius for TMB 2-Bladed SC Propeller Series, EAR = 0.5
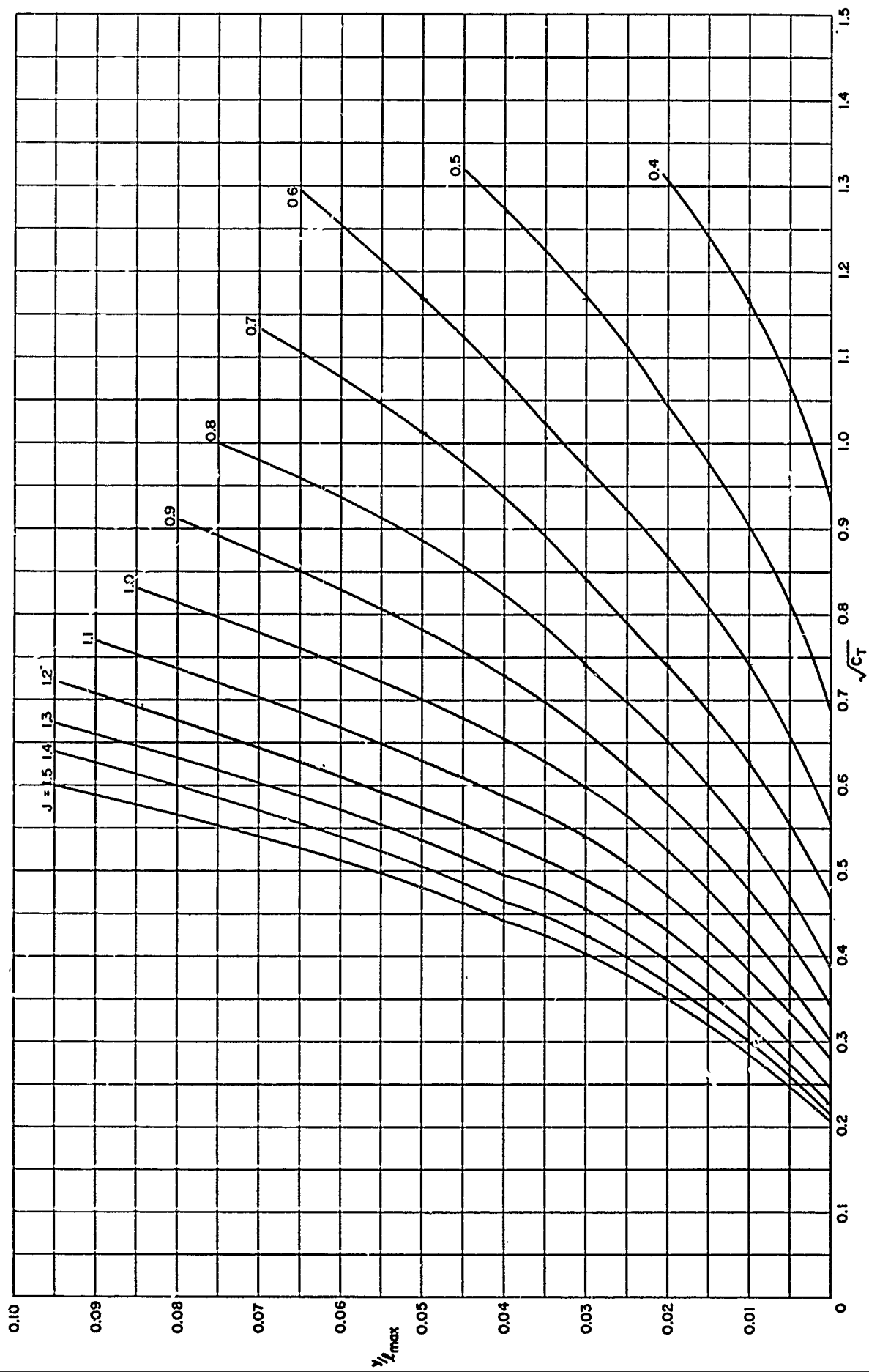
57
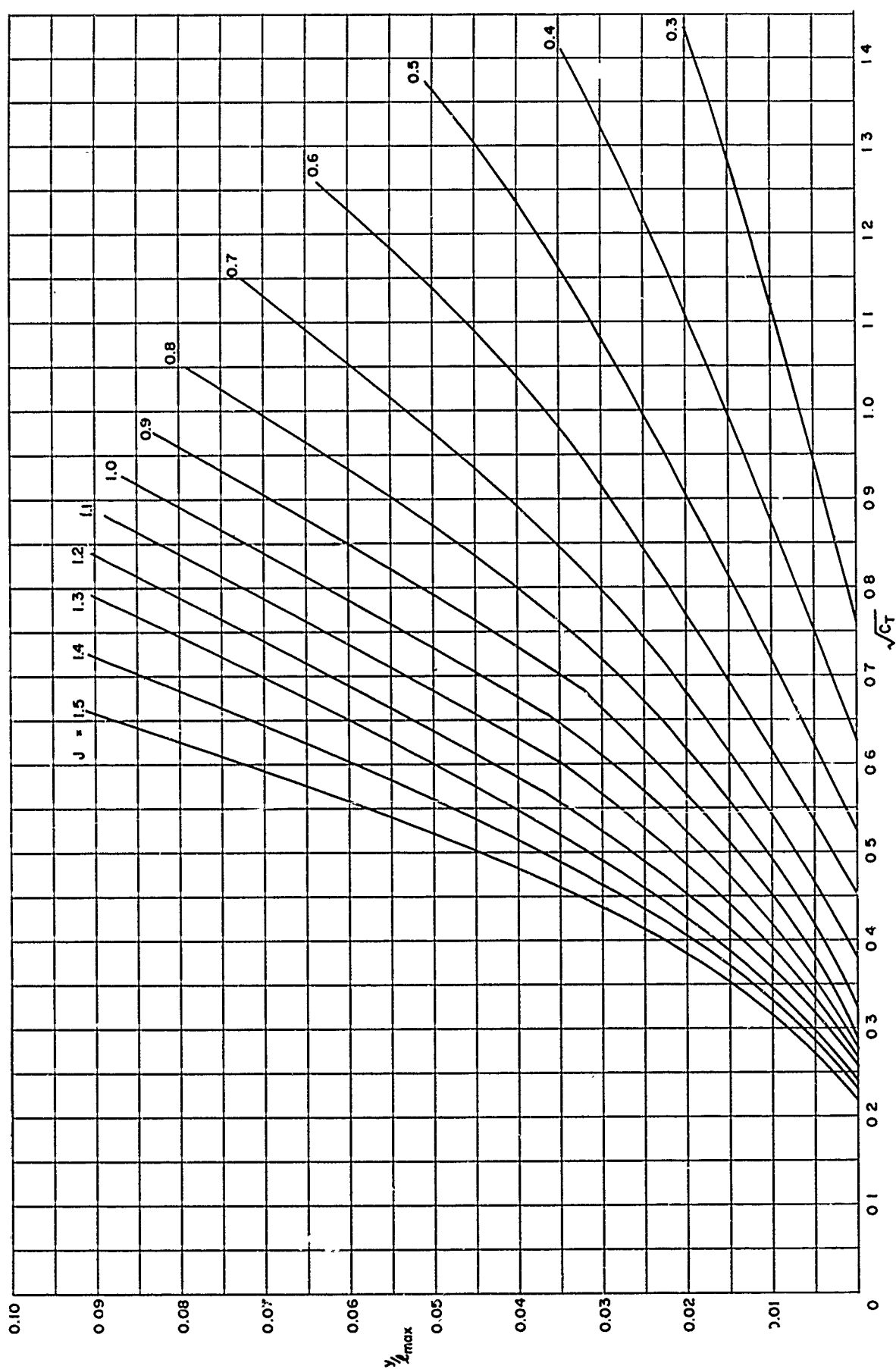
Figure 5d — Maximum Face Ordinate at 0.3 Radius for TMB 3-Bladed SC Propeller Series, EAR = 0.4

58
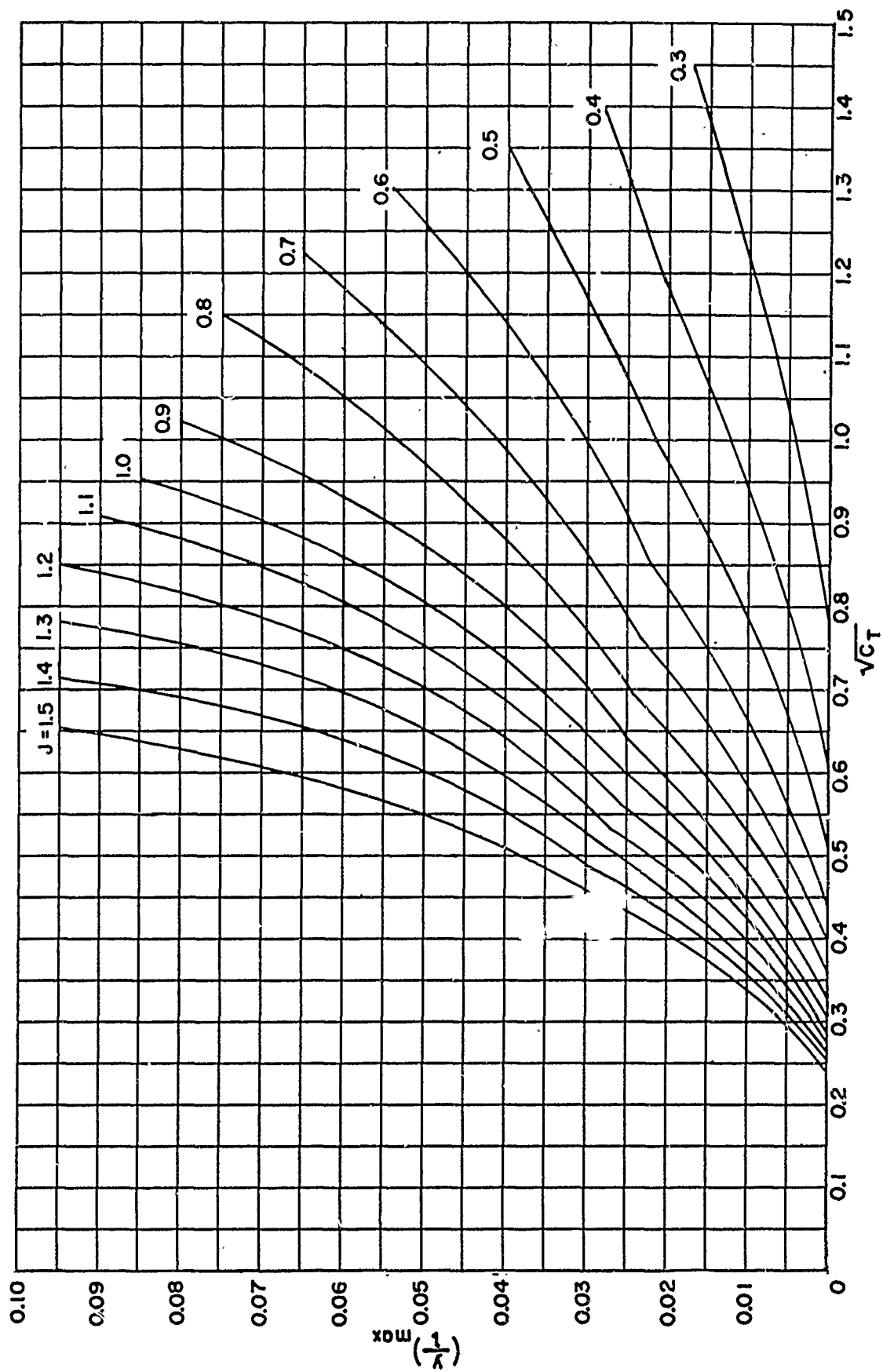
Figure 5e — Maximum Face Ordinate at 0.3 Radius for TMB 3-Bladed SC Propeller Series, EAR = 0.5

59
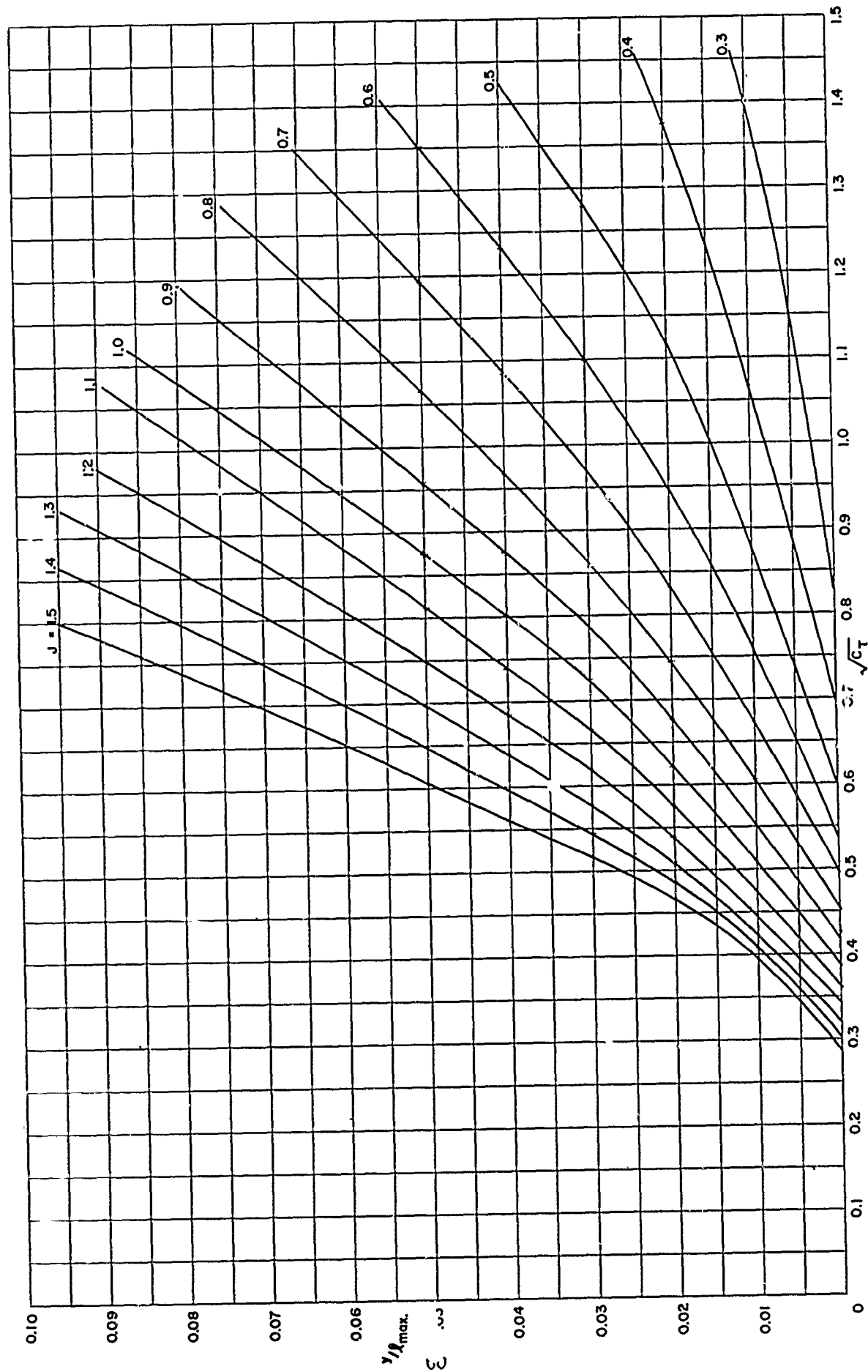
Figure 5f – Maximum Face Ordinate at 0.3 Radius for TMB 3-Bladed SC Propeller Series, EAR = 0.6
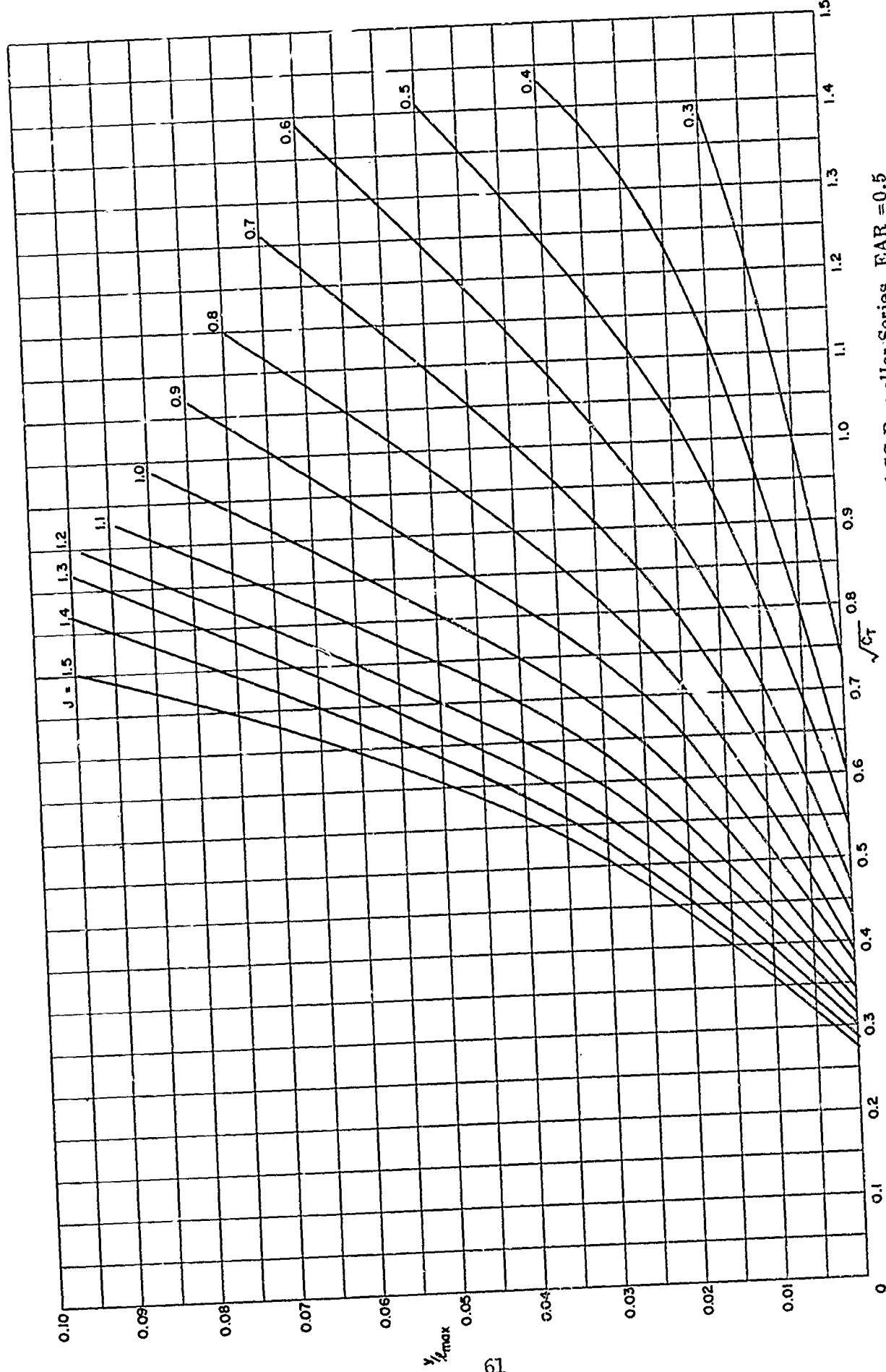
Figure 5g – Maximum Face Ordinate at 0.3 Radius for TMB 4-Bladed SC Propeller Series, EAR = 0.5

61
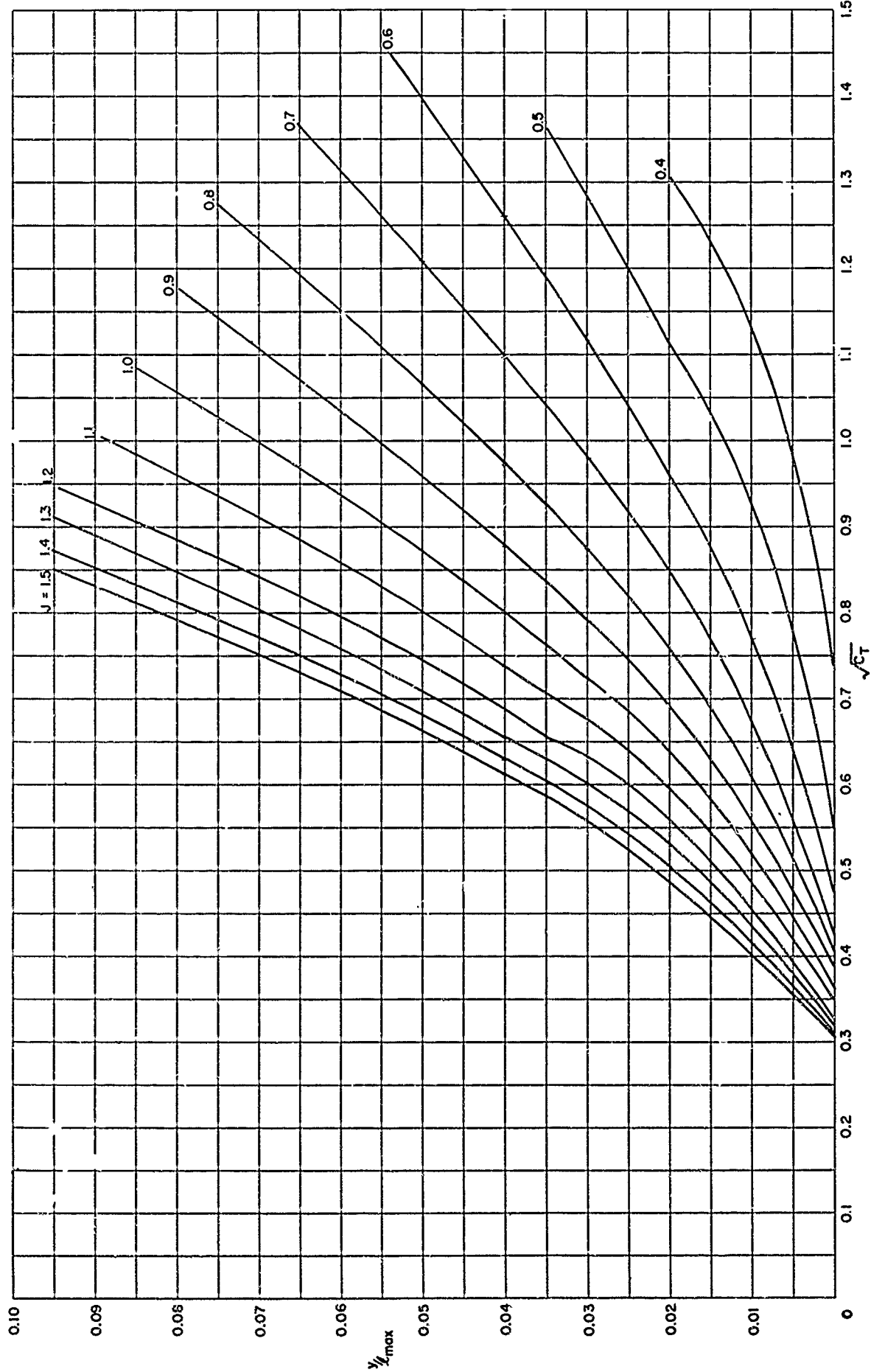
Figure 5h – Maximum Face Ordinate at 0.3 Radius for TMB 4-Bladed SC Propeller Series, EAR = 0.6
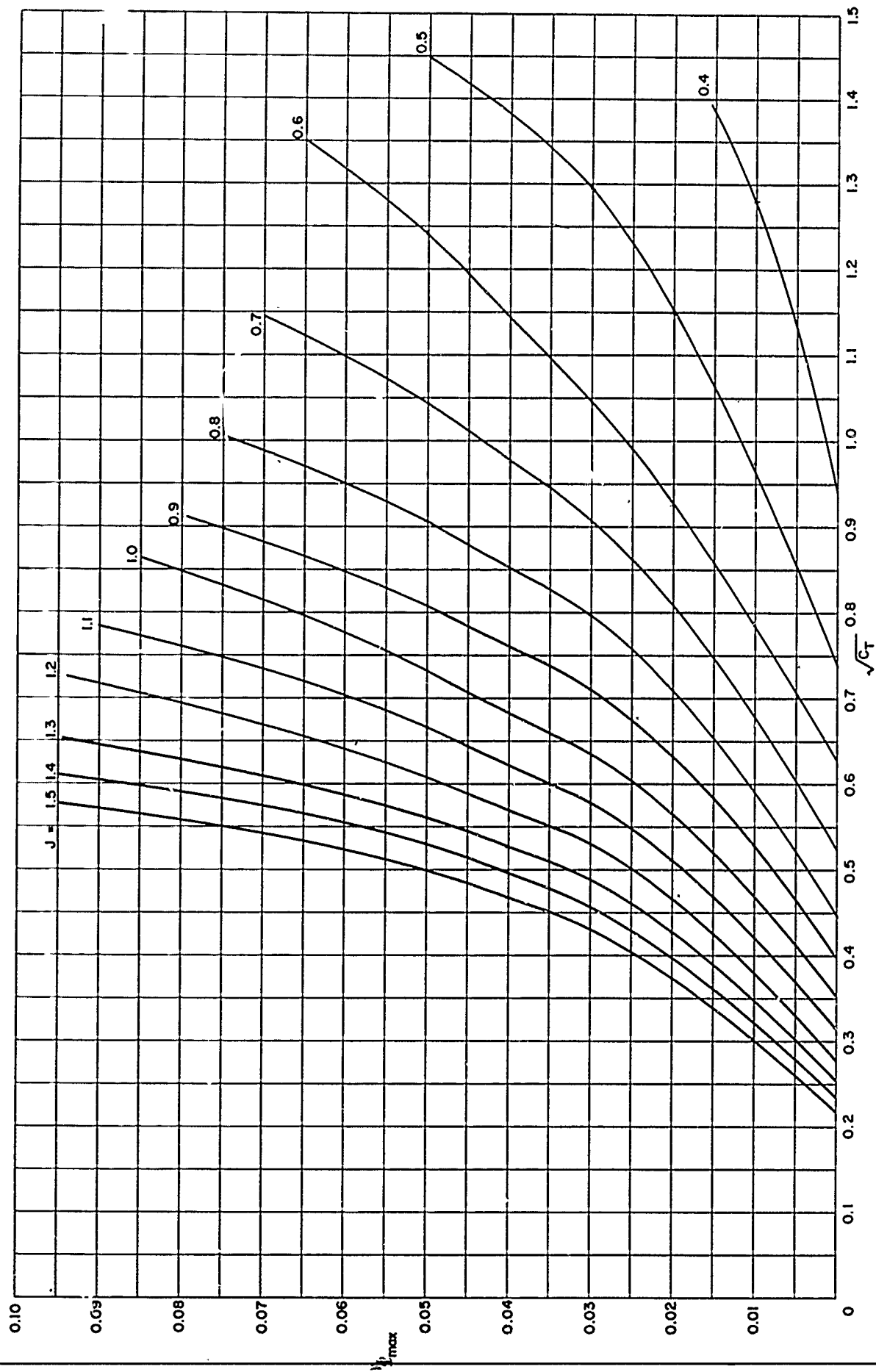
62
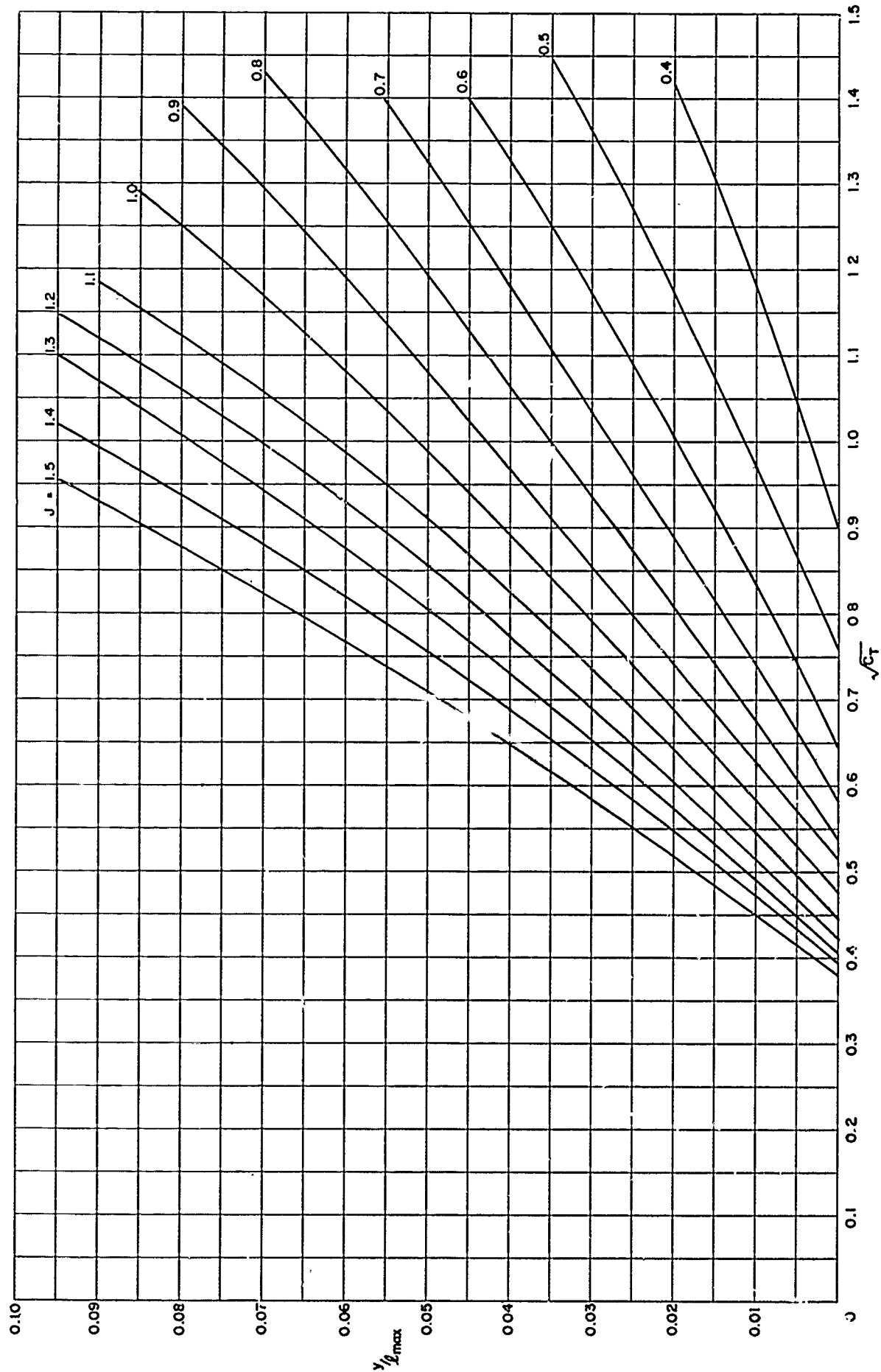
Figure 5i — Maximum Face Ordinate at 0.3 Radius for TMB 4-Bladed SC Propeller Series, EAR = 0.7
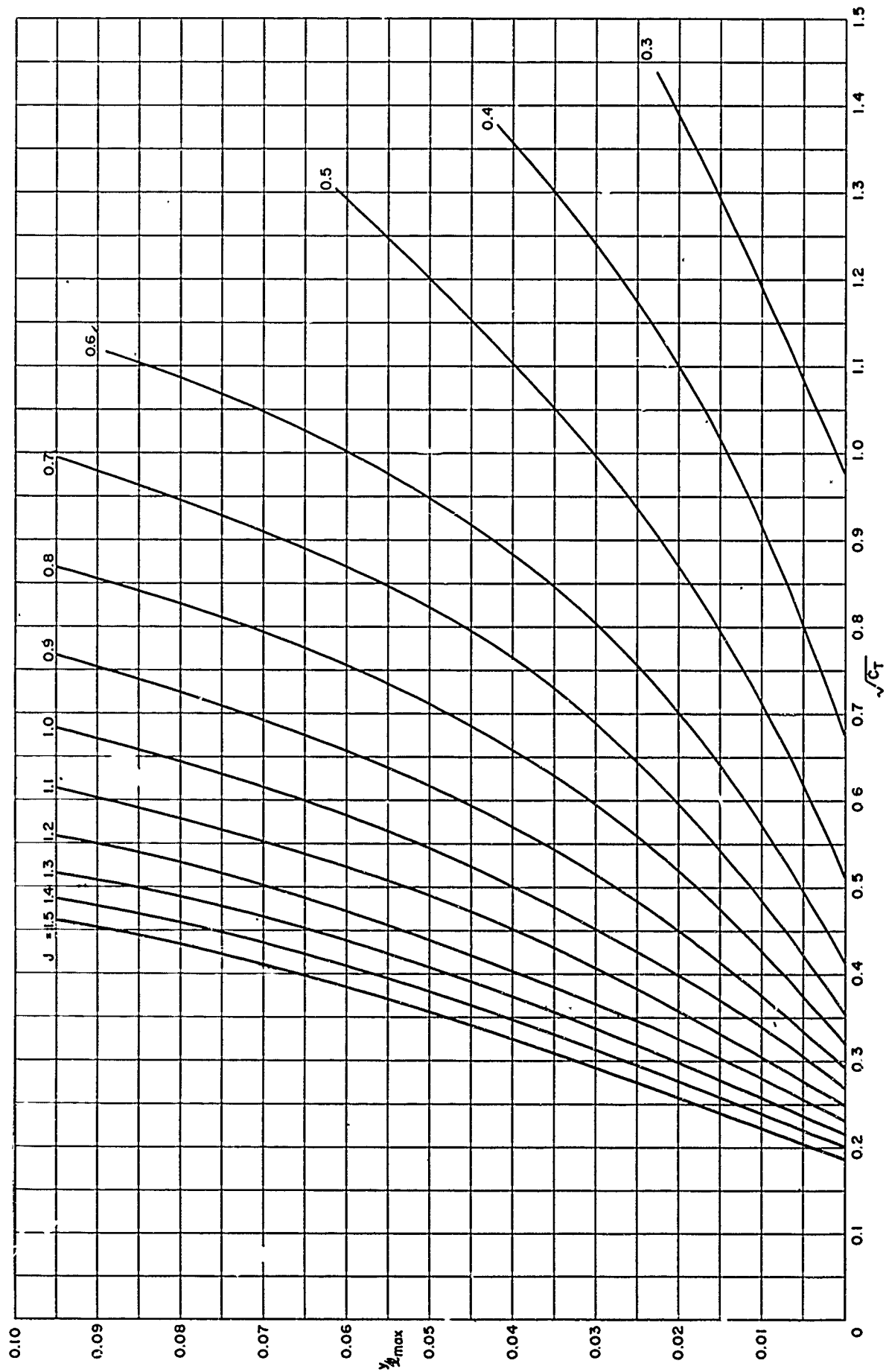
63
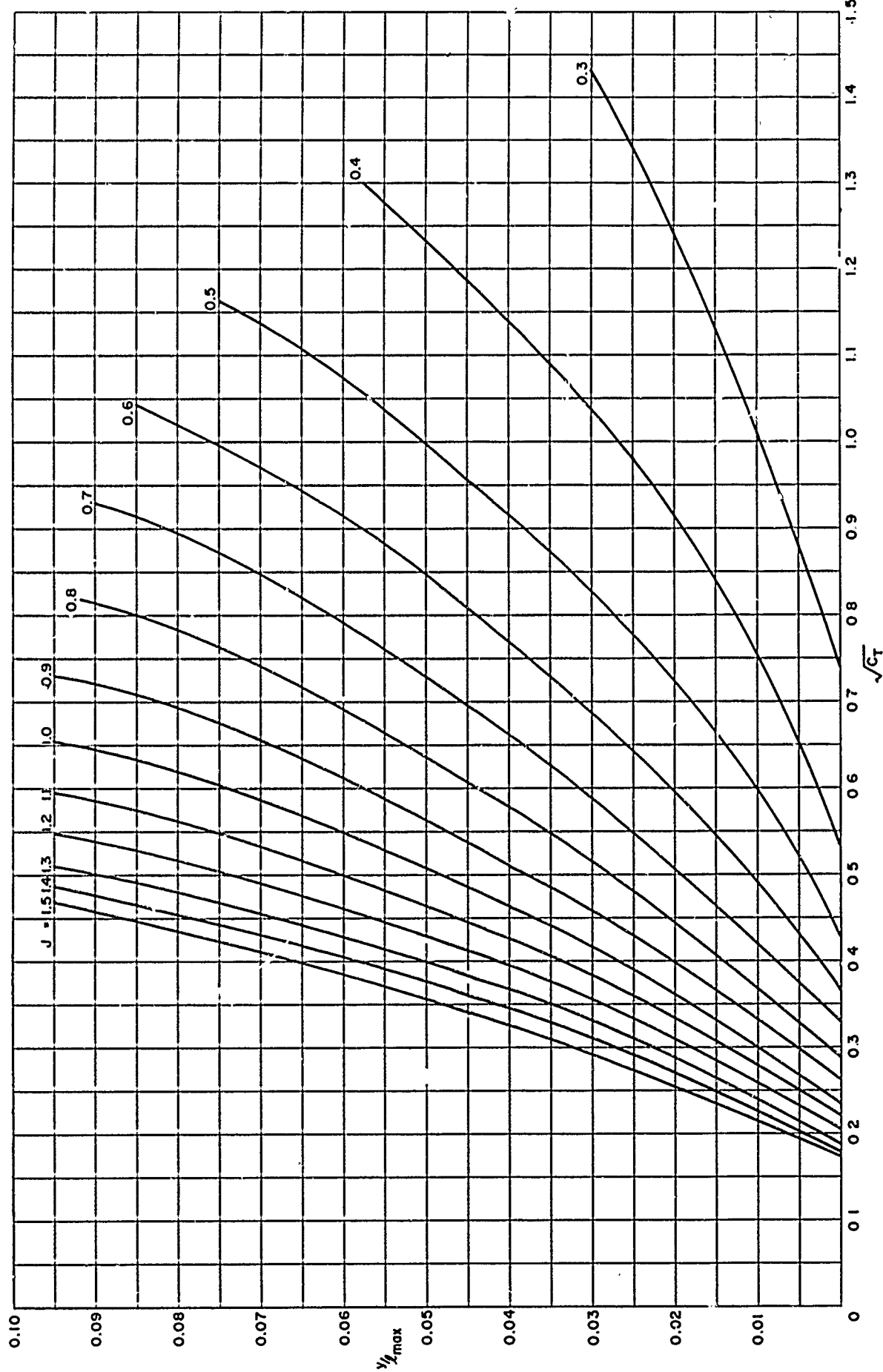
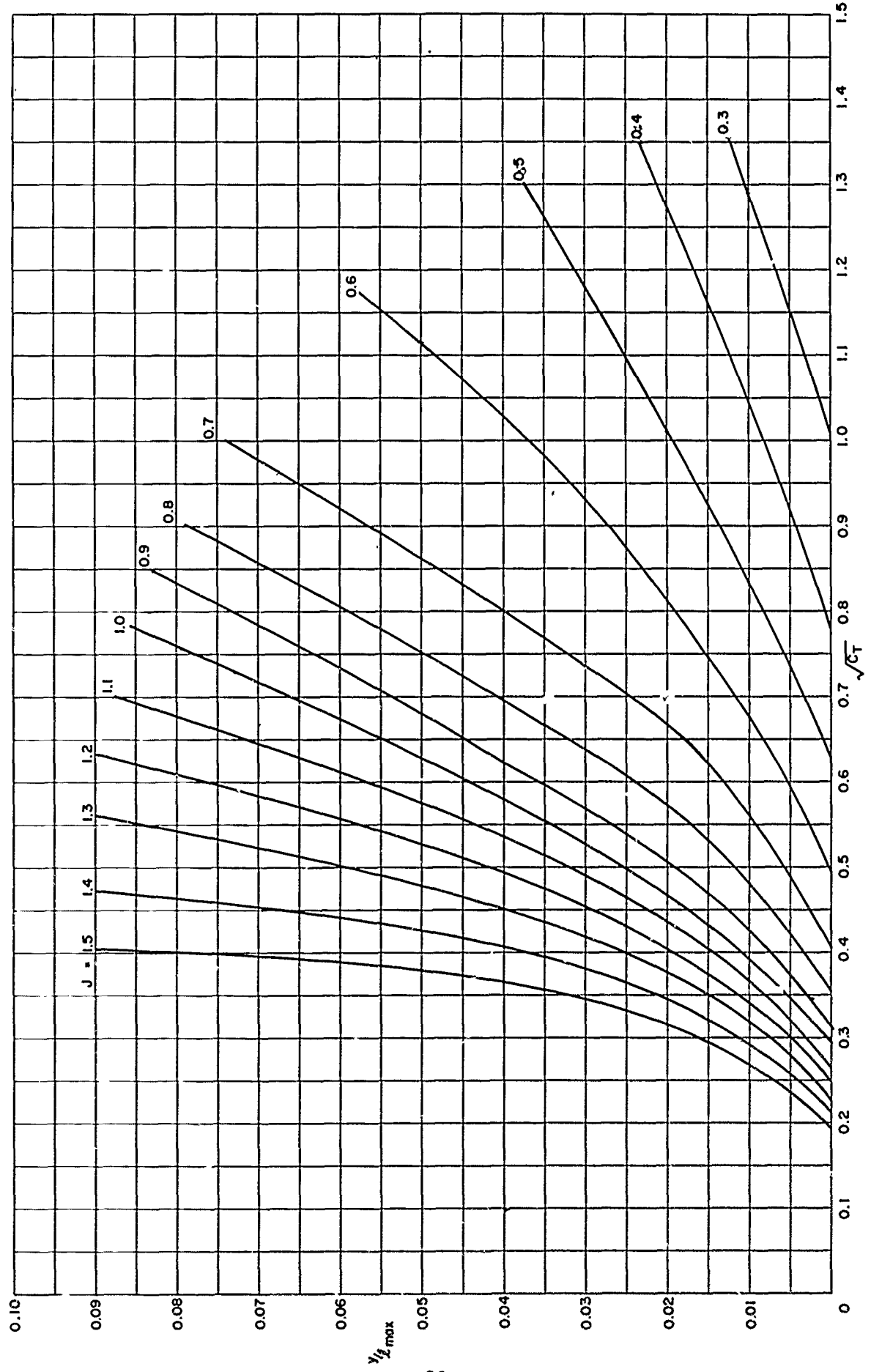Figure 6a — Maximum Face Ordinate at 0.5 Radius for TMB 2-Bladed SC Propeller Series, EAR = 0.3

64
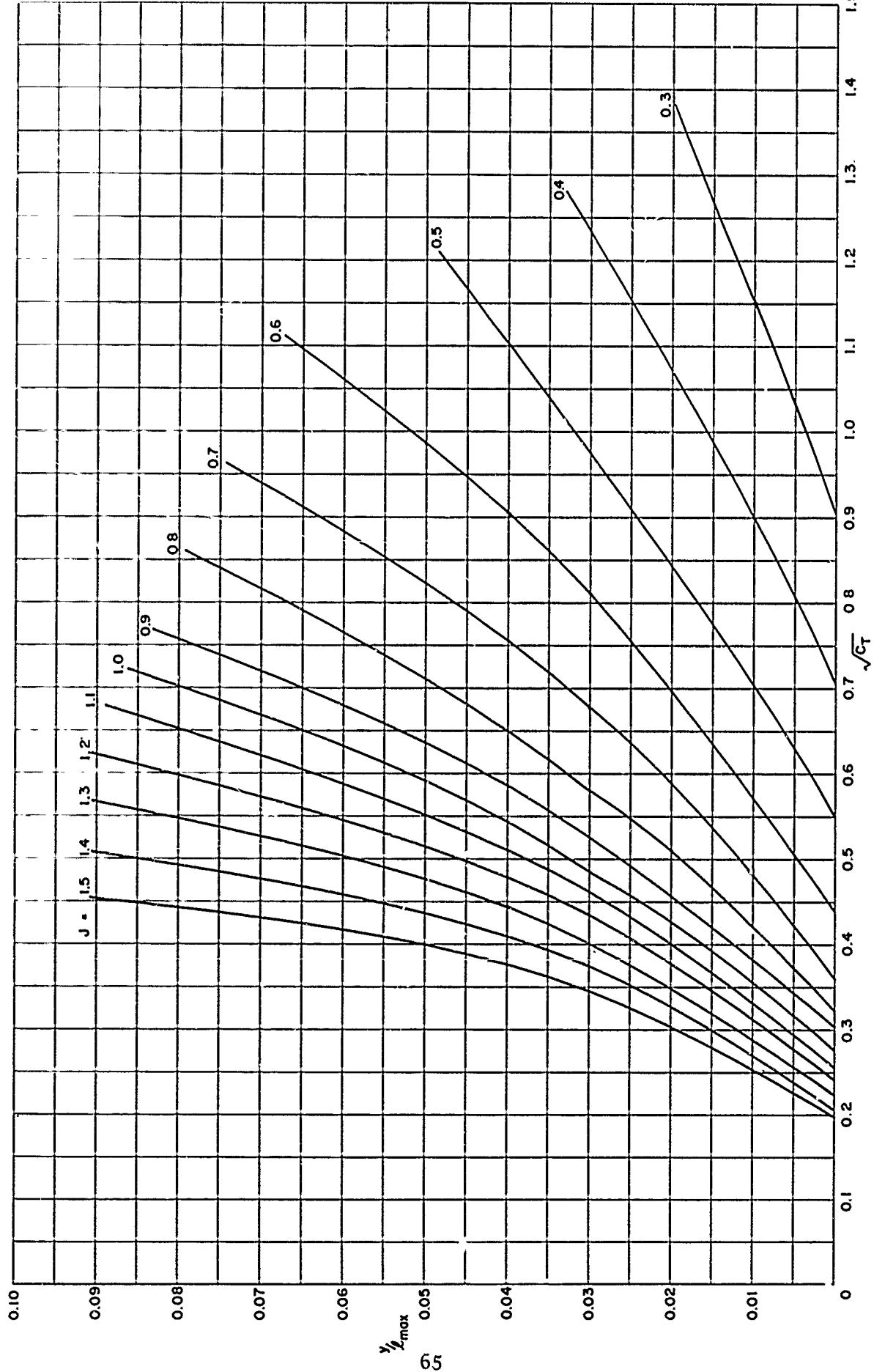
Figure 6b – Maximum Face Ordinate at 0.5 Radius for TMB 2-Bladed SC Propeller Series, EAR = 0.4
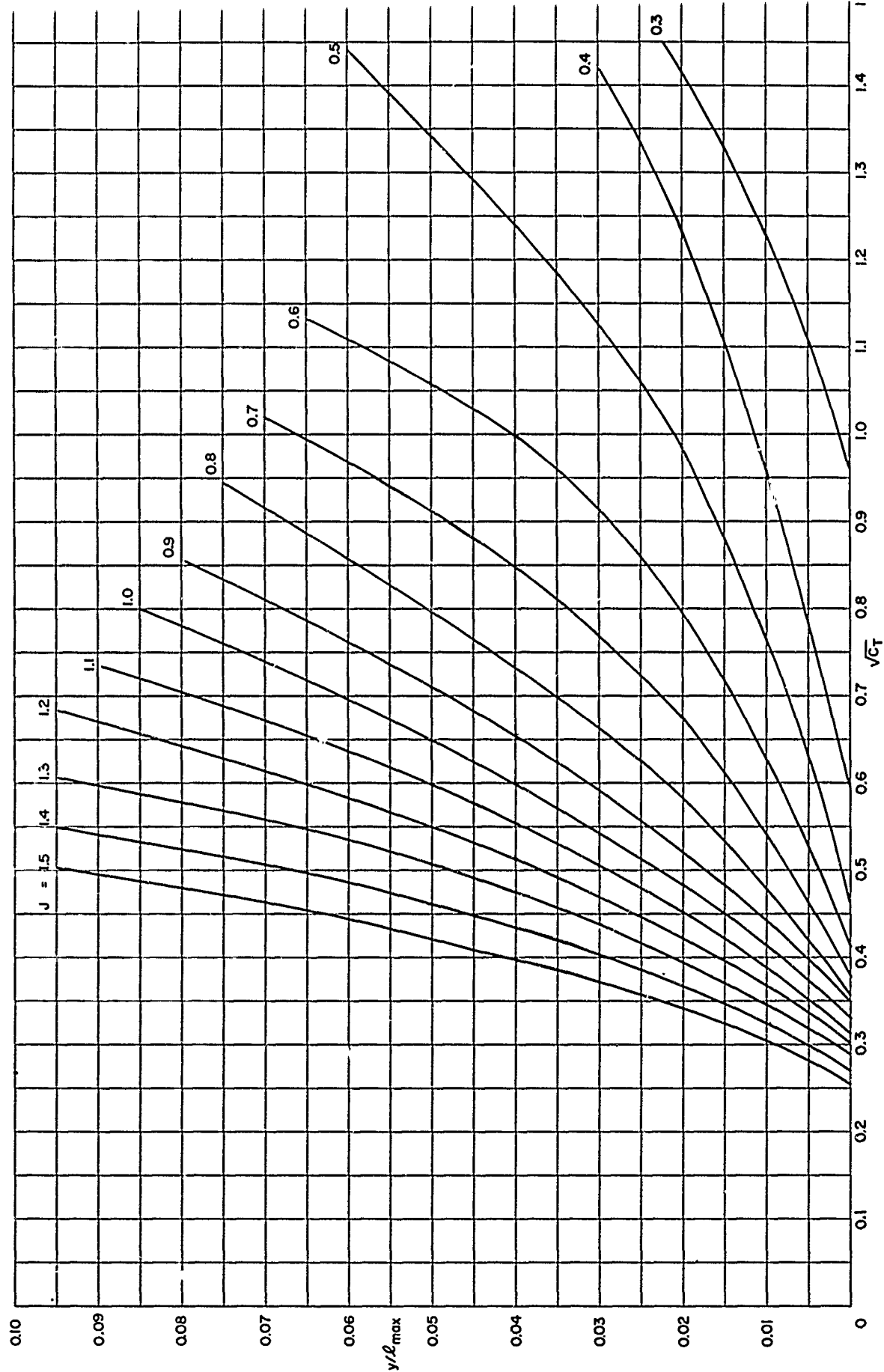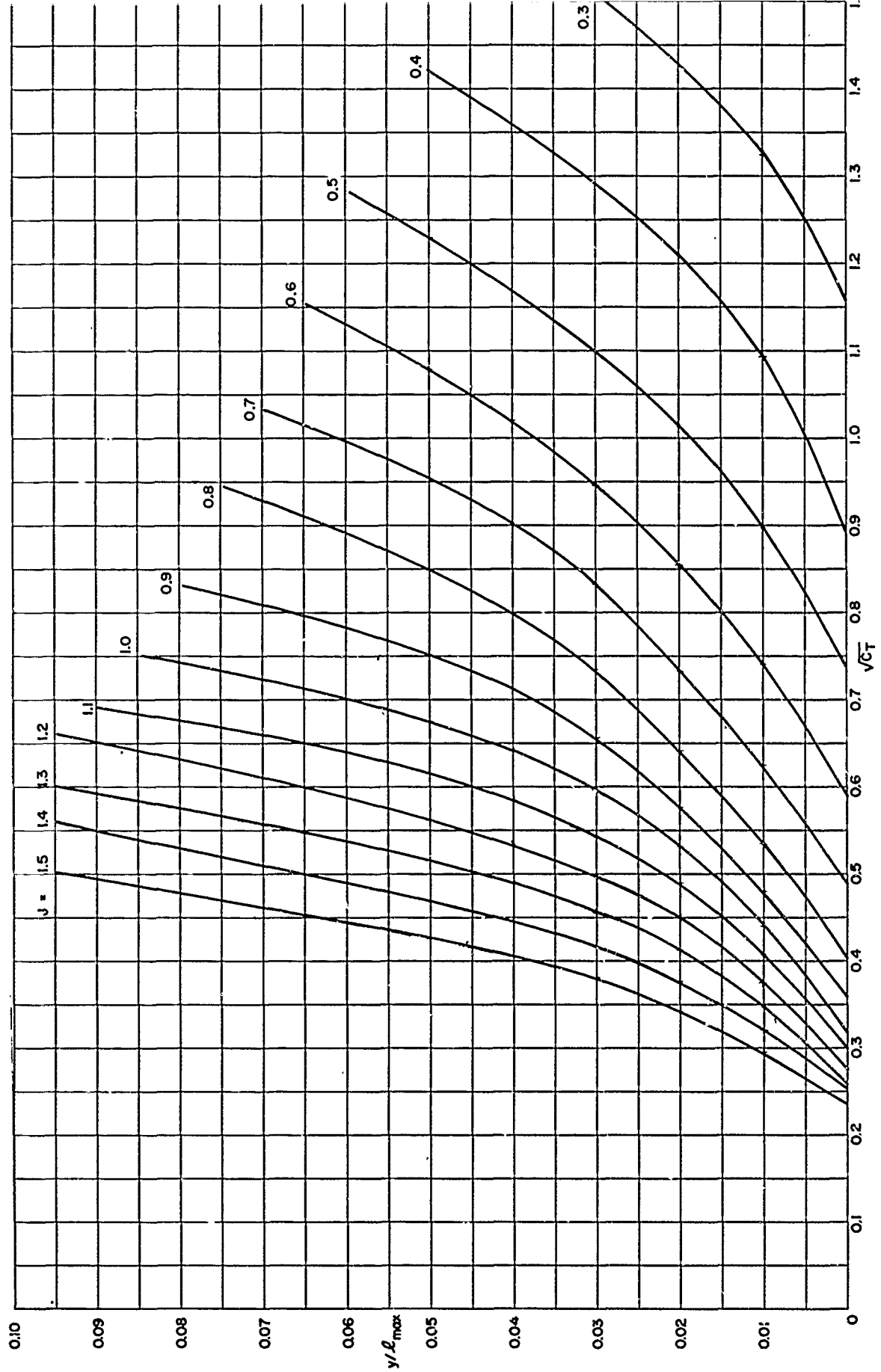
65

Figure 8c – Maximum Face Ordinate at 0.5 Radius for TMB 2-Bladed SC Propeller Series, EAR = 0.5
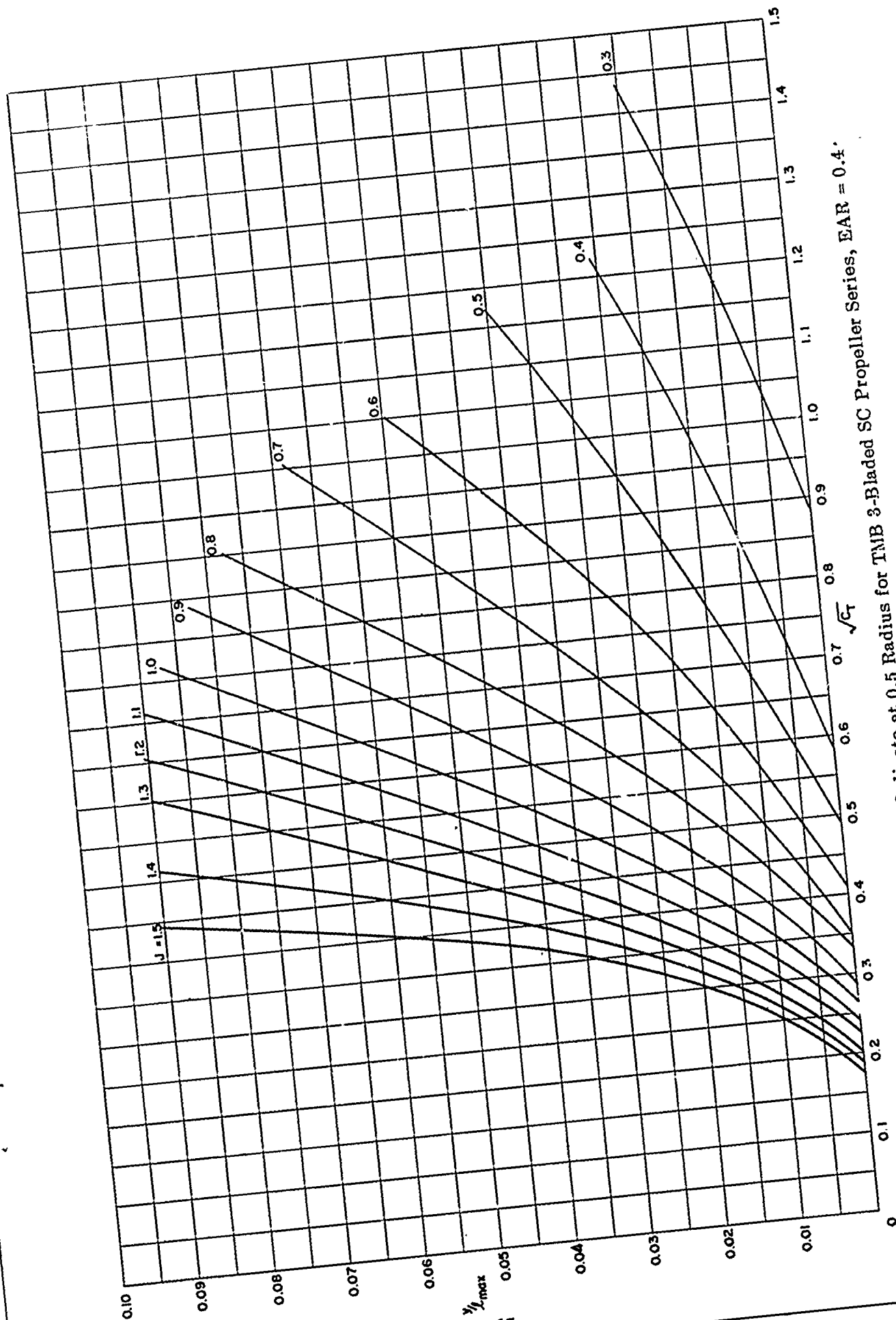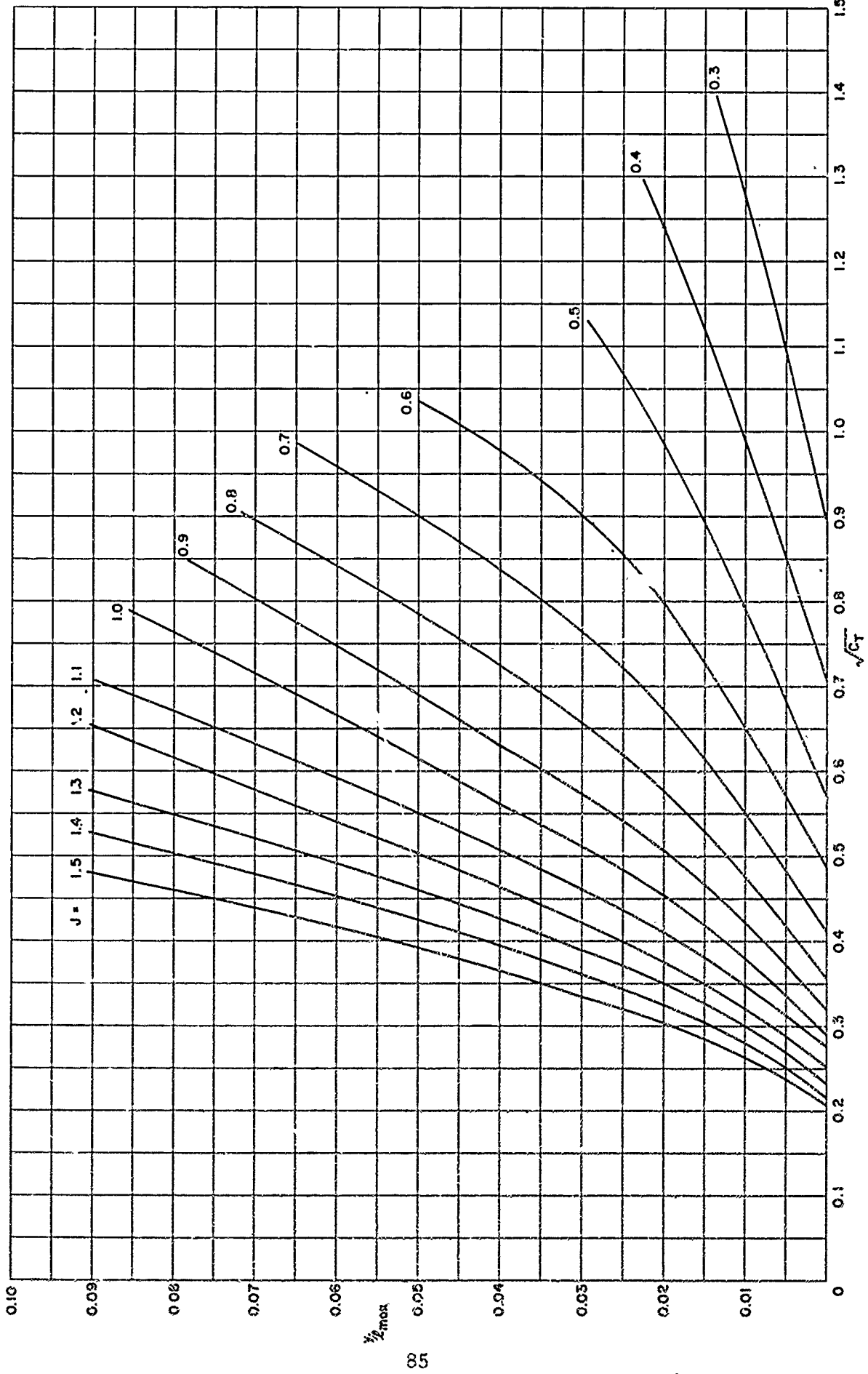
Figure 6d -- Maximum Face Ordinate at 0.5 Radius for TMB 3-Bladed SC Propeller Series, EAR = 0.4
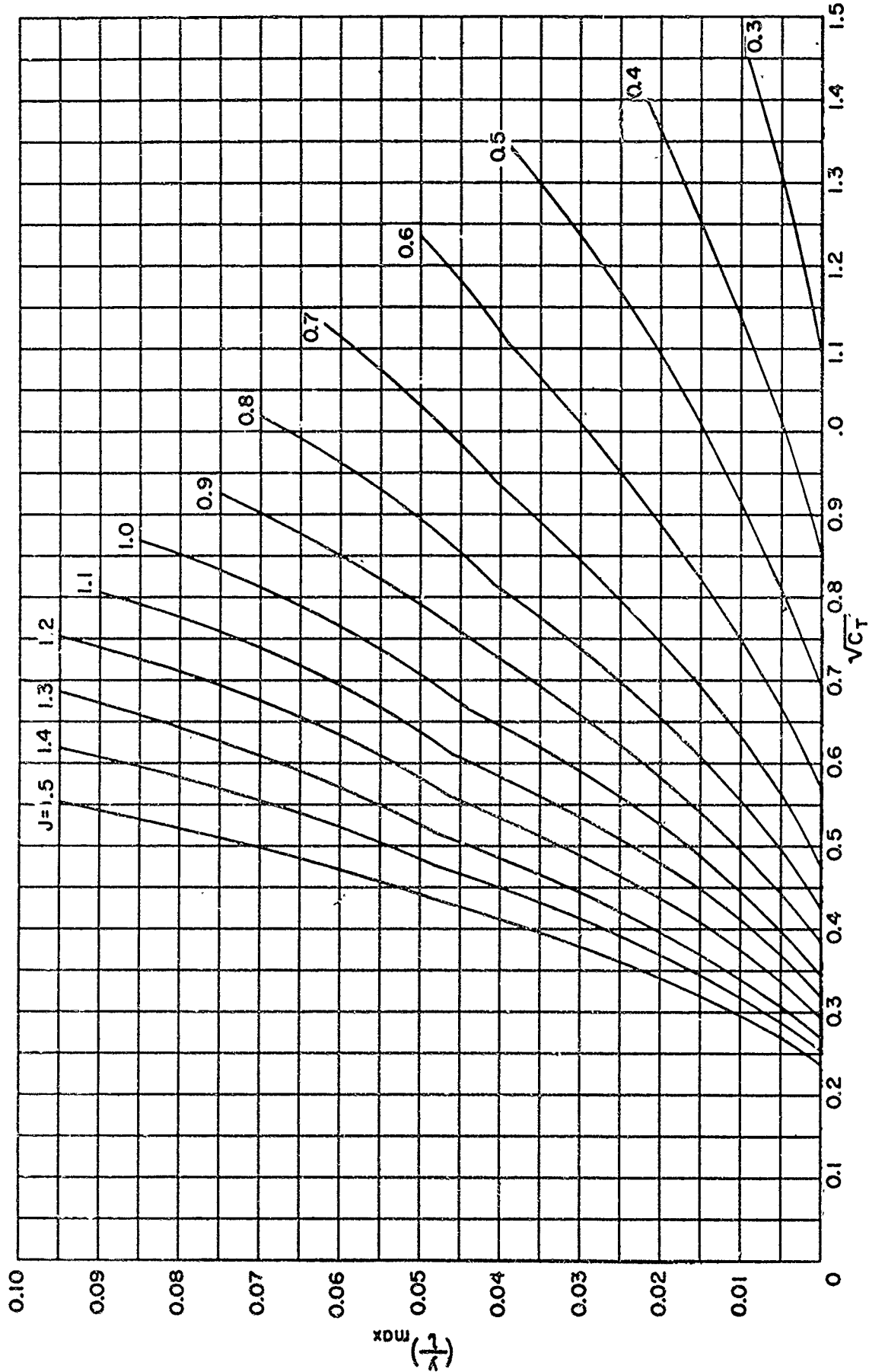
67
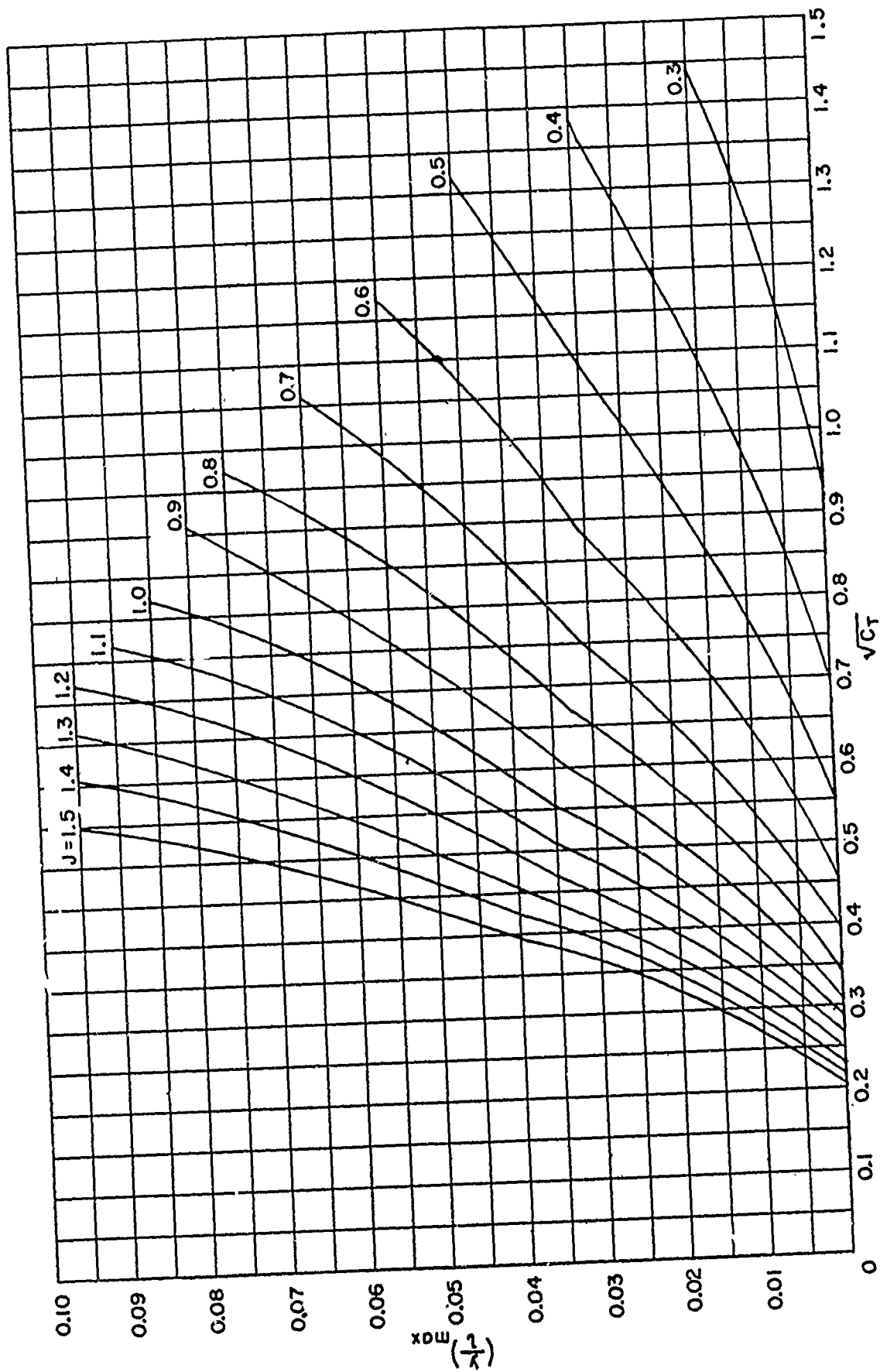
Figure 6e – Maximum Face Ordinate at 0.5 Radius for TMB 3-Bladed SC Propeller Series, EAR = 0.5
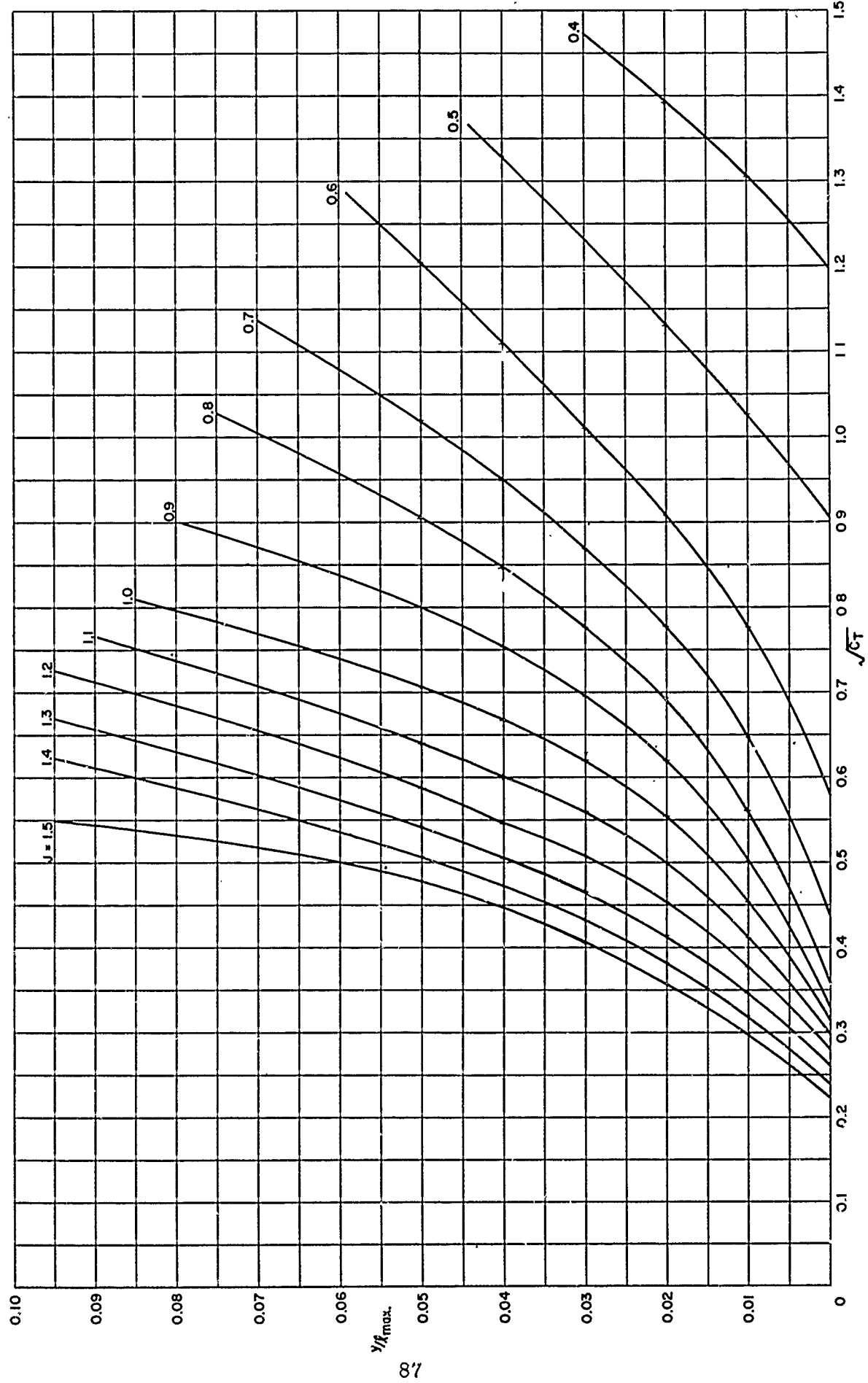
68
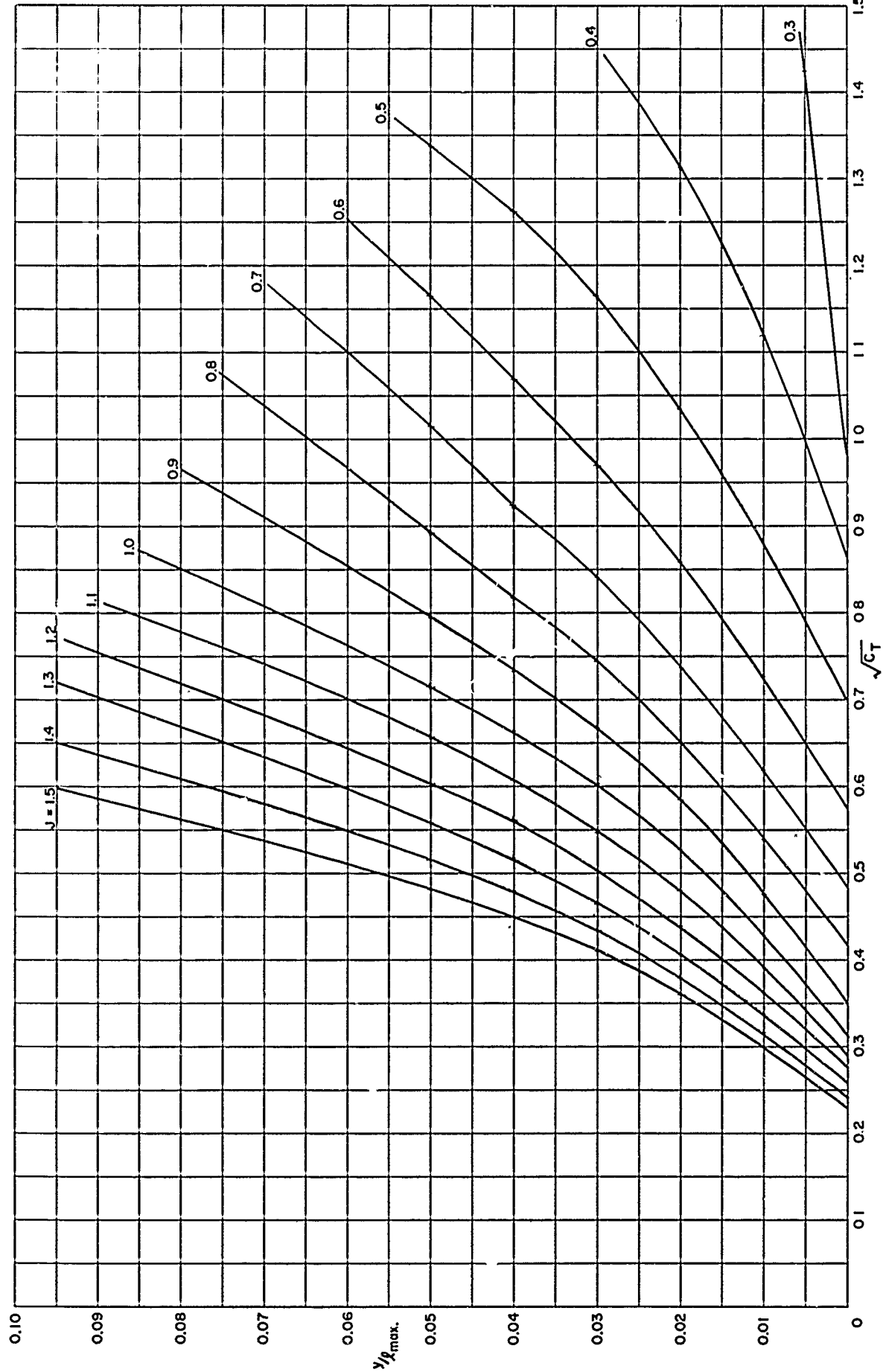
Figure 6f — Maximum Face Ordinate at 0.5 Radius for TMB 3-Bladed SC Propeller Series, EAR = 0.6

69
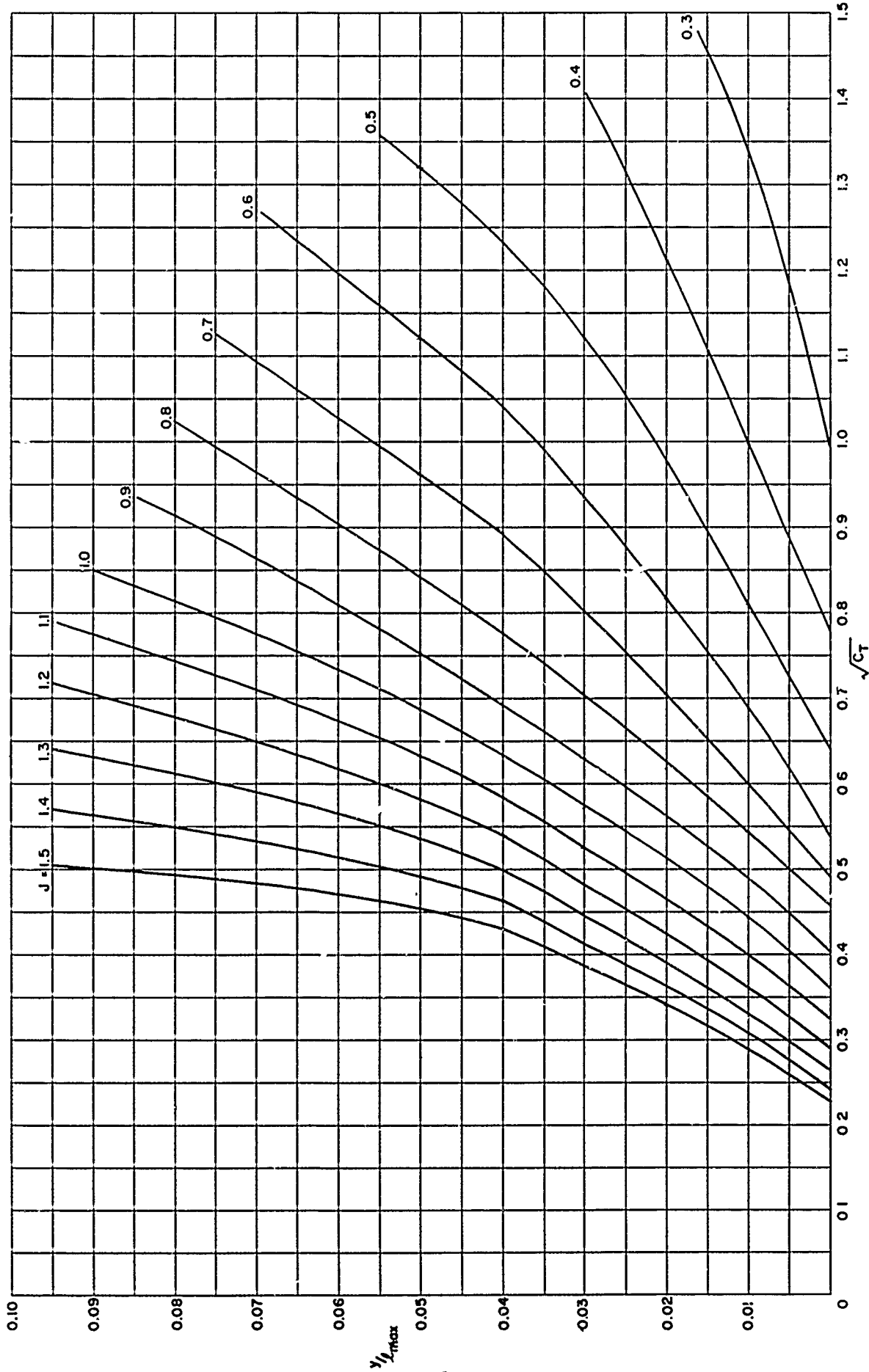
Figure 6g — Maximum Face Ordinate at 0.5 Radius for TMB 4-Bladed SC Propeller Series, EAR = 0.5

70
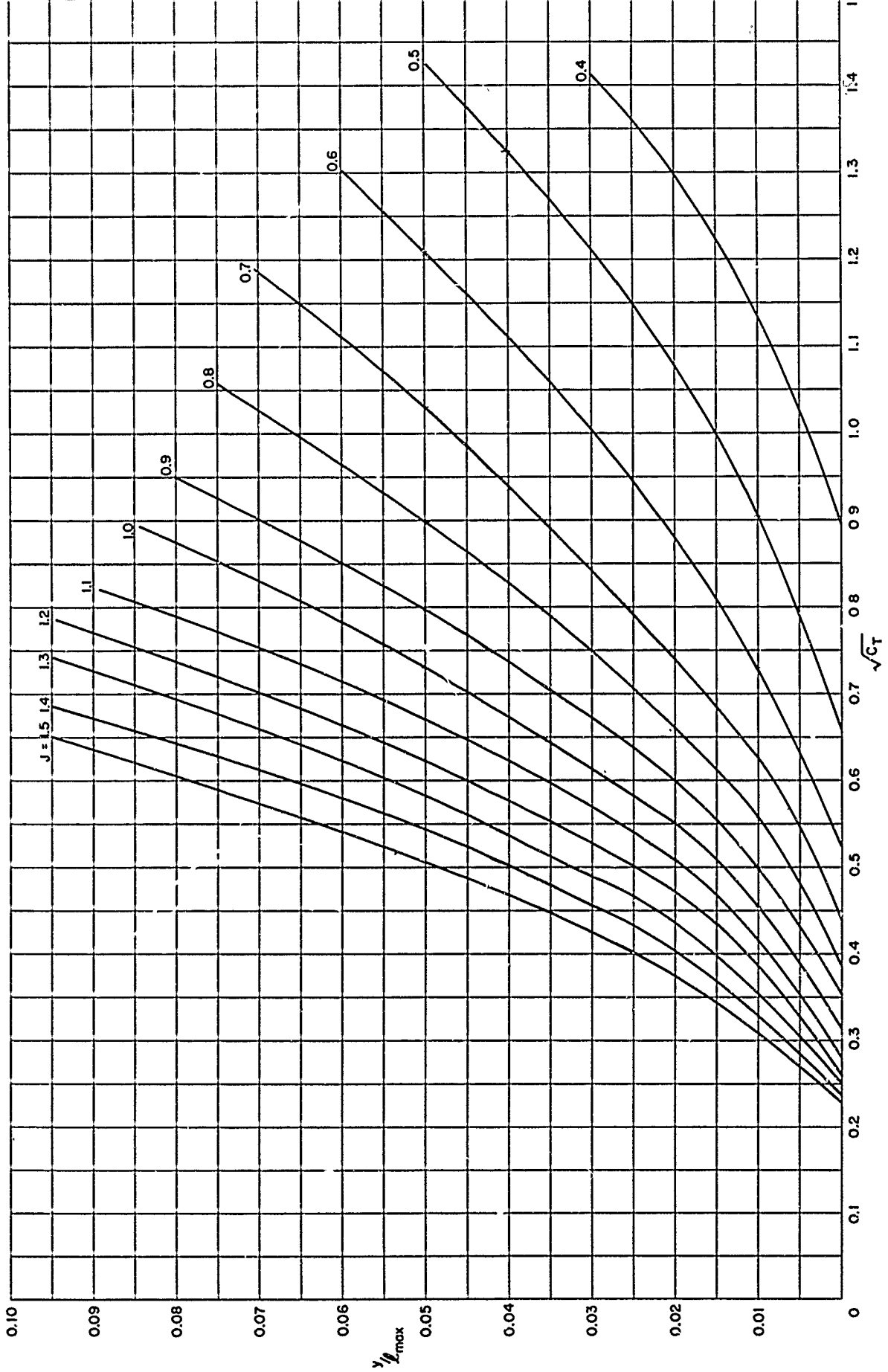
Figure 6h — Maximum Face Ordinate at 0.5 Radius for TMB 4-Bladed SC Propeller Series, EAR = 0.6

71
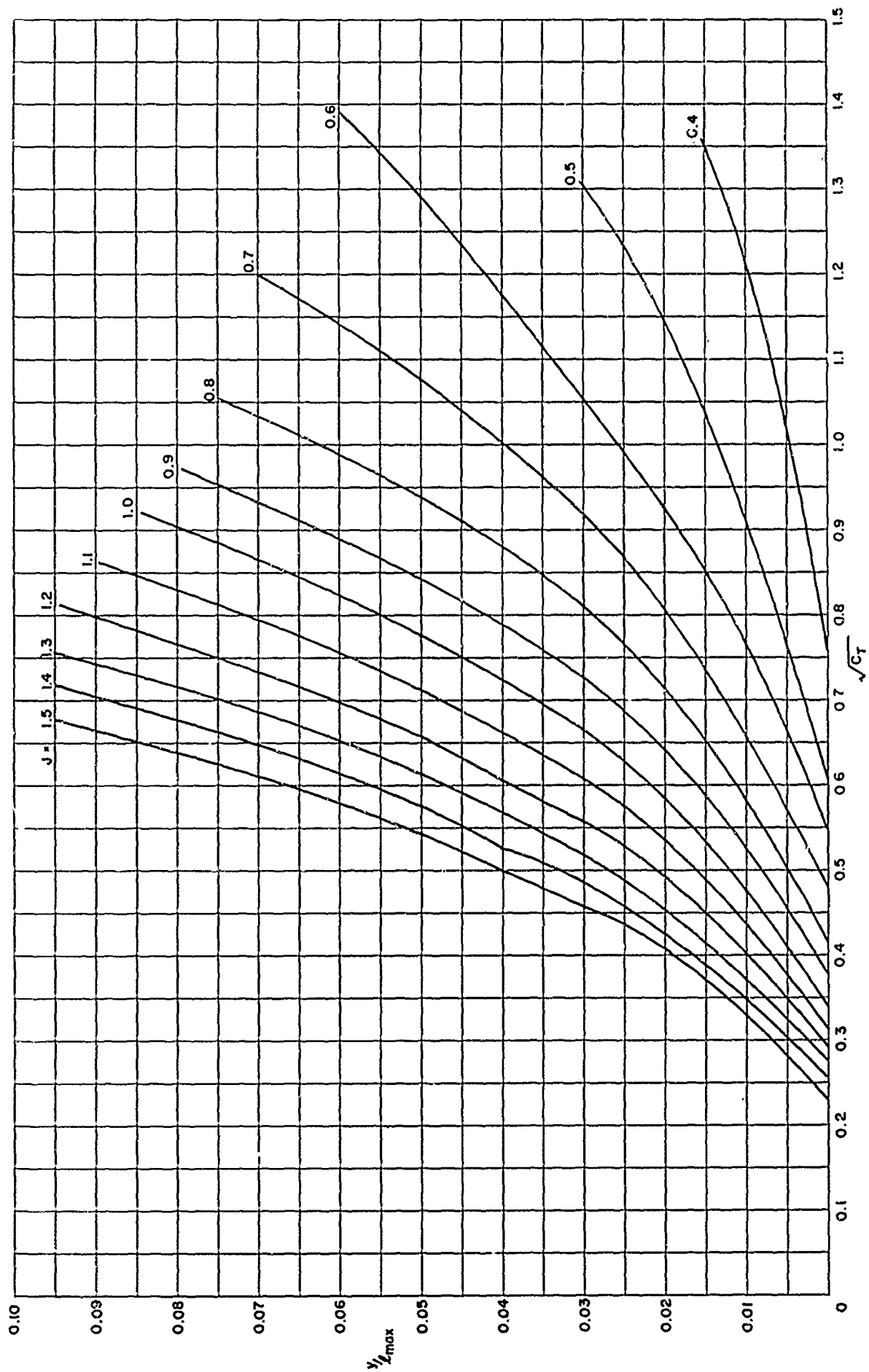
Figure 6i — Maximum Face Ordinate at 0.5 Radius for TMB 4-Bladed SC Propeller Series, EAR = 0.7

72
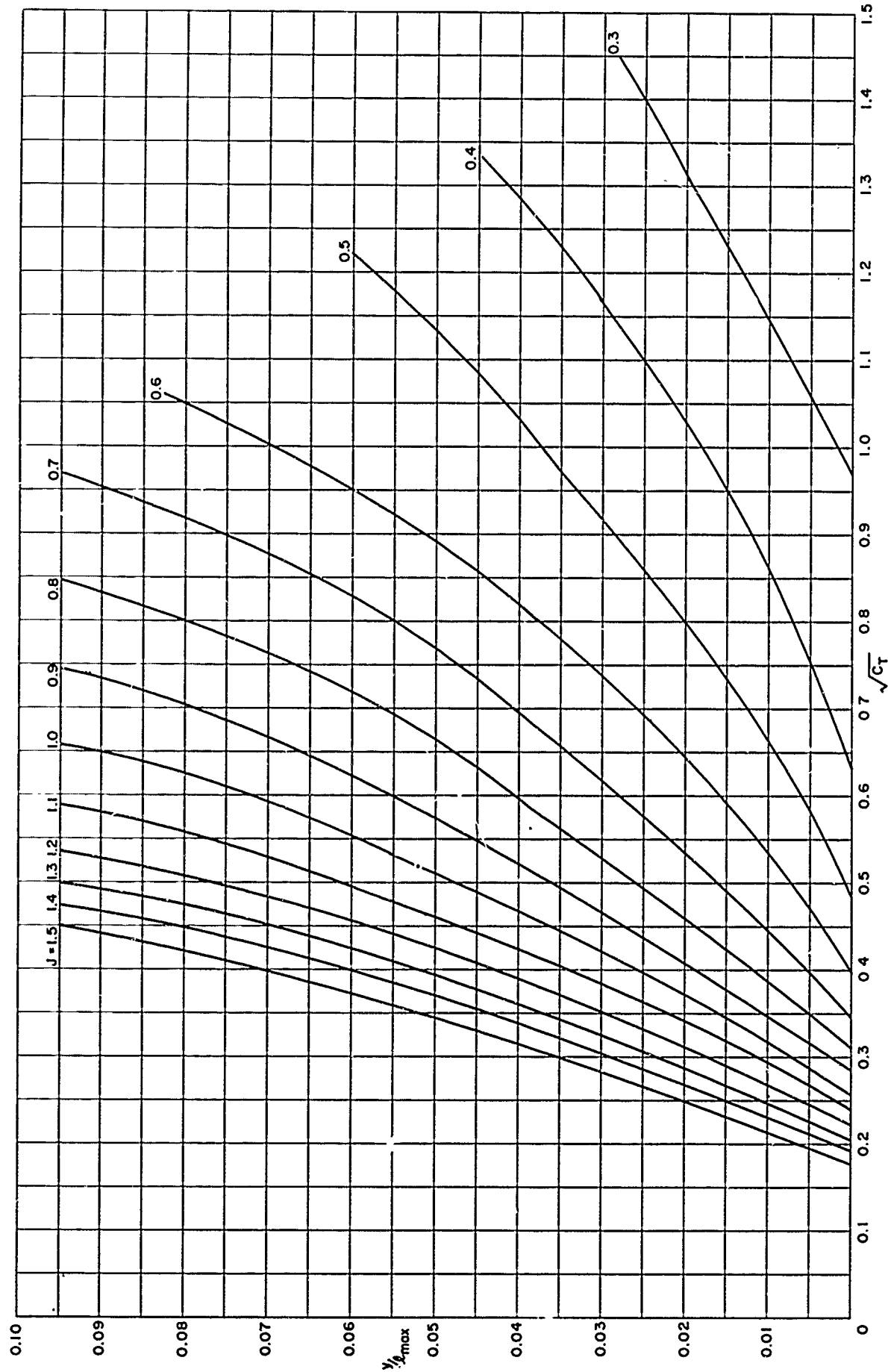
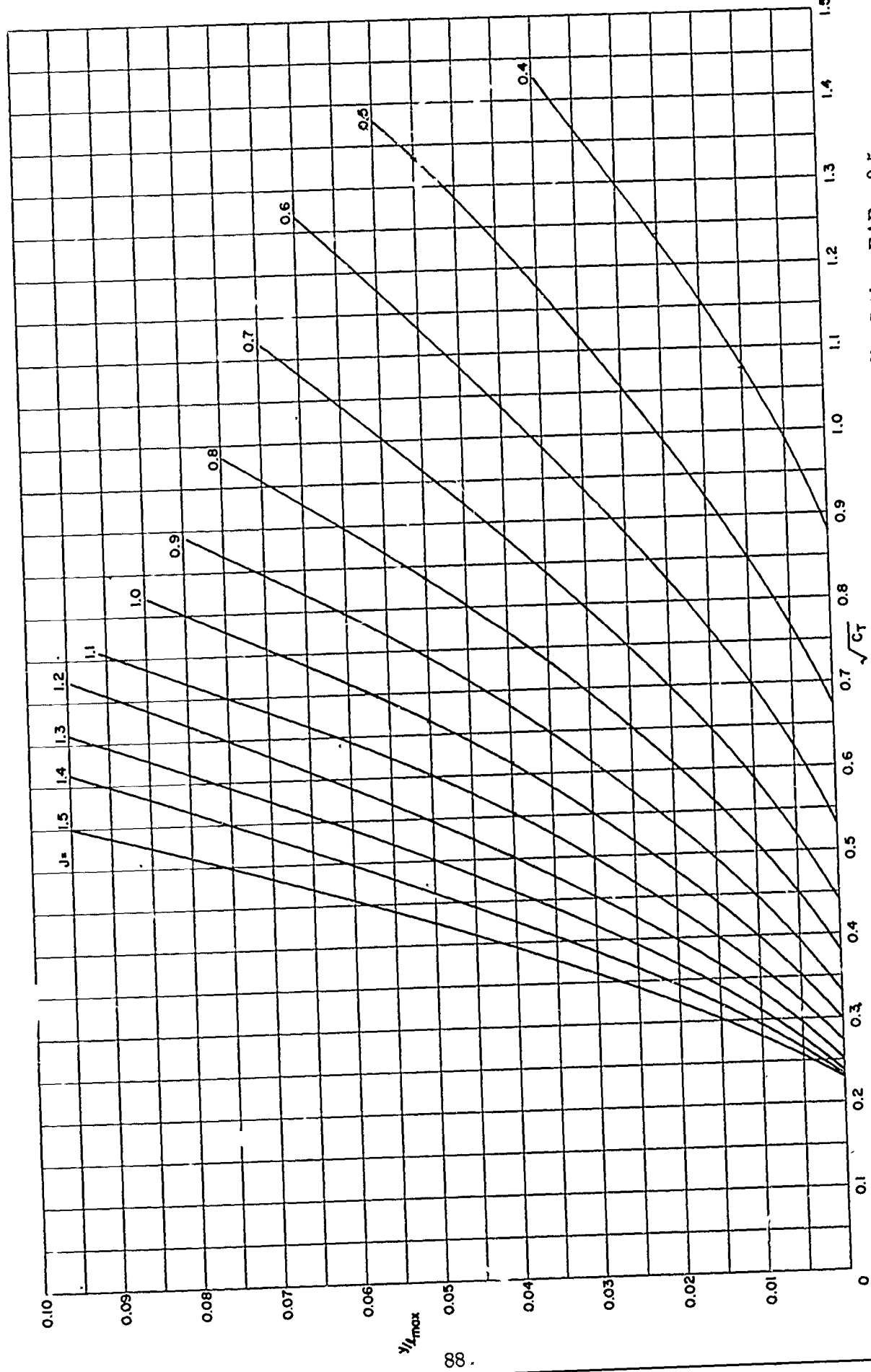Figure 7a — Maximum Face Ordinate at 0.7 Radius for TMB 2-Bladed SC Propeller Series, EAR = 0.3
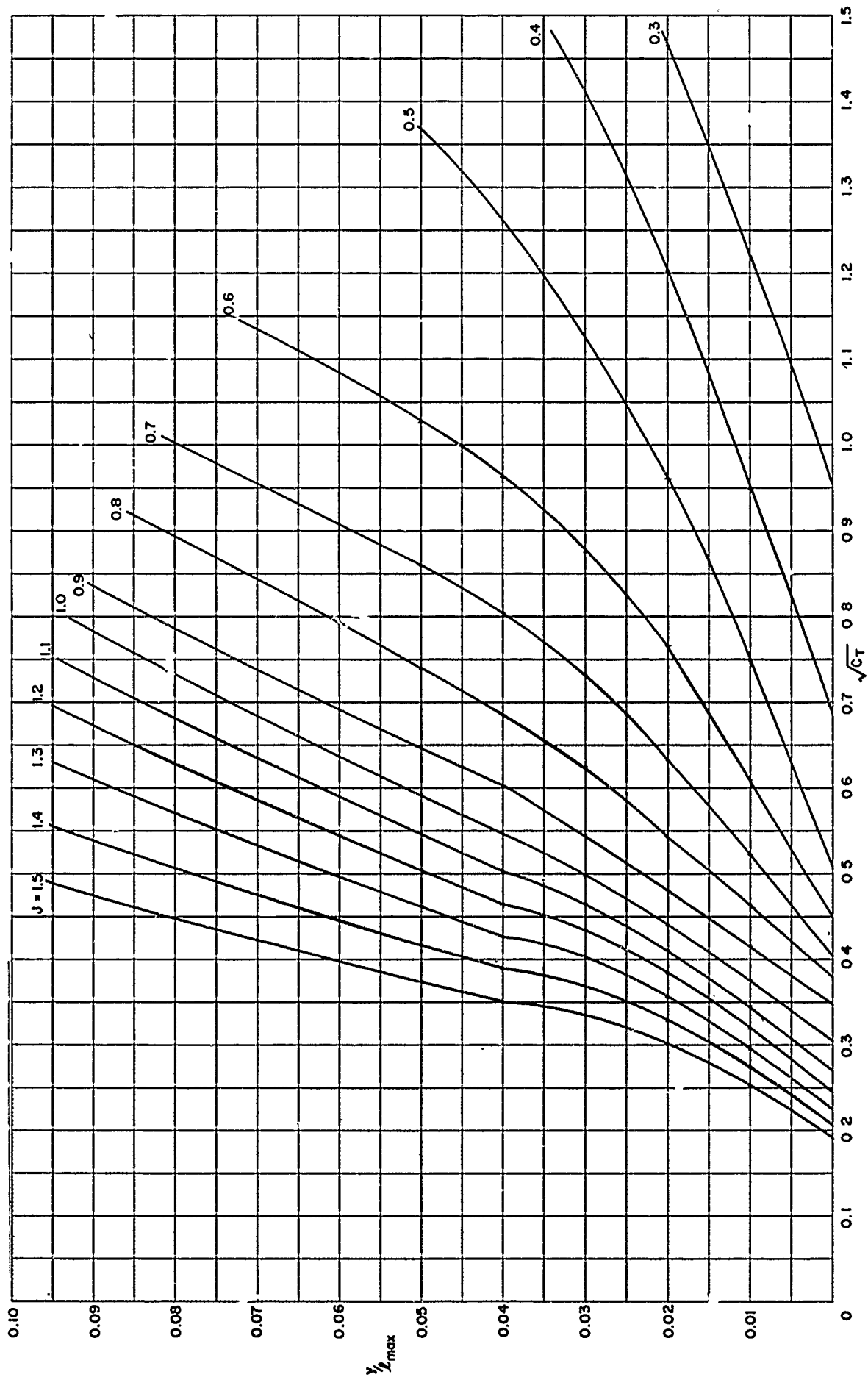
Figure 7b – Maximum Face Ordinate at 0.7 Radius for TMB 2-Bladed SC Propeller Series, EAR = 0.4
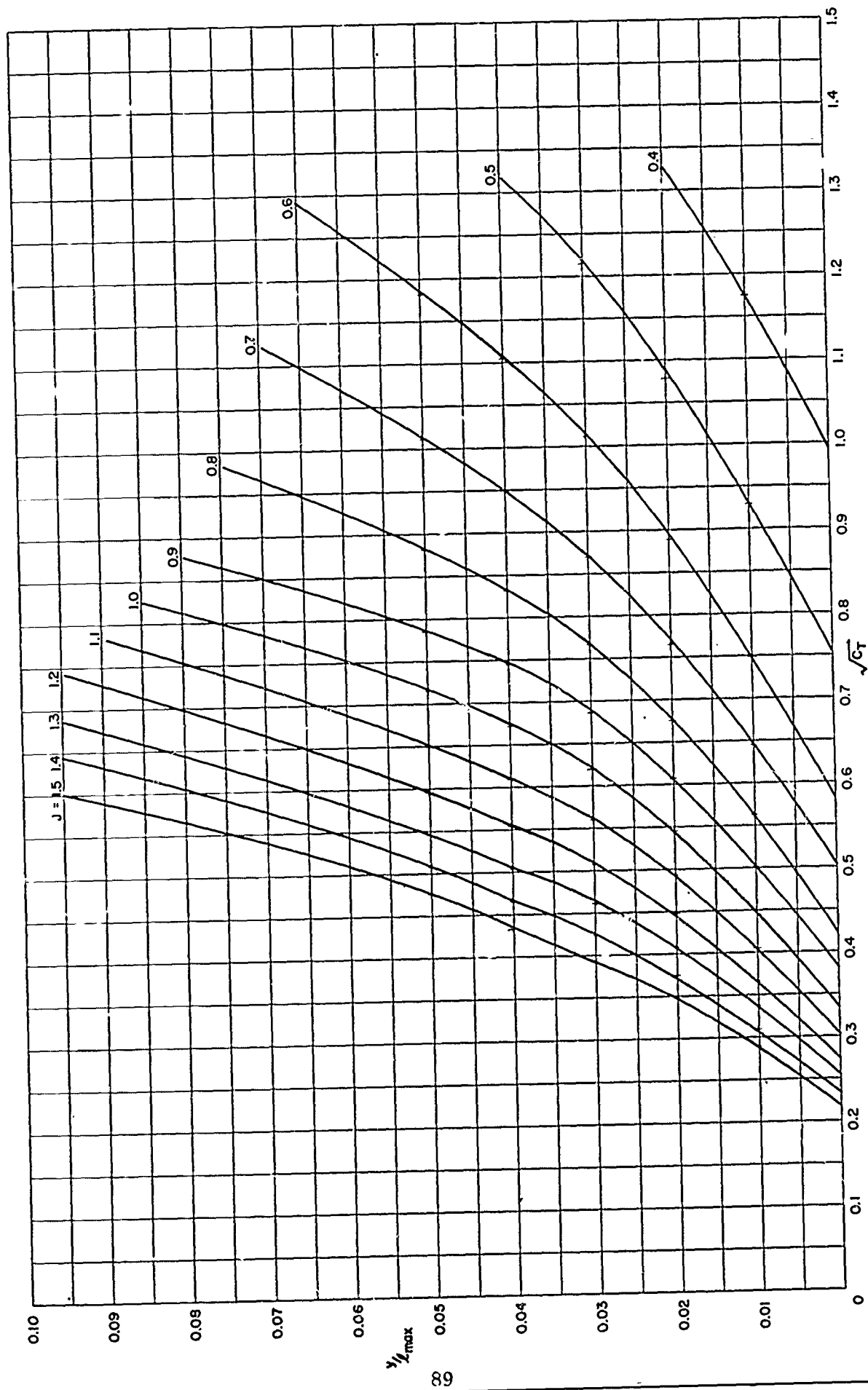
74
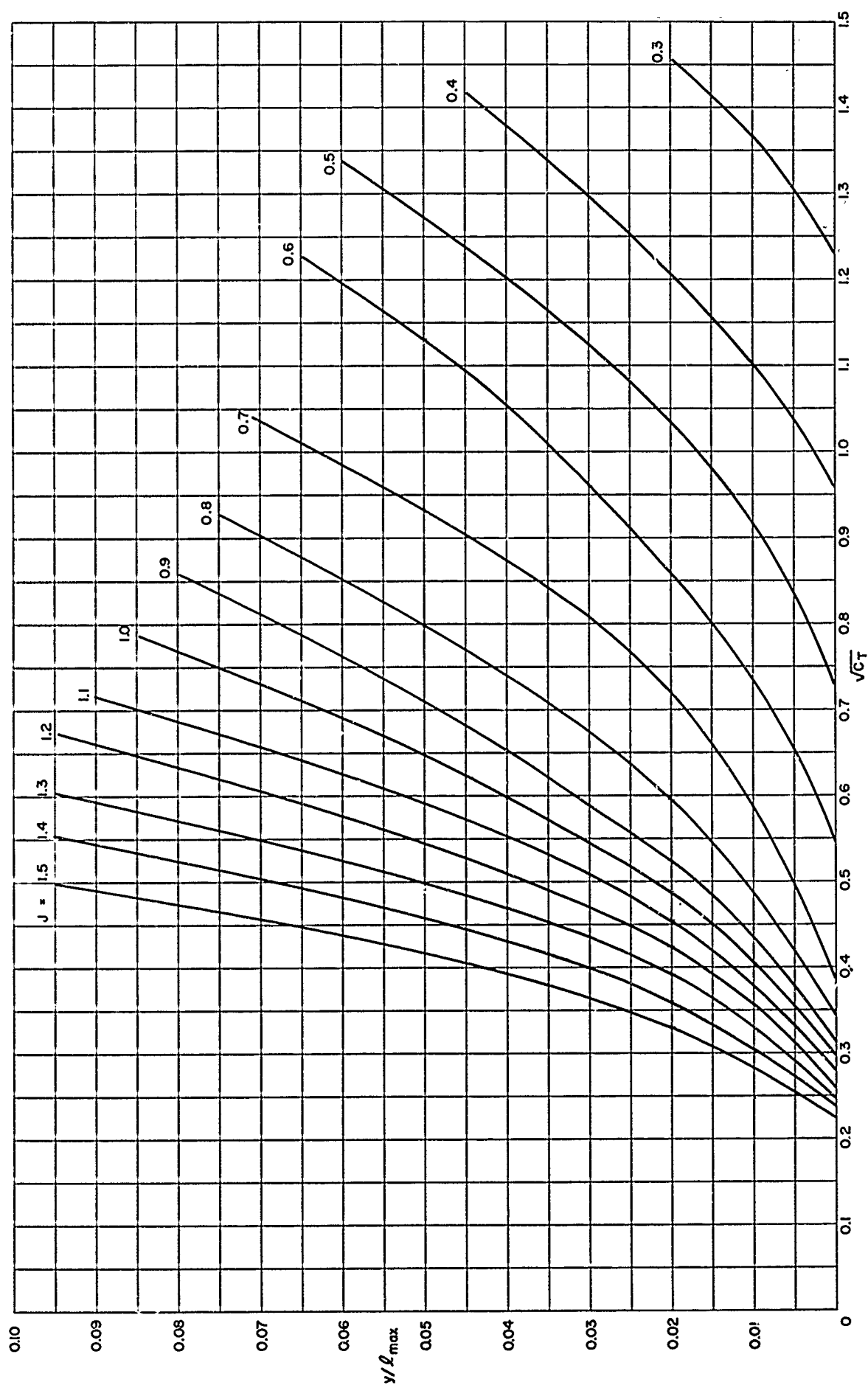
Figure 7c — Maximum Face Ordinate at 0.7 Radius for TMB 2-Bladed SC Propeller Series, EAR = 0.5

75

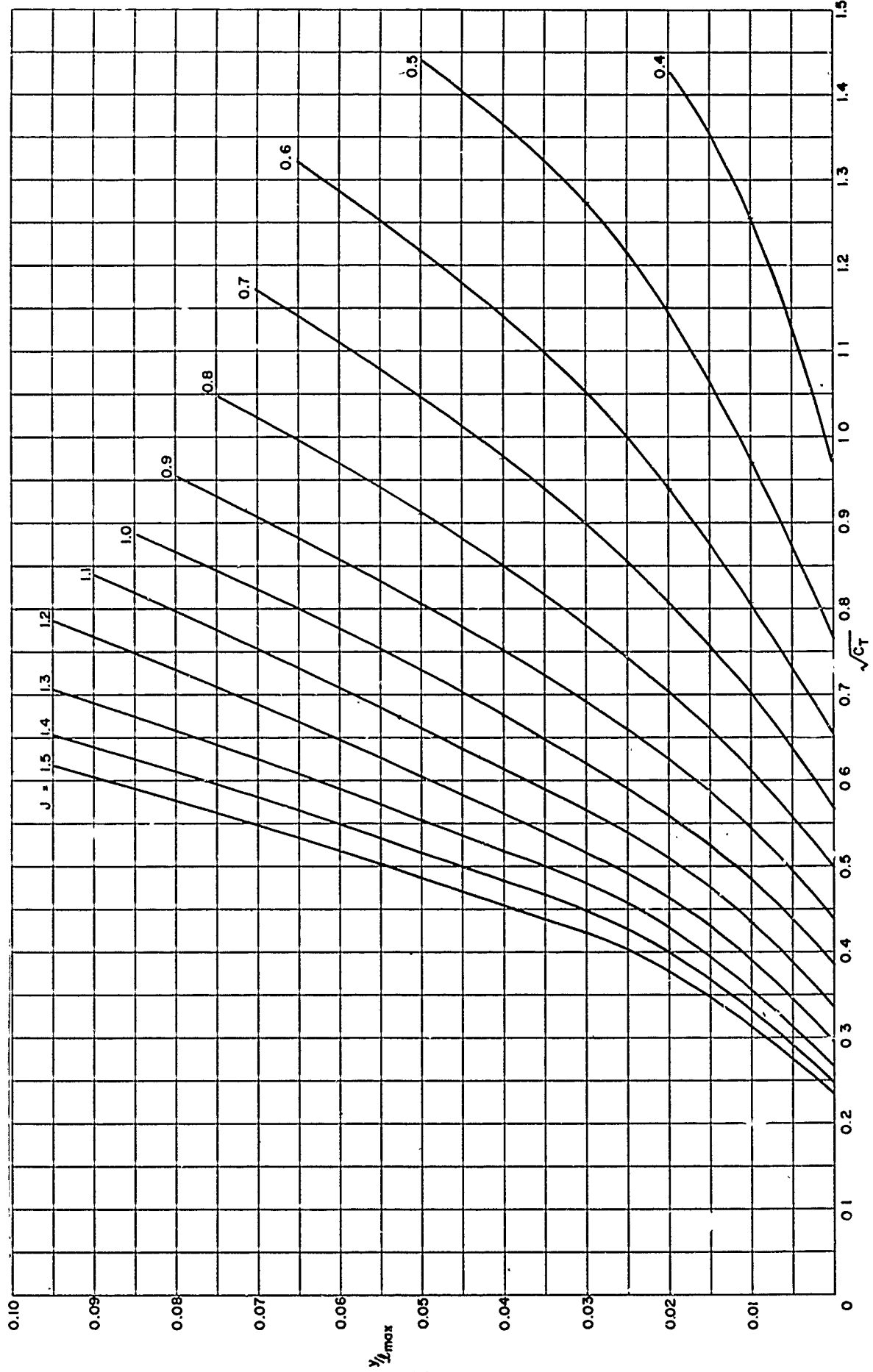Figure 7d — Maximum Face Ordinate at 0.7 Radius for TMB 3-Bladed SC Propeller Series, EAR = 0.4

76

Figure 7e — Maximum Face Ordinate at 0.7 Radius for TMB 3-Bladed SC Propeller Series, EAR = 0.5

77

Figure 7f — Maximum Face Ordinate at 0.7 Radius for TMB 3-Bladed SC Propeller Series, EAR = 0.6

Figure 7g — Maximum Face Ordinate at 0.7 Radius for TMB 4-Bladed SC Propeller Series, EAR = 0.5

79

Figure 7h – Maximum Face Ordinate at 0.7 Radius for TMB 4-Bladed SC Propeller Series, EAR = 0.6

Figure 7i — Maximum Face Ordinate at 0.7 Radius for TMB 4-Bladed SC Propeller Series, EAR = 0.7

Figure 8a -- Maximum Face Ordinate at 0.9 Radius for TMB 2-Bladed SC Propeller Series, EAR = 0.3

82

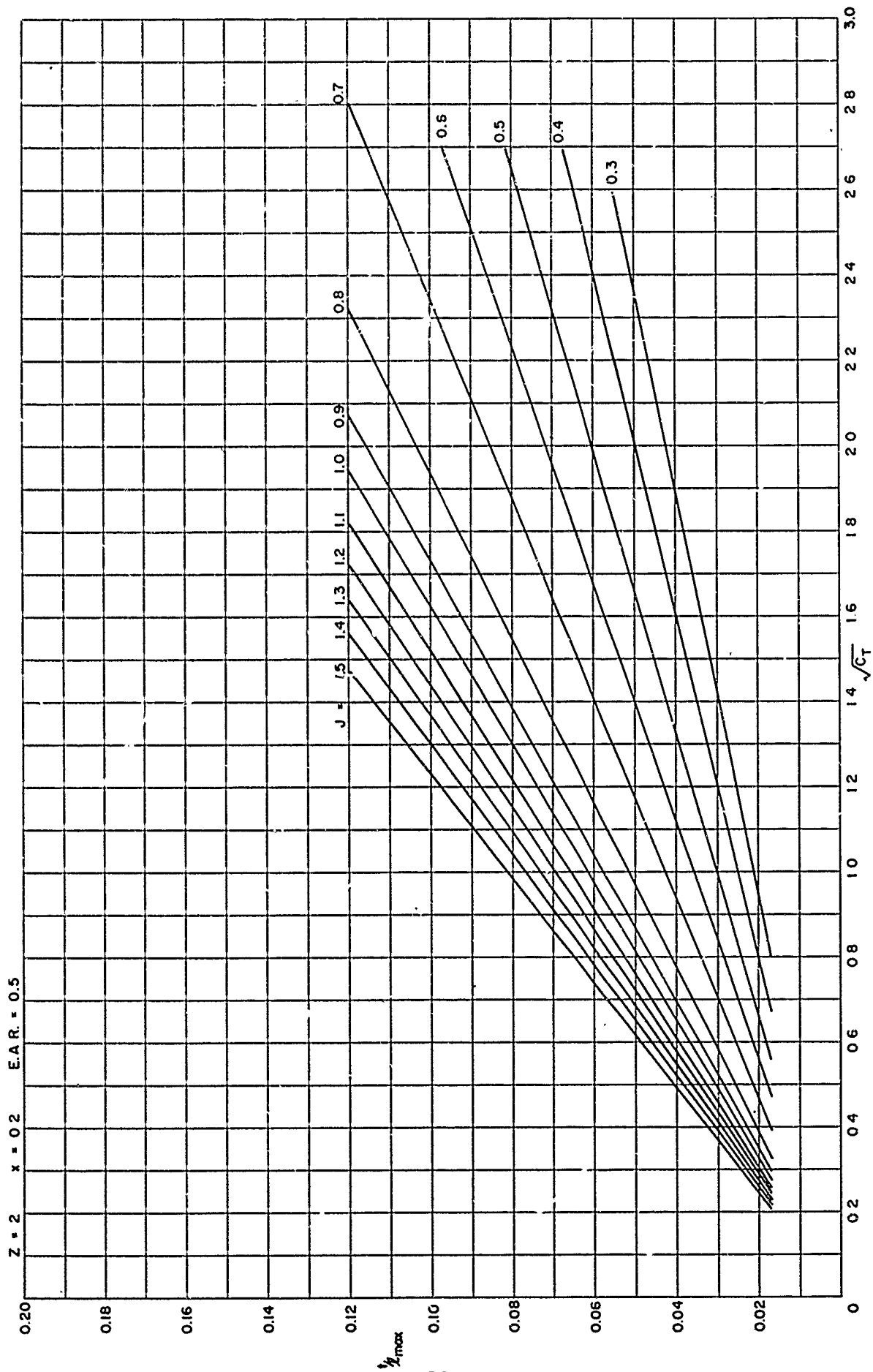Figure 8b — Maximum Face Ordinate at 0.9 Radius for TMB 2-Bladed SC Propeller Series, EAR = 0.4

Figure 8c – Maximum Face Ordinate at 0.9 Radius for TMB 2-Bladed SC Propeller Series, EAR = 0.5
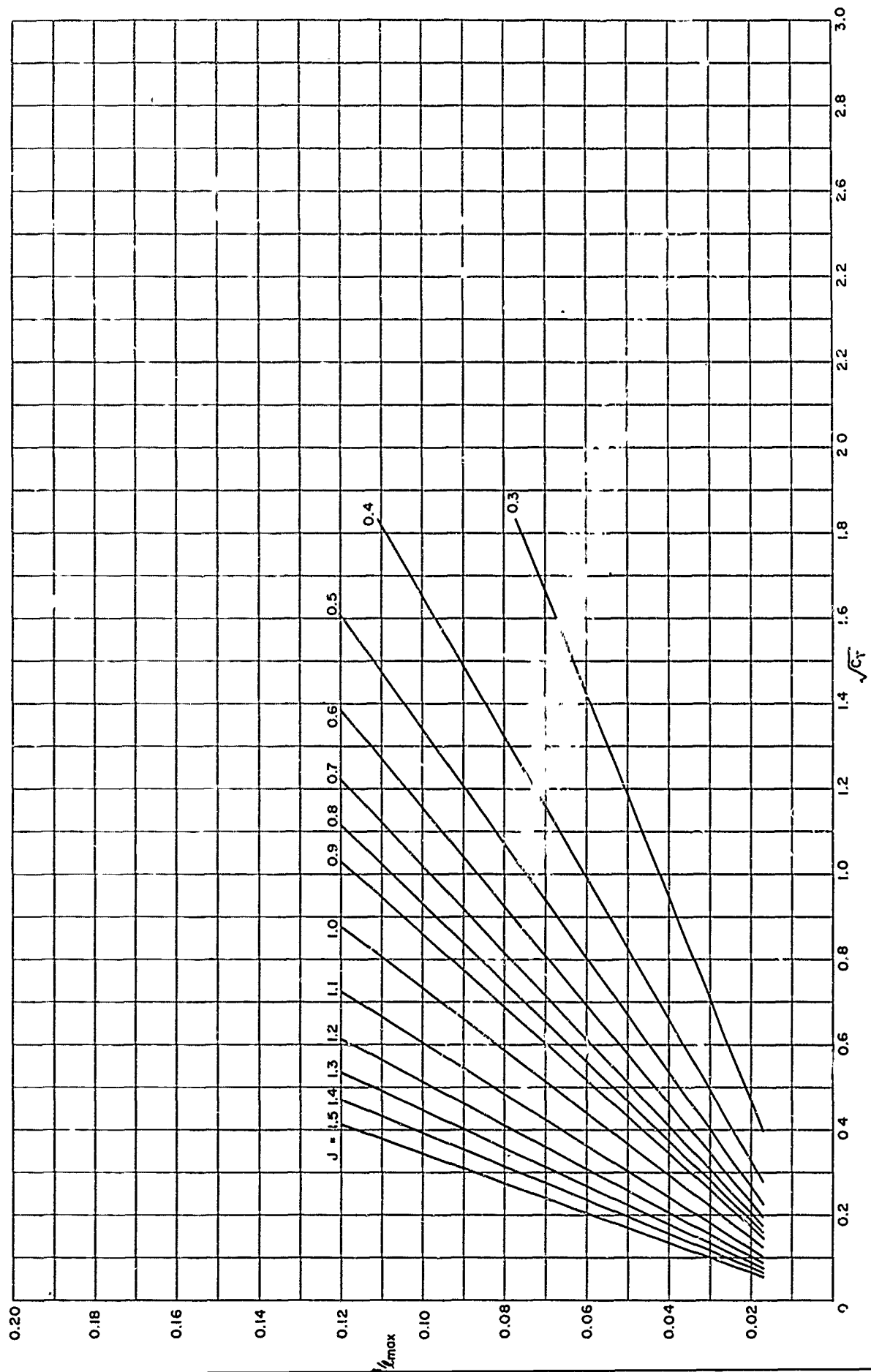
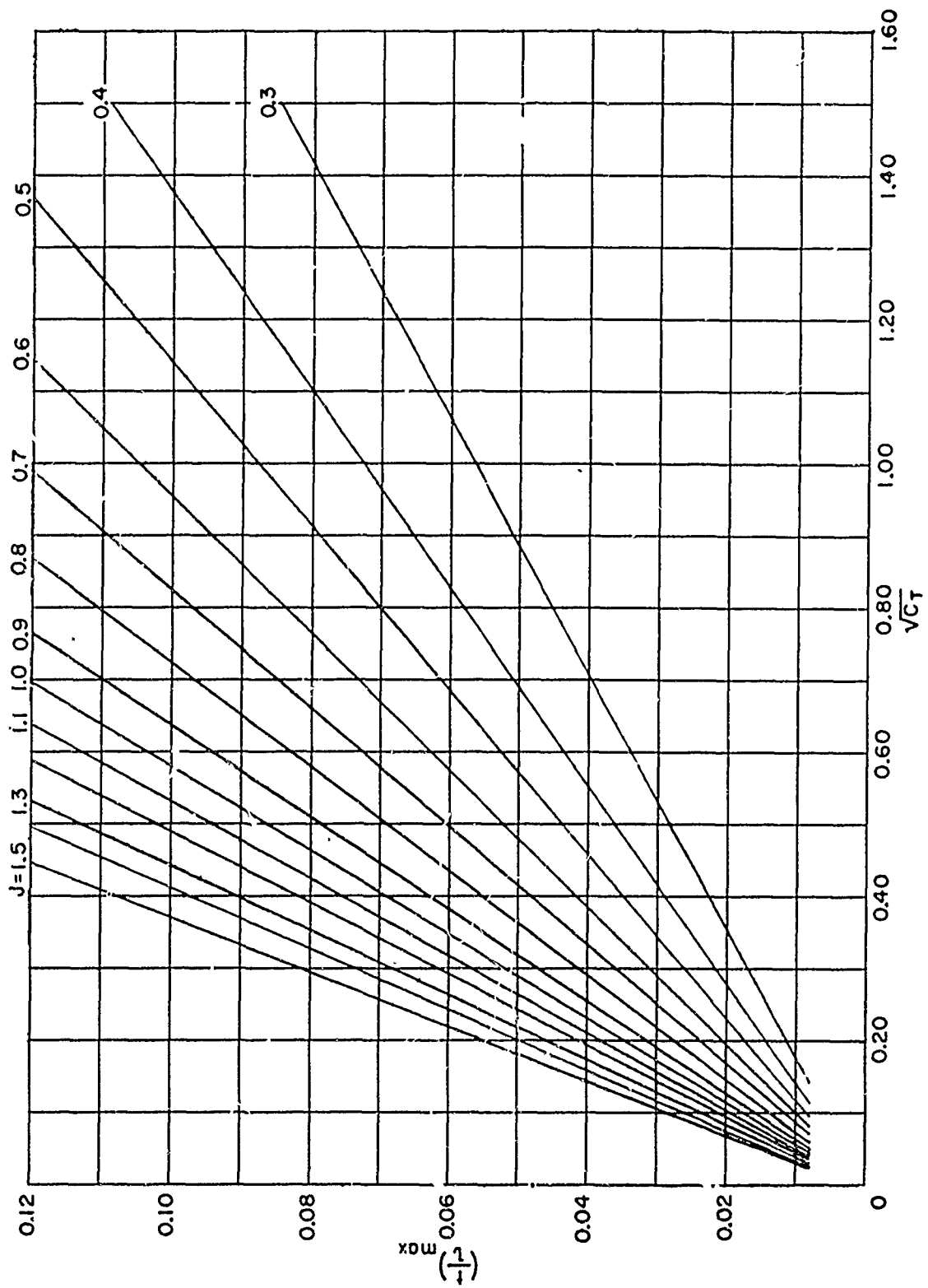Figure 8d — Maximum Face Ordinate at 0.9 Radius for TMB 3-Bladed SC Propeller Series, EAR = 0.4

Figure 8e — Maximum Face Ordinate at 0.9 Radius for TMB 3-Bladed SC Propeller Series, EAR = 0.5

Figure 8f – Maximum Face Ordinate at 0.9 Radius for TMB 3-Bladed SC Propeller Series, EAR = 0.6

Figure 8g — Maximum Face Ordinate at 0.9 Radius for TMB 4-Bladed SC Propeller Series, EAR = 0.5
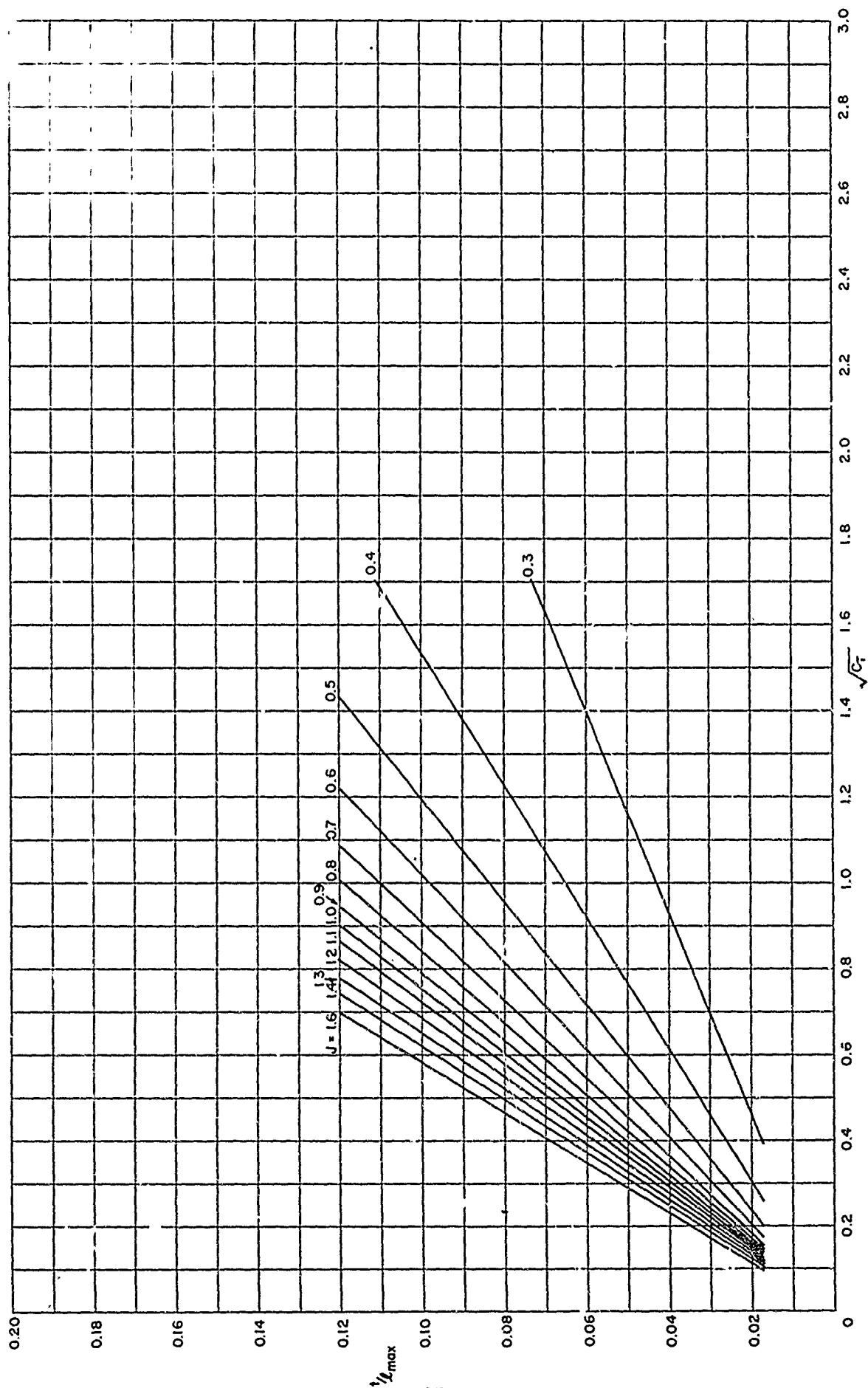
88.

Figure 8h – Maximum Face Ordinate at 0.9 Radius for TMB 4-Bladed SC Propeller Series, EAR = 0.5

Figure 8i – Maximum Face Ordinate at 0.9 Radius for TMB 4-Bladed SC Propeller Series, EAR = 0.7

90

APPENDIX F

MAXIMUM THICKNESS ORDINATES AT 0.2, 0.5, 0.7, AND 0.9 RADIUS FOR
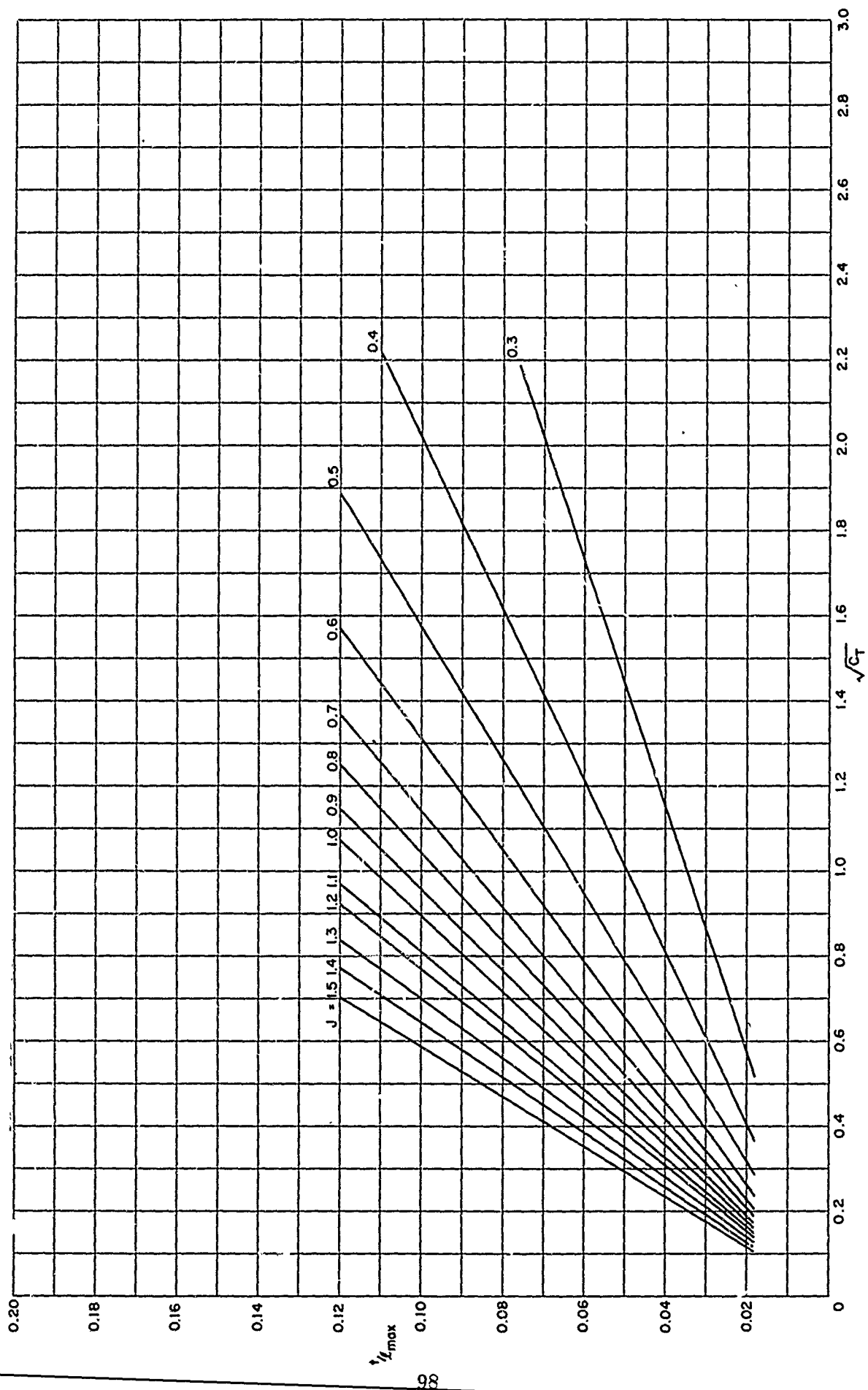TMB SC PROPELLER SERIES
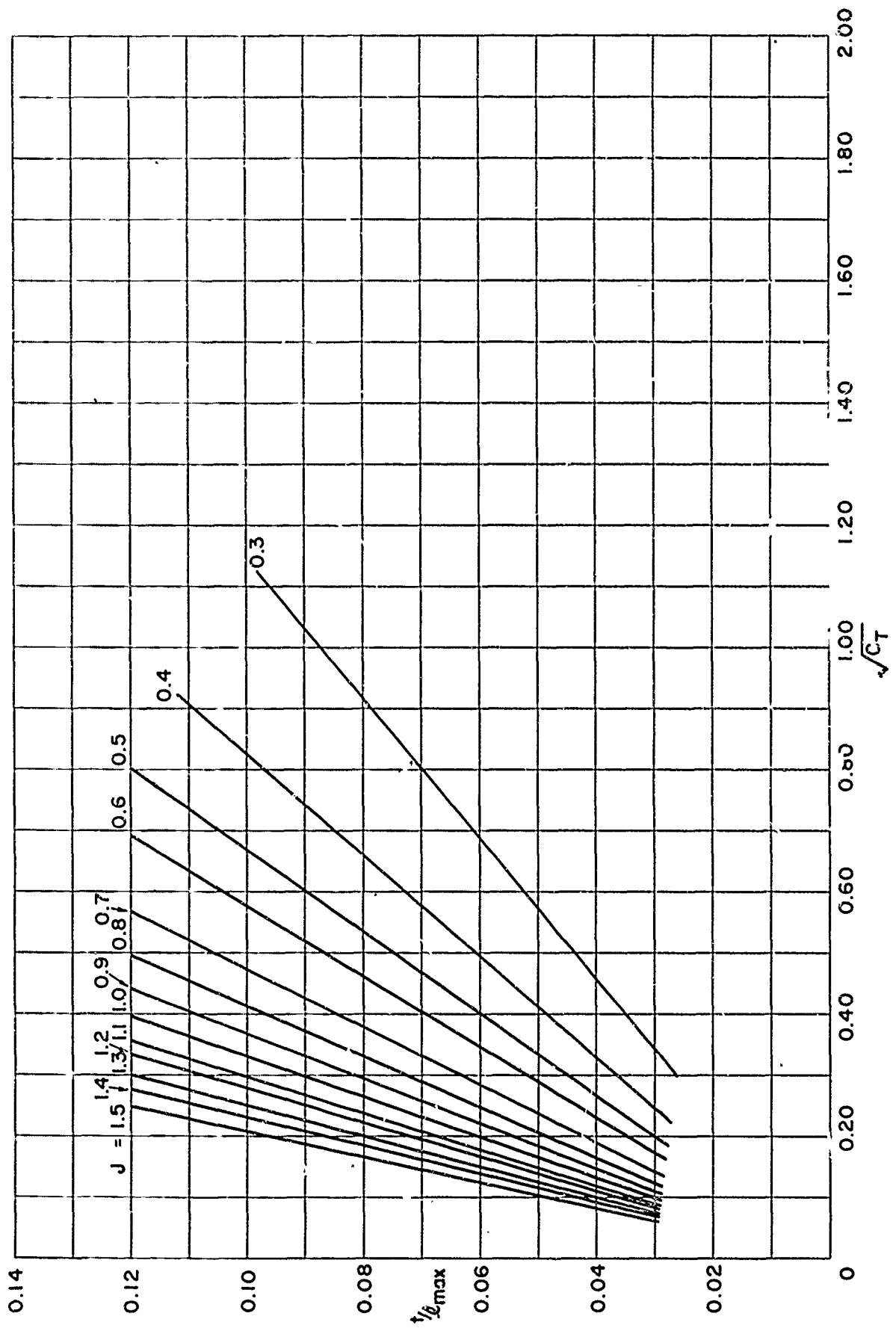
Figure 92 — Maximum Thickness at 0.2 Radius for TMB 2-Bladed SC Propeller Series, EAR = 0.3

92
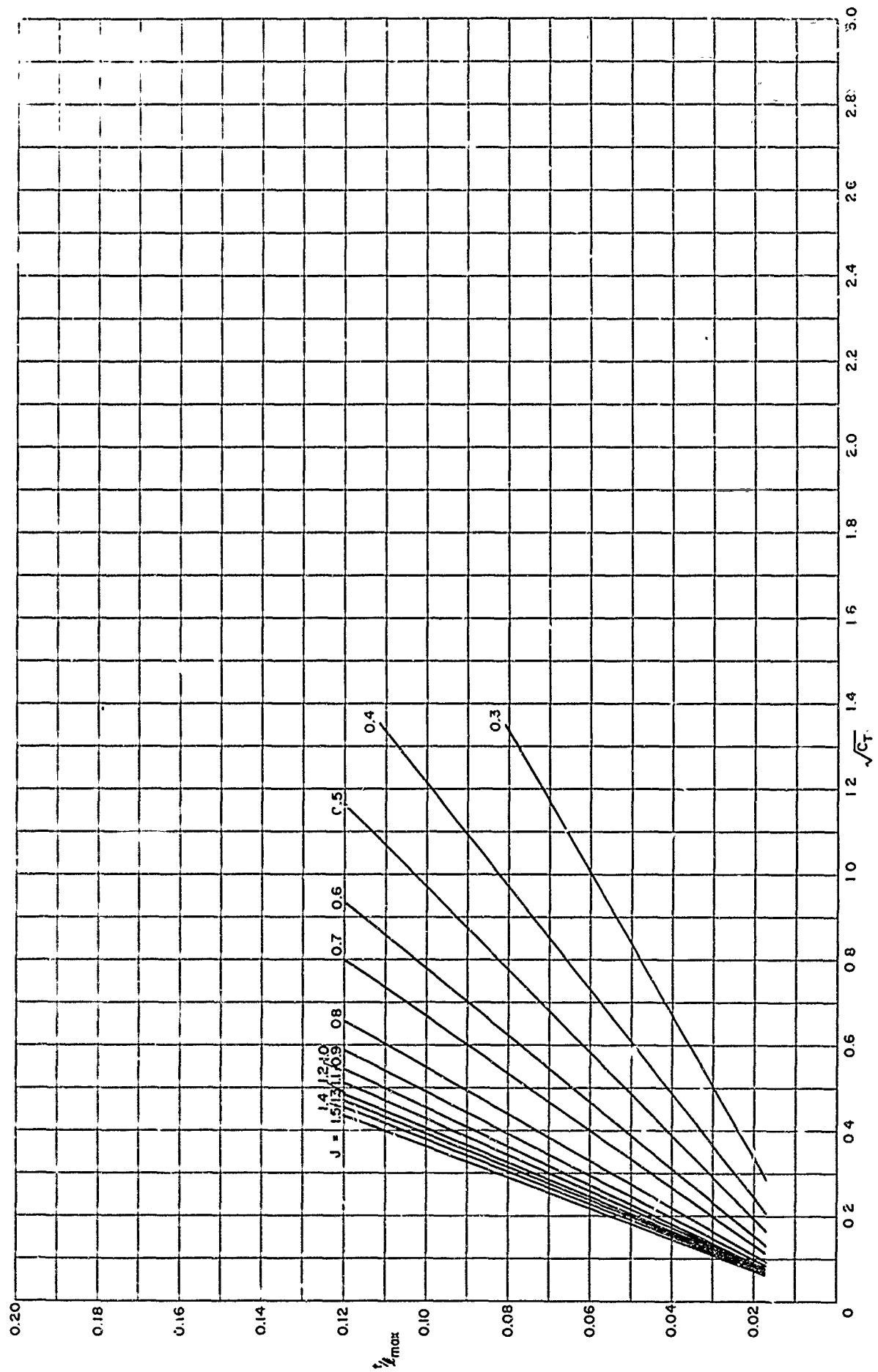
Figure 9b – Maximum Thickness at 0.2 Radius for TMB 2-Bladed SC Propeller Series, EAR = 0.4
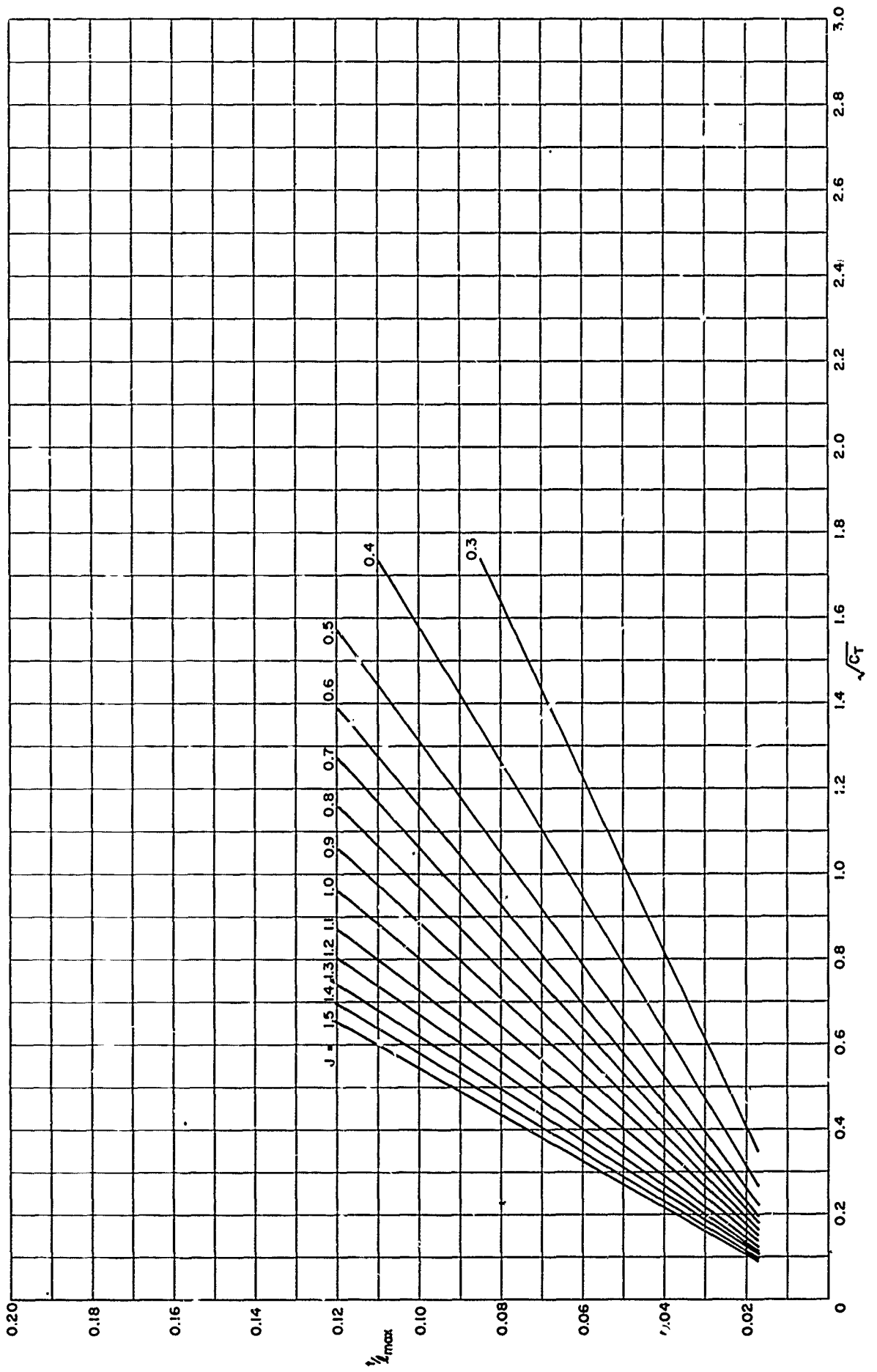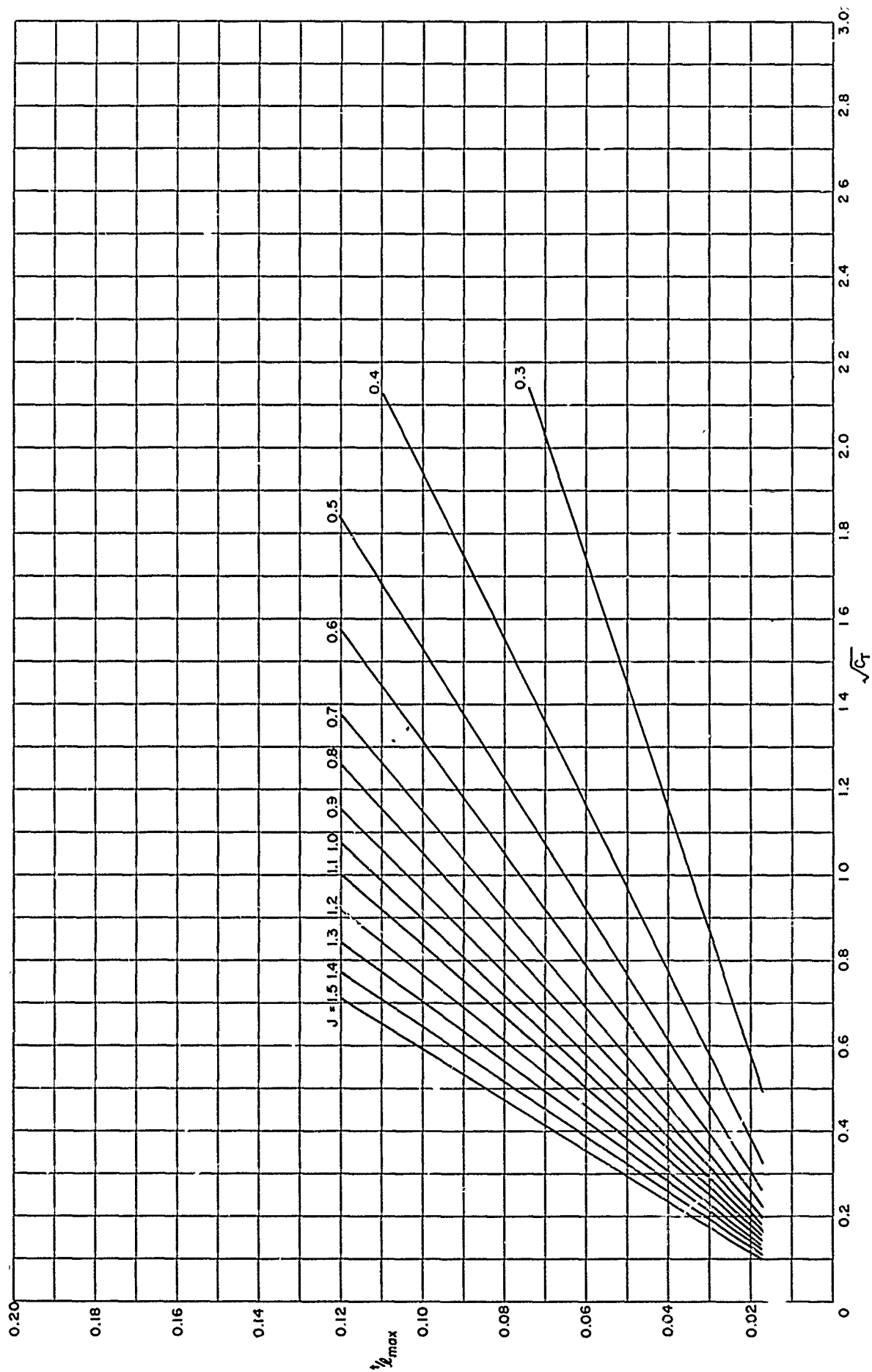
Figure 9c — Maximum Thickness at 0.2 Radius for TMB 2-Bladed SC Propeller Series, E.A.R. = 0.5

Figure 9d — Maximum Thickness at 0.2 Radius for TMB 3-Bladed SC Propeller Series, EAR = 0.4

Figure 9e — Maximum Thickness at 0.2 Radius for TMB 3-Bladed SC Propeller Series, EAR = 0.5

96
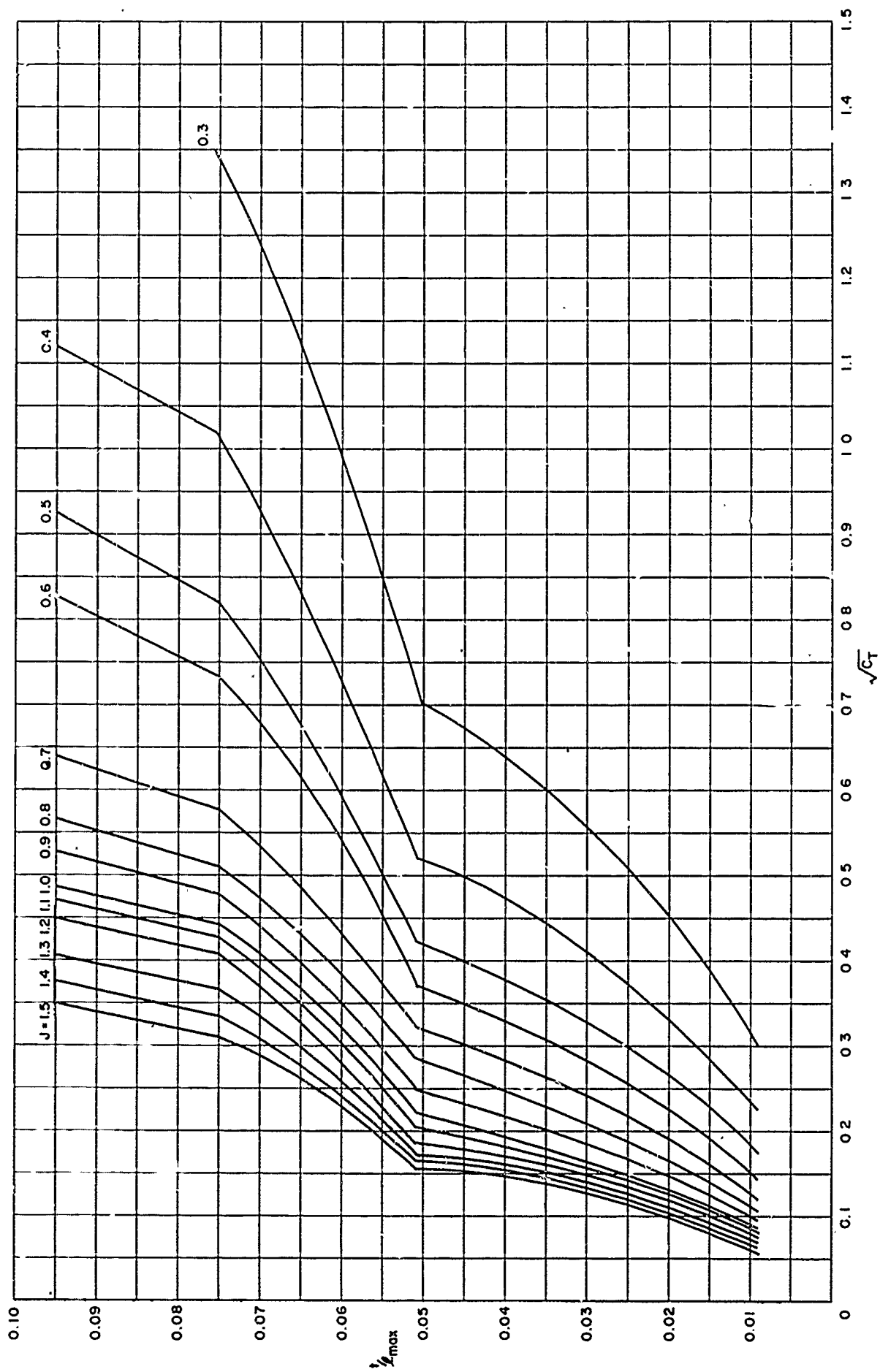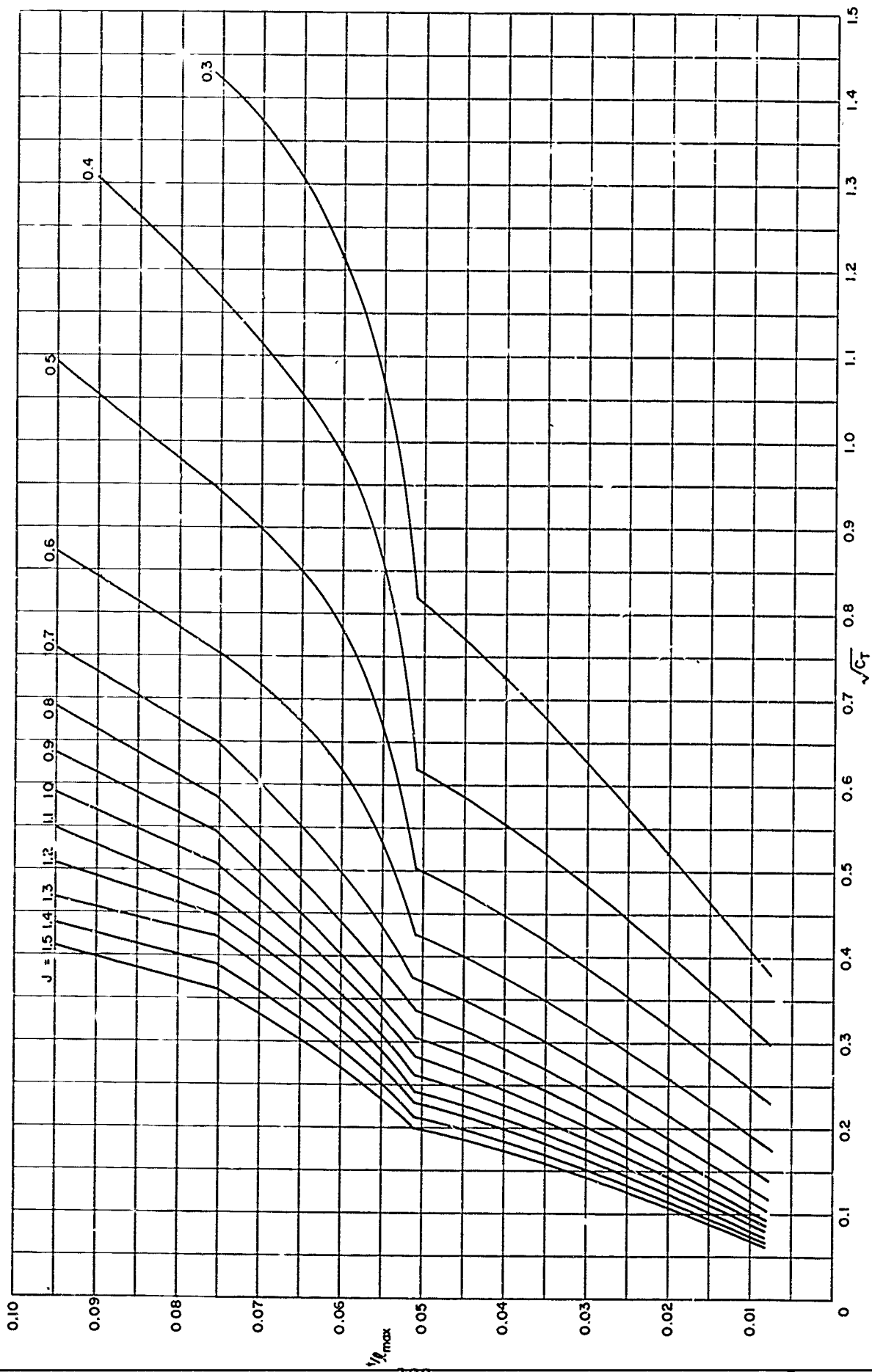
Figure 9f -- Maximum Thickness at 0.2 Radius for TMB 3-Bladed SC Propeller Series, EAR = 0.6

Figure 9g — Maximum Thickness at 0.2 Radius for TMB 4-Bladed SC Propeller Series, EAR = 0.5

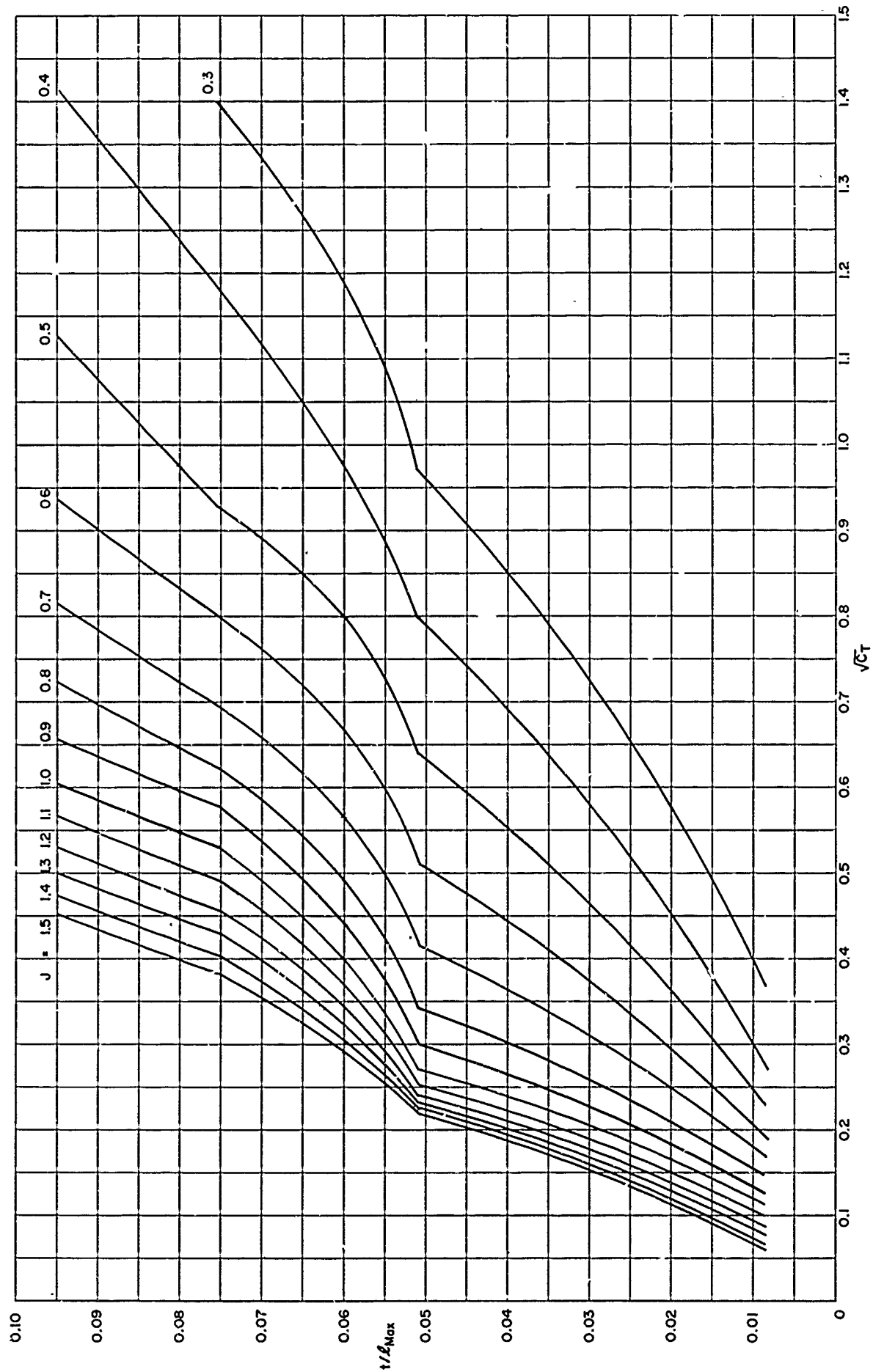Figure 9h — Maximum Thickness at 0.2 Radius for TMB 4-Bladed SC Propeller Series, $\nabla AR = 0.5$

Figure 9i — Maximum Thickness at 0.2 Radius for TMB 4-Bladed SC Propeller Series, EAR = 0.7

100

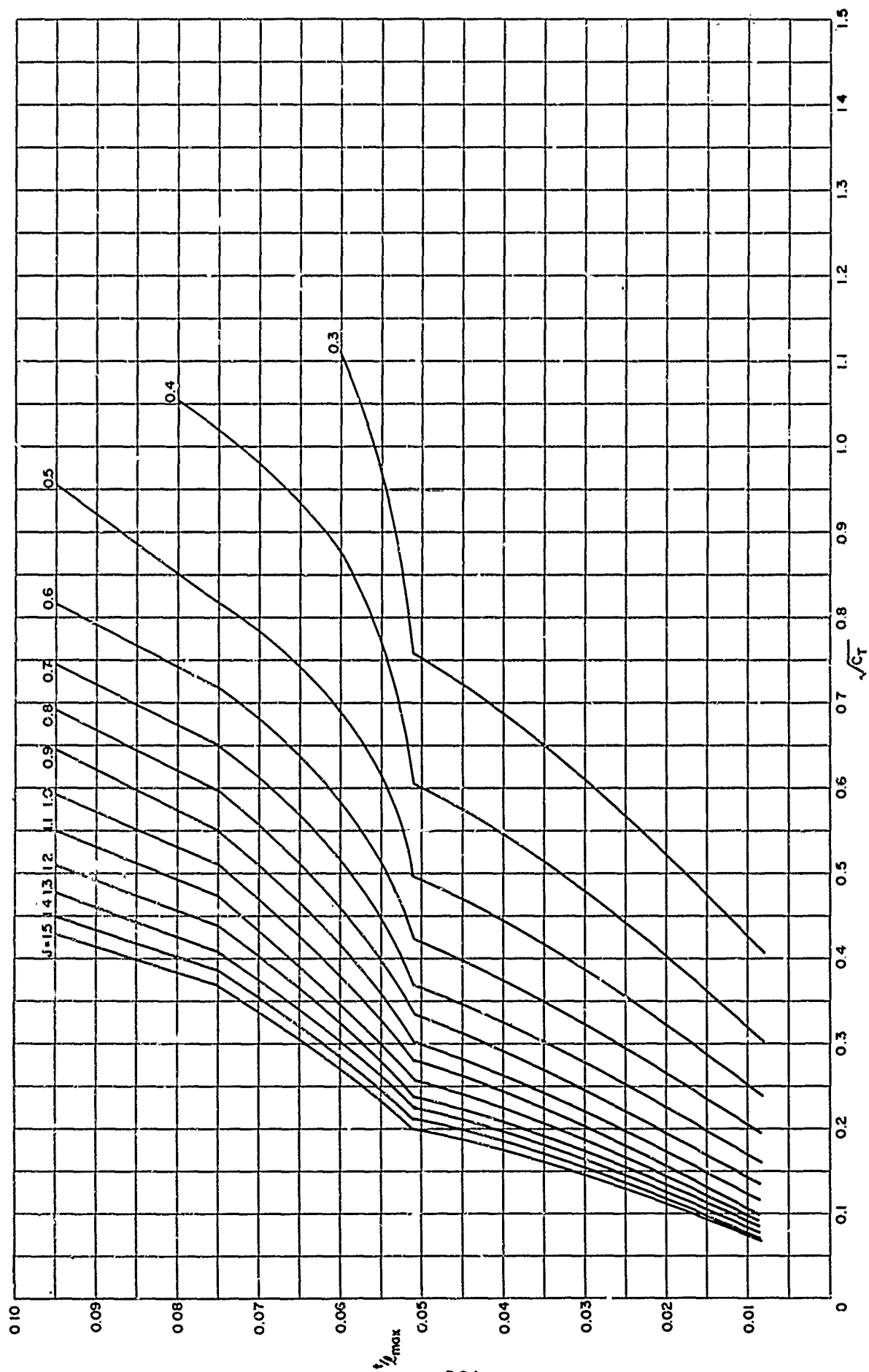Figure 10a — Maximum Thickness at 0.5 Radius for TMB 2-Bladed SC Propeller Series, EAR = 0.3

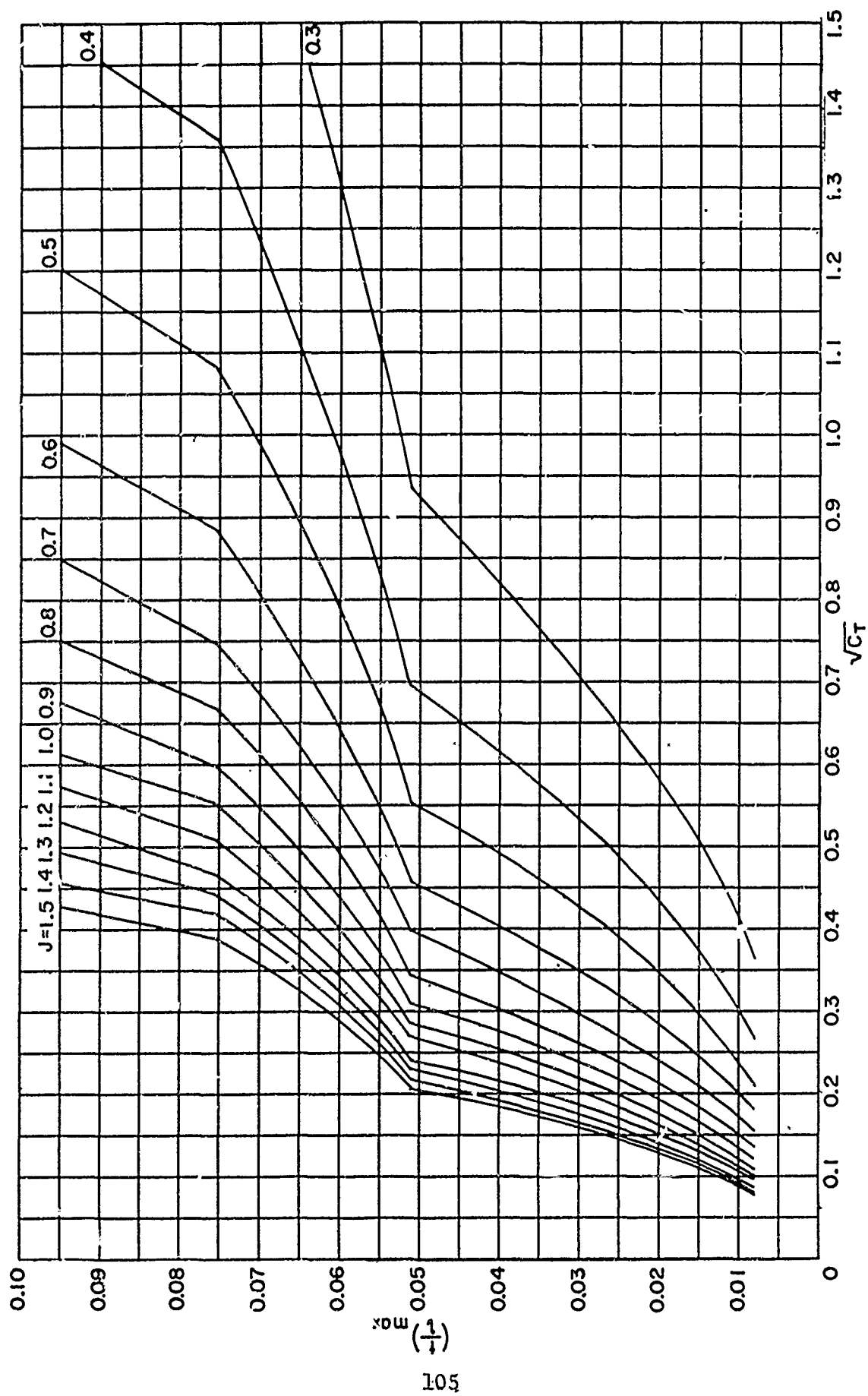Figure 10b – Maximum Thickness at 0.5 Radius for TMB 2-Bladed SC Propeller Series, FAR = 0.4

Figure 10c — Maximum Thickness at 0.5 Radius for TMB 2-Bladed SC Propeller Series, EAR = 0.5

103

Figure 10d — Maximum Thickness at 0.5 Radius for TMB 3-Bladed SC Propeller Series, EAR = 0.4

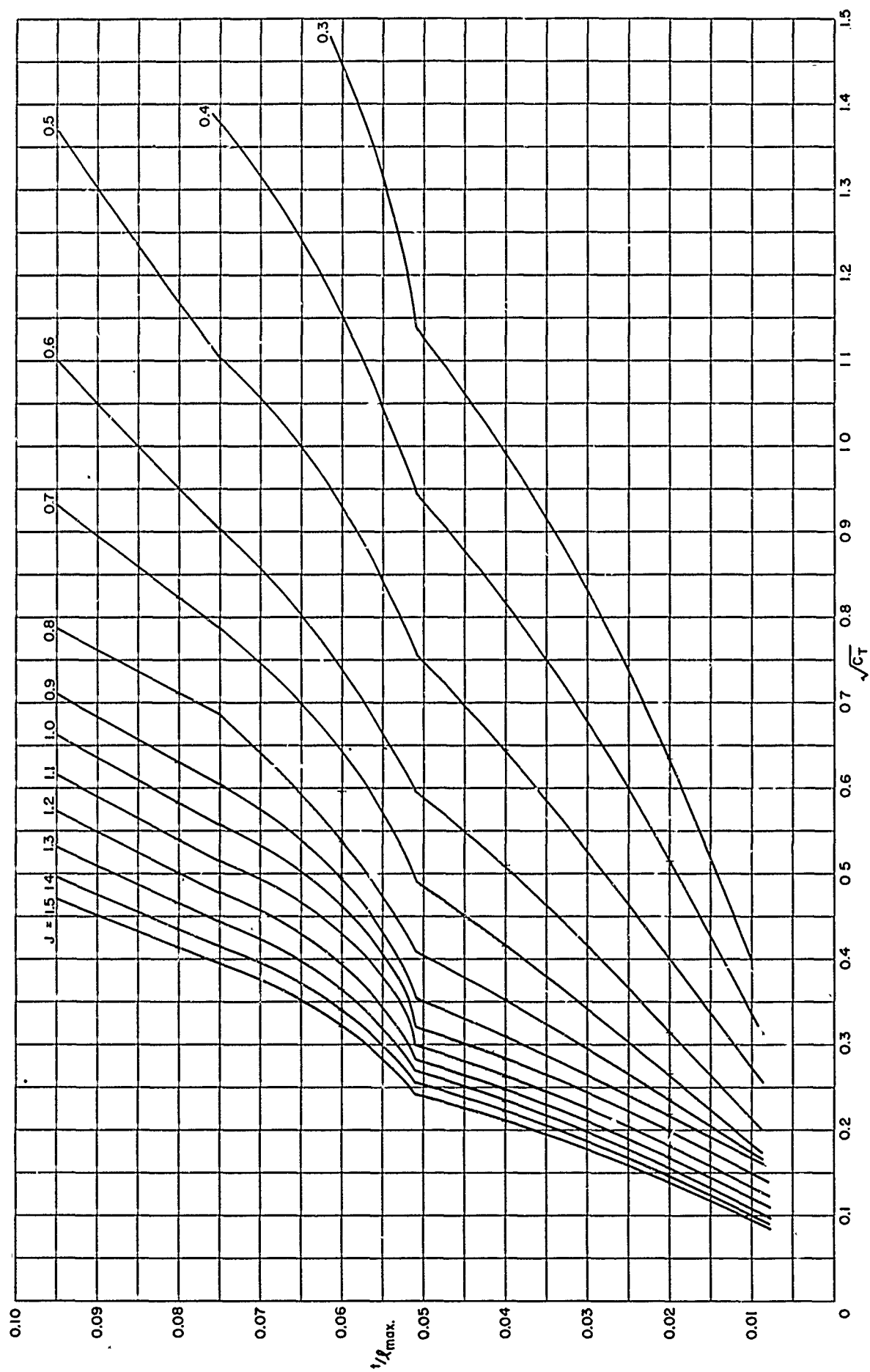Figure 10e – Maximum Thickness at 0.5 Radius for TMB 3-Bladed SC Propeller Series, EAR = 0.5

105

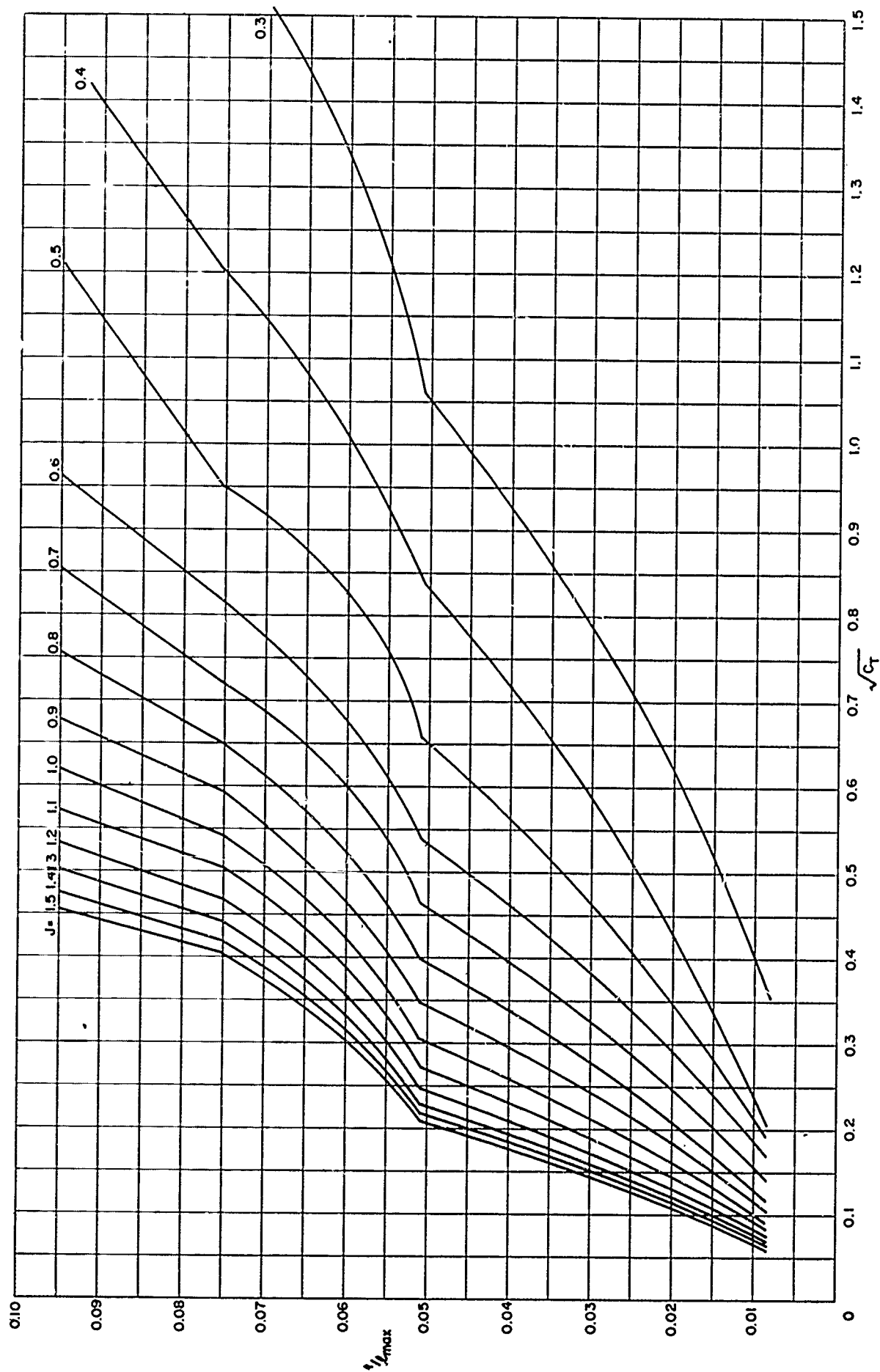Figure 10f — Maximum Thickness at 0.5 Radius for TMB 3-Bladed SC Propeller Series, EAR = 0.6

Figure 10g — Maximum Thickness at 0.5 Radius for TMB 4-Bladed SC Propeller Series, EAR = 0.5
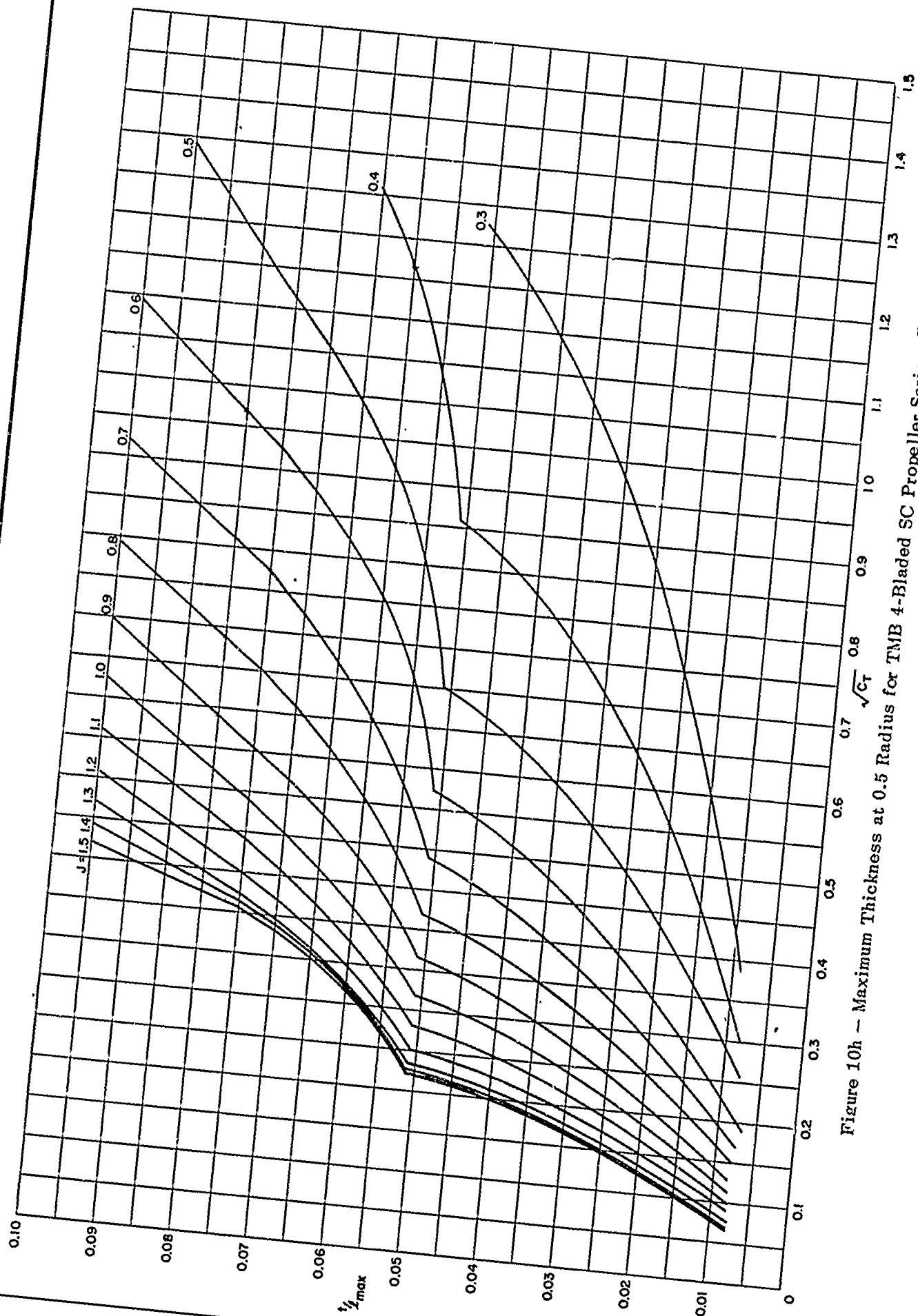
107

Figure 10h — Maximum Thickness at 0.5 Radius for TMB 4-Bladed SC Propeller Series, EAR = 0.6
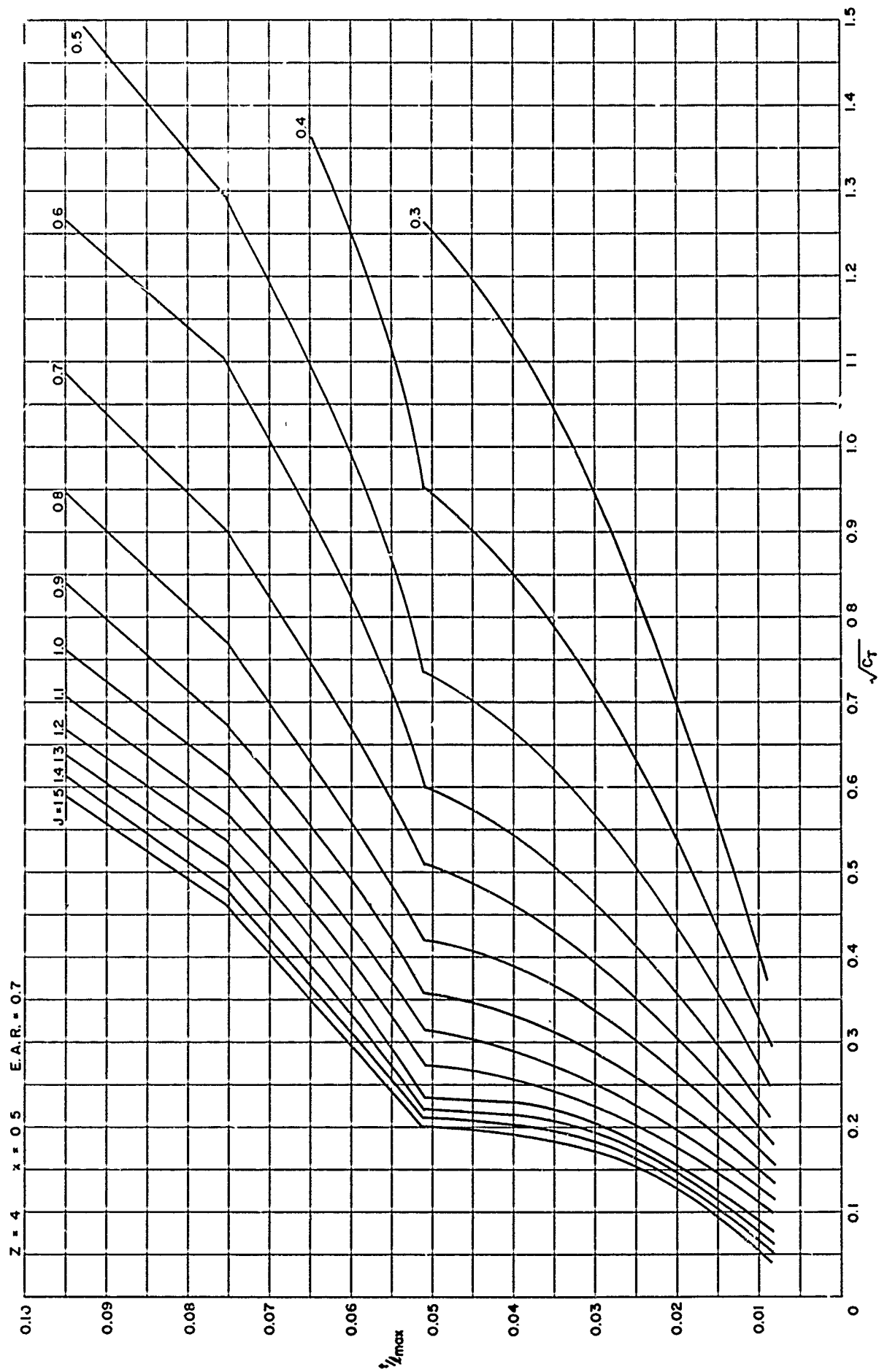
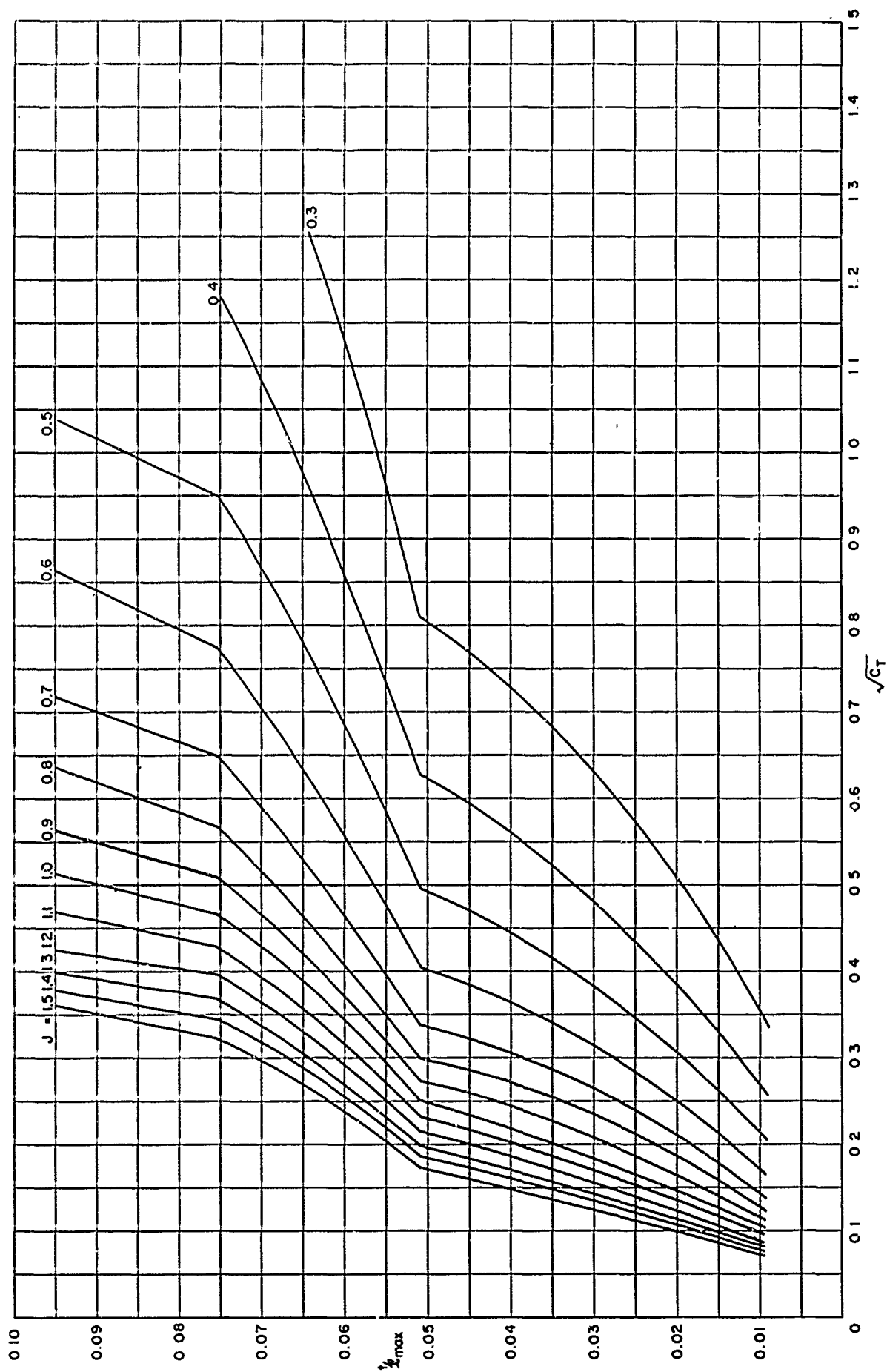Figure 10i — Maximum Thickness at 0.5 Radius for TMB 4-Bladed SC Propeller Series, E.A.R. = 0.7

109

Figure 11a – Maximum Thickness at 0.7 Radius for TMB 2-Bladed SC Propeller Series, EAR = 0.3

Figure 11b – Maximum Thickness at 0.7 Radius for TMB 2-Bladed SC Propeller Series, EAR = 0.4

Figure 11c – Maximum Thickness at 0.7 Radius for TMB 2-Bladed SC Propeller Series, EAR = 0.5
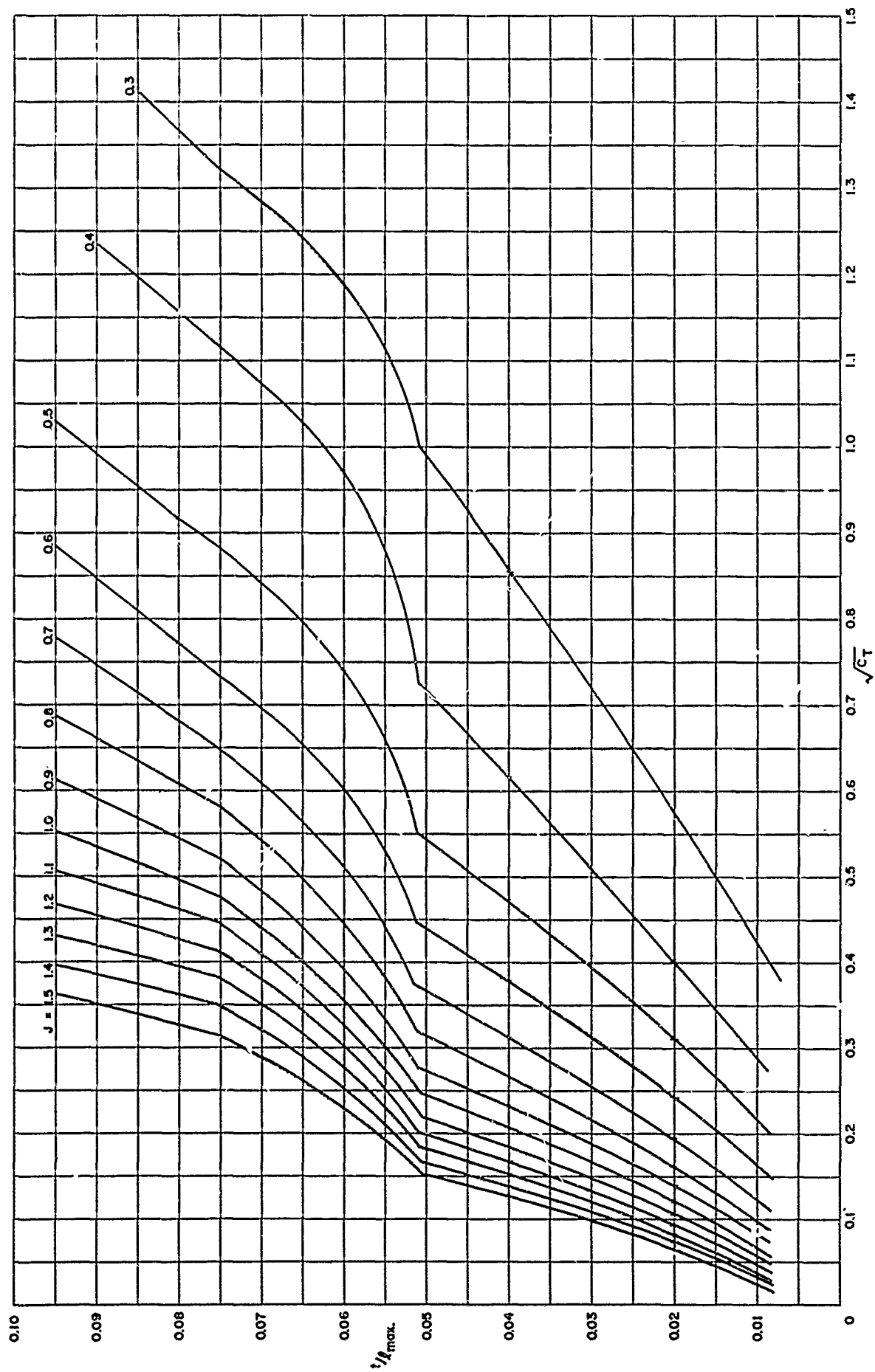
Figure 11d — Maximum Thickness at 0.7 Radius for TMB 3-Bladed SC Propeller Series, EAR = 0.4

Figure 11e — Maximum Thickness at 0.7 Radius for TMB 3-Bladed SC Propeller Series, EAR = 0.5

Figure 11f – Maximum Thickness at 0.7 Radius for TMB 3-Bladed SC Propeller Series, EAR = 0.6

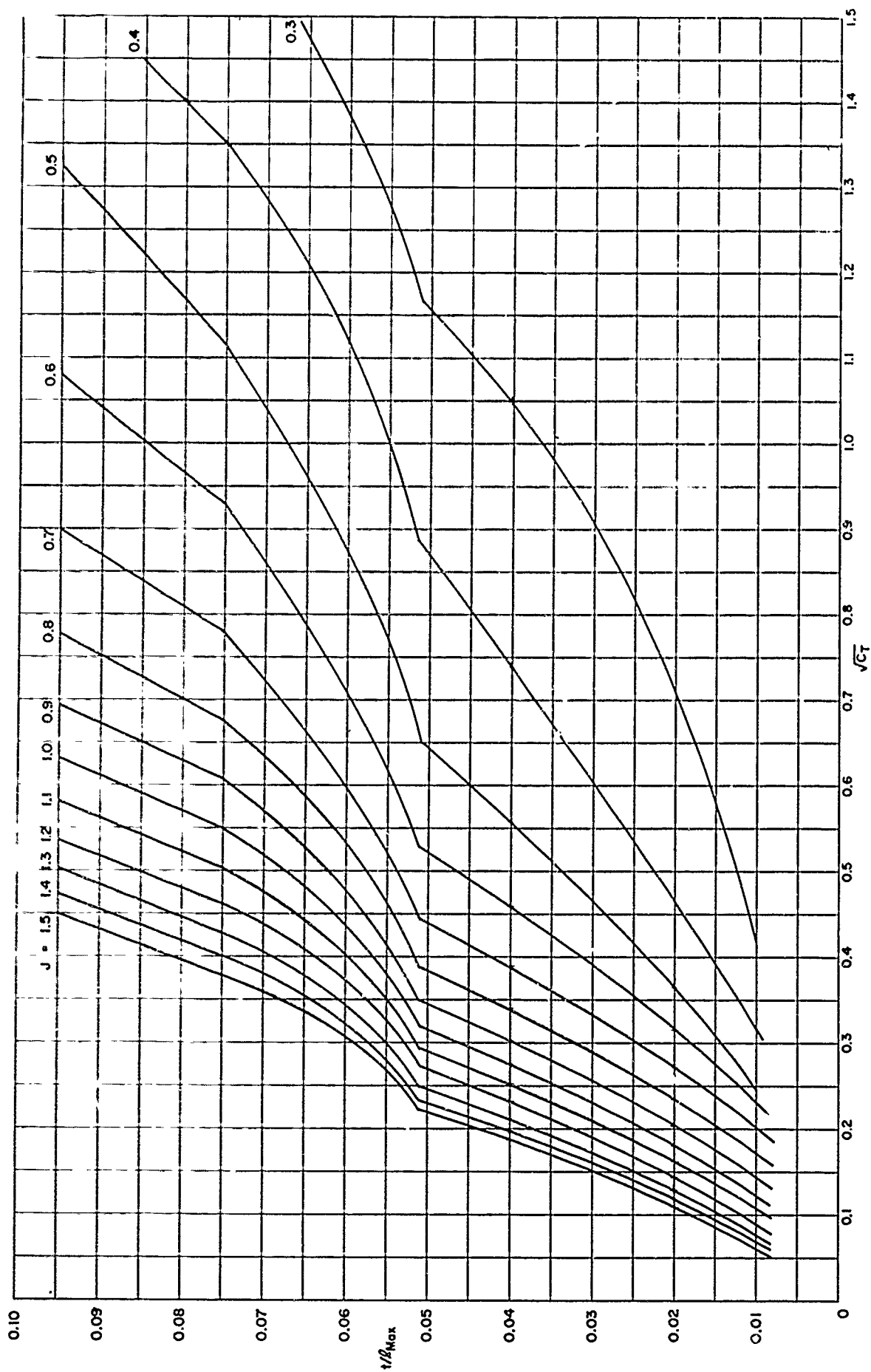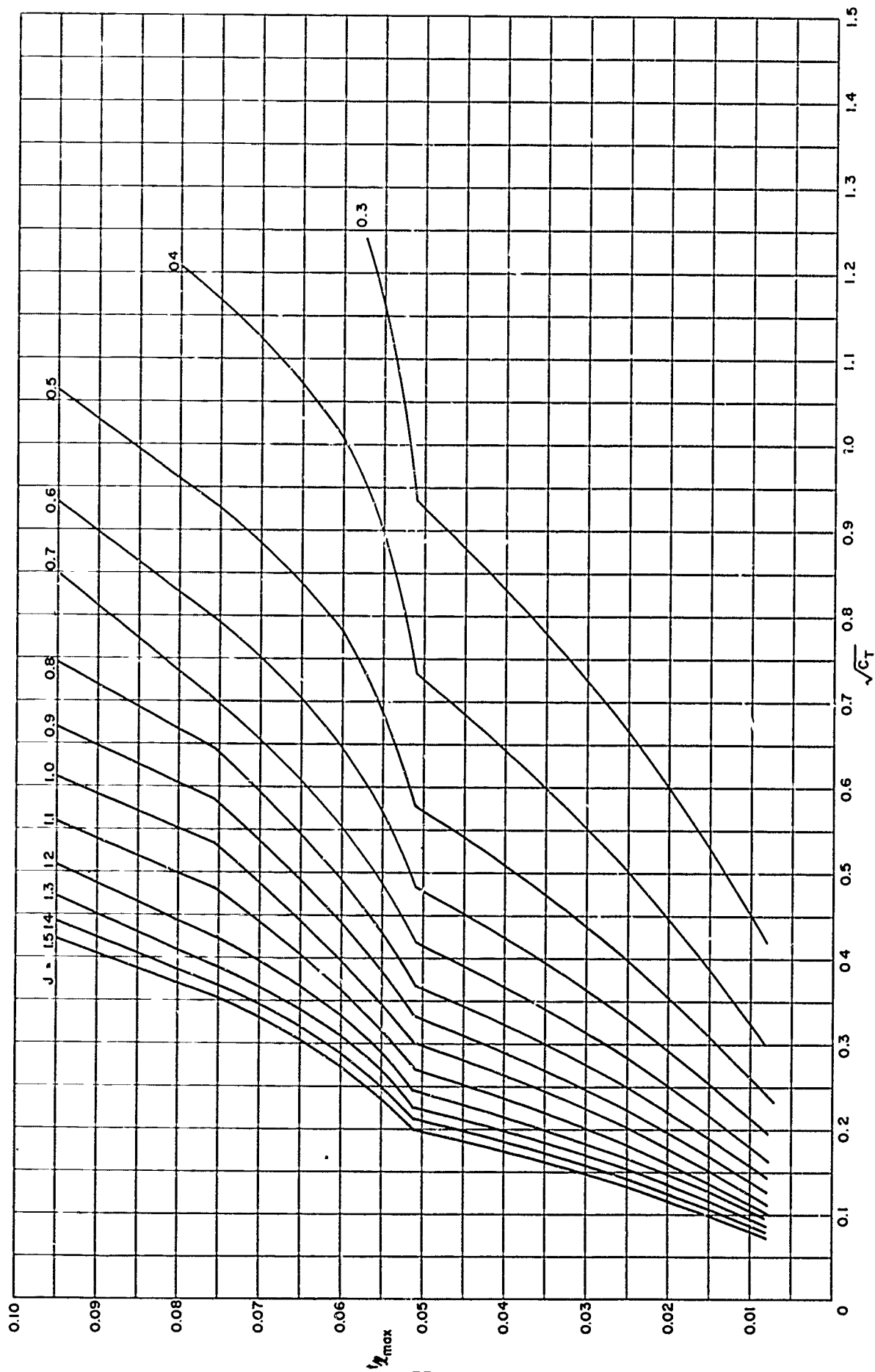Figure 11g — Maximum Thickness at 0.7 Radius for TMB 4-Bladed SC Propeller Series, $EAR = 0.5$

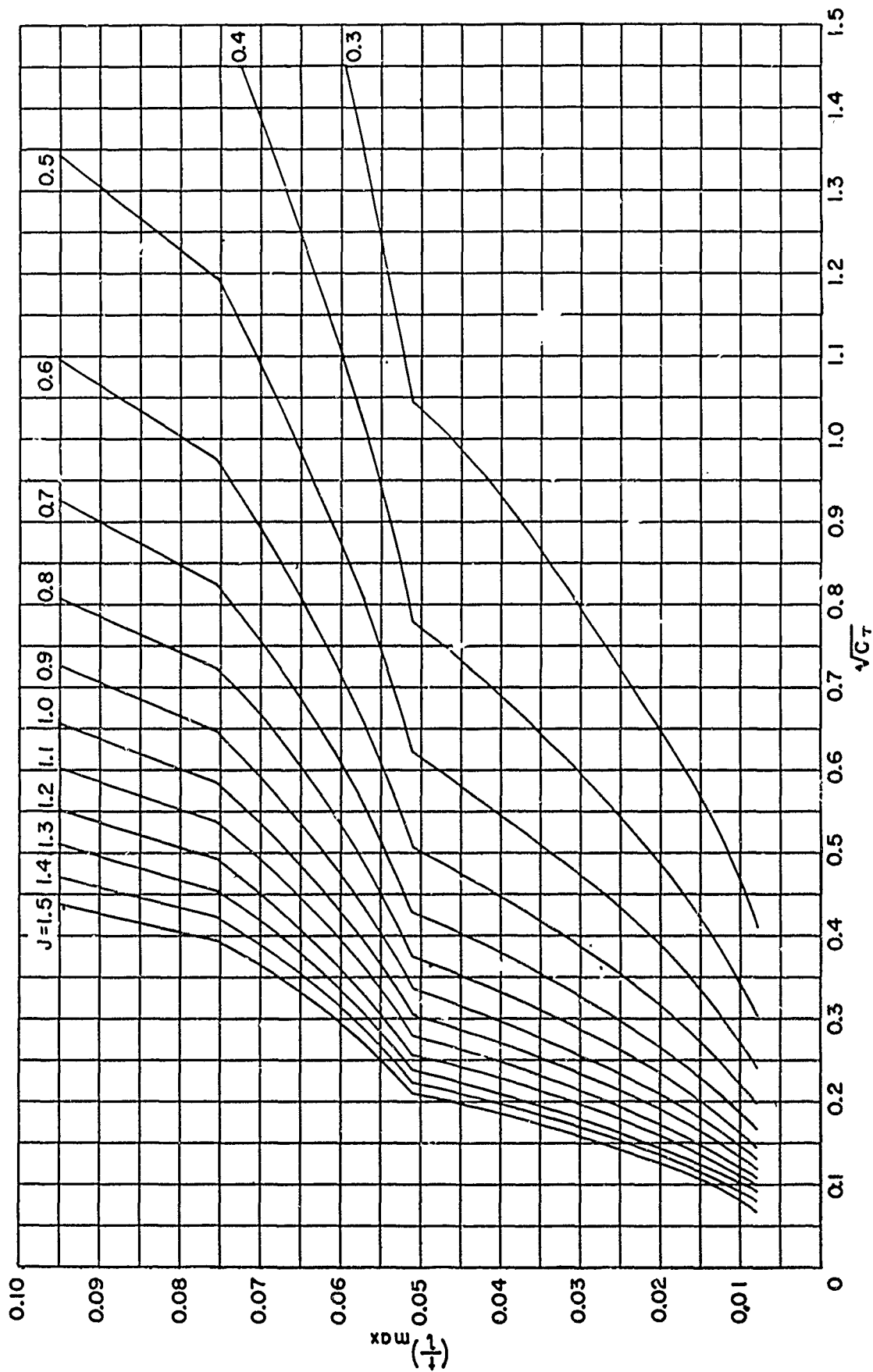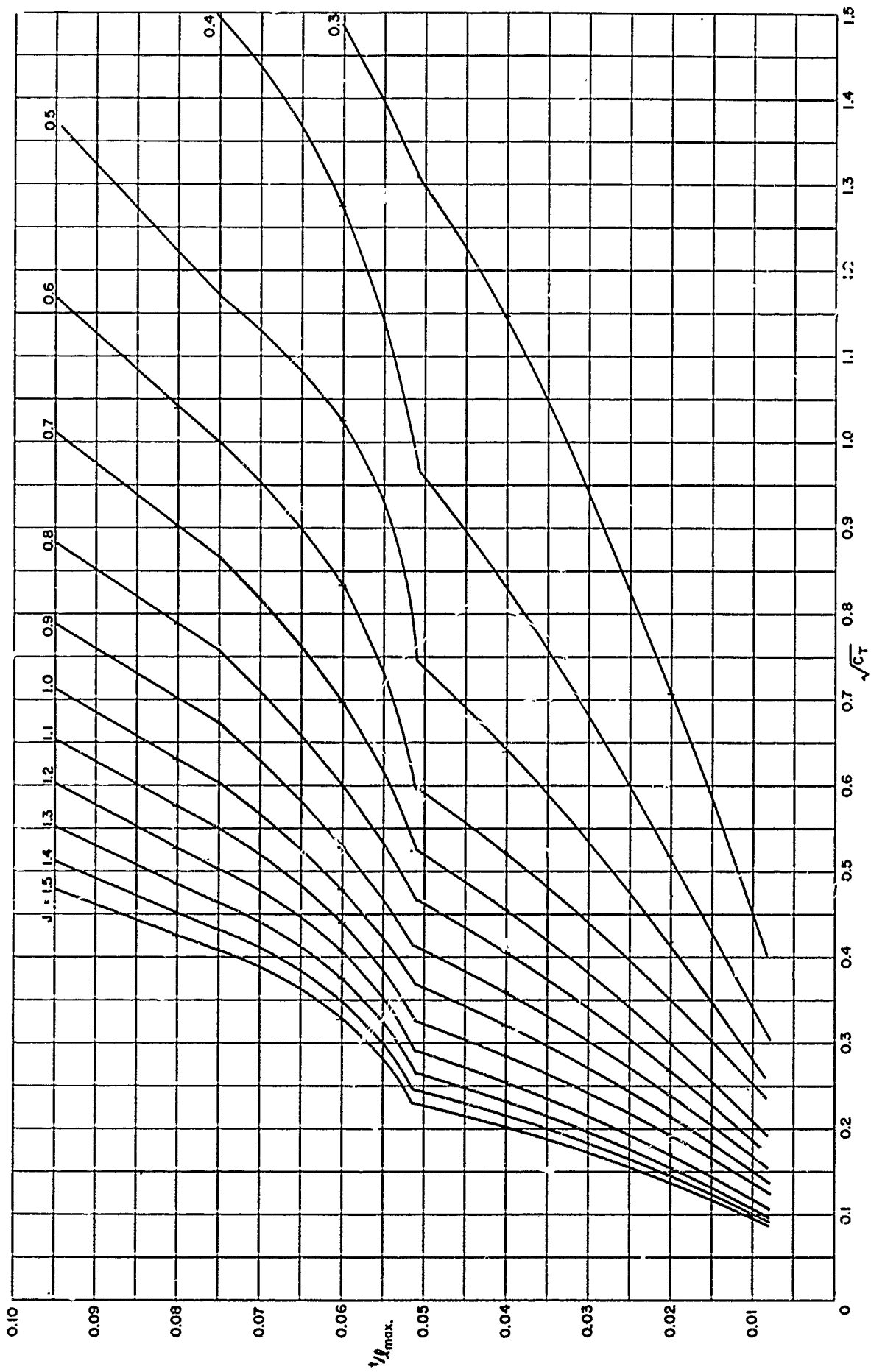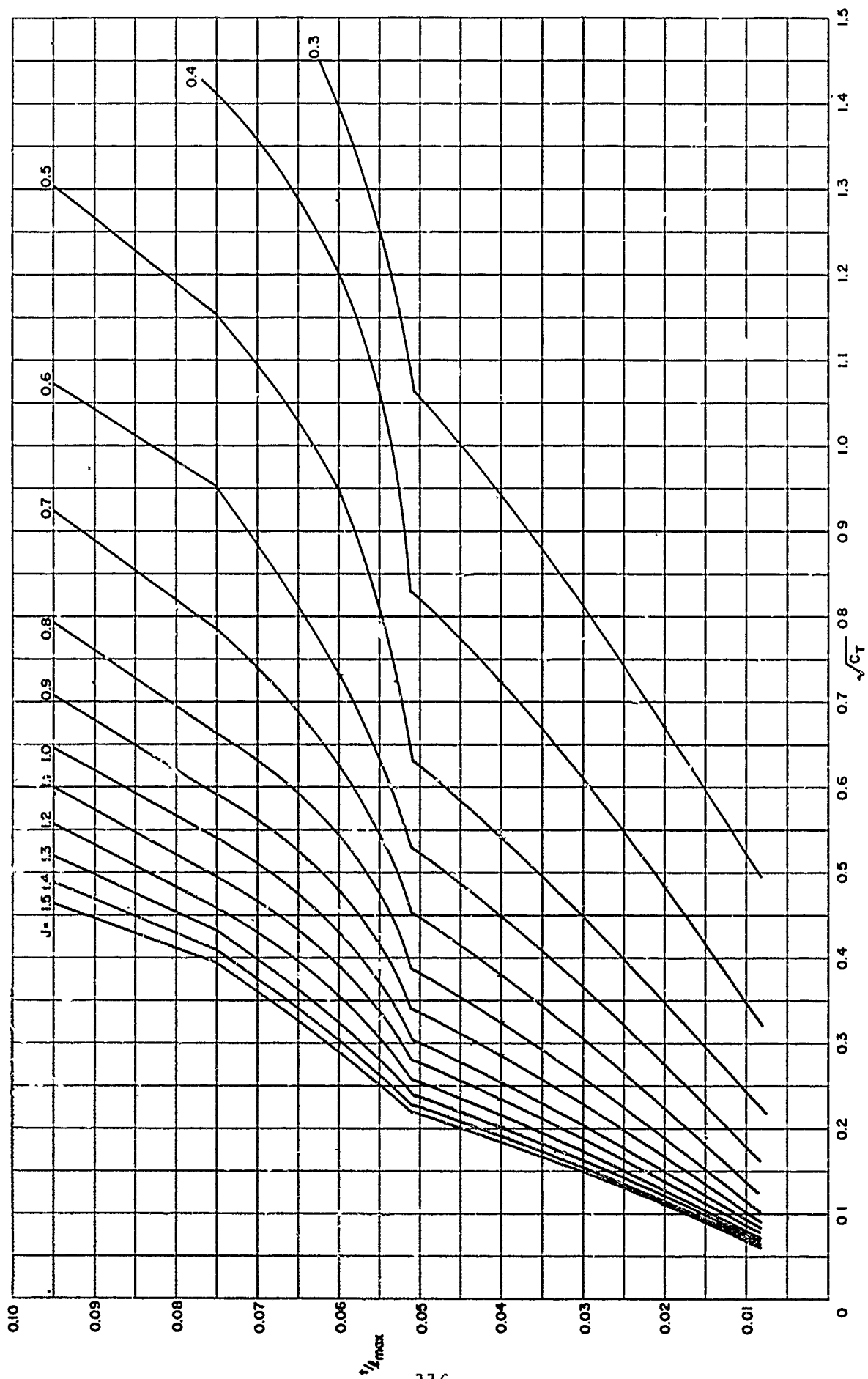Figure 11h – Maximum Thickness at 0.7 Radius for TMB 4-Bladed SC Propeller Series, EAR = 0.6

117

Figure 11i – Maximum Thickness at 0.7 Radius for TMB 4-Bladed SC Propeller Series, EAR = 0.7

118

Figure 12a — Maximum Thickness at 0.9 Radius for TMB 2-Bladed SC Propeller Series, EAR = 0.3

119

Figure 12b -- Maximum Thickness at 0.9 Radius for TMB 2-Bladed SC Propeller Series, EAR = 0.4

120

Figure 12c — Maximum Thickness at 0.9 Radius for TMB 2-Bladed SC Propeller Series, EAR = 0.5
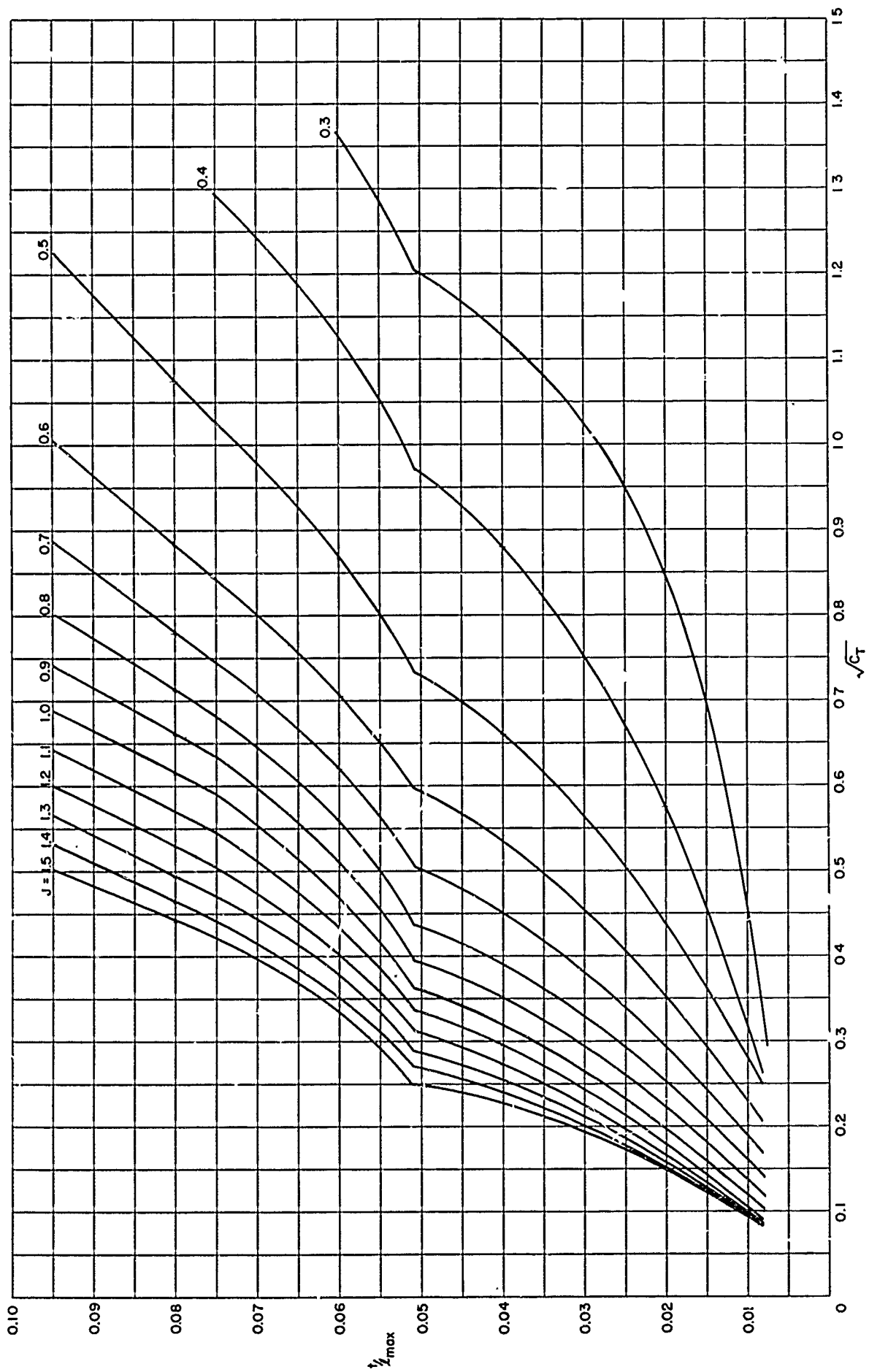
121
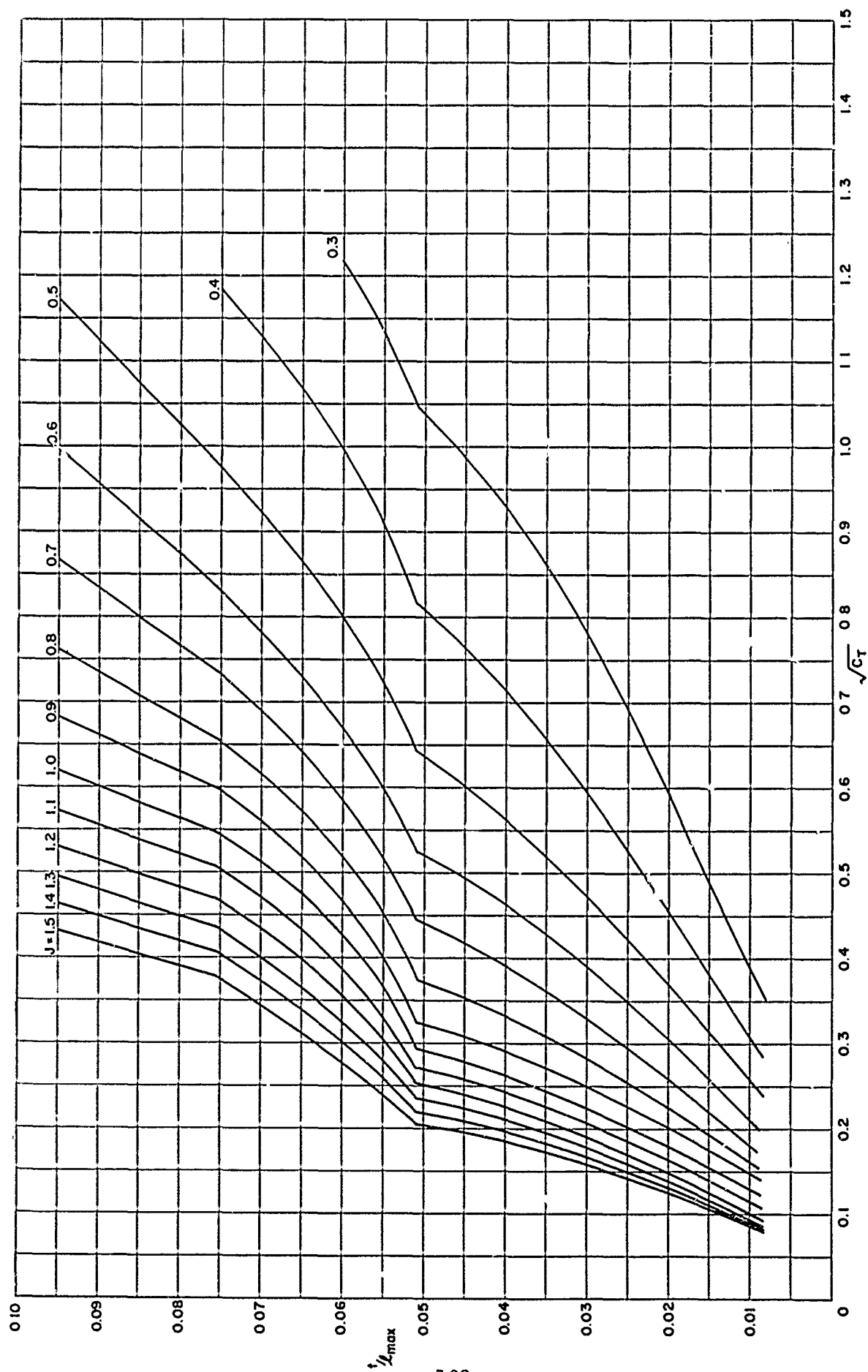
Figure 12d — Maximum Thickness at 0.9 Radius for TMB 3-Bladed SC Propeller Series, EAR = 0.4
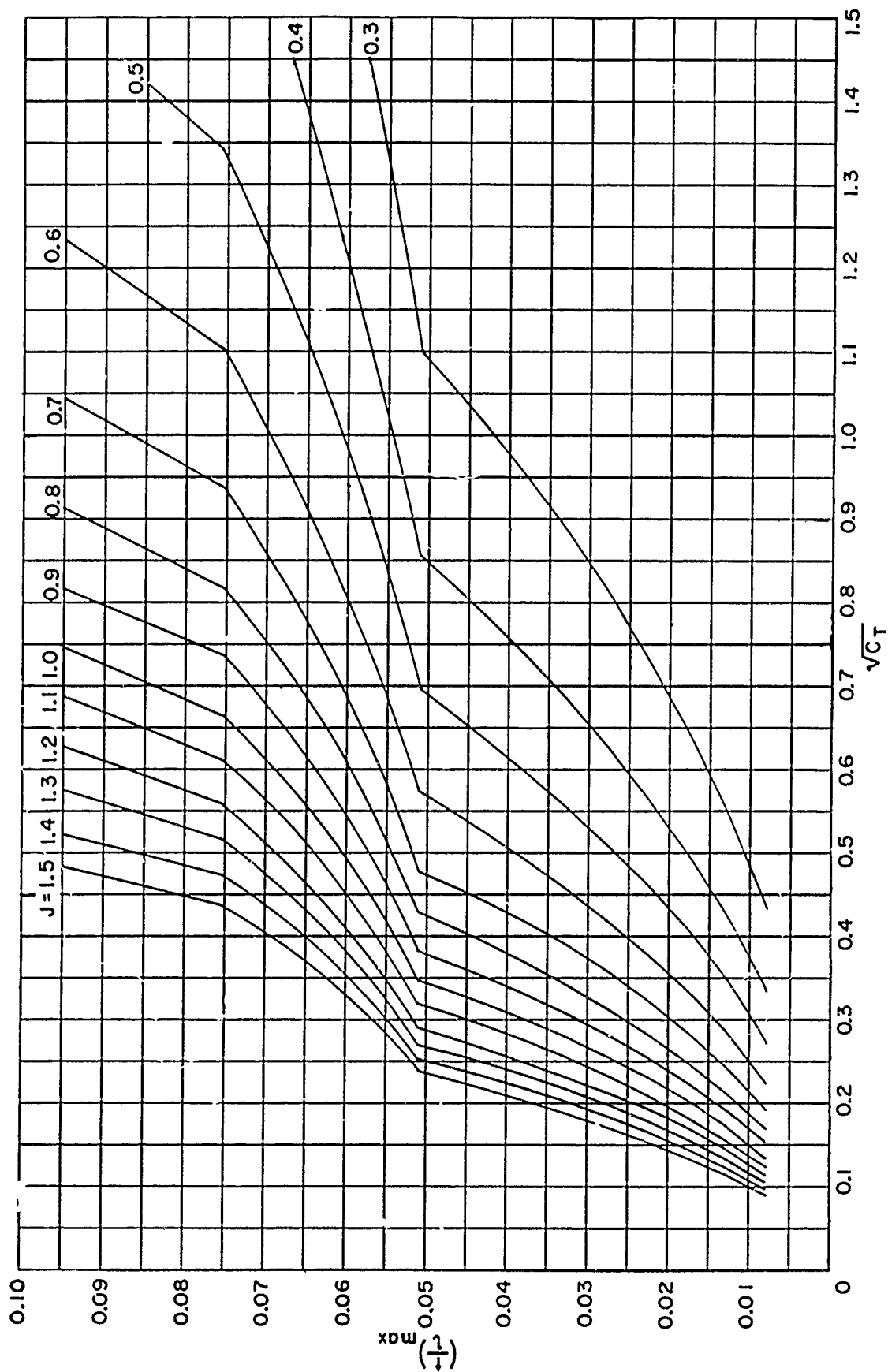
Figure 12e — Maximum Thickness at 0.9 Radius for TMB 3-Bladed SC Propeller Series, EAR = 0.5

123
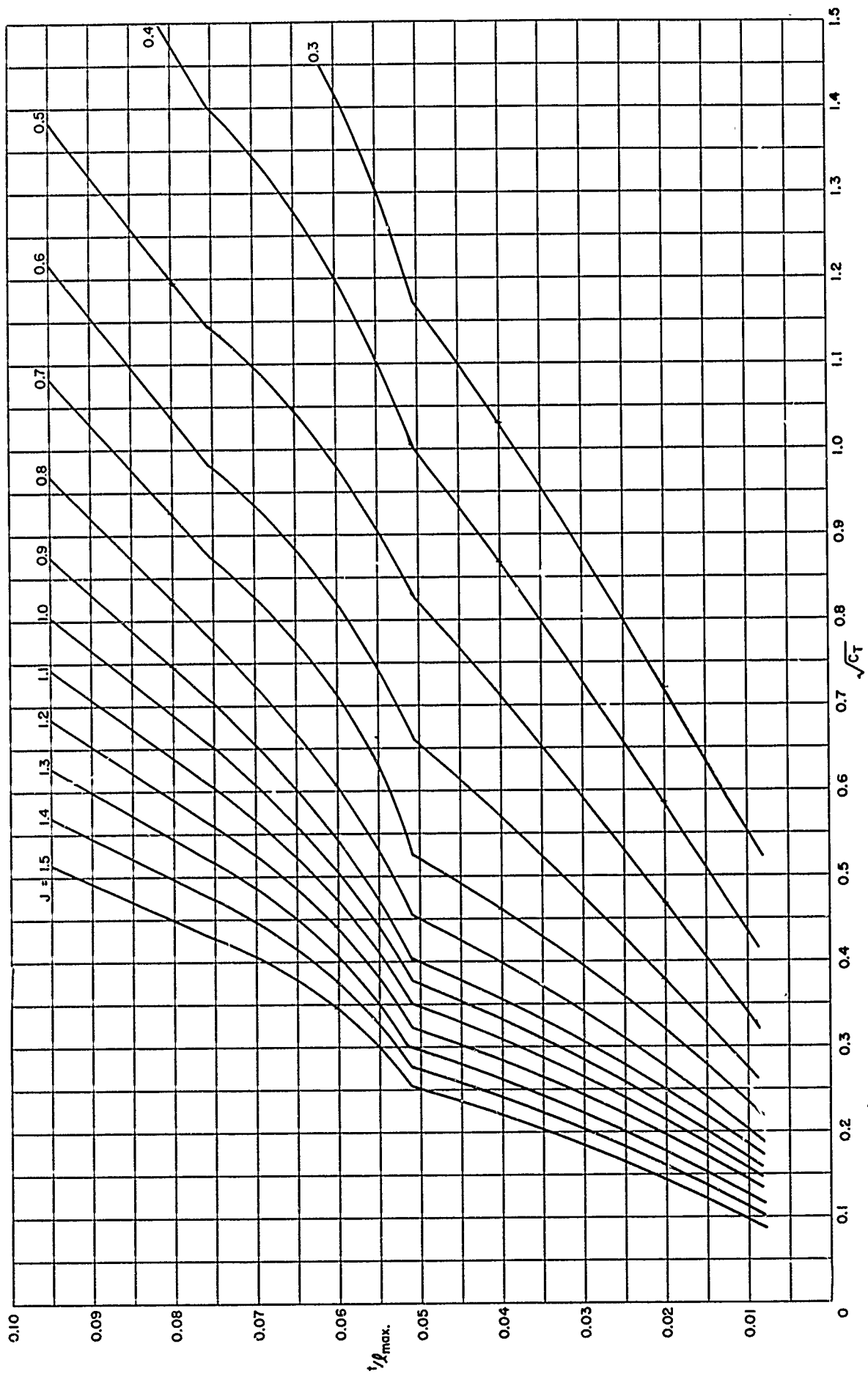
Figure 12f – Maximum Thickness at 0.9 Radius for TMB 3-Bladed SC Propeller Series, E.A.R. = 0.6

124
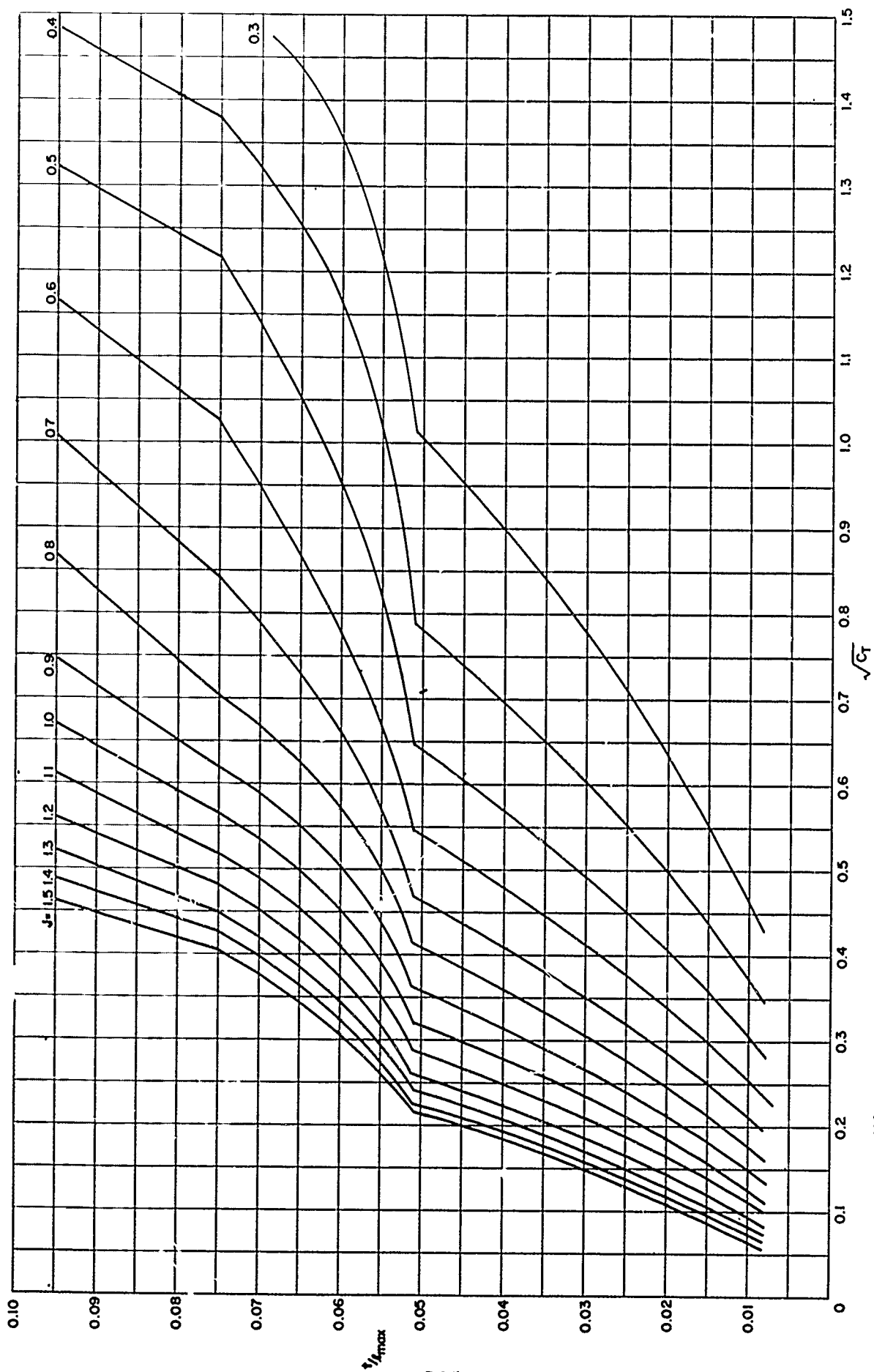
Figure 12g — Maximum Thickness at 0.9 Radius for TMB 4-Bladed SC Propeller Series, EAR = 0.5

125
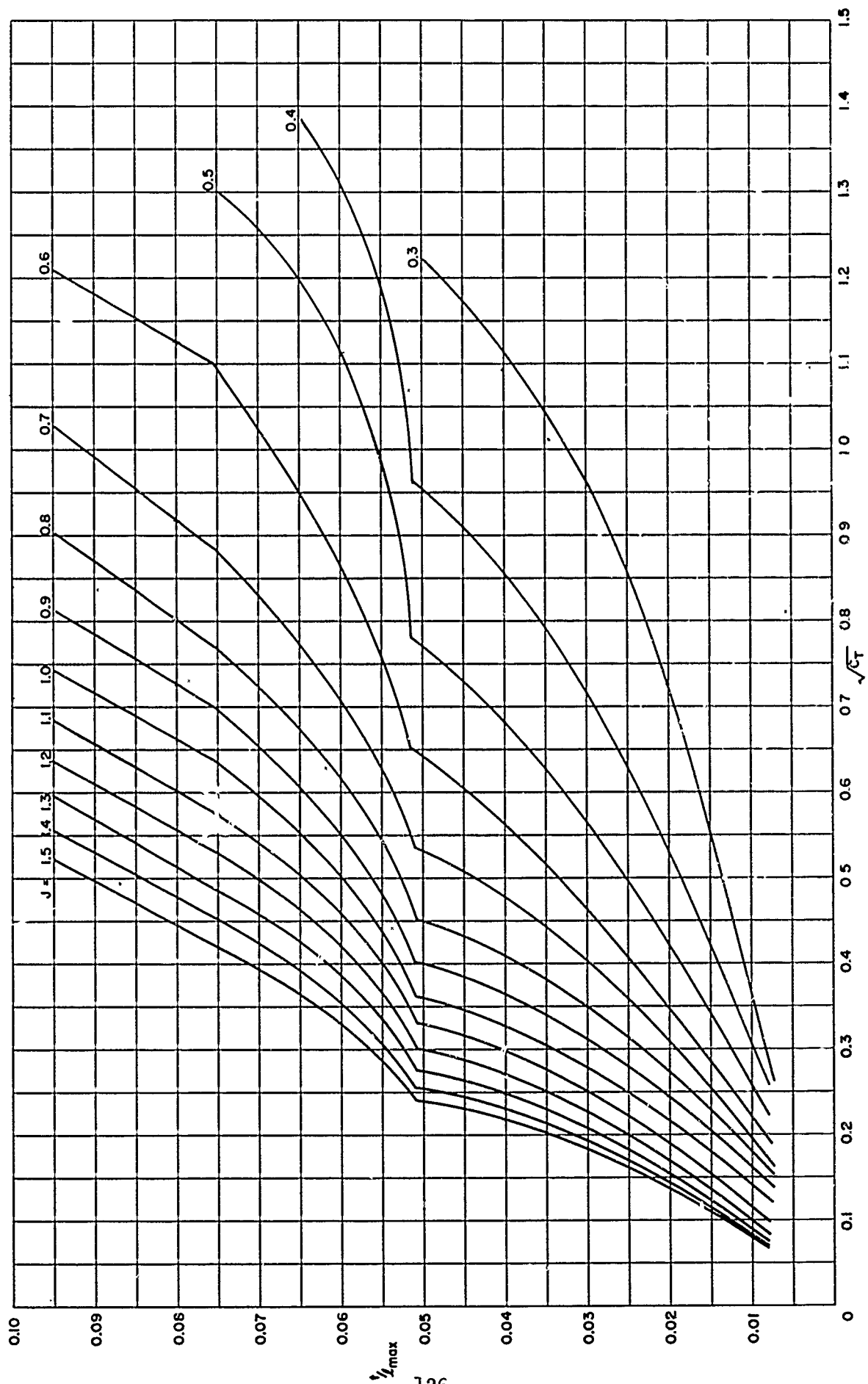
Figure 12h — Maximum Thickness at 0.9 Radius for TMB 4-Bladed SC Propeller Series, FAR = 0.6
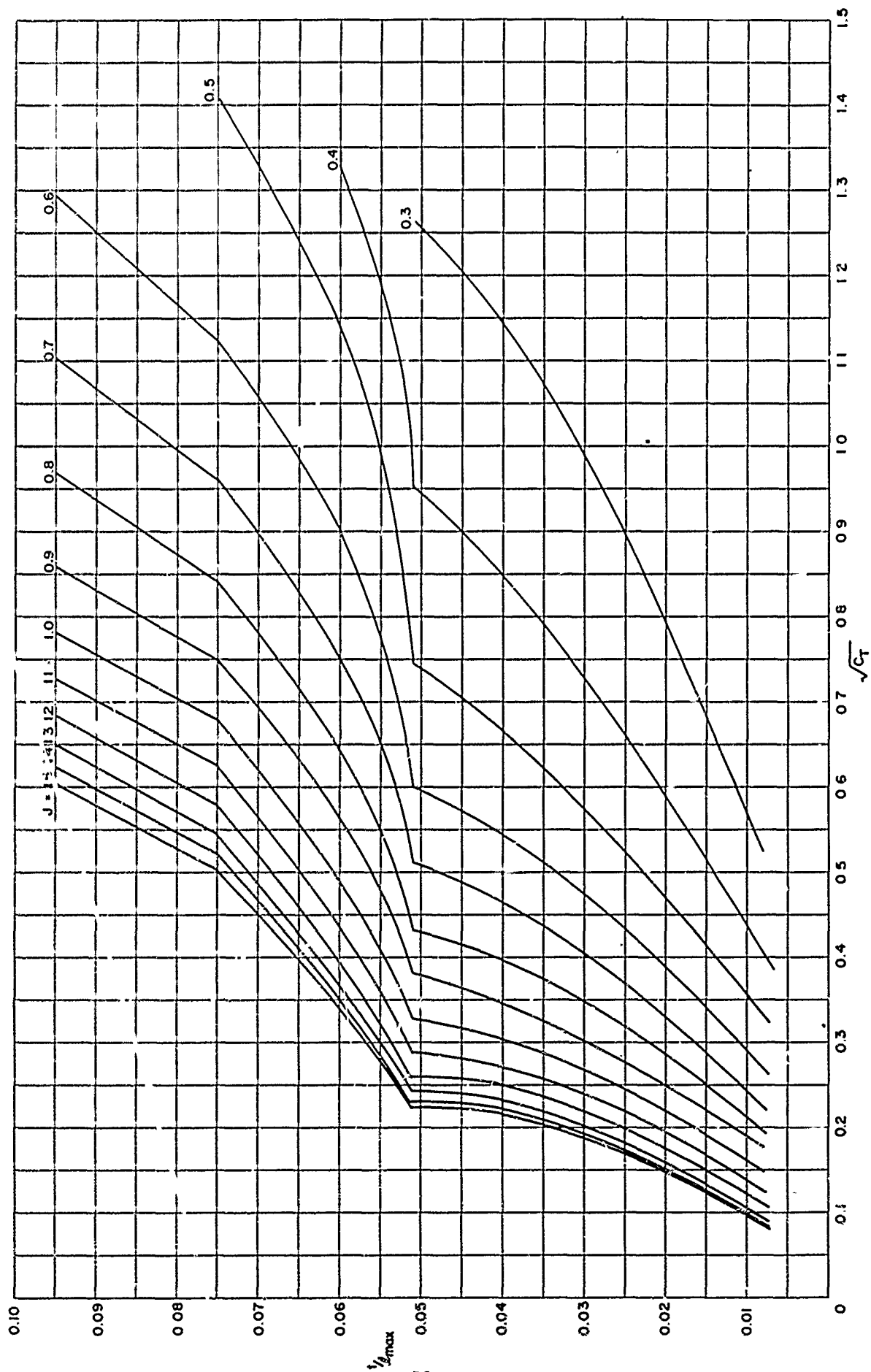
126

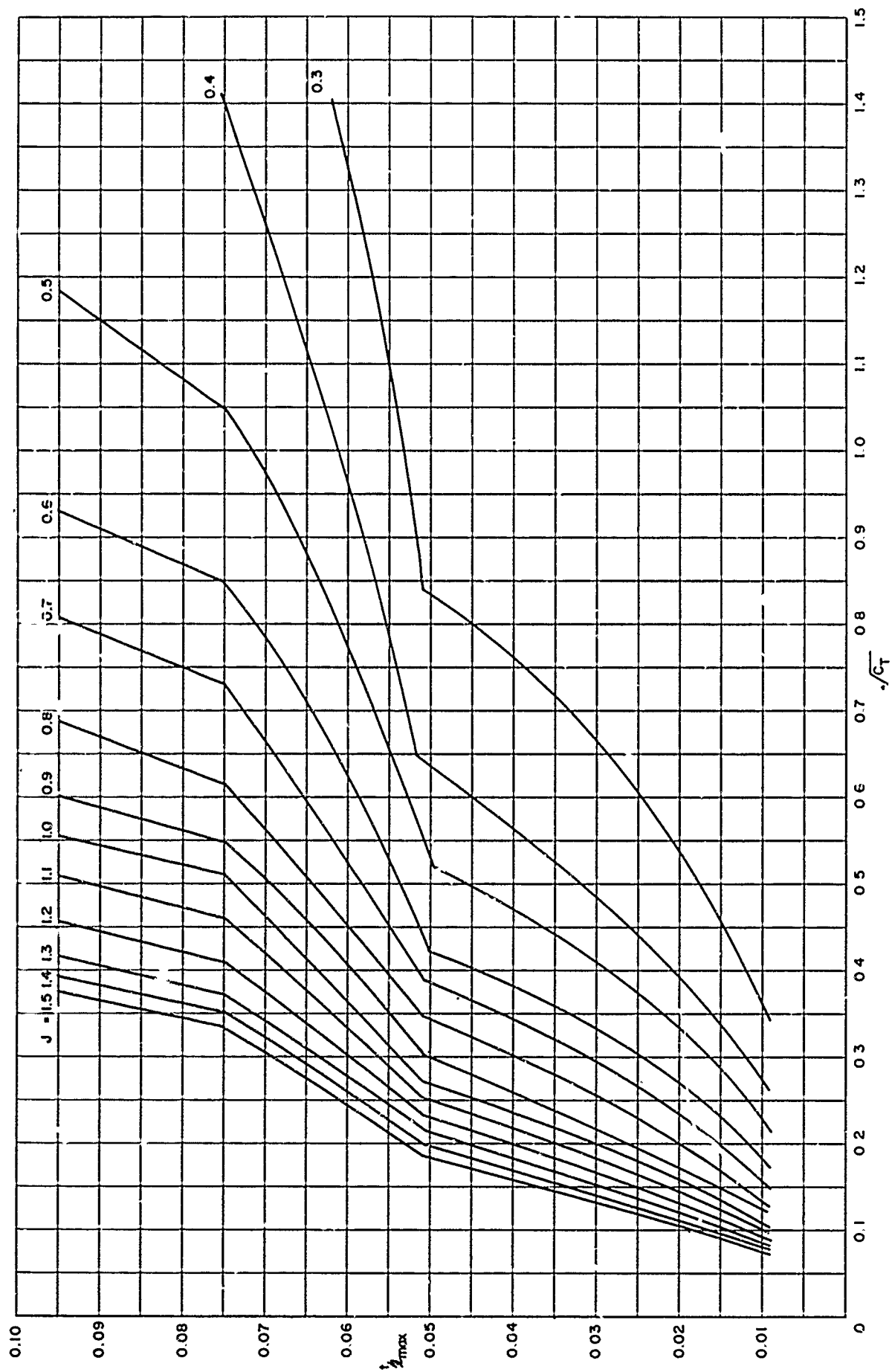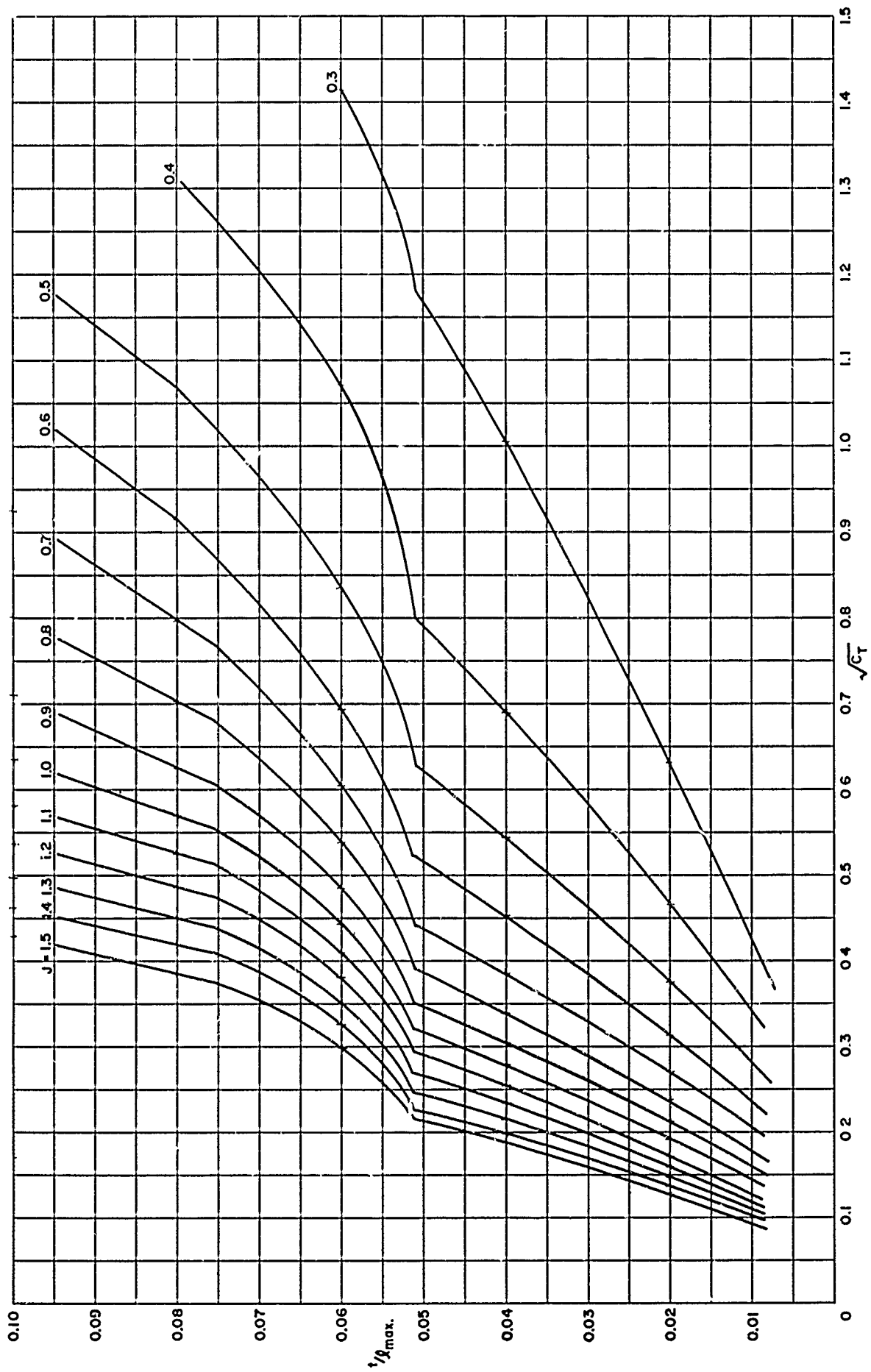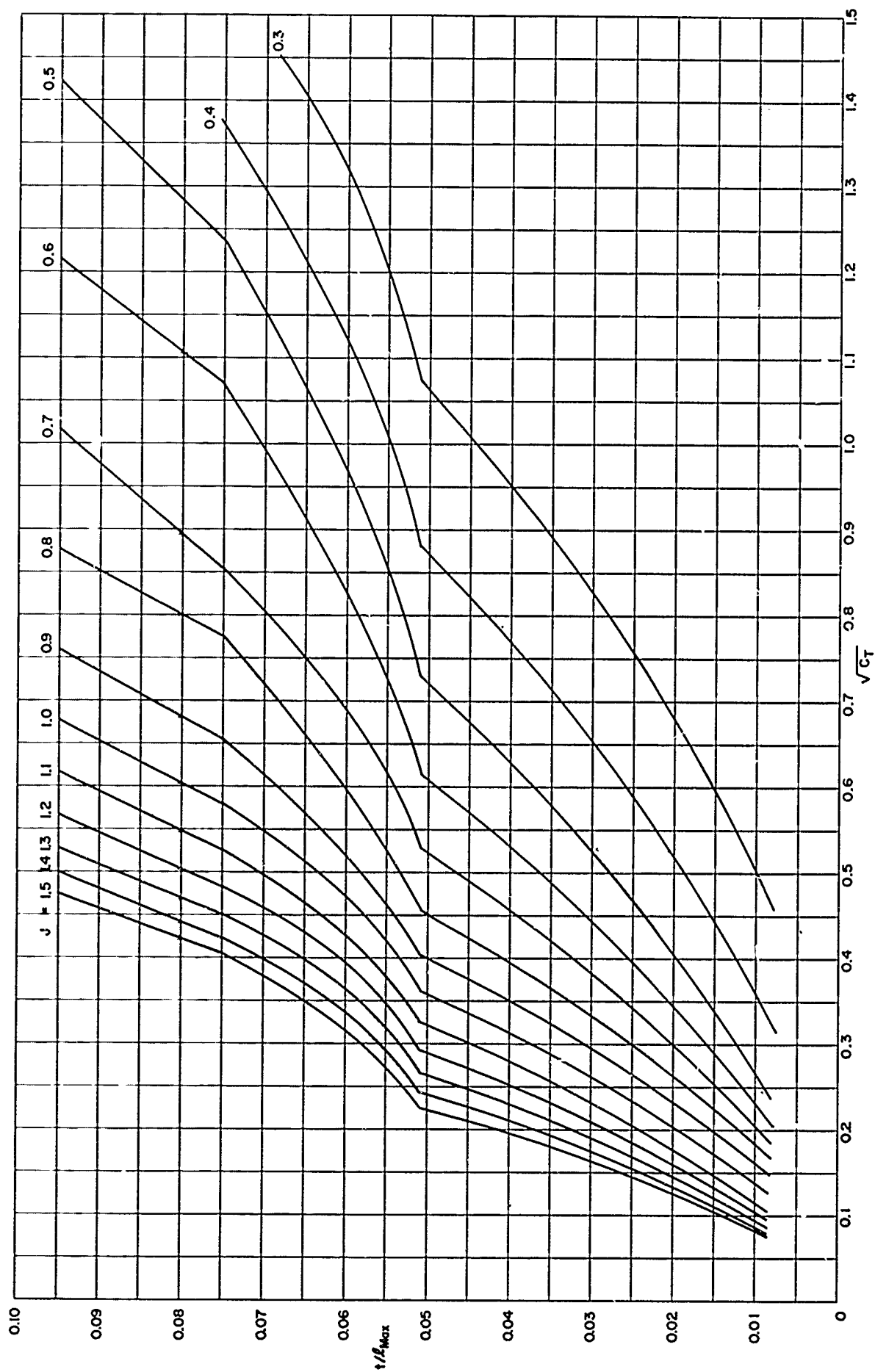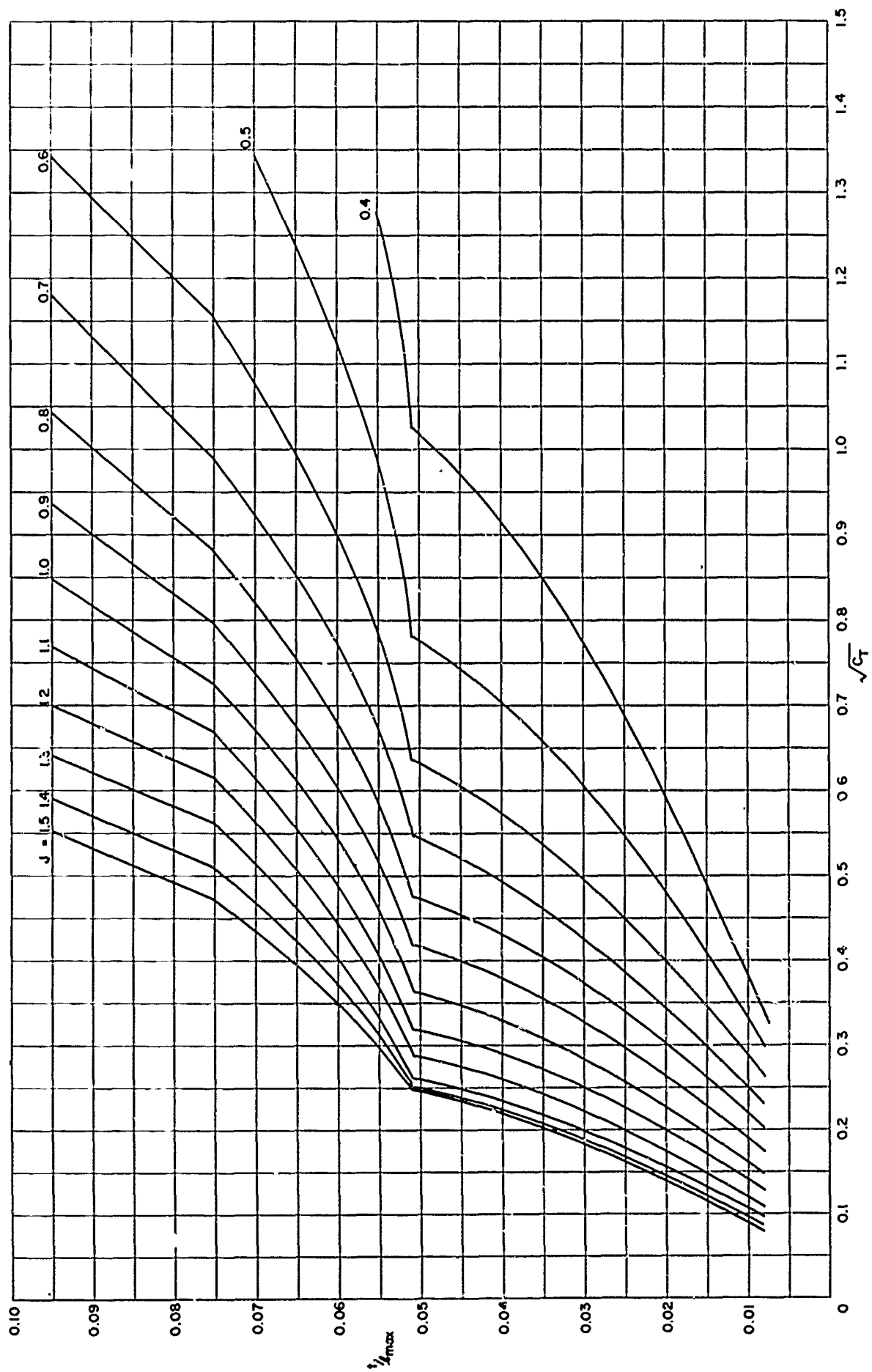Figure 12i – Maximum Thickness at 0.9 Radius for TMB 4-Bladed SC Propeller Series, EAR = 0.7

127
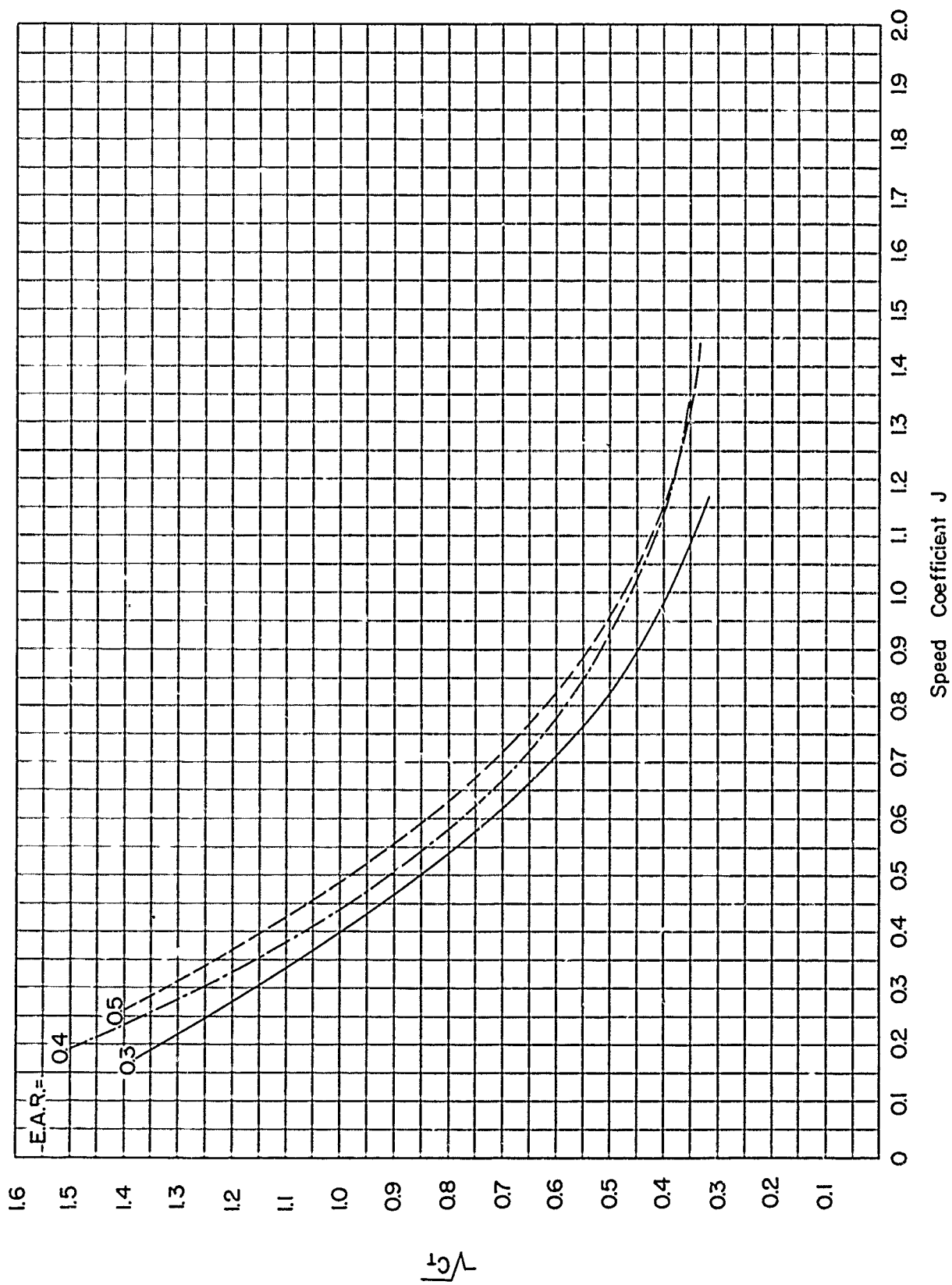
Figure 13 – Curve of Maximum Efficiency for a Given C_T for TMB 2-Bladed SC Propellers
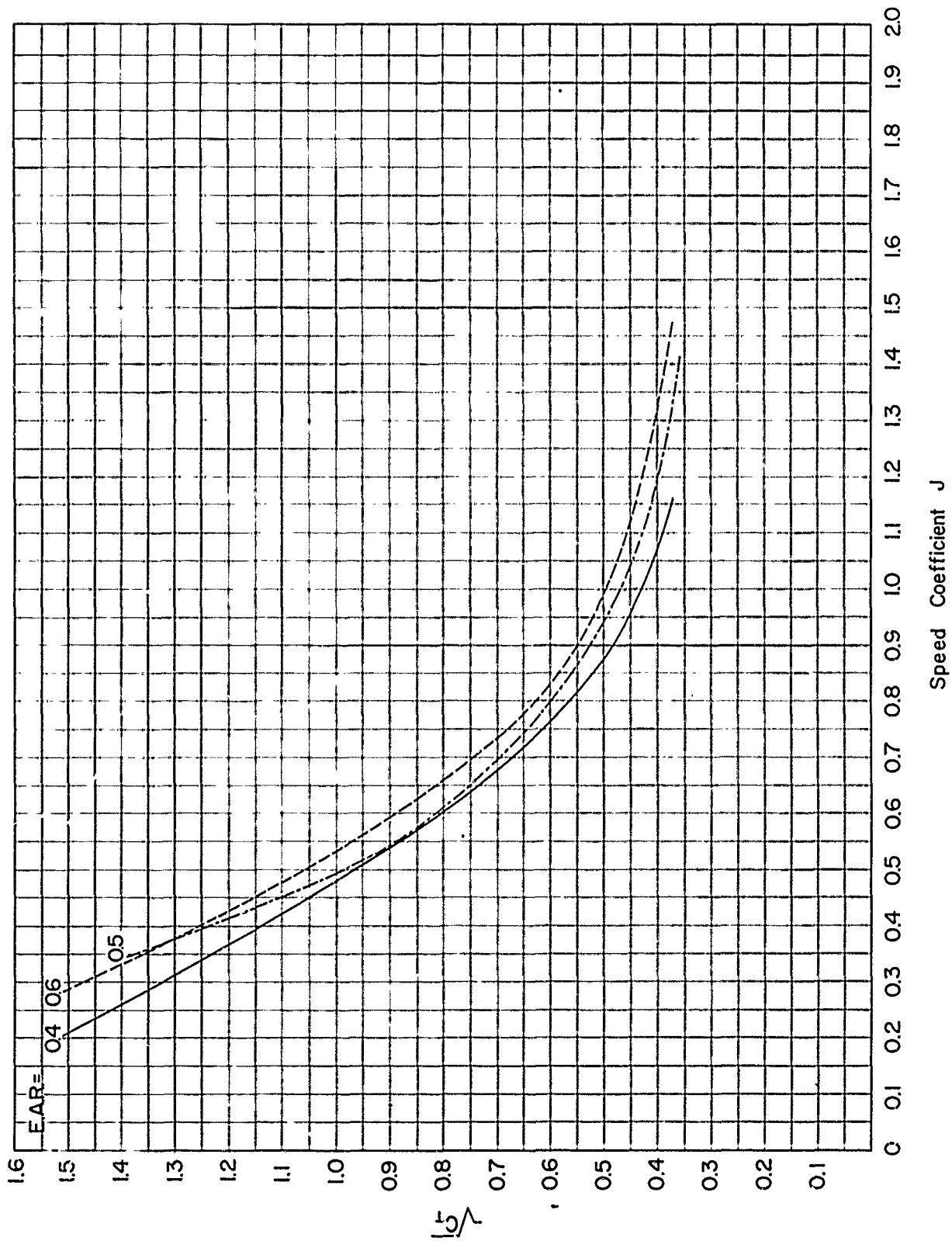
Figure 14 — Curve of Maximum Efficiency for a Given C_T for TMB 3-Bladed SC Propellers

129
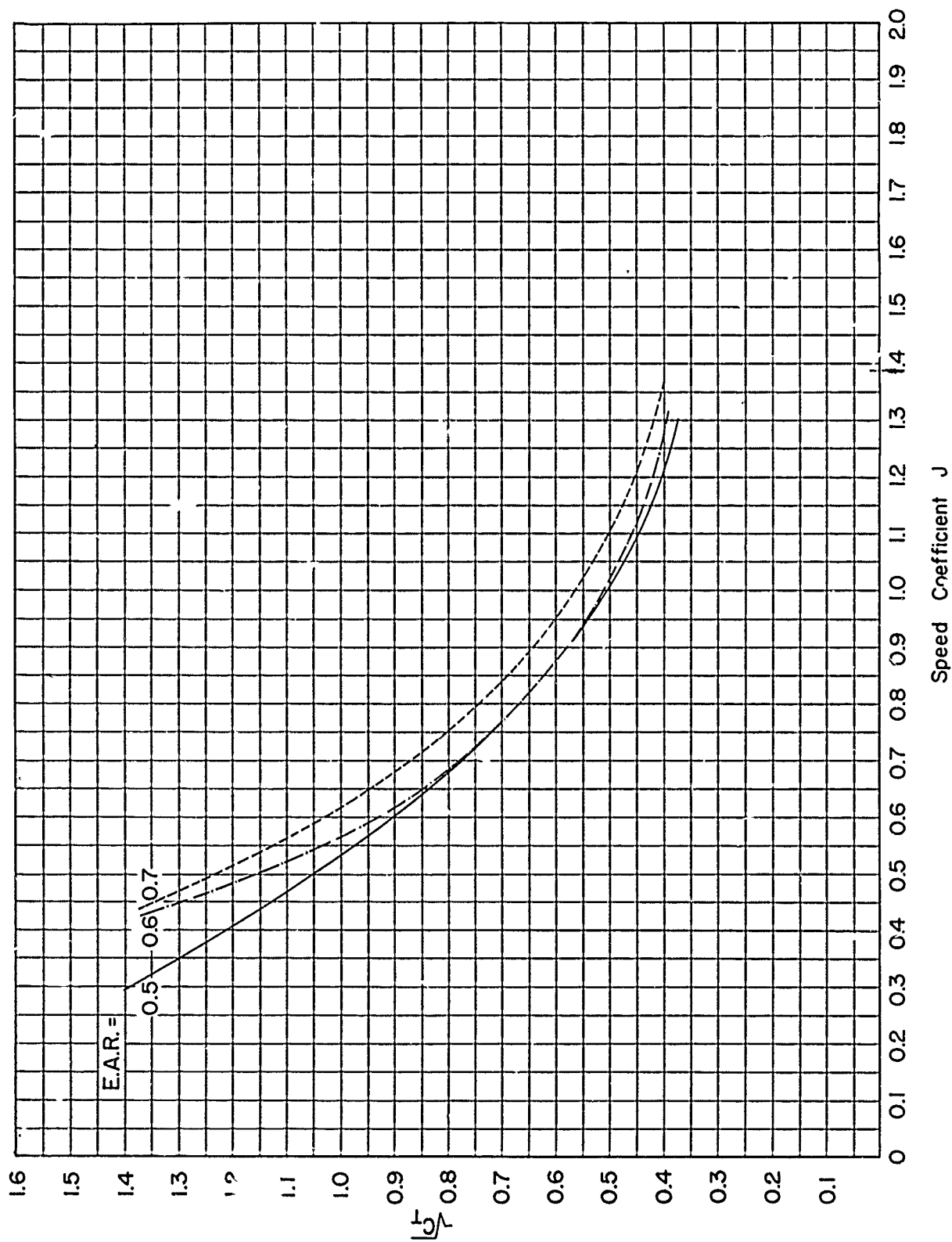
Figure 15 — Curve of Maximum Efficiency for a Given C_T for TMB 4-Bladed SC Propellers

Speed Coefficient J

E.A.R. = 0.5 0.6 0.7

130
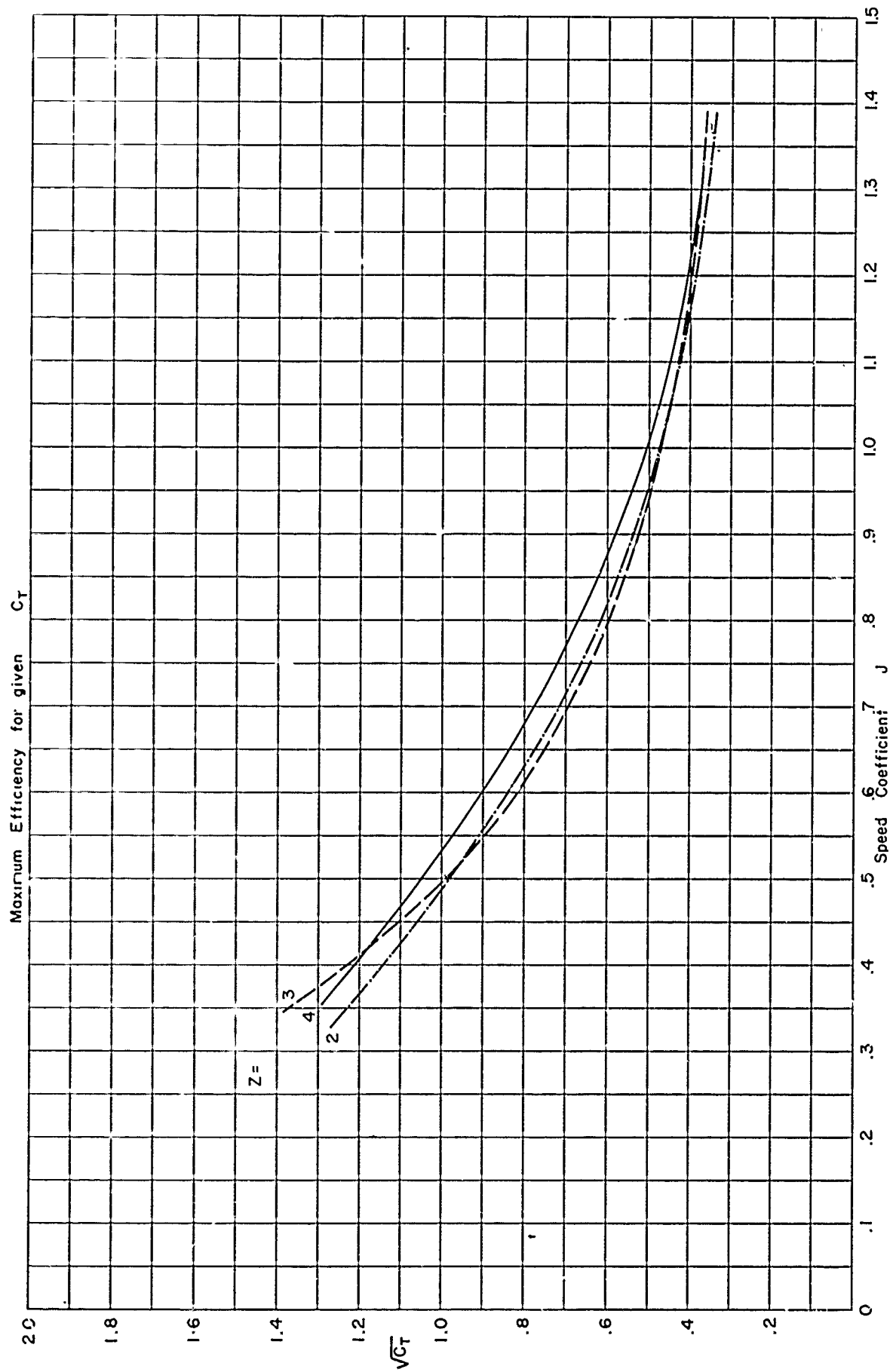
Figure 16 – Curve of Maximum Efficiency for a Given C_T for TMB 2-, 3-, and 4-Bladed SC Propellers, EAR = 0.5
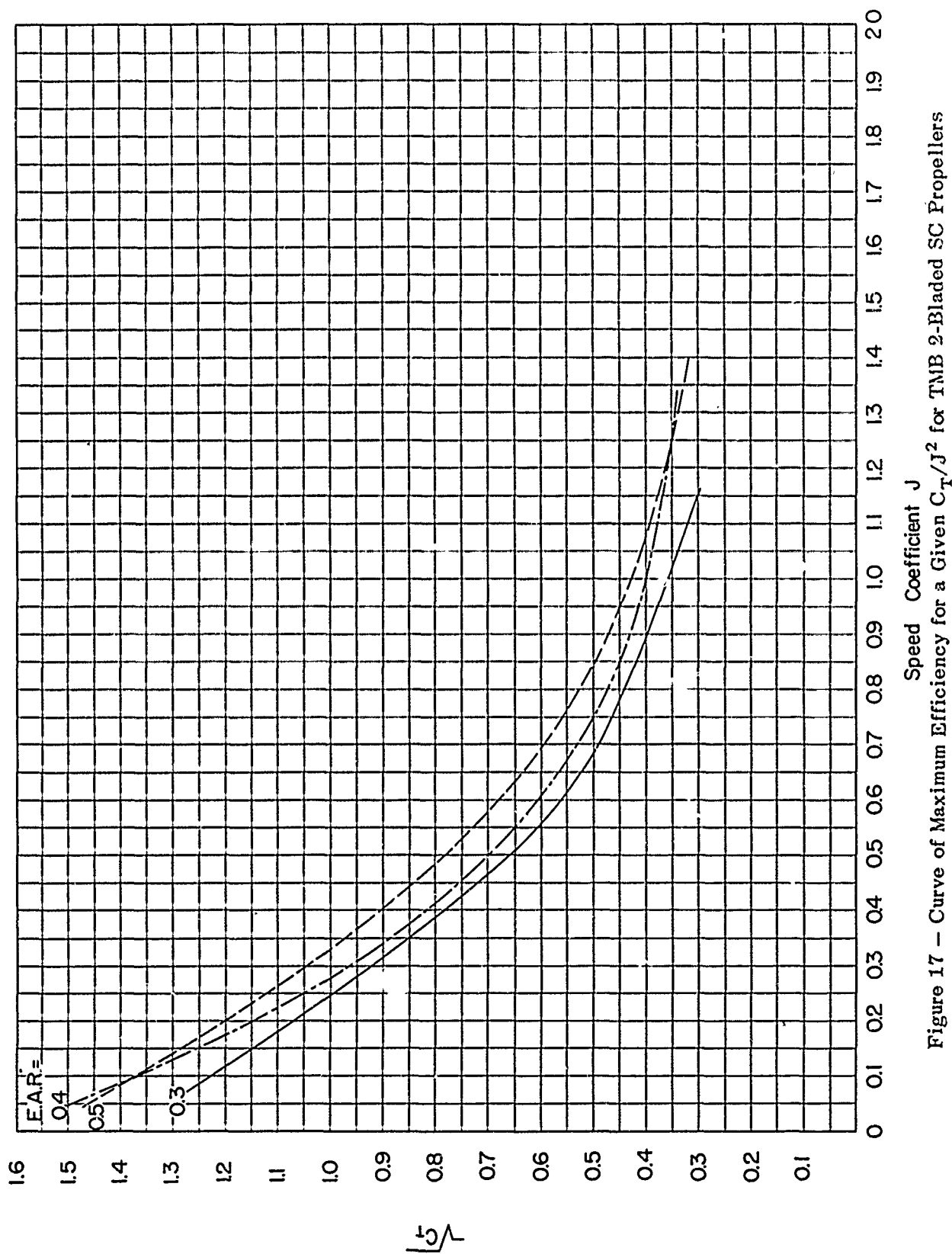
Figure 17 — Curve of Maximum Efficiency for a Given C_T/J^2 for TMB 2-Bladed SC Propellers

132
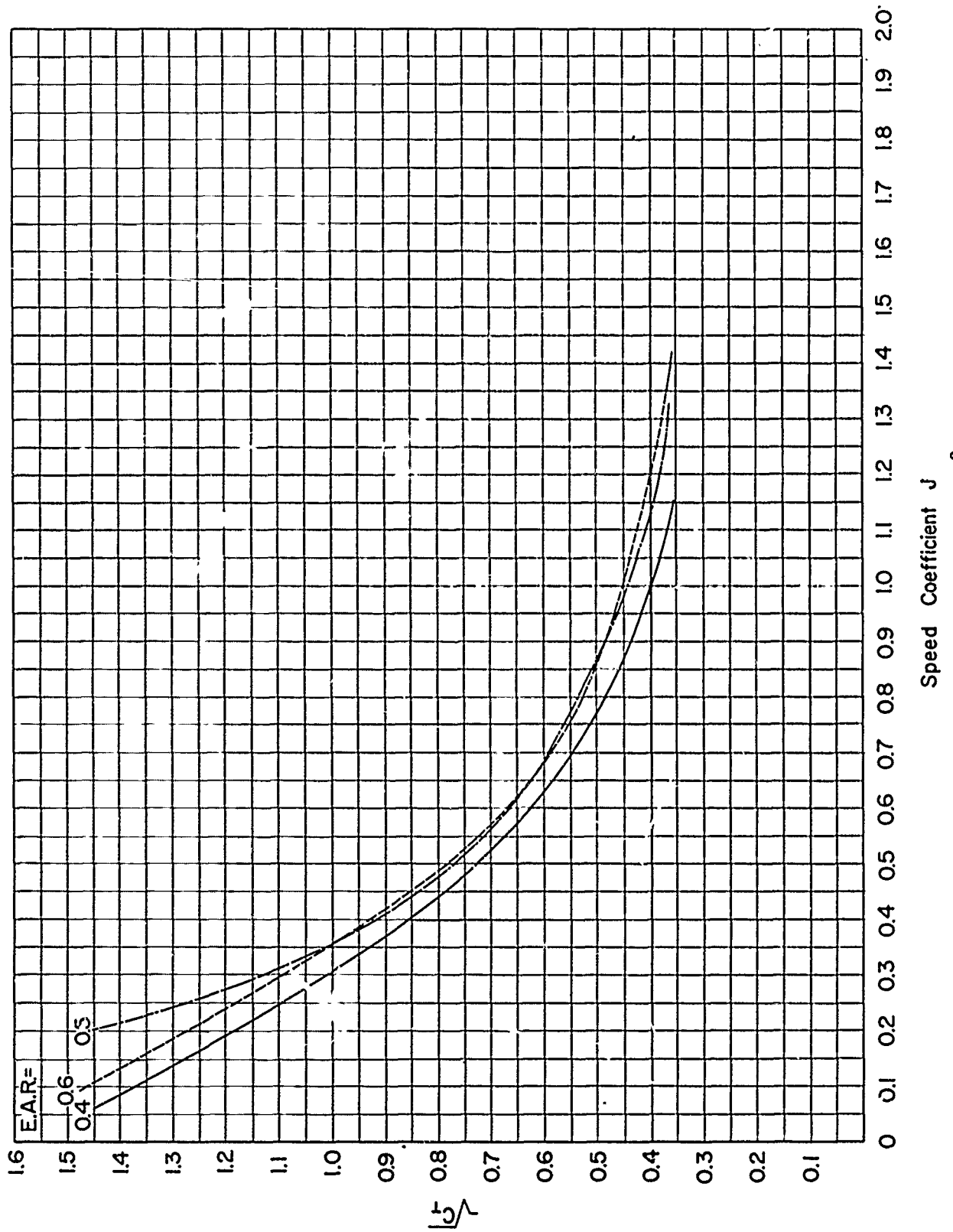
Figure 18 – Curve of Maximum Efficiency for a Given C_T/J^2 for TMB 3-Bladed SC Propellers

Speed Coefficient J

133
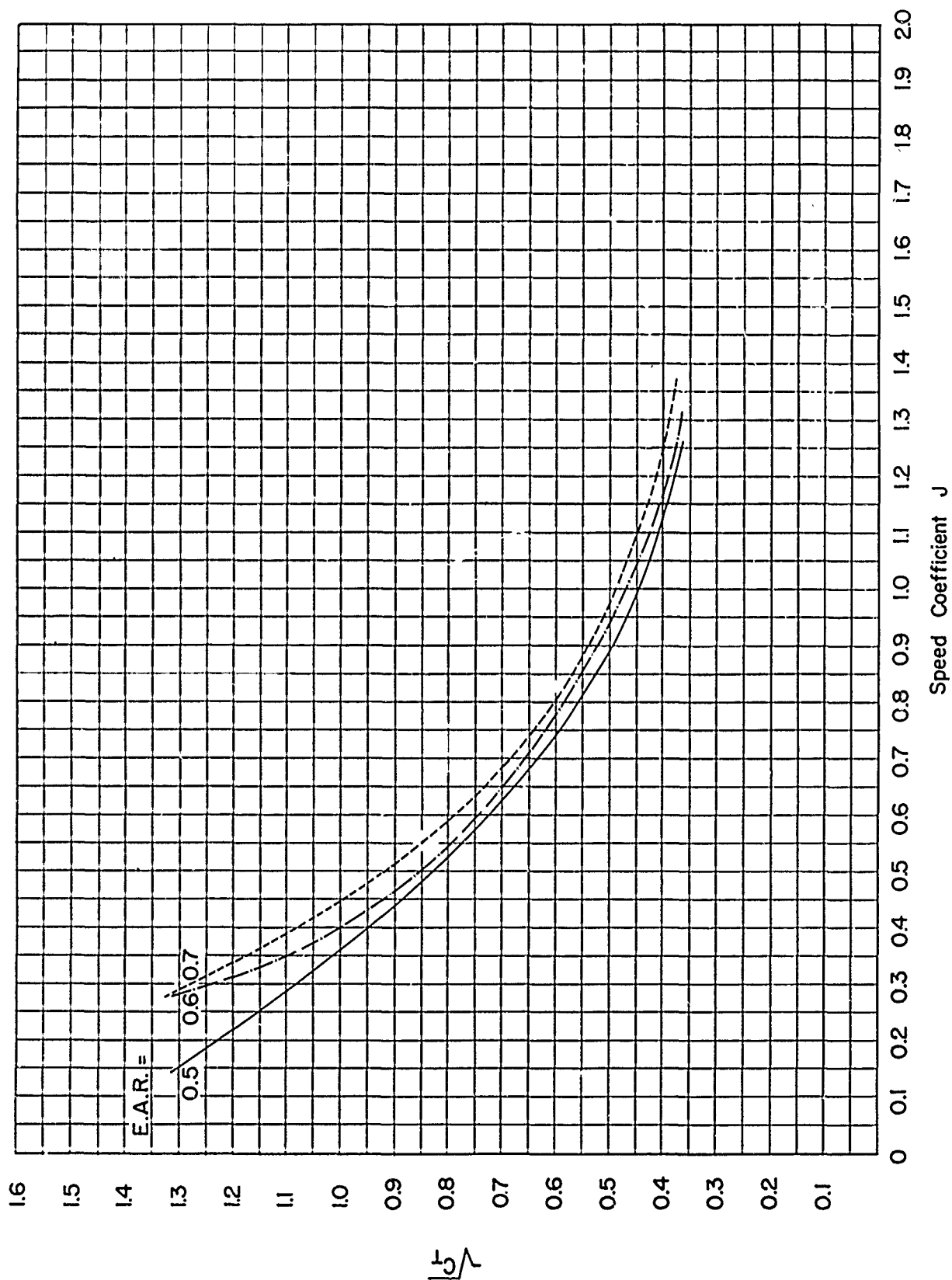
Figure 19 — Curve of Maximum Efficiency for a Given C_T/J^2 for TMB 4-Bladed SC Propellers

134
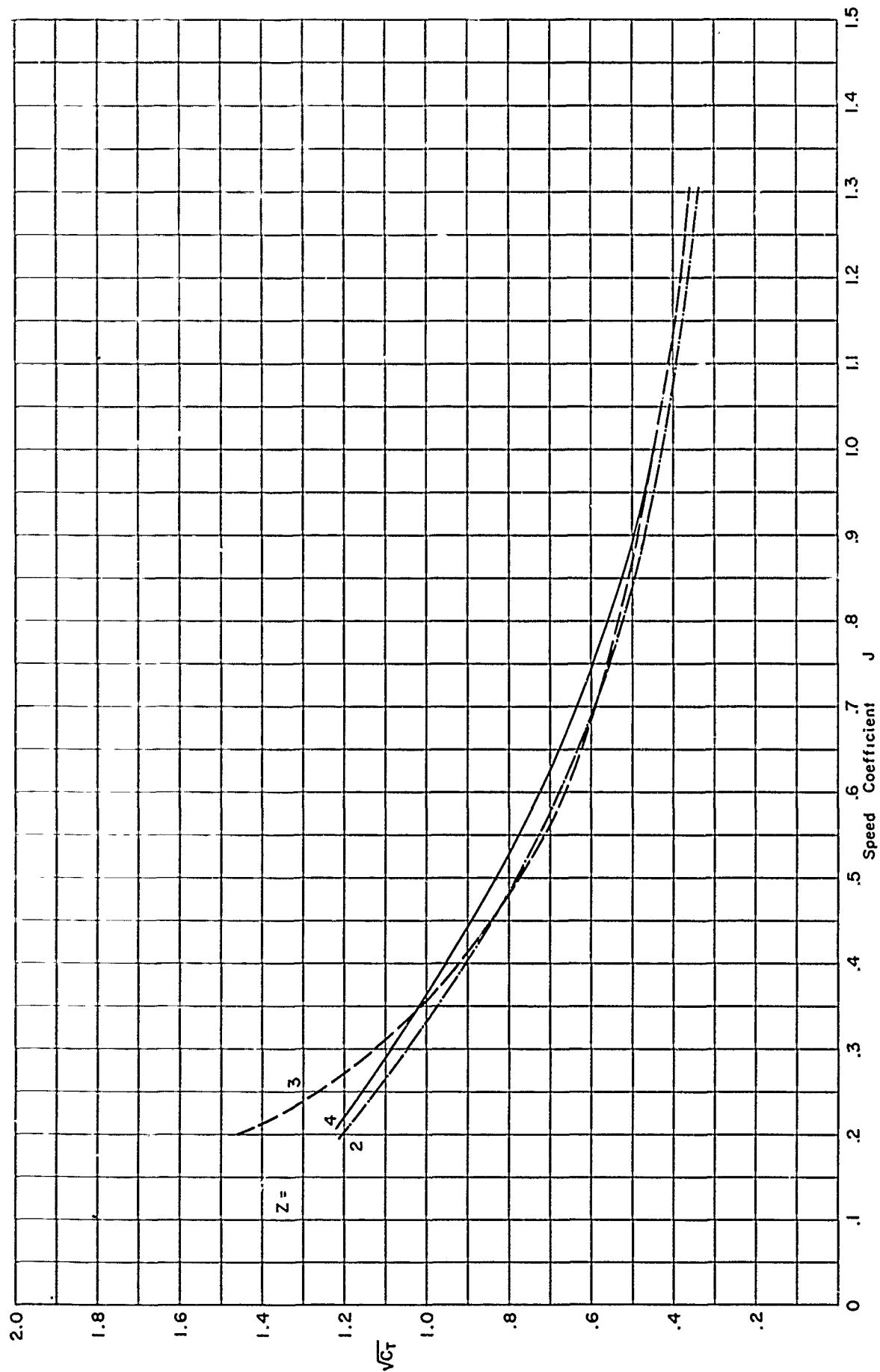
Figure 20 – Curve of Maximum Efficiency for a Given C_T/J^2 for TMB 2-, 3-, and 4-Bladed SC Propellers, EAR = 0.5

135

Copies

10   CHBUSHIPS
      3 Tech Info Sec (Code 335)
      1 Appl Research (Code 340)
      1 Prelim Des (Code 420)
      1 Mach Des (Code 430)
   1 Mach Sci & Res (Code 436)
      1 Hull Des (Code 440)
      2 Prop Shafting & Bearing (Code 644)

3   CHBUWEPS
      1 Library (DLI 3)
      1 Res & Components (RuSD-342)
      1 HydroPropulsion Sec. (RuTO-32)

3   CHONR
      2 Fluid Dynamics (Code 438)
      1 Undersea Programs (Code 466)

1   CDR, USNOTS, Pasadena Annex

1   CDR, USNOL

1   DIR, USNRL

1   DIR, USNEES

1   SUPT, USNAVPGSCOL

    ADMIN, Maritime Adm

    Gibbs and Cox, Inc.,

1   HD, NAME MIT

1   Hydro Lab, CIT,

1   DIR, Iowa Inst of Hydraulic Res,

1   DIR, St. Anthony Falls Hydraulic Lab,

1   PIB, Dept of Aero Eng & Appl Mech

1   DIR, ORL

1   Aerojet-General Corp, Azusa, Calif.

1   DIR, Davidson Lab, SIT,

1   Dir, Inst of Eng Res, Univ of Calif.

1   HD, DEPT of NAME, Univ of Mich

1   ADMIN, INST NAVARCH, Webb

2   University of California, Berkeley
      1 Librarian
      1 Head, Dept. of Nav. Arch.

1   Hydronautics

10	ASTIA
1	SNAME
1	George G. Sharp, Inc.
1	Grumman Aircraft Co.
1	Boeing Aircraft Corp.
1	Electric Boat Div. General Dyn Corp., Groton
1	Lockheed, Sunnyvale, Calif.

David Taylor Model Basin. Report 1637.
TMB 2-, 3-, AND 4-BLADED SUPERCAVITATING PROPELLER
SERIES, by E. B. Caster. Jan 1963. iv, 138p.
illus., graphs, tables, refs.   UNCLASSIFIED

This report presents theoretically derived series
of 2-bladed supercavitating propellers with expanded
area ratios of 0.3, 0.4, and 0.5; 3-bladed SC pro-
pellers with expanded area ratios of 0.4, 0.5, and
0.6; and 4-bladed SC propellers with expanded area
ratios of 0.5, 0.6, and 0.7. These propellers have
a specified radial distribution of the section chord
and a hub radius of 0.2 of the propeller radius.
The series data are plotted in the form of non-

1. Supercavitating
   propellers--Design--
   Theory
2. Supercavitating
   propellers--Per-
   formance--Prediction
3. Supercavitating
   propellers--TMB Series
I. Caster, E. B.
II. S-R009 01 01

David Taylor Model Basin. Report 1637.
TMB 2-, 3-, AND 4-BLADED SUPERCAVITATING PROPELLER
SERIES, by E. B. Caster. Jan 1963. iv, 138p.
illus., graphs, tables, refs.   UNCLASSIFIED

This report presents theoretically derived series
of 2-bladed supercavitating propellers with expanded
area ratios of 0.3, 0.4, and 0.5; 3-bladed SC pro-
pellers with expanded area ratios of 0.4, 0.5, and
0.6; and 4-bladed SC propellers with expanded area
ratios of 0.5, 0.6, and 0.7. These propellers have
a specified radial distribution of the section chord
and a hub radius of 0.2 of the propeller radius.
The series data are plotted in the form of non-

1. Supercavitating
   propellers--Design--
   Theory
2. Supercavitating
   propellers--Per-
   formance--Prediction
3. Supercavitating
   propellers--TMB Series
I. Caster, E. B.
II. S-R009 01 01

David Taylor Model Basin. Report 1637.
TMB 2-, 3-, AND 4-BLADED SUPERCAVITATING PROPELLER
SERIES, by E. B. Caster. Jan 1963. iv, 138p.
illus., graphs, tables, refs.   UNCLASSIFIED

This report presents theoretically derived series
of 2-bladed supercavitating propellers with expanded
area ratios of 0.3, 0.4, and 0.5; 3-bladed SC pro-
pellers with expanded area ratios of 0.4, 0.5, and
0.6; and 4-bladed SC propellers with expanded area
ratios of 0.5, 0.6, and 0.7. These propellers have
a specified radial distribution of the section chord
and a hub radius of 0.2 of the propeller radius.
The series data are plotted in the form of non-

1. Supercavitating
   propellers--Design--
   Theory
2. Supercavitating
   propellers--Per-
   formance--Prediction
3. Supercavitating
   propellers--TMB Series
I. Caster, E. B.
II. S-R009 01 01

David Taylor Model Basin. Report 1637.
TMB 2-, 3-, AND 4-BLADED SUPERCAVITATING PROPELLER
SERIES, by E. B. Caster. Jan 1963. iv, 138p.
illus., graphs, tables, refs.   UNCLASSIFIED

This report presents theoretically derived series
of 2-bladed supercavitating propellers with expanded
area ratios of 0.3, 0.4, and 0.5; 3-bladed SC pro-
pellers with expanded area ratios of 0.4, 0.5, and
0.6; and 4-bladed SC propellers with expanded area
ratios of 0.5, 0.6, and 0.7. These propellers have
a specified radial distribution of the section chord
and a hub radius of 0.2 of the propeller radius.
The series data are plotted in the form of non-

1. Supercavitating
   propellers--Design--
   Theory
2. Supercavitating
   propellers--Per-
   formance--Prediction
3. Supercavitating
   propellers--TMB Series
I. Caster, E. B.
II. S-R009 01 01

dimensional coefficients so that the performance of the propellers can be easily predicted and a complete design obtained if desired.

dimensional coefficients so that the performance of the propellers can be easily predicted and a complete design obtained if desired.

dimensional coefficients so that the performance of the propellers can be easily predicted and a complete design obtained if desired.

dimensional coefficients so that the performance of the propellers can be easily predicted and a complete design obtained if desired.